# STUDIES FOR ANTI-TUMOR ACTIVITIES AND REVERSING P-GLYCOPROTEIN MEDIATED MULTIDRUG RESISTANCE INDUCED BY NOVEL QUINOLINE DERIVATIVES

**ZHOU YUANYUAN**

**PhD**

**The Hong Kong Polytechnic University**

**2019**

**The Hong Kong Polytechnic University**

**Department of Applied Biology and Chemical Technology**

# Studies for Anti-tumor Activities and Reversing P-glycoprotein Mediated Multidrug Resistance Induced by Novel Quinoline Derivatives

**ZHOU Yuanyuan**

**A thesis submitted in partial fulfillment of requirements for the degree of Doctor of Philosophy**

**January**
**2019**

# CERTIFICATE OF ORIGINALITY

I hereby declare this thesis is my own work and that, to the best of my knowledge and belief, it reproduces no material previously published or written, no material that has been accepted for award of any other degree or diploma, except where due acknowledgement has been made in the text.

(Signed)

Zhou Yuanyuan

# ABSTRACT

Cancer is a major health threaten worldwide. P-glycoprotein mediated multidrug resistance is one of the main obstacles for successful cancer chemotherapy. Quinoline core has been shown to possess a promising role in the development of novel anti-cancer agents. The development of novel anti-cancer drugs with high efficacy, low toxicity and minimal anti-cancer drug resistance is thus essential and still a great challenge.

In the study of the anti-cancer effect of a novel synthesized quinoline compound 91b1, cytotoxic effect on the four cancer cell lines (A549, AGS, KYSE150, and KYSE450) and one non-tumor cell line NE3 was determined by MTS cytotoxicity assay compared with the widely used chemotherapeutic drug CDDP. The $MTS_{50}$ values of compound 91b1 were 15.38 μg/mL, 4.28 μg/mL, 4.17 μg/mL, 1.83 μg/mL, and 2.17 μg/mL for A549, AGS, KYSE150, KYSE450, and NE3 cells respectively. The $MTS_{50}$ values of CDDP were 6.23 μg/mL, 13.00 μg/mL, 13.2μg/mL, 6.83 μg/mL, and 1.17 μg/mL for A549, AGS, KYSE150, KYSE450, and NE3 cells respectively. The compound 91b1 showed stronger cytotoxicity to cancer cells and less toxicity to non-tumor cells compared with CDDP. cDNA microarray analysis on the compound 91b1treated (9.5μg/mL) KYSE150 cells compared with the parental cells identified lumican as one of the most significantly downregulated targets. By qPCR analysis, lumican was shown to be suppressed in mRNA with compound 91b1 treatment in a dose-dependent manner. Cell proliferation assay was performed on four cancer cell

lines (A549, AGS, KYSE150, and KYSE450), which all showed an obvious reduction in proliferation rate after treated with compound 91b1 (10 μg/mL). Cell cycle analysis was performed on A549 and KYSE450 cells to identify the effect of compound 91b1 on cancer cell growth. Cancer cells were observed to be arrest at G2/M phase and decreased at G0/G1 phase after compound 91b1 (10 μg/mL) treatment. Wound healing assay for A549, KYSE150, AGS, KYSE70, and KYSE510 cell lines showed that compound 91b1 suppressed cancer cell migration *in vitro*. What's more, compound 91b1 inhibited solid tumor (KYSE150 and KYSE450) growth in nude mice xenograft model using KYSE450 with the reduction of tumor volume by 51.06 % compared with the vehicle control group after 25 days' treatment). The compound 91b1 showed mild liver damage with no significant changes being observed on liver functional parameters including levels of ALT, AST, TP, and Tbile in animal serum after treatment and was relatively safe than doxorubicin at therapeutic dose in the mouse model. These results implied that the compound 91b1 could effectively induce anti-cancer activity both *in vitro* and *in vivo* on the studied tumors.

In the study of the functions of lumican in cancer cells, up-regulation of lumican was detected in cancer cell lines (KYSE30, KYSE70, KYSE150, KYSE510, and SLMT1) and tumor samples isolated from cancer patients with esophageal carcinoma. The trans-well matrigel invasion assay demonstrated that lumican protein enhanced the migration ability of KYSE150 cells. Cell proliferation assay on four cancer cell lines (A549, AGS, KYSE150, and KYSE450) showed that protein lumican (250 ng/mL) increased cancer cell proliferation rate. Wound healing test of A549, AGS,

and KYSE150 cell lines showed that protein lumican enhanced cancer cell invasion. Subcutaneous injection of lumican transfected NIH 3T3 cells (NIH 3T3/Lum) generated a subcutaneous mass in athymic nude mice. Bio-Plex cell signaling assay was performed on KYSE150 cells treated with either compound 91b1 or human recombined lumican protein in order to identify the most associated pathway by which compound 91b1 suppressed cancer cell progression and tumor development via down-regulating lumican expression. The phosphorylated level of Erk1/2 revealed consistent trend of increase or decrease after treatment with either compound 91b1 or protein lumican respectively (phosphorylated level of Erk1/2 was increased after compound 91b1 treatment and decreased after reclumican treatment; while compound 91b1 down-regulated lumican expression in KYSE150 cells). The overall results suggested that protein lumican promoted cancer cell proliferation, invasion and migration in esophageal carcinoma cells KYSE150, by enhancing tumor development. It is inferred that compound 91b1 induced anti-cancer effect through Erk1/2 signaling pathway by downregulating lumican expression.

In the study of reversal effect of p-glycoprotein modulated multi-drug resistance (MDR)of compound 160a, DOX-resistance cancer cells of lung cancer (A549) and esophageal cancer (KYSE150) were established from parental cancer cells and cultured in 1.0 μg/mL doxorubicin in medium to maintain its resistance to doxorubicin. P-glycoprotein was predicted to be the possible interaction target of compound 160a by molecular docking analysis using Similarity Ensemble Approach (SEA). The synergistic effect of compound 160a combined with doxorubicin was

determined based on cytotoxicity (A549/DOX and KYSE150/DOX cell lines) and cell proliferation (A549/DOX, KYSE150, LCC6/MDR, and MX100 cell lines) tests and analyzed by Compusyn program with CI value being smaller than 1. The above results demonstrated that the compound 160a showed synergistic effect to enhance the cytotoxicity and inhibition of cell proliferation induced by doxorubicin against the DOX-resistance cancer cell lines. The effect of compound 160a on p-glycoprotein was also tested by multi-drug resistance assay using calcein AM as the substrate of p-glycoprotein, and detected by flow cytometry and confocal microscopy. It was indicated that the compound 160a increased the intracellular calcein AM concentration by inhibiting the MDR effect induced by p-glycoprotein. Doxorubicin accumulation test also offered consistent results that160a exhibited greater potency by increasing DOX accumulation against DOX-resistance cancer cells (LCC6/MDR, KYSE150/DOX, and A549/DOX cells) than verapamil, a positive control. The duration of reversal MDR effect test also showed that the compound 160a could persist the MDR effect for 1 hour. The overall results of this part showed that the novel quinoline compound 160a possessed synergistic effect when combined with doxorubicin against DOX-resistance cancer cells. The molecular mechanism of the synergistic effect of the compound 160a was explained by being able to reverse the multi-drug resistance modulated by the p-glycoprotein based drug-efflux effect.

To conclude, the results of the overall work provided the possible novel therapeutic directions for cancer therapy at molecular level. The findings of the anti-cancer actions of the novel quinoline compound 91b1 and the mechanisms

associated with lumican offered a new therapeutic target. The results about the MDR reversal effect of the novel quinoline compound 160a showed the great potential of 160a to overcome the chemoresistance in cancer treatment in future.

# PUBLICATIONS

## Manuscripts under preparation (directly related to this thesis)

1. **Anti-cancer effect of a novel quinoline derivative 91b1 through ERK 1/2 signaling pathway to down-regulate the expression of lumican**

2. **Development of a novel quinoline derivative 160a asp-glycoprotein inhibitor to reverse multi-drug resistance in cancer cells.**

**Yuanyuan Zhou**, Po-yee Chung, Jessica Yuen-wuen Ma, Alfred King-yin Lam, Simon Law, Kwok-wah Chan, Albert Sun-chi Chan, Xingshu Li, Kim-hung Lam, Chung-hin Chui, and Johnny Cheuk-on Tang

Biology 2019, 8(4), 75

## Other Publications

1. **Anti-cancer Effects of a Novel Quinoline Derivative 83b1 on Human Esophageal Squamous Cell Carcinoma through Down-Regulation of COX-2 mRNA and $PGE_2$**

Ivan Ho Yuen Pun, BScDessy Chan, BSc, Sau Hing Chan, PhD, Po Yee Chung, BSc, **Yuan Yuan Zhou**, MSc, Simon Law, MBBChir, MS, Alfred King Yin Lam, MD, PhD, Chung Hin Chui, PhD, Albert Sun Chi Chan, PhD, Kim Hung Lam, PhD, Johnny Cheuk On Tang, PhD
Cancer Research and Treatment 2017; 49(1): 219-229.

2. **Expression of Insulin-Like Growth Factor Binding Protein-5 (*IGFBP5*) Reverses Cisplatin-Resistance in Esophageal Carcinoma**

Dessy Chan,**Yuanyuan Zhou**,Chung Hin Chui,Kim Hung Lam,Simon Law,Albert Sun-chi Chan,Xingshu Li,Alfred King-yin Lam, and Johnny Cheuk On Tang

Cells. 2018 Oct; 7(10): p.15.

3. **Targeting DNA Binding for NF-κB as an Anticancer Approach in Hepatocellular Carcinoma**

Po Yee Chung,Pik Ling Lam,**Yuanyuan Zhou**,Jessica Gasparello,Alessia Finotti,Adriana Chilin,Giovanni Marzaro,Roberto Gambari,Zhaoxiang Bian,Wai Ming Kwok,Wai Yeung Wong,Xi Wang,Alfred King-yin Lam,Albert Sun-chi Chan,Xingshu Li,Jessica Yuen Wuen Ma,Chung Hin Chui,Kim Hung Lam, and Johnny Cheuk On Tang

Cells. 2018 Oct; 7(10): p.14.

4. **Downregulation of chemokine (C-C motif) ligand 5 (CCL5) suppresses tumor invasiveness in esophageal carcinoma. Submitted to Frontiers_in_Cell_and _Developmental_Biology**

# ACKNOWLEDGEMENTS

I would like to express my most sincerely gratitude to my supervisor, Dr. Johnny Tang Cheuk-On, who provided me the enthusiastic supervision, supportive guidance and valuable suggestions throughout the whole period of my research project. This project can only be finished because of Dr. Johnny Tang's novel ideas, frequent discussion, valuable comments, and clear directions. Dr. Johnny Tang's attitude and spirit to research and science also gave me great examples when I encountered difficulties.

I would like to express my deepest thanks to the group members of Dr. Tang's group, including Mr. Ivan Ho-Yuen Pun, Dr. Dessy Chan, Miss Yami Yeung, Miss Po-Yee Chung, and Mr. Yannick Ying-Lung Hung for their assistance on laboratory work, discussion about project difficulties, research-experience sharing, and continuous encouragement.

I also would like to thank Dr. Penny Sau-hing Chan for the synthesis of the novel quinoline derivatives 91b1 and 160a.

I would like to express my special thanks to Prof. Larry Chow from the Department of Applied Biology and Chemical Technology of Hong Kong Polytechnic University for kindly offer me LCC6, LCC6/MDR, and MX100cell lines for the important part of the whole work. That's a great help to finish this project.

I would like to extend my sincerely thanks to all laboratory staffs from the Department of Applied Biology and Chemical Technology, including Dr. Lam Kim-hung, Dr. Iris Wong, Mr. Kwan Wing-kong, Ms. Echo Wan, Dr. Karen Gu, Miss

Sarah Yeung, Mr. Kim Chi-fai, Miss Sharon Chan, Ms. Ivy Teo for their great help to assist me to finish every test of my project.

I would like to express my deeply thanks to staff from the ULS, including Dr. Rachel Li, Dr. Clara Hung, Dr. Carol Tsang, and Dr. So Pui-kin to help me operate the equipment and offered me the technical suggestions.

I would like also to thank colleagues from Shenzhen Research Institute of the Hong Kong Polytechnic University, including Ms. Xie Xiujuan, Mr. Liu Xingxian, Ms. Xiao Huihui, and Mr. Yang Qing for their support on animal experiment and UPLC/MS analysis.

Special thanks are also given to my family and friends, especially Mr. Zhou Chengcai, Mrs. Yuan Dongmei, Mr. Zhou Zhongguo, Mr. Li Ming, and Ms. Su Xiaochun for always giving me support and encouragement.

# TABLE OF CONTENT

# LIST of TABLES

# LIST of FIGURES

# LIST OF ABBREVIATIONS

| | |
|---|---|
| 91b1 | : 5,7-dibromo-1,2,3,4-tetrahydro-2-methylquinolin-8-ol |
| 160a | : 8-(3-methoxybenzyloxy) quinoline-2-carbaldehyde |
| ATCC | : American Type Culture Collection |
| CDDP | : Cisplatin;cis-diamminedichloroplatinum (II); cis-diammineplatinum (II) dichloride |
| DOX | : doxorubicin |
| DMSO | : Dimethyl Sulfoxide |
| MDR | : multi drug resistance |
| SEA | : similarity ensemble approach |
| DMEM | : Dulbecco’s modified Eagle’s medium |
| DNA | : Deoxyribonucleic acid |
| dNTP | : Deoxyribonucleoside triphosphate |
| ESCC | : Esophageal squamous cell carcinoma |
| FBS | : Fetal bovine serum |
| IHC | : Immunohistochemistry |
| KSFM | : Keratinocyte serum-free medium |
| MTS | : [3-(4,5-dimethylthiazol-2-yl)-5-(3-carboxymethoxyphenyl)-2-(4-sulfophenyl)-2H-tetrazolium] |
| p | : p value |
| PBS | : Phosphate buffered saline |

| | |
|---|---|
| qPCR | : Quantitative polymerase chain reaction analysis |
| RNA | : Ribonucleic acid |
| RT-PCR | : Reverse transcription-polymerase chain reaction |
| Cq | : cycle of quantification |
| ALB | : albumin |
| ALP | : alkaline phosphatase |
| ALT | : alanine aminotransferase |
| AST | : aspartate transaminase |
| TP | : total protein |
| TBil | : total bilirubin |
| Ip | : Intraperitoneal |
| PEG | : Poly(ethylene) Glycol |
| LC/MS | : Liquid Chromatography/ Mass Spectrometry |
| UPLC | :Ultra-Performance Liquid Chromatography |
| TQD | : Triple Quadrupole |
| ESI | : Electron Spray Ionization |
| TBE | : Tris-borate-EDTA |
| EDTA | : Ethylenediaminetetraacetic acid |
| reclumican | : recombined lumican protein |
| CI | : combination index |
| IPA | : Ingenuity Pathway Analysis |

# LIST OF ABBREVIATION FOR UNITS

| | |
|---|---|
| °C | : degree Celsius |
| bp | : base pair |
| M | : molar |
| nm | : nanometer |
| μm | : micrometer |
| m | : meter |
| μL | : microliter |
| mL | : milliliter |
| L | : liter |
| sec (s) | : second(s) |
| min(s) | : minute(s) |
| Hr(s) | : hour(s) |
| ng | : nanogram |
| μg | : microgram |
| mg | : milligram |
| g | : gram |
| kg | : kilogram |
| p | : p value |
| rpm | : revolutions per minute |

# Chapter 1 Introduction and Literature review

## 1.1. Introduction of cancer

### 1.1.1. General situation

Cancer is a major public health thread worldwide [1, 2]. Lung cancer is the leading cause of cancer death, while breast cancer remains the most popular site among females and prostate cancer is the most popular site among males. There are most cancer cases in Asia among different parts of the world. Figure 1.1 shows the general situation of cancers including mortality, numbers, sites, and prevalence distribution worldwide in 2012[3, 4]. Thus the development of anticancer drugs with high efficacy and low toxicity is still a great challenge.

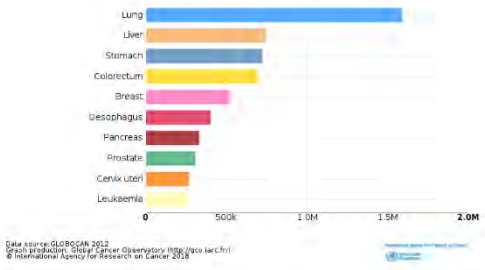


A

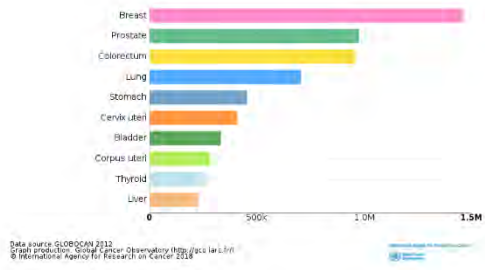


B

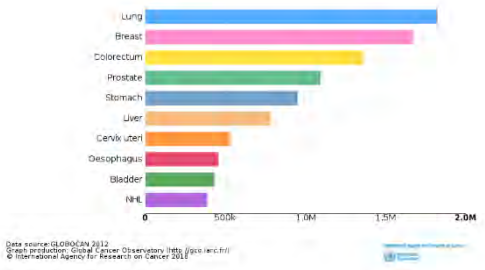


C

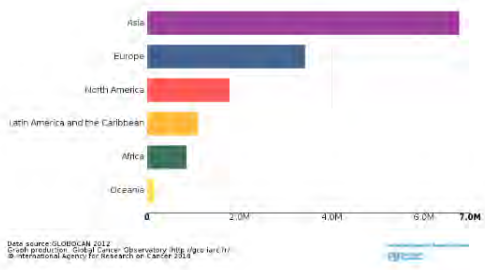


D

**Figure 1.1 General estimated situations of cancers worldwide in 2012. A: Estimated number of deaths of top 10 cancer sites worldwide in 2012; B: Estimated number of prevalent cases of top 10 cancer sites worldwide in 2013; C: Estimated number of incident case of top 10 cancer sites worldwide in 2012; D: Estimated number of incident cases of all cancers worldwide in 2012.**

Cancer cells are completely different from normal cells in different aspects. A series of mutations in oncogenes, tumor suppressor genes, or other functional genes caused by environmental factors or inherited genetics play important role in tumorigenesis[5]. The gene expression, morphology, unregulated proliferation, escaping from programmed cell death, and the ability of invasion to distant tissues let cancer cells form an aggressive tumor population with metastasis[6].

### 1.1.2. Oncogenes

It has been reported that a multistep process of alterations of oncogenes, tumor-suppressor genes or microRNA genes induce cancer formation. Most cancers are initiated by functional defects of tumor suppressor genes and then followed by mutations of oncogenes. Oncogenes encode proteins which control cell proliferation, differentiation, apoptosis or many other functions[7]. When oncogenes are activated by mutation or gene fusion, the defects will be over exhibited by overexpression of their encoded protein products[8]. These protein products can be classified as transcription factors[9], growth factors[10], growth factor receptors[11], chromatin remodelers[12], signal transducers[13] and apoptosis regulators[14]. Along with more and more comprehensive understanding of the tumor initiation behaviors and progression of oncogenic properties, some novel anticancer drugs which target at

ontogenetic products have been developed[15]. Treatment strategies for targeting oncogenes could affect cancer cells exclusively without serious harm for normal cells.

### 1.1.3. Apoptosis

Apoptosis is a programmed cell death process which controls the balance of cells by regulating cell destruction[16]. Lack of apoptosis makes cancer cells escape from death by either over proliferation or decreased removal of cells[17]. Cancer cells can get resistance to apoptosis by overexpression of pro- and anti-apoptotic members of the BCL-2 protein family, or mutation of pro-apoptotic protein Bax, which influenced cytochrome c[18]. Once cytochrome c is released, pro-caspase-p and its downstream pro-caspase-2, and pro-caspase-7 will be activated to induce cell death[19]. Many cytotoxic agents arrest the cell cycle at G1, S or G2/M phase and then induce apoptotic cell to death, thus have been widely used clinically in cancer therapy[19, 20]. For examples, nitrogen mustard can delay G2 phase by affect cyclin A/cdk2 and cyclin B1/ckc2-kinase complexes[21], mitoxantrone can affect proliferation dynamics and cell-cycle progression[22], and ellipticine can arrest cell cycle to cause apoptosis[23].

### 1.1.4. Metastasis

Metastasis is one of the distinguished features of cancer cells and induces as much as 90% of cancer-associated mortality[24]. When metastasis occurs, cancers cells from their primary tumor invade the surrounding normal tissue, enter the blood system, and

adapt at the microenvironment of distant tissues and finally cause death[25]. Combination therapy using anti-metastatic drugs and cytotoxic chemotherapy shows high potential in clinical use. Celecoxib ($COX_2$ inhibitor) and cetuximab (anti-EGFR antibody), which target at two metastatic progression genes respectively, could effectively block lung metastases of highly lung-metastatic breast cancer[26].

### 1.1.5. Epidemiology

#### 1.1.5.1. Esophageal cancer

Esophageal cancer is the 8th most common cancer worldwide and the 6th top cause of cancer death and affected more than 450,000 people with high increasing incidence in the world[27]. Esophageal cancer is mainly classified into squamous cell carcinoma and adenocarcinoma. The incidence of esophageal cancer varies widely by regions. Turkey, Northeastern Iran, Kazakhstan and China comprised of so-called Asian belt with the incidence of 0.1% every year[28]. Tobacco use, alcohol consumption, obesity, caustic injury to the esophagus, and history of head and neck cancer are the most primary risk factors of esophageal cancer[29]. Barium esophagography, esophagogastroduodenoscopy, bronchoscopy, and biopsy are used to diagnose esophageal cancer and its stages[30]. Surgery is applied to treat locally advanced disease[31], while radiotherapy or endoscopic therapy are used to treat advanced disease[32].

#### 1.1.5.2. Lung cancer

Lung cancer is the most common cancer with the highest mortality in the world. It is estimated that there are 1.8 million new confirmed cases and 1.6 million deaths in 2012 in the world[4, 33]. Tobacco and smoking[34], environmental factors including radon, asbestos, pollution and air quality[35], HIV infections[36], and genetically associated with high risks of chromosome regions 5p15, 15q25-26, and 6q21, which all play important roles in lung cancer occurrence and development. Computed tomography or positron emission tomography is applied after initial diagnosis to determining accurate staging of lung cancer[37]. Surgical resection is the main choice for feasible lung cancer, while chemotherapy is adopted for patients with metastasis, and radiation is introduced for stage 3 lung cancer. Meanwhile, angiogenesis, epidermal growth factor receptor inhibitors, and vascular endothelial growth factor inhibitors are applied more frequently in target-based lung cancer therapy[38].

#### 1.1.5.3. Breast cancer

Breast cancer is the most popular cancer and the leading cause of cancer-associated death among females. There were almost 1.4 million cases were diagnosed and about 459,000 deaths of breast cancer worldwide in 2008 worldwide[39]. Increasing age, the age of first pregnancy, family history, radiation, and lifestyle are the main risk factors for breast cancer[40]. Surgery is still the main treatment for breast cancer, instead of total mastectomy, lumpectomy alone or lumpectomy combined with breast irradiation has been recognized as a more appropriate therapy strategy[41].

Comprehensive radiation is a benefit for clinical T3 tumors, stage Ⅲ-Ⅳ disease, or patients with four or more positive nodes[42]. Adjuvant CMF (cyclophosphamide, methotrexate, and fluorouracil) treatment is effective for patients at risk of relapse after operation[43]. With the development of molecular mechanisms of cell growth, differentiation and apoptosis, new selective molecular targeting agents such as trastuzumab, celecoxib, and anti-cyclin dependent kinases show promising prospect against breast cancer[44].

### 1.1.6. Prevention and Diagnosis

Majority of cancer cases are due to environmental risk factors, which affect oncogenes, tumor suppressor genes, or other somatic genes. Cancer is therefore potentially preventable by avoiding risk factors such as tobacco and alcohol consumption, obesity, lack of physical activity, unhealthy dietary, and environmental pollution.[45]. On the other side, cancers caused by hereditary genetic disorders are difficult to prevent. Moreover, vaccination is beneficial for some cancers caused by viruses' infection. For example, by the beginning of 2012, Human papillomavirus (HPV) vaccines have been introduced into at least 40 countries and is expected to reduce the absolute lifetime risk of cervical cancer and other HPV-associated diseases by 94%[46].

Although there is no definite diagnostic method before examination of the tissue sample, early stage or suspected cancers can be predicted, screened or examined by molecular changes. Identification of different expression level of biomarkers

including genes and proteins for cancers at different stages could give suggestions for cancer diagnosis and therapy[47]. Peptide receptors have been successfully used for targeting human cancers. Receptor scintigraphy of radiolabeled peptides can indicate tumor localization and metastases[48]. It is recognized that microRNA plays an important role in maintaining cellular machinery and stability. The circulating miRNAs in the blood of cancer patients could be a novel cancer diagnostic biomarker[49].

### 1.1.7. Signaling Pathway

Oncogenes, tumor-suppressor genes, and other homeostatic genes are usually responsible for tumorigenesis. Multiple mutations of different genes affect cellular pathways that they control, which also contribute to the causes of cancers[50]. The high activity of B-RAF mutations of oncogene B-RAF directly phosphorylate MEK, which is associated with the signal to downstream targeting at ERK, leading to aberrant growth[51]. Activating mutations of RAS genes or alternation in upstream signaling substrates contribute to cell growth and malignant transformation[52]. Multiple components of the phosphatidylinositol-3-kinase (PI3K)/AKT pathway are frequently targeted by amplification, mutation, and translocation in cancer patients. PI3K also crosstalk with the p53 and its downstream regulator AKT to comprise a signaling network to promotes tumor initiation and progression[53]. By increased activity of (PI3K)/AKT or inactivity of TSC proteins, pathways upstream of TOR (target of rapamycin) are frequently upregulated in cancer. TOR regulates the

translation of ribosomal protein by phosphorylating and inactivating eukaryotic initiation factor 4E binding proteins[54]. Alternations of upstream or downstream components which affect p53 pathway occur in many cancers. P53 protein acts as a tumor suppressor protein, and thus the reactivation of p53 pathway therapeutic strategy has been developed to treat cancer[55].

## 1.1.8. Treatment

### 1.1.8.1. General strategies

Currently, the primary treatments of cancers include surgery, chemotherapy, radiation therapy, hormonal therapy, and target therapy. The choice of treatment strategies depends on the types of cancer, tumor size, different stages, metastasis progressions, and patient's individual health conditions. These treatment methods are usually combined to generate cooperation effect[56]. Surgery is the first choice for early-stage patients without metastasis. For some types of cancer at the early stage, removal of entire tumor mass together with involved lymph nodes is sufficient to cure cancer[57]. Radiation therapy could damage the DNA of the tumor together with surrounding normal tissue from multiple angles. Low energy X-rays are usually applied to treat skin cancer, while high energy X-rays are used for cancers within the body. Radiation therapy is usually used and combined with chemotherapy or after surgery[58]. Chemotherapy with one or more cytotoxic anticancer agents is the primary treatment targeting at specific cellular mechanisms in early cancer stage or combined with surgery or radiotherapy[59]. Alkylating agents such as cyclophosphamide,

dacarbazine, and procarbazine, could damage DNA by forming covalent bonds to generate DNA cross-linking[60]. Platinum compounds include cisplatin, carboplatin, and oxaliplatin, which are clinically used in cancer treatment by the formation of covalent bonds of DNA cross-links[61]. Tubulin-binding drugs such as paclitaxel, taxotere, and vincristine could interfere with tubulin function, while tubulin plays a very important role in maintaining cell shape, intracellular transportation, mitosis and meiosis[62]. Topoisomerase inhibitors such as topotecan, irinotecan, and epipodophyllotoxins could stabilize the cleavable complex during the DNA replication and transcription[63]. Tyrosine kinase inhibitors such as imatinib, erlotinib, and lapatinib could target tyrosine kinase domain to inactive the downstream signaling pathways to affect cancer cell functions leading to cancer death[64].

#### 1.1.8.2. Anti-cancer Drug Cisplatin

Cisplatin (cisplatinum, cis-diamminedichloroplatinum (II) or CDDP) is widely used clinically for the treatment of numerous human cancers including bladder, head, and neck, lung, ovarian, and testicular cancers[65]. Figure 1.2 shows the structure of cisplatin. Cisplatin is a DNA-damage agent, which could cross-link with the purine bases of DNA to form both intra- and inter-strand CDDP-DNA adducts to interfere DNA repairing, inducing DNA damage, arresting G1, S, or G2-M stage of the cell cycle and finally resulting in apoptosis of cancer cells[65].

It was also reported that CDDP could induce severe side effects such as renal disorders, allergic reactions, gastrointestinal disorders, and hemorrhage because of its

general cytotoxic damages on normal cells[66]. Additionally, the development of drug resistance is one of the major limits in cisplatin-based treatment. Combination therapies of cisplatin with other anti-cancer drugs such as carboplatin or oxaliplatin are employed to overcome drug-resistance and reduce side effects[67].

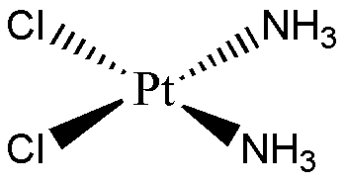


**Figure 1.2 Structure of cisplatin.**

### 1.1.8.3. Anti-cancer Drug Doxorubicin

Doxorubicin is extensively used to treat leukemias, Hodgkin's lymphoma, bladder cancer, breast cancer, stomach cancer, lung cancer and many other cancers[68]. Figure 1.3 shows the structure of doxorubicin. By intercalating with DNA base pairs or binding to DNA−associated enzymes, and targeting multiple molecular receptors, doxorubicin inhibits nucleic acid synthesis and induces apoptosis. At the same time, doxorubicin also induces apoptosis and necrosis in healthy tissues, and causes toxicity in brain, liver, kidney, and heart [69].

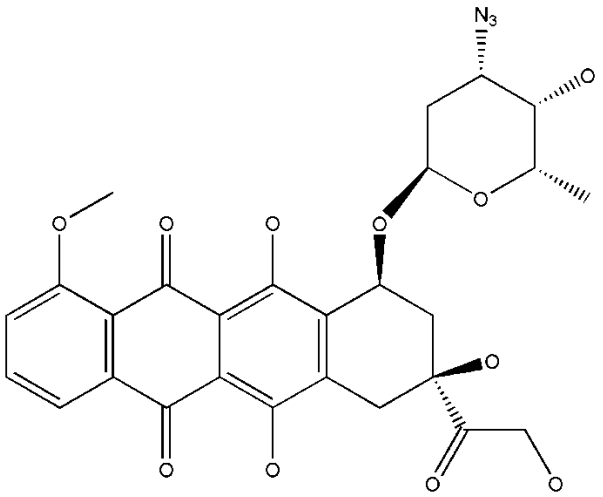


**Figure 1.3 Structure of doxorubicin.**

The development of multidrug resistance in cancer therapy is one of the main causes of treatment failure. The increase of drug efflux which is mediated by P-glycoprotein is one of the most important reasons to induce multidrug resistance. P-glycoprotein could pump out intracellular drugs out of cells, resulting in decreased intracellular drug concentration and therefore causes low therapeutic efficacy[70]. It is well known that doxorubicin is a P-glycoprotein substrate. Thus, the efficacy of doxorubicin is strongly limited by overexpression of P-glycoprotein. As a result, doxorubicin is usually combined with P-glycoprotein inhibitors to reverse doxorubicin-resistance caused by P-glycoprotein to achieve a satisfactory effect in various cancer therapies[71].

## 1.1.9. Roles of lumican in cancers

### 1.1.9.1. Introduction of lumican

Lumican belongs to Class II of small leucine-rich proteoglycan family (SLRPs),

which comprises an important part of the non-collagenous extracellular matrix (ECM) proteins[72]. Lumican expressed in many tissues including skin, artery, lung, in vertebral discs, kidney, bone, aorta, and articular cartilage[73]. Lumican has a molecular weight of about 40 kDa, and consists of four major domains, which are a presumed 18 residues' signal peptide, a N-terminal domain containing four cysteine residues with disulfide bonds and sulfated tyrosine, a central part of tandem leucine-rich repeats characterized by a common molecular architecture adapted for protein-protein interaction, and a C-terminal domain containing two conserved cysteines. Figure 1.4 shows the structural domains of lumican[74].

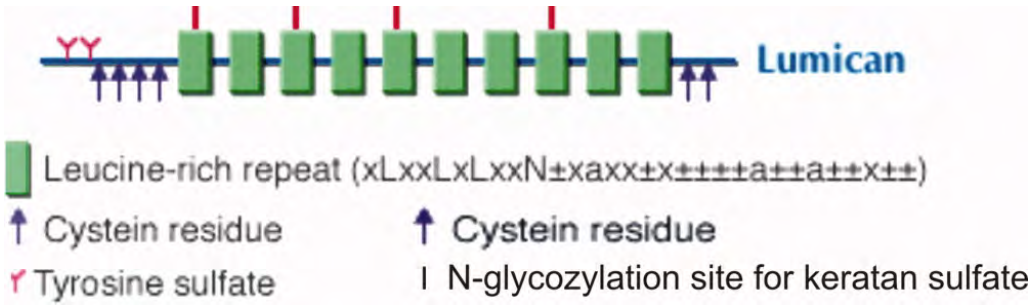


**Figure 1.4 The structural domains of lumican.**

Lumican gene was localized at chromosome 12q21.3-q22 and encodes a 338-residue protein, whose expression varies in different tissues[75]. lumican contains a unique core protein but shows different structures in different tissues or at different ages[76].

### 1.1.9.2. Expression and Function of lumican

Recent studies have shown that lumican is a key regulator of collagen fibrillogenesis, and participates in the maintenance of tissue homeostasis and modulates cellular functions including cell proliferation, migration, and differentiation[77].

During the wound healing process, lumican was found overexpressed in the cornea to promote cell migration and proliferation. Soluble lumican glycoprotein which was purified from human amniotic membrane could promote corneal epithelial wound healing[78]. Overexpression of lumican could induce $\alpha_2\beta_1$ integrin expression via extracellular signal‐regulated kinase (Erk)1/2 signaling to promote migration[79]. lumican was found in keratocytes cells of eye to collagen fibrillogenesis and increases migration[80], in acinar cells and α-cells of pancreas to maintain islet cell function[81], and in epithelial cells and fibroblasts of colon and rectum to increase cell growth[82].

The expression of lumican is reported to be positively correlated with cell growth, adhesion, migration, and metastasis in different kinds of cancers. The different glycosylation patterns of lumican or receptors in cell signaling pathways involve different cancer-cell behaviors[83]. As mentioned before, lumican consists of four main domains, of which the core protein was reported to increase melanoma cell adhesion, while lumican glycosylated protein inhibits melanoma cell migration and invasion[84]. In pancreatic cancer, lumican expresses in fibroblasts, acinar cells, and α‐cells of islets, and is associated with an advanced stage and retroperitoneal and duodenal invasion[81, 85]. In breast cancer, lumicans expressed in fibroblasts, but

reduced lumican protein expression is related to poor outcome of breast cancer[86]. In lung cancer, lumicans expressed in carcinoma cells and stromal tissues and regulates tumor aggressiveness[87]. Table 1. Summarized the different functions of lumican is different kinds of cancers.

**Table 1.1 Lumican expression and functions in different kinds of cancers.**

| Cancer type | Lumican expression | Reported functions |
|---|---|---|
| Pancreatic cancer | Overexpression | Increase cell growth<br>Increase cell adhesion<br>Decrease cell invasion[87] |
| Colon cancer | Overexpression | Decrease cell migration[88] |
| Breast cancer | Overexpression | Decrease cell migration[86] |
| Lung cancer | Overexpression | Increase cell aggressiveness[89] |
| Prostate cancer | Overexpression | Decrease cell migration<br>Decrease cell invasion[85] |
| Malignant melanoma | Overexpression | Decrease tumor growth<br>Decrease tumor metastasis[84] |
| Osteosarcoma | Overexpression | Increase cell migration[88] |
| Gastric cancer | Overexpression | Increase cell migration[90] |

### 1.1.9.3. Mechanism of anti-cancer effect target lumican

The hypothesized mechanisms of lumican's actions in modulating key cellular functions are summarized in Figure 1.4[91]. lumican interacts with integrin $\alpha_2\beta_1$ and $\beta_1$ to active signaling pathways by adhesion kinase (FAK). Adhesion kinase regulates cell motility, invasion, and metastasis by playing an important role of focal adhesion turnover, actin cytoskeleton reorganization, and matrix metalloproteinase (MMP) expression. lumican also inhibits cyclin expression to regulates cell growth by active FAK downstream pathways Erk1/2 and Akt [92]. In bone tumor cell, lumican was found to modulate Smad signaling pathway by interacting with TGF‐β to affect integrin expression, and finally resulted in inhibiting cell adhesion[93]. Lumican was discovered to regulate innate immune response by interacting with CD14 on macrophages to enhance phagocytosis or with toll‐like receptor (TLR) 4 to regulating MyD88 followed by downstream NF-κB[94]. lumican was also reported to interact with Fas‐Fas ligand, which is critical for mediating cell apoptosis and immune-privileged status[95]. Figure 1.5 shows the postulated mechanisms of the action of lumican in modulating cellular functions[91].

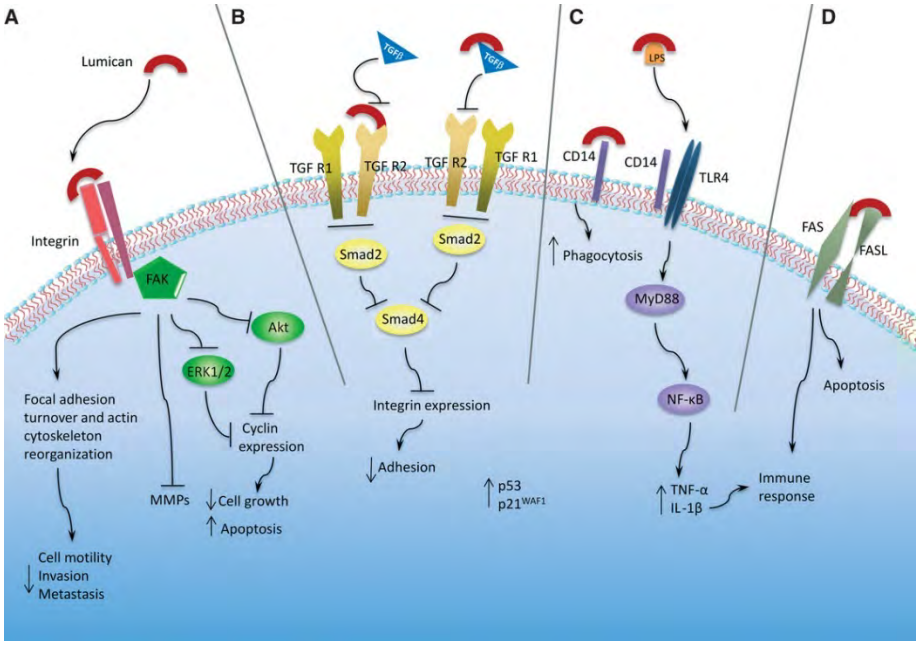


**Figure 1.5 Postulated mechanisms of the action of lumican in modulating key cellular functions[91].**

## 1.2. Introduction of Quinoline compounds

### 1.2.1. Quinoline compounds and their bioactivities

Quinolines are one of the most important classes of heterocyclic alkaloids. Quinoline-bearing structures exist in many biologically active drugs, including Quinine, Quinidine, Mefloquine and Chloroquine (Figure 1.6 shows the examples of structures of quinoline compounds) [96-98].

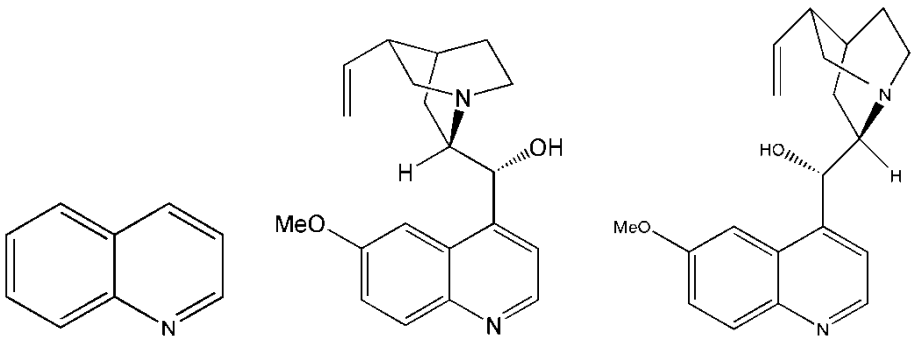


**1** **2** **3**

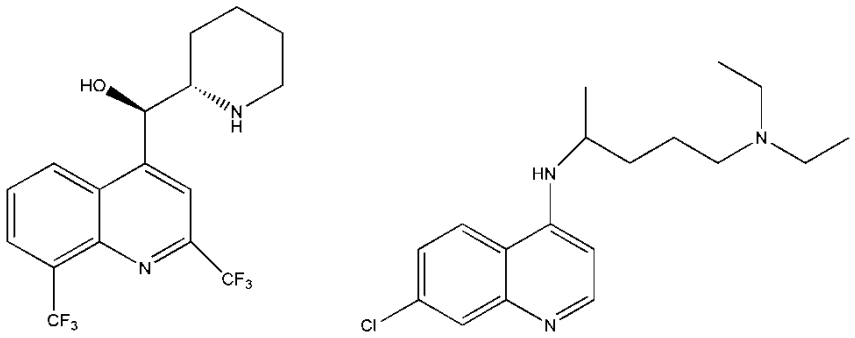


**4** **5**

**Figure 1.6 Structures of quinoline compouds with biological activities. 1: Quinoline, 2: Quinine, 3: Quinidine, 4: Mefloquine, and 5: Chloroquine.[96-98]**

Quinoline derivatives have been widely reported to possess a broad range of pharmaceutical activities and can be isolated from different natural sources [99]. One of the first well-known natural quinoline compounds 4-hydroxy-6-methoxy-quinoline-2-carboxylic acid (Figure1.7) was extracted from *Ephedra pachyclada ssp. Sinaica*[100, 101].

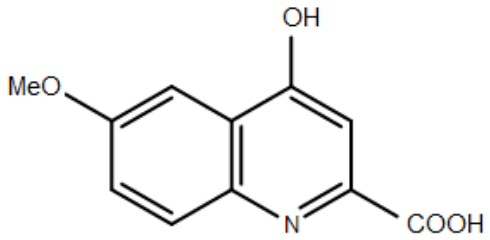


**Figure 1.7 Structure of 4-hydroxy-6-methoxyquinoline-2-carboxylic acid.**

Natural products with quinoline core usually exhibit a broad spectrum of biological activities and therefore provide promising drug candidates for different kinds of

diseases. Quinoline and its heterocyclic derivatives were tested by various groups and were proved to have many biological activities, examples include anti-malarial[102], antibacterial[103], anti-HIV[104], and anticonvulsant[105] agents. Quinolines provide promising drug candidates, and many of them are clinically and commercially available[106].

### 1.2.2. Mechanisms of the anti-cancer effects of quinoline compounds

Quinoline derivatives have been extensively studied as potential antitumor agents. With the development of cytobiology and molecular biology, the essential principles of tumorigenesis, invasion, migration, and metastasis induced by quinoline derivatives have been further explained. Anti-tumor mechanisms of quinoline derivatives include alkylating DNA[107], inhibiting c-Met kinase[108],epidermal growth factor receptor (EGFR)[109], and vascular endothelial growth factor(VEGF)[110]. Some of them were also proven to be the inhibitor of tubulin[111], histone deacetylase, histone acetyltransferase[112], and P-glycoprotein[113].

Anti-cancer activity of quinoline derivates has been widely recognized and investigated. The identification of the precise mechanisms of quinolines is an important step in advancing the field of drug development.

## 1.3. Introduction of P-glycoprotein

### 1.3.1. Multidrug resistance

Cancer continues to be the top threatening disease worldwide, and development of anti-cancer drugs with high efficacy and minimal side effects remains to be a challenge for both academia and pharmaceutical industry[4]. The development of drug resistance during chemotherapy is seriously limited and this decreases the survival of cancer patients[114]. Multidrug resistance (MDR) in cancer cells is a phenomenon manifested as cross-resistance to a variety of structurally and mechanistically unrelated anticancer drugs. MDR renders cancer cells immune to standard treatments and is a major challenge in cancer therapy[115].The development of strategies to overcome MDR in cancer cells is a key challenge for effective targeting the drug delivery system for a successful chemotherapy.

Drug resistance can occur in many ways, such as altering the targets or the metabolism of the drug to make cells become resistant to one or more chemotherapeutic drugs. The drug resistance mechanisms against anticancer drugs are summarized in Table 1.2[116]:

**Table 1.2 Drug resistance mechanisms of anticancer drugs**

| Class | Example | Cytotoxicity mechanism | Molecular in the resistance mechanism |
|---|---|---|---|
| **Intercalators** | Doxorubicin<br>Daunomycin | Topoisomerase II inhibitor, superoxides, and free radicals | P-gp, Topoisomerase II, MRP, GST |
| **Alkylators** | Cyclophosphamide<br>Cisplatin | DNA alkylation<br>DNA alkylation | $O^6$-alkylguanine-DNA alkyltransferase, Glutathione, Aldehyde dehydrogenase |

| | | | |
|---|---|---|---|
| | | | Glutathione, Metallothionein, DNA repair enzyme, multispecific organic anion transporter |
| **Antimetabolites** | BCNU<br>Methotrexate | DNA alkylation<br>Folic acid antagonist | $O^6$-alkylguanine- DNA alkyltransferase<br>Amplification of dihydrofolate reductase, MRP, decreased reduced folate carrier expression |
| **Vinca alkaloids** | 5-Fluorouracil<br>Vinblastine<br>Vincristine | Uracil analog<br>Tubulin Polymerization inhibitor | Amplification of thymidylate synthase<br>P-gp, MRP, Tubulin Mutation |
| **Epidophylotoxins** | Etoposide | Topoisomerase II inhibitor | MRP, Glutathione, P-gp, Topoisomerase I |
| **Taxanes** | Paclitaxel | Microtubule assembly inhibitor | P-gp, altered α/β Tubulin |

There are many potential mechanisms of MDR, such as ABC transporter family, apoptosis, autophagy, cancer stem cell regulation, miRNA regulation, hypoxia, DNA damage and repair, and epigenetic regulation[117].

There are at least 48 members in ABC transporter family, including P-glycoprotein which are encoded by ABCB1 gene, MDR-associated protein1 which are encoded by ABCC1 gene, and breast cancer resistance protein (BCRP) which are encoded by ABCG2 gene. ABC transporters are found overexpressed on the membrane of resistance cells, therefore increased drug efflux, resulting in resistance to chemotherapy treatment[118].

Autophagy is responsible for the maintenance of intracellular homeostasis by delivering cytoplasmic components to lysosomes for bulk degradation. It was found

that apoptosis induction by anticancer drugs caused apoptosis together with autophagy, followed by the cyto-protective effect of degrading of drug molecules caused by autophagy. As a result, cancer cells escaped from apoptosis[119].

Many antitumor drugs have the anti-cancer effects by damaging tumor cell DNA, while DNA repair in cancer cells contribute to drug resistance by excises lethal DNA lesions. Additionally, the disorder of one DNA repair pathway could counteract with another compensatory DNA damage response pathway, which induces multi-drug resistance to DNA-damaging chemotherapy[120].

Epigenetic changes also account for a large part of multi-drug resistance. Up-regulation of the expression of the MDR-linked genes, such as ABC transporters, *Bcl-2* family gene, or bone morphogenetic protein 4 genes inversely correlated with multi-drug resistance[121].

To overcome multi-drug resistance in cancer treatment, many strategies are adopted including combination chemotherapy with anti-tumor drug and P-gp inhibitor, inactivation of the MDR-associated gene by targeting specific mRNA, and development of nanocarrier drug delivery system[122, 123].

### 1.3.2. P-glycoprotein

One of the major mechanisms of MDR in cancer therapy is the overexpression of P-glycoprotein (P-gp). P-gp belongs to the first member of ATP-binding cassette (ABC) superfamily which is encoded by MDR1 gene[124], and is widely expressed in epithelial cells of normal tissues involved in drug disposition including the liver,

intestine and kidney[125].

Multi-drug resistance proteins (MRPs) family has currently been found to have seven members which also confer a broad range of anti-cancer drug resistance to the tumor cells and hence this usually dramatically reduces the effectiveness of clinical drugs to suppress the growth of cancer cells. Some of the mechanisms of MRPs have been elucidated such as alterations of the checkpoints in cell cycle, suppression of apoptosis and reduction of drug accumulation inside of the cells. All MRPs are also the ATP-binding cassette (ABC) efflux transporters which can export the carcinostatic drugs to the outside of the cells[126]. It has been reported that P-gp (also called ABCB1 or MDR1) can actively bind and pump out the drugs against the concentration gradient by hydrolysis of ATP and is an ATP-powered drug efflux pump membrane transporter, therefore the anti-cancer drug cannot accumulate inside the cells to trigger the cytotoxic effects. There are some commonly used anti-cancer drugs which have been shown to be weakened by P-gp including vincristine, etoposide, and doxorubicin[116].

#### 1.3.2.1. Structure and Function of P-glycoprotein

P-glycoprotein is one of the most prevalent mediators of drug efflux based multi-drug resistance in various cancers because of the large and poly-specific drug-binding pocket and the wide distribution in different tissue and organs which localized in the luminal membrane of the endothelial cells[127, 128]. P-gp belongs to ABC superfamily and is encoded by *MDR1* gene in human tissue including liver, kidney,

pancreas, small and large intestine. P-gp is an ATP-powered drug efflux pump membrane transporter, which is a 170-kDa phosphorylated proteins containing more than 1289 amino acids[128, 129]. P-gp is composed of two homologous halves, each of which contains six transmembrane domains and ATP binding or utilization domain. Figure 1.14 shows the structure of P-glycoprotein[130].

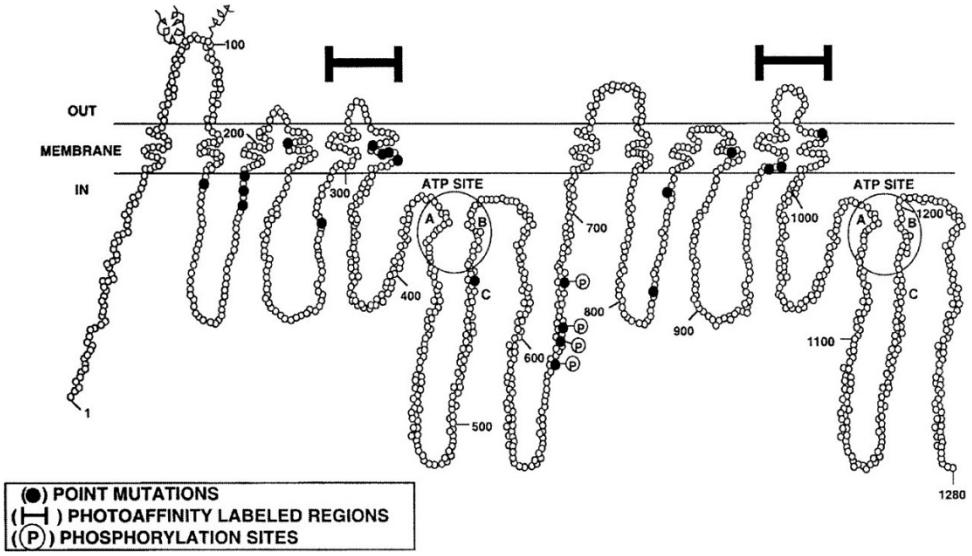


**Figure 1.8 The structure of P-gp[130].**

It is proposed that different binding sites of P-gp interact with different kinds of molecules. The ATP molecule binds with NBD1 and NBD2 for ATP hydrolysis. The two bundles of six transmembrane helices formed a large internal cavity, which binds to the substrate, modulator, and inhibitor. Figure 1.15 shows the 3D structure of P-glycoprotein[131].

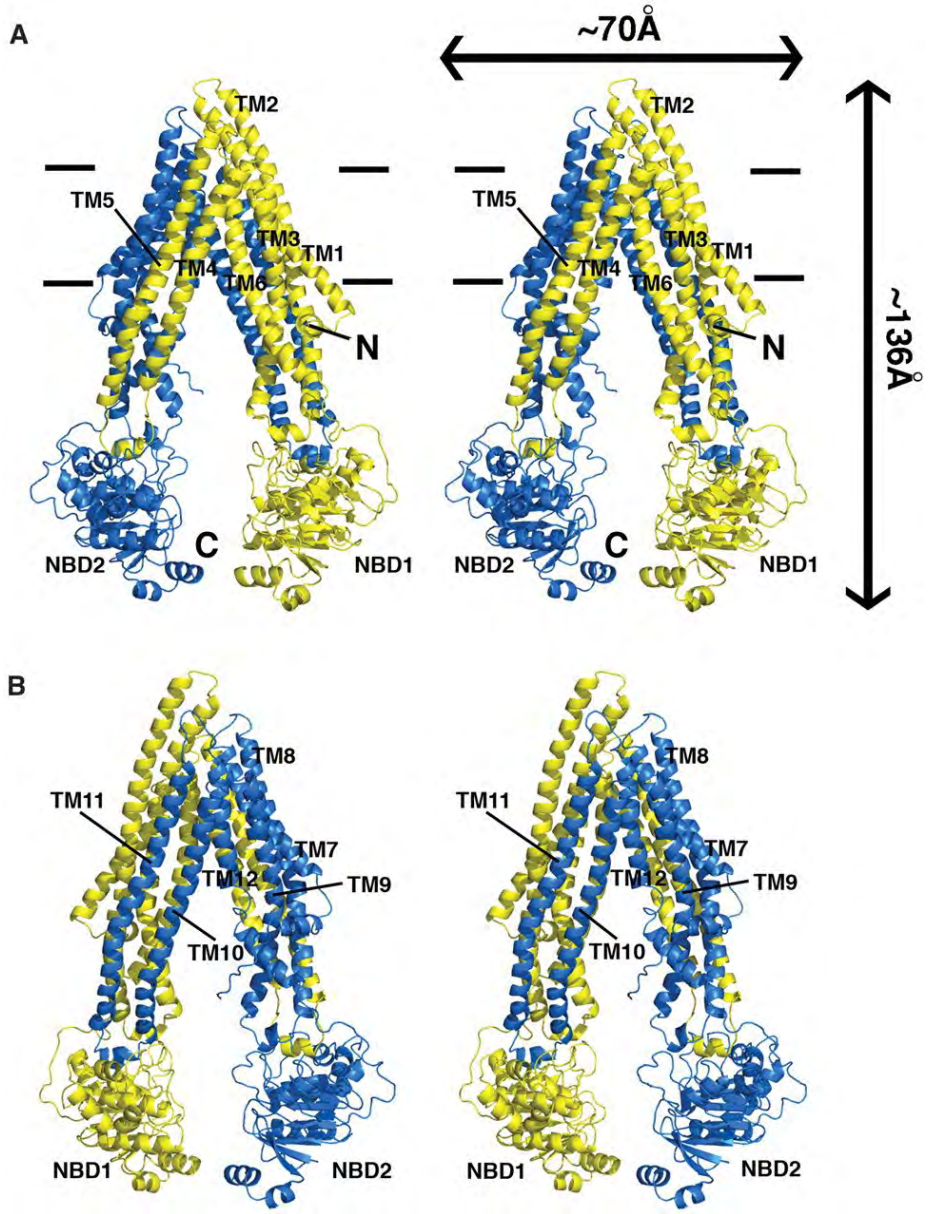


**Figure 1.9 The 3D molecular structure of P-gp. (A) Front view of P-gp; (B) Back view of P-gp; NBDs: the nucleotide-binding domains; TMs: transmembrane helices. The N-terminal is colored yellow, while the C-terminal is colored blue[131].**

P-glycoprotein is widely expressed in nearly all the cancer types including solid tumors and hematological malignancies. The overexpression of P-gp in human cancer cells may due to intrinsic factors or exposure to chemotherapeutic drugs. Many of the P-gp substrates vary greatly in structures or functions[132]. The development of

P-glycoprotein inhibitors has been applied clinically to overcome P-glycoprotein regulated multi-drug resistance.

#### 1.3.2.2. P-glycoprotein inhibitors

First generation P-gp inhibitors including Verapamil, Trifluoperazine, Cyclosporine-A, Quinidine and Reserpine, Vincristine, Yohimbine, Tamoxifen, and Toremifene, which are all competitive substrates of P-glycoprotein. They are not selective hence high dosage is required to reverse multi-drug resistance, resulting in serious side effect. Low affinity, high toxicity, and unpredictable pharmacokinetic behaviors of these first-generation P-gp inhibitors limited their clinical use. More and more novel P-glycoprotein inhibitors were developed to replace the old ones for reversing multi-drug resistance[133].

Second generation P-gp inhibitors including Dexverapamil, Dexniguldipine, Valspodar (PSC 833), and Biricodar citrate (VX-710), which are structurally modified based on first generation P-gp inhibitors for reducing toxicity and having better tolerability. Combination of second generation P-gp inhibitors and chemotherapy drugs successfully increased therapy efficacy and reversed multi-drug resistance in cancer treatment[134].

Third-generation inhibitors including Tariquidar-XR9576, Zosuquidar-LY335979, Laniquidar-R101933, and ONT-093, which have high potency and specificity for P-gp compared to second generation of P-gp inhibitors. The third-generation inhibitors do not interfere with cytochrome P450 3A4 enzyme, which plays important role in drug

metabolism, therefore they do not change drug plasma concentrations or pharmacokinetic behaviors. They have shown promised potential in cancer therapy to reverse P-gp mediated multi-drug resistance. [135].

Recently, quinoline derivatives are founded to be capable of reversing MDR phenotype in P-gp overexpressing tumor cells. It has been showed that the chloroquine resistance of Plasmodium falciparum malaria parasites shares many similarities to MDR in tumor cells[136].

Jing Qi found that pyronaridine (structure of pyronaridine is showed in Figure 1.10) was capable of reversing MDR phenotype in P-gp overexpressing tumor cells, and the MDR-modulating effect of pyronaridine persisted for longer than 24h after removal of the agent from the culture medium. In nude mice bearing K562/A02 xenografts, pyronaridine also showed significant enhancement on the effect of antitumor drug doxorubicin but without increasing its toxicity[137].

**(A)**

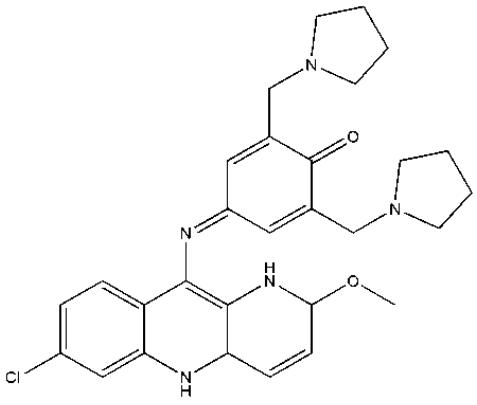

**(B)**

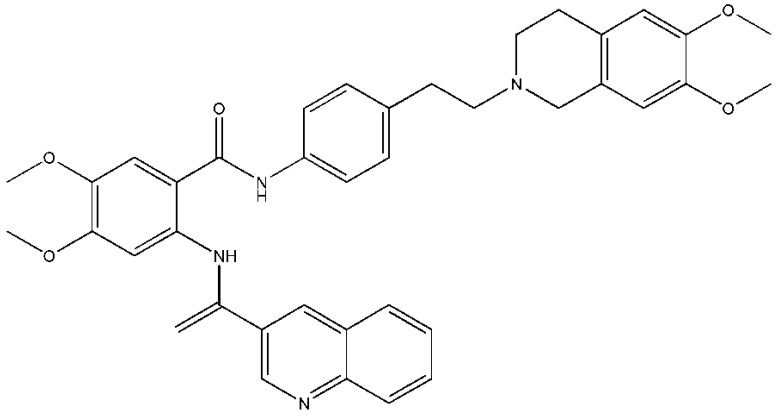


**Figure 1.10 Quinolone-based P-glycoprotein inhibitors. A: structure of pyronaridine; B：structure of XR9576.**

Roe synthesized and evaluated the *in vitro* and *in vivo* modulatory activities of compound XR9576 (structure of XR9576 is showed in Figure 1.10). It was found that compound XR9576 could potentiate the cytotoxicity of several anticancer drugs including doxorubicin, paclitaxel, etoposide, and vincristine *in vitro*. Meanwhile, in animal models, compound XR9576 could also potentiate the anti-tumor activities of doxorubicin, paclitaxel, etoposide, and vincristine without increasing its toxicity when they are co-administrated[138].

Therefore, many P-gp inhibitors have been developed to reduce the chemo-resistance of cancers through reversing their multi-drug resistance, so that the commonly used front-line anti-cancer agents will show better efficacy against cancers with MDR phenotype. In this study, based on the former experience in organic synthesis and drug-development studies, a series of novel quinoline derivatives were prepared to analysis their anticancer activity and MDR reversal effect.

# Chapter 2 Aims and Objectives

To address the proposed study on the novel quinoline compound 91b1 for its anti-cancer effects, the roles of lumican in cancer cells and the novel quinoline compounds 160a for reversing the MDR phenotype, the following study aims and objectives have been defined:

## Aim #1: To evaluate the anti-cancer effect of compound 91b1

## Objectives:

1.1 To determine the dose-dependent cytotoxic effects of the compound 91b1on cancer cells;

1.2 To identify the changes in gene expression profile which is induced by the compound 91b1;

1.3To study the effect of the compound 91b1 on cancer cell proliferation, invasion, cell-cycle changes

1.4 To evaluate the anti-cancer activity of the compound 91b1 on animal model;

1.5 To assess the toxicity of compound 91b1 using animal model;

1.6 To establish a reliable method of analysis to measure the compound 91b1 qualitatively and quantitatively by UPLC/MS;

1.7 To identify the most associated signaling pathways with compound 91b1.

## Aim #2: To study the roles of lumican in cancer cells.

## Objectives:

2.1 To identify the lumican expression level in cancer cells and patients' tumor samples;

2.2To validate the dose-depend suppression effect of lumican expression level caused by the compound 91b1 in cancer cells;

2.3To study the effect of lumican on cancer cell proliferation, invasion and migration;

2.4To investigate the effect of lumican in tumorigenesis on animal model;

2.5To correlate the down-regulating effect of compound 91b1 on lumican expression and the role of lumican in cancer-cell progression; the mechanisms of the compound 91b1-inducedanti-cancer effects will also be studied.

## Aim #3: To study the modulation effect of the compound 160a on P-glycoprotein induced MDR

## Objectives:

3.1 To identify the possible target of the compound 160a in human cells;

3.2To determine the synergistic effect of the compound 160a when combined with doxorubicin in cancer cells in terms of cytotoxicity and proliferation;

3.3To confirm the inhibitory effect of the compound 160a on drug-efflux function of P-glycoprotein in cancer cells;

3.4To evaluate the duration of reversing MDR using the compound 160a as a P-glycoprotein modulator.

The completion of the above study will provide the first time the useful information about its anti-cancer actions of 91b1 and 160a for the future drug development. Moreover, the study on the roles of lumican, which is downregulated by 91b1 treatment, will also open a new path for the future detailed study about the roles of lumican in other cancers.

# Chapter 3 Materials and Methods

## 3.1. Cell lines and cell culture

### 3.1.1. Parental cell lines

A total of 11 cell lines were examined in this project. Three esophageal squamous cell carcinoma (ESCC) cell lines KYSE70, KYSE150，and KYSE450[139] were purchase from DSMZ (Deutsche Sammlung van Mikroorganismen und Zellkulturen, Braunschweig, Germany). A metastatic breast cancer cell line MCF-7, a lung cancer cell line A549, and a gastric adenocarcinoma cell line AGS was purchased from ATCC (American Type Culture Collection, Manassas, USA).A non-tumor esophageal epithelial cell lines NE-3[140] was kindly provided by Professor George S.W. Tsao from the Department of Anatomy of The University of Hong Kong. A human breast cancer cell line LCC6[141] was kindly provided by Prof. Larry Chow from the Department of Applied Biology and Chemical Technology, The Hong Kong Polytechnic University. Mouse embryo embryonic fibroblast cell line NIH 3T3 was purchased from ATCC and it was used for DNA transfection studies

KYSE70 cells were cultured in 90% RPMI-1640 medium (Gibco, USA) and supplemented with 10% heat-inactivated fetal bovine serum (Biosera, France) and 100 units/ml penicillin (Gibco, USA). KYSE150 cells and KYSE450 cells were cultured in 45% RPMI-1640(Gibco, USA) and 45% F12 medium and supplemented (Gibco, USA) with 10% heat-inactivated fetal bovine serum (Biosera, France) and 100 units/ml penicillin (Gibco, USA). MCF-7, A549, AGS, and LCC6 cell lines were

cultured in Dulbecco's Modified Eagle Medium (Gibco, USA) and supplemented with 10% heat-inactivated fetal bovine serum (Gibco, USA) and 100 units/ml penicillin (Gibco, USA). NE-3 were cultured in KSFM Medium and supplemented EGF Human Recombinant (Gibco, USA), Bovine Pituitary Extract and 100 units/ml penicillin (Gibco, USA). NIH 3T3 cells were cultured in Dulbecco's Modified Eagle Medium (Gibco, USA) and supplemented with 10% heat-inactivated fetal bovine serum (Biosera, France) and 100 units/ml penicillin (Gibco, USA). Cultures were maintained in a humidified atmosphere of 95% air and 5% $CO_2$ at 37°C. The cultures were passaged at pre-confluent densities of about 80% using a solution of 0.25% trypsin (Invitrogen, USA). Cells were washed briefly with phosphate- buffered saline (PBS), treated with 0.25% trypsin, and harvested by centrifugation for sub-culturing.

### 3.1.2. Drug-resistance cell lines

LCC6/MDR cell lines (LCC6 cell line with multi-drug resistance)[141] and MX100 cell lines (MCF-7 cell line with Doxorubicin-resistance) were kindly provided by Dr. Larry Chow from the Department of Applied Biology and Chemical Technological of The Hong Kong Polytechnic University.

LCC6/MDR and MX100 cell lines were cultured in Dulbecco's Modified Eagle Medium (Gibco, USA) and supplemented with 10% heat-inactivated fetal bovine serum (Biosera, France) and 100 units/ml penicillin (Gibco, USA). Cultures were maintained in a humidified atmosphere of 95% air and 5% $CO_2$ at 37°C. The cultures were passaged at pre-confluent densities of about 80% using a solution of 0.25%

trypsin (Invitrogen, USA). Cells were washed briefly with phosphate- buffered saline (PBS), treated with 0.25% trypsin, and harvested by centrifugation for sub-culturing.

Three doxorubicin-resistant cell line, DOX-KYSE70, DOX-A549, and DOX-AGS were established from parental cell lines (KYSE70, A549, and AGS cell lines) by culturing in an increasing concentration of doxorubicin (Sigma-Aldrich, USA). The starting concentration of doxorubicin used was 0.1 μg/mL. Survived cells were repeatedly sub-cultured in medium containing an increasing concentration of doxorubicin from 0.1 μg/mL, 0.2 μg/mL,0.5 μg/mL, 0.75 μg/mL to final 1.00 μg/mL. DOX-KYSE70 cells were cultured in 90% RPMI medium and supplemented with 10% heat-inactivated fetal bovine serum and 100 units/ml penicillin with 1.00 μg/mL of doxorubicin. DOX-A549 and DOX-AGS cell lines were cultured in 90% DMEM medium and supplemented with 10% heat-inactivated fetal bovine serum and 100 units/ml penicillin with 1.00 μg/mL of doxorubicin. Cultures were maintained in a humidified atmosphere of 95% air and 5% $CO_2$ at 37°C. The cultures were passaged at pre-confluent densities of about 80% using a solution of 0.25% trypsin. Cells were washed briefly with phosphate- buffered saline (PBS), treated with 0.25% trypsin, and harvested by centrifugation for sub-culturing.

### 3.1.3. Transfected cell lines

For the study of lumican, NIH-3T3/Lum and NIH-3T3/Mock cells were established from Mouse embryo embryonic fibroblast cell line NIH 3T3 cells which were transfected with lumican expression vector (Human LUM ORF mammalian

expression plasmid, C-Myc tag, Sino Bioglogical Inc) or mock vector (pCMV/hygro-Negative Control Vector, Myc-tagged, Sino Biological Inc) as negative control. The detailed procedures for the establishment of these two cell lines were described in Section 3.11. NIH-3T3/Lum and NIH-3T3/Mock cells were maintained in DMEM medium supplemented with 10% FBS, 100 μg/mL penicillin and 400 μg/mL hygromycin (Invitrogen, USA) at 37℃ in a humidified incubator with 5% $CO_2$. Trypsinization was performed as previously described in section 3.1 when the density of cells reached 80% confluence.

## 3.2. Animals and animal raise

### 3.2.1. Sprague-Dawley rats

Male Sprague-Dawley rats, each weighted 180g, were purchased from Guangzhou Medicinal Experiment Animal Center. The animal approval code was 44007200003486 and the certificate number was SCXK (Guangdong) 2008-0002.

The animals were kept in the SPF-grade animal laboratory which was conformed to the SPF grade requirement of animal testing facility, where temperature was within the range of 22°C (± 2°C), the humidity was within the range of 30~70 %, the diurnal lighting and darkness cycle was 12 hours and the number of air change per hour was within the range of 10-20 times. The approval no. of the SPF animal laboratory was SYXK (Guangdong) 2005-0062. The rat chow was the SPF-grade full pellet for rats, which was bought from Guangdong Medicinal Laboratory Animal Center. The nutritional values and the sanitation condition were conformed to the SPF-grade

requirement for animal testing. Antiseptic water was given *ad libitum*.

### 3.2.2. NIH mice

Male NIH mice, each weighted 18g, were purchased from Guangzhou Medicinal Experiment Animal Center. The animal approval code was 44007200006623 and the certificate number was SCXK (Guangdong) 2013-0002.

The animals were kept in the SPF-grade animal laboratory which was conformed to the SPF grade requirement of animal testing facility, where temperature was within the range of 22℃ (± 2℃), the humidity was within the range of 30~70 %, the diurnal lighting and darkness cycle was 12 hours and the number of air change per hour was within the range of 10-20 times. The approval no. of the SPF animal laboratory was SYXK (Guangdong) 2005-0062. The mice chow was the SPF-grade full pellet for mouse, which was bought from Guangdong Medicinal Laboratory Animal Center. The nutritional values and the sanitation condition were conformed to the SPF-grade requirement for animal testing. Antiseptic water was given *ad libitum*.

### 3.2.3. Balb/c nude mice

Female Balb/c-nu mice, each weighted 18g, were purchased from Beijing Charles River Laboratories. The animal approval code was 440072000011798and the certificate number was SCXK（Beijing）2012-0001.

The animals were kept in the SPF-grade animal laboratory which was conformed to the SPF grade requirement of animal testing facility, where temperature was within

the range of 22°C (± 2°C), the humidity was within the range of 30~70 %, the diurnal lighting and darkness cycle was 12 hours and the number of air change per hour was within the range of 10-20 times. Individual Ventilated Cages (IVC) system was applied to culture nude athymic mice. The approval no. of the SPF animal laboratory was SYXK (Guangdong) 2005-0062. The mice chow was the SPF-grade full pellet for mouse, which was bought from Guangdong Medicinal Laboratory Animal Center. The nutritional values and the sanitation condition were conformed to the SPF-grade requirement for animal testing. Antiseptic water was given *ad libitum*.

All animals were quarantined for at least 7 days in a germ-free environment with a 12-hour diurnal lighting and darkness cycle to confirm they were in healthy condition for experiments. All animal experiments in this project were conducted following the Cap 340 Animal License from Department of Health (HKSAR Government) and ethical approval from Animal Ethics Subcommittee of the Hong Kong Polytechnic University.

## 3.3. Patient specimens

Twenty archival esophageal squamous cell carcinoma (ESCC) paired patient specimens (non-tumor and tumor) were used for the study of lumican expression. The ESCC tumor specimens were collected from the Department of Surgery, Queen Mary Hospital, Hong Kong, during 1990-2001 after ESCC patients had undergone esophagectomy. Their corresponding non-tumor epithelial tissue specimens were collected for comparison and located at least 10cm away from the tumor.

## 3.4. Quinoline Compounds used in this study

More and more quinolines have been designed and synthesized along with the mechanisms being researched and explained. 8-Hydroxyquinoline and its derivatives were also reported to have phytotoxic activities [142], antibacterial, and antifungal activities[31]. Our previous findings also revealed that the 8-hydroxyquinoline derivatives showed relatively promising *in vitro* and *in vivo* anti-cancer effects [99, 143], anti-bacterial effects, and anti-inflammation effects implying the importance of the 8-hydroxyl group for their biological actions[144]. A series of novel 2-substituted 8-hydroxyl quinoline derivatives were synthesized by our research group. Compounds studied in this project were selected according to the structural-activity study conducted by the previous PhD study of Dr. Penny Chan Sau-hing from our research group. The bioactivities of the core structures of the 8-hydroxyquinoline derivatives were also reported by our group before [99, 145, 146].

### 3.4.1. Compound 91b1

The chiral5,7-dibromo-2-methyl-1,2,3,4-tetrahydroquinolin-8-ol (R/S **91b**) was prepared by asymmetric hydrogenation reaction of 5,7-dibromo-2-methylquinolin-8-ol. 5,7-dibromo-2-methylquinolin-8-ol was synthesized by commercially available 2-methyl-8-quinolinol (1.6 g, 10 mmol), which was dissolved in 150 mL MeOH with drop-wise added $Br_2$(1 mL). The molarity weight of 91b1 is 318.9207 g/mol. Compound 91b1 is very soluble in dimethyl sulfoxide (DMSO), methanol, and acetonitrile, but very slightly soluble in water. Dr.

Penny Chan from our research group has demonstrated that both anti-tumor effect of compound (R/S) 91b showed promising MTS50 compared with CDDP, but R emantiomer of 91b (91b1) exhibited better anti-tumor activities than S emantiomer of 91b (91b2) on most of tested cancer lines (Hep3B, HKESC-1, HKESC-4, and KYSE150 cell lines). According to Dr.. Penny Chan's work, it is inferred that the chemical structure of 91b1 was more favourable approaching to cancer cell membrane and kill the cancer cells more effectively than 91b2. Thus, compound 91b1 was further studied in this project. Compound 91b1 was used in this project to examine the *in vitro and in vivo* anti-cancer effects and its mechanisms. The structure of compound 91b1 was examined by $^{1}$H-NMR and UPLC/MS-MS (Ultra Performance Liquid Chromatography/ Mass-Mass Spectrometry). Figure 3.1 shows the structure of compound 91b1. Figure 3.2 shows the $^{1}$H-NMR Spectrum of compound 91b1.

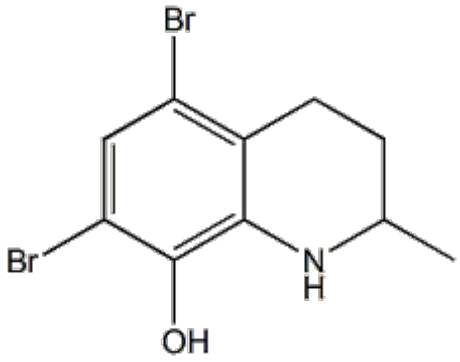


**Figure 3.1 Structure of compound 91b1.**

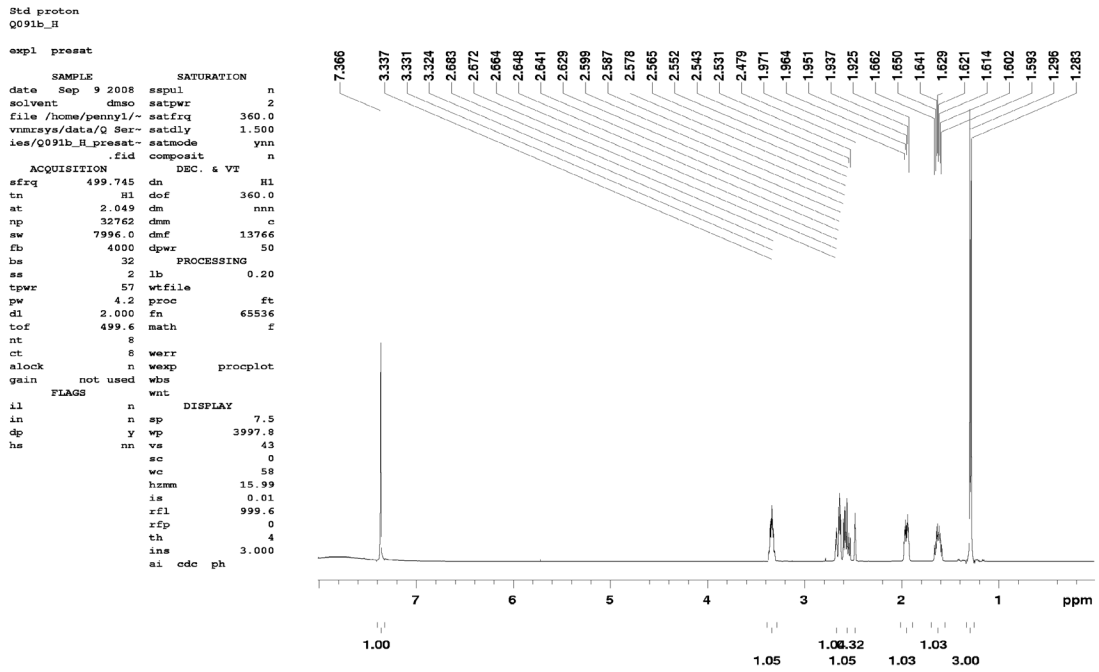


**Figure 3.2 $^{1}$H-NMR Spectrum of 91b1.**

In this project, the attempt was further made to investigate the novel quinoline derivative 91b1, and to examine its *in vitro* and *in vivo* anti-cancer effects and investigate the changes in gene expression and pathways affected by the compound 91b1 after treatment.

## 3.4.2. Compound 160a

160a (8-(3-methoxybenzyloxy) quinoline-2-carbaldehyde was synthesized by oxidation of 8-(3-methoxybenzyloxy)-2-methylquinoline by Dr. Penny Chan Sau-hing from our research group. The structure of 160a has been confirmed by NMR test. Compound 160a was completely dissolved in dimethyl sulfoxide (DMSO).

A novel 8-substituted 2-carbaldehyde quinoline derivative(8-(3-methoxybenzyloxy) quinoline-2-carbaldehyde (160a) was prepared by oxidation of 8-(3-methoxybenzyloxy)-2-methylquinoline with addition of selenium dioxide,

pre-dried 1,4-dioxane and water in reflux for 24 hours. 8-(3-Methoxybenzyloxy)-2-methylquinoline was synthesized by nucleophilic substitution of commercially available 2-methyl-8-quinolinol with 3-methoxybenzyl bromide in DMF at room temperature. The molarity weight of 160a is 293.1052 g/mol. Compound 91b1 is very soluble in dimethyl sulfoxide (DMSO), methanol, and acetonitrile, but very slightly soluble in water. Compound 160a was used in this project to examine its *in vitro* reverse multi-drug resistance effect and its mechanisms on cancer cells. The structure of compound 83b1 was examined by $^{1}$H-NMR and UPLC/MS-MS (Ultra Performance Liquid Chromatography/ Mass-Mass Spectrometry). Figure 3.3 shows the structure of compound 160a, and Figure 3.4 shows the $^{1}$H-NMR Spectrum of compound 160a.

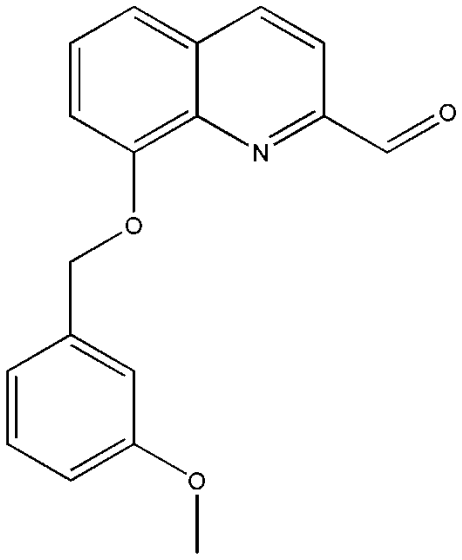


**Figure 3.3 Structure of compound 160a.**

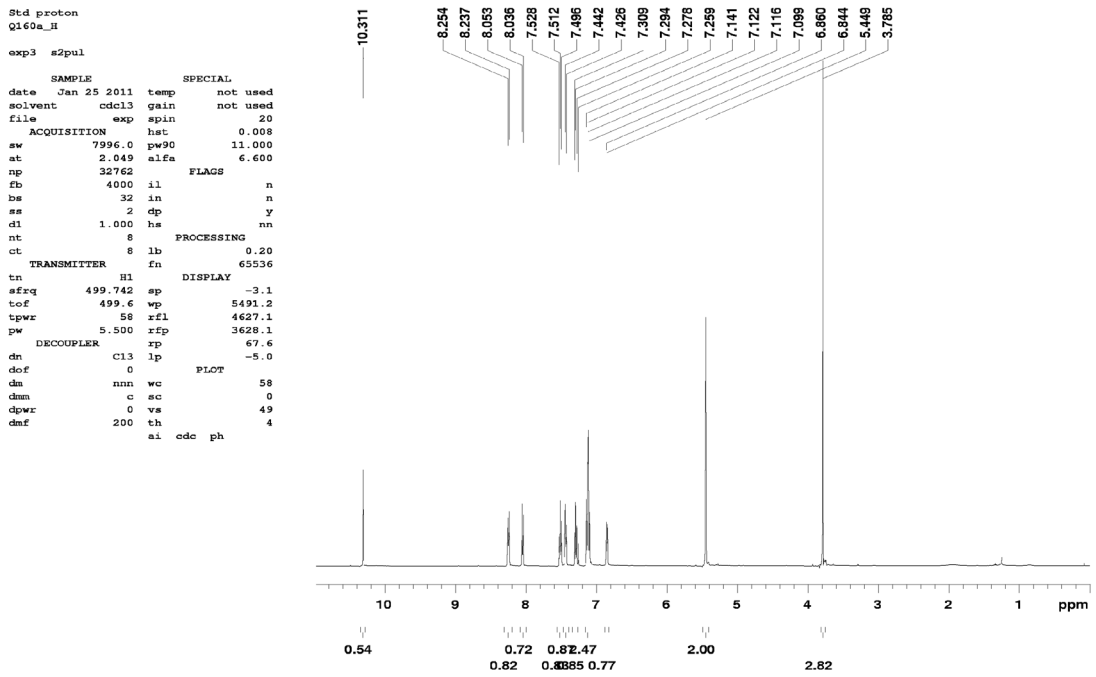


**Figure 3.4 $^{1}$H-NMR spectrum of compound 160a.**

## 3.4.3. Compound 83b1

8-(4-(trifluoromethyl)benzyloxy)-1,2,3,4-tetrahydro-2-methylquinoline (**83b1**) was prepared by our previously reported method[147]of asymmetric hydrogenation of 8-(4-(trifluoromethyl)benzyloxy)-2- methylquinoline (83b) under the conditions of 0.15 mmol of 83b, $[Ir(COD)Cl]_2$ (0.0015 mmol), P-Phos ligand (0.0032 mmol), and $I_2$ (0.015 mmol) in 1.5 ml tetrahydrofuran (THF) as solvent at room temperature and 700 psi $H_2$ for 20 hours. Compound 83b was obtained via nucleophilic substitution of commercially available 2-methyl-8-quinolinol with 4-trifluoromethylbenzyl bromide in DMF at room temperature. The structure of compound 83b1 was examined by $^{1}$H-NMR and liquid UPLC/MS-MS (Ultra Performance Liquid Chromatography/ Mass-Mass Spectrometry) [148]. Figure 3.5 shows the structure of compound 83b1,

and Figure 3.6 shows the $^{1}$H-NMR Spectrum of compound 83b1.

The former reported work for the PhD study of Mr. Pun Ho Yuen from our research group evaluated the *in vitro* and *in vivo* cytotoxicity of compound 83b1 on human esophageal cancer cells and showed that compound 83b1 played anti-cancer effects associated with onco-target PPARδ to down-regulate cancer-related genes and molecules[149].

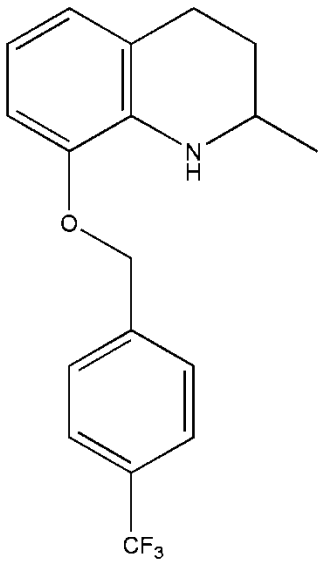


**Figure 3.5 Structure of compound 83b1.**

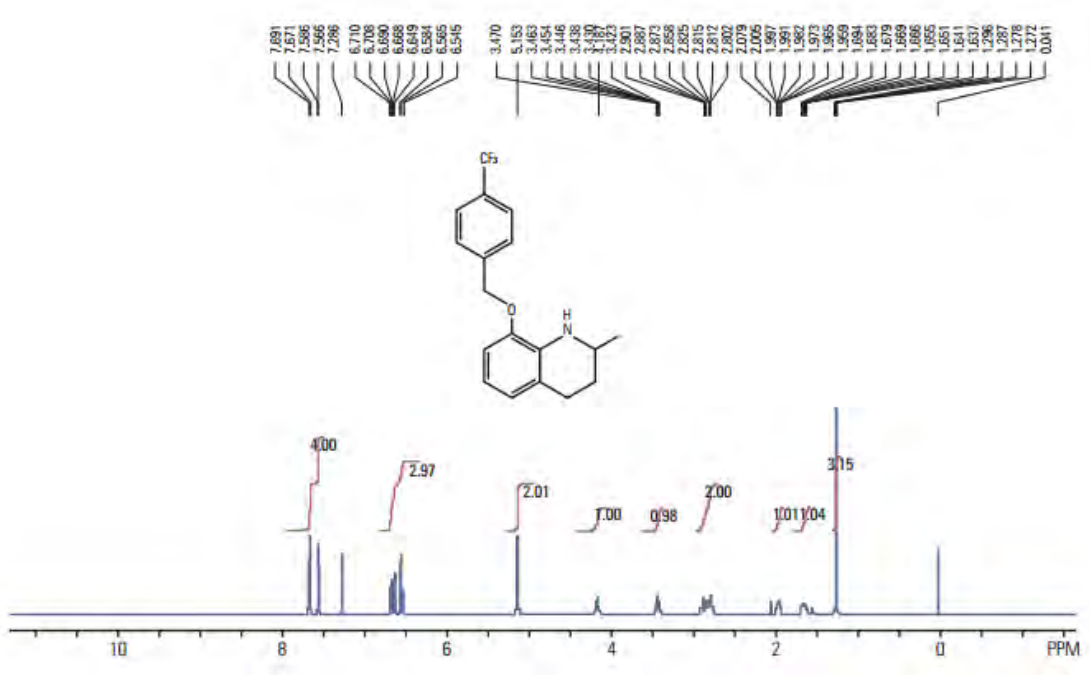


**Figure 3.6 $^{1}$H-NMR spectrum of compound 83b1.**

## 3.5. Cytotoxicity Assay by MTS

3-(4,5-Dimethylthiazol-2-yl)-5-(3-carboxymethoxyphenyl)-2-(4-sulfophenyl)-2H-tetr azolium (MTS) assay was performed to evaluate the cytotoxic effect of quinoline compounds 91b, 160a, 83b, and positive control (widely used first-line anti-tumor drugs: doxorubicin or cisplatin) on selected cell lines (cancer cell lines and immortalized non-tumor cell lines) by using CellTiter96 AQueous One Solution Cell Proliferation (Promega, Madison, WI) following the manual instructions.

Briefly, the cells under test were harvested by trypsinization as described in section 3.1 and total cell numbers were counted by a Neubauer Chamber Cell Counting (Celeromics, France) under a microscope (Olympus CKX41, Japan). About $5\times10^{3}$ cells were seeded into each well of a flat-bottom 96-well cell culture plate in 100µl

recommended culture medium and were allowed to grow for 24 hours at 37$^{o}$C with 5% $CO_2$ to settle down. After 24-hour incubation, old culture medium was replaced by fresh medium, and the concentrations were gradually increased for 91b1, 160a, cisplatin (CDDP) or doxorubicin (DOX)and were added to treat the cells (n= 4). For 91b1, 160a, and CDDP, the concentrations of treatment were increased from 0μg/mL to 50 μg/mL (0, 1.562, 3.125, 6.250, 12.500, 25.000, and 50.000 μg/mL), while for DOX, the concentrations were increased from 0μg/ml to 5 μg/ml (0, 0.156, 0.312, 0.625, 1.250, 2.500, and 5.000 μg/ml), and 0.1% DMSO were added in medium as vehicle control. The seeded 96-well plates were then incubated for 48 hours at 37$^{o}$C with 5% $CO_2$. After incubation, the supernatant including old medium and dead cells were removed totally without disrupting the attached cells, and then 100 μl of diluted MTS solution (MTS/PBS (v/v) = 1:4) was added into each well. The plates were then incubated at 37$^{o}$C with 5% $CO_2$ in dark for a period (45 mins, 1 hour, or 2 hours depending on different kinds of cell lines) before reading the results. The absorbance at 492 nm was measured by a micro-plate reader (Bio-RAD, Ultrmark, Microplate Imaging System, USA) to determine the cell viability. The background was normalized by blank wells which were treated with the same conditions but without adding any cells or medium. The control value corresponding to untreated cells was taken as 100% and the viability of treated samples was expressed as a percentage of the control. Finally, the curves of cells viability against compound concentrations were plotted and the $MTS_{50}$(concentration of tested compounds that have 50% inhibition on MTS activity) value of the tested compound was determined.

## 3.6. Proliferation Assay by MTS

3-(4,5-Dimethylthiazol-2-yl)-5-(3-carboxymethoxyphenyl)-2-(4-sulfophenyl)-2H-tetr azolium (MTS) assay was performed to analyze the effect of cell proliferation of adding the compounds 91b1, 160a, doxorubicin, and human lumican protein. The tumor cell lines A549, AGS, KYSE150, and KYSE450 cells were tested with the compound 91b1 or the human lumican protein for the cell proliferating effect. A549/A549-DOX, KYSE150/KYSE150-DOX, MCF-7/MX100, and LCC6/LCC6 MDR cell lines were applied to assess the MDR-reversal effect with the treatment of compound 160a. A549-DOX and MX100 cell lines were used to evaluate the duration of MDR-reversal effect of compound 160a.

The tested cells were harvested by trypsinization as described in Section 3.1 and the cell number was counted by hemocytometer under a microscope. Approximately 5,000 cells were plated in a flat-bottom 96-well plate in 100 μL of respective culture medium in each well. After incubation at 37ºC with 5% $CO_2$overnight, culture medium was replaced by 200 μl of 10 μg/mL compound 91b1, 10 μg/mL compound 160a, 0.15 μg/mL doxorubicin, 0.05 μg/mL doxorubicin, or 250 ng/ml lumican of proper culture medium as a test group, and 0.1% DMSO culture medium as vehicle control group. MTS reagent was used for the quantification of cell viability to indicate cell proliferation. MTS working solution was prepared by diluting five times with autoclaved PBS before use (MTS/PBS (v/v) = 1:4). 100 μL of the MTS working solution was added to each well after removal of culture medium at 0 h, 6 h, 24 h, 48 h, and 72 h respectively without disturbing the attached cells, and then incubated at

37 ℃with 5% $CO_2$for a period of time depending on the cell types. The cell viability was then determined by measuring the absorbance of the well at 492 nm using microplate reader (Bio-RAD, Ultrmark, Microplate Imaging System, USA). Relative growth (compared with the cell viability at 0 hours) of each cell line was calculated by $\frac{[A]_T}{[A]_{T0}}$. Where $[A]_T$ is the absorbance at different time points and $[A]_{T0}$ is the absorbance at 0 hour. This assay was performed in triplicate.

## 3.7. Duration of MDR Reversal

To evaluate the duration of action of compound 160a as a modulator, approximately 5,000 tested DOX-resistance cells (A549/DOX and MX100) were plated in a flat-bottom 96-well plate in 100μL of respective culture medium in each well. After the cells were settled down, the old culture medium was replaced by fresh medium with 10 μg/ml quinoline compound 160a and the cells were incubated at 37ºC with 5% $CO_2$ overnight. Then the cells were washed with fresh culture medium to remove compound 160a and were incubated in fresh culture medium for 0, 0.5, 1, 2 hours before the addition of doxorubicin (0.15 μg/mL for A549/DOX cells, 0.05 μg/mL for MX100 cells). MTS working solution (MTS/PBS (v/v) = 1:4) was prepared by diluting five times with autoclaved PBS before use. 100μL of the MTS working solution was added to each well after removal of culture medium at 0 h, 6 h, 24 h, 48 h, and 72 h respectively to determine cell viability, and incubated at 37 ℃ with 5% $CO_2$ in dark for a period of time (1-hour incubation for A549/DOX cells, 2-hourincubation for MX100 cells). The cell viability was then determined by

measuring the absorbance of the well at 492 nm using microplate reader (Bio-RAD, Ultrmark, Microplate Imaging System, USA). Relative growth (compared with the cell viability at 0 hour) of each cell line was calculated by $\frac{[A]_T}{[A]_{T0}}$. Where $[A]_T$ is the absorbance at different time points and $[A]_{T0}$ is the absorbance at 0 hour. This assay was performed in triplicate[150].

## 3.8. Molecular Docking Analysis

Prediction of possible molecular binding targets of the selected compound was performed based on the similarity ensemble approach (SEA) by the search engine http://sea.bkslab.org[151]. The binding behavior of compounds including compound 91b1, compound 160a, or positive control including doxorubicin and verapamil to protein targets was investigated based on their molecular structures, which were matched against the ChEMBL medicinal chemistry database (version16). Program ChemDraw Ultra 8.0 was applied to identify the mol format of the previously mentioned compounds' structures, and STRUCTURE-TO-SMILE translator (https://cactus.nci.nih.gov/index.html) was used for translating the compound structure to their corresponding SMILE format, which was input to the search engine (http://sea.bkslab.org)to determining the corresponding possible binding proteins according to the expected value (P-value) and the maximum target complementary value (MaxTC).

After protein targets were predicted by the SEA program, another molecular docking program DockingServer: http://www.dockingserver.com/web was used to determine

the binding affinity of the compound to its predicted target compare to protein's natural ligand by estimated the released free energy of binding reactions respectively. The three-dimensional structures, possible interactions, interacted amino acids, and released interaction energy of either compound, natural ligands or antagonists to their protein targets respectively were then identified.

## 3.9. Transformation of plasmid to bacteria

For the study of lumican function, lumican expression vector pCMV3-LUM-Myc (Figure 3.7, Sino Biological Inc.) and Myc tagged pcMV/hydro-negative control vector (Figure 3.8, Sino Biological Inc.) were transformed into E. coli to extract corresponding vector for transfection into cells as described in section 3.10 and Section 3.13.

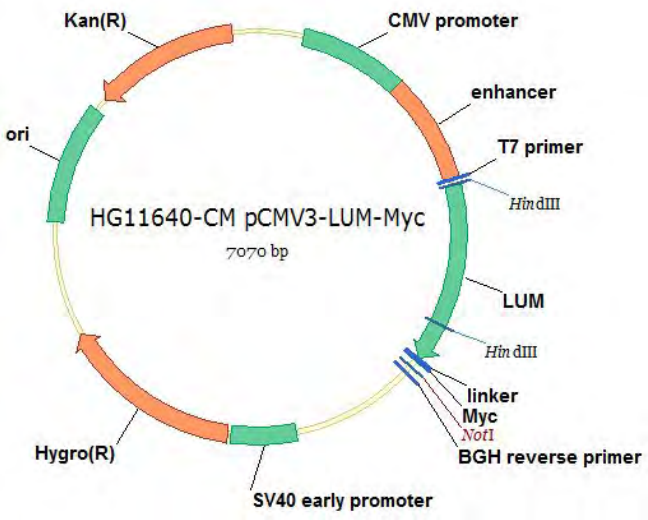


**Figure 3.7 Physical map of lumican-expression vector (LUM/pcMV3-C-Myc).** (Adopted from Datasheet of Human LUM ORF mammalian expression plasmid, C-Myc tag).

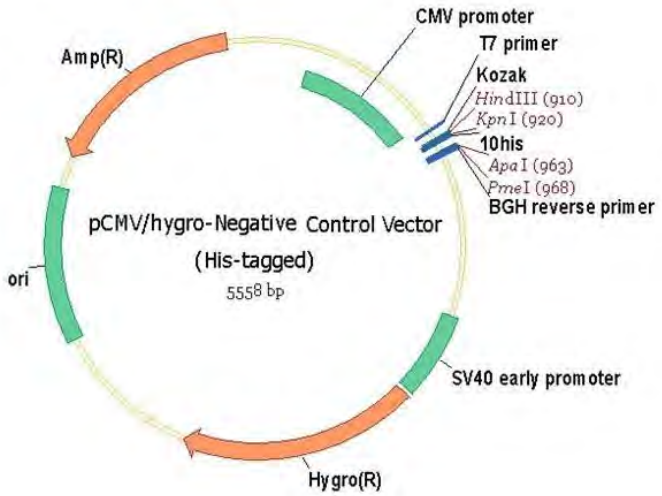


**Figure 3.8 Physical map of pcMV/hygro-negative control vector (Myc-tagged).** (Adopted from Datasheet of pcMV/hygro-Negative Control Vector, Myc-tagged).

ArcticExpress (DE3) RP competent cells (Agilent Technology, USA) was used for transformation. Competent cells were thawed on ice and then mixed with 2µl of diluted XL10-Gold β-mercaptoethanol (provided by the kit), the cells were swirled gently on ice for 10 minutes, and then50ng of expression plasmid DNA containing the gene of interest (Human Lum ORF mammalian expression plasmid, C-Myc tag, or pCMV/hgro-Negative Control Vector, Myc-tagged, Sino Biological Inc. Beijing) was added, followed by incubation for 30 minutes on ice, and was then incubated at 42$^{o}$C water bath for 25 seconds with gently shaking and was immediately put on ice for 2 minutes. Then 600µL of pre-warmed super optimal broth with catabolite repression medium (SOC) was added and incubated at 37$^{o}$C for 1 hour on a shaker at 225 rpm. LB agar plates were prepared by mixing 100mL of LB molten agar with 50 µg/mL kanamycin. 100 µl of the cells (1:1, 1:10, 1:50 samples respectively) were added and spread on the agar plates, therefore, the plasmid DNA containing the kanamycin-resistant gene can be selected and the positive colonies were grown on the

plates at 37°C overnight on a shaker at 225 rpm.

On the second day, a single colony was picked out with a pre-autoclaved tooth stick and was incubated in 5 mL LB broth with 50 μg/mL kanamycin for 18 hours at 37°C on a shaker at 225 rpm. The bacterial cells were then used for plasmid extraction or kept at -80°C in 50% glycerol/LB for further use.

## 3.10. Plasmid extraction

Hybrid-QTM Plasmid Rapidprep kit (GeneAll, USA) was used for plasmid extraction. 3 ml of bacterial cells was pelleted by centrifugation at 10,000 rpm for 1 minute in 1.5 mL Eppendorf tube (by repeating centrifuge twice). The supernatant was discarded and 170 μL of re-suspension buffer (buffer S1) was added to thoroughly re-suspend the cell pellet. 170μL of lysis buffer (buffer S2) was added to the bacterial cells and mixed by inverting for 5 times. The bacterial cells were then incubated at room temperature for 4 minutes for cell lysis. Afterward, 250 μL of precipitation buffer (buffer G3) was added to the cell lysate for DNA precipitation, the tube was gently inverted for 10 times for complete precipitation of DNA. The lysate was then transferred to EzClear™ filter column and centrifuged at 10,000 rpm for 1 minute, the upper EzClear™ filter column unit and the flow-through were discarded. 700 μL of washing buffer (buffer PW) was added to wash the filter membrane and centrifuged at 10,000 rpm for 1 minute, this washing step was repeated once. The column was put into a new 1.5 mL Eppendorf tube, 50 μL of nuclease-free water was carefully added exactly on the filter membrane of the column and incubated at room temperature for 1

minute for high recovery. Finally, the plasmid DNA was obtained by centrifugation at 10,000 rpm for 1 minute.

## 3.11. RNA extraction from cell lines

Total RNA of cells was extracted by RNeasy Mini Kit (Qiagen, USA) according to the manuals' instruction. RNA extraction was performed when cells grew to approximately 80% confluency in a 75 $cm^3$ flask. Cells were firstly suspended by scrapper, and then suspended cells together with medium were collected and centrifuged at 1,500 rpm for 3 mins. The medium was removed after centrifuge, and 4ml of phosphate buffer saline (PBS) was added in the former flask, and then re-suspended cell pellet to collect more cells. Suspended cells in PBS were also centrifuged at 1,500 rpm for 3 mins to get final cell pellet, which was kept in -80 $^oC$ until RNA extraction.

The thawed cell pellet was firstly re-suspended by adding 300 μl lysis buffer RLT, then 700 μL of 70% ethanol was added to get the lysate. Each lysate was transferred into a RNeasy spin column and centrifuged at 12,000 rpm at room temperature for 1 minute. Flow-through was discarded and 700 μL washing buffer RW1 was added to the column and then the column was centrifuged at 12,000 rpm at room temperature for 1 minute. The flow-through was discarded and 500 μL of another washing buffer PRE was added to the column and the column was then centrifuged at 12,000 rpm at room temperature for 1 minute. The PRE washing step was repeated once. After that, the flow-through was discarded and the column was put into a new 1.5 mL Eppendorf

tube. 50 μL of RNase-free water was added into the column and incubated for 1 minute on ice to dissolve more RNA product. Finally, the RNA was collected by centrifuging the column at 12,000 rpm for 1 minute. The concentration of extracted RNA was measured by CLARIOstar microplate reader (BMG LABTECH, Germany) and the quality of RNA was analyzed by 1.5% agarose gel electrophoresis. Extracted RNA was kept in -80 $^{o}$C for future use.

## 3.12. cDNA synthesis

cDNA (complementary DNA) was synthesized from mRNA by reverse transcriptase (Promega, USA). About 6μL of extracted total RNA(extraction progress was described in Section 3.11) was mixed with 4 μL of 5X reaction buffer, 2 μL of $MgCl_2$ (20 mM), 1 μL of random primers and oligo$(dT)_{15}$ primers, 1 μL of PCR Nucleotide Mix (10 mM), 0.5 μL of ribonuclease inhibitor, 0.5 μL of reverse transcriptase, and 4μL of Nuclease-Free Water to get a final total volume of 20 μL in a PCR tube on ice. The tubes with the samples were put in a thermo-cycler (Primus 96 plus, MWG Biotech AG, Germany) with the thermal cycling profile as follow: 25$^{o}$C for 5 minutes, 40$^{o}$C for 1 hour and 70$^{o}$C for 15 minutes. Afterwards, the synthesized cDNA was kept at -20$^{o}$C for further use. The concentration of cDNA was measured by CLARIOstar microplate reader (BMG LABTECH, Germany).

## 3.13. Transfection

The pCMV/hygro-negative control with or without cloned lumican insert was transfected into mouse fibroblast cell line NIH-3T3 using FuGENE 6 transfection reagent (Promega, USA) with 3:1 reagent DNA ratio according to manual's instructions. Approximately 30% confluent cells grown on 6-well plates were transfected with 2 ng of interested plasmid DNA.2ng of plasmid (final concentration of plasmid is 20 ng/mL) and 3 μL of transfection reagent were added to pure medium without adding FBS at a final volume of 100 μL in a PCR tube. The tube was vortexed and then incubated at room temperature for 15 minutes. The medium in the 6-well plate was replaced by the fresh medium, the transfection mixture was then added to the well drop by drop. Afterwards, the cells were incubated in a humidified incubator at 37$^{o}$C with 5% $CO_2$ for 3 days to let the cells grow under the transfection. After 72 hours of transfection, the cells were harvested as described in Section 3.1 and cultured in medium containing Hygromycin B (Thermo Scientific, USA) at a concentration of gradually increased from 100 to 400 μg/mL to select the transfected cells to proliferate. The expression of the gene of interest was examined by PCR and gel electrophoresis.

After selection in hygromycin B for 2 months, approximately $2\times10^{6}$NIH 3T3 parental, NIH 3T3/Lum or NIH 3T3/Mock cells were harvested and subcutaneously injected into each frank of female Balb/cathymic nude mice (n=5). Total RNAs of the parental NIH 3T3 cells, NIH 3T3/Mock cells, NIH 3T3/Lum cells and the cells cultured from tumor issues are extracted and cDNAs were synthesized as described in

Section 3.12. The lumican expression level is examined by qRTPCR as described in Section 3.16 and gene β-actin was used as the reference gene for normalization.

## 3.14. Amplification of cDNA by PCR

PCR reaction was performed by using AmpliTaq Gold DNA polymerase (Applied Biosystems, USA) to amplify cDNA. 4 μL of cDNA template(synthesized from total RNA as described in Section 3.11) was mixed with 2 μL of 10 X PCR buffer, 1μL of $MgCl_2$ (25 mM), 0.4 μL of dNTP mix (10 mM), 0.25 μL of AmpliTaq Gold DNA polymerase, 0.2 μL of β-actin (reference gene) forward and 0.2 μL reverse primers respectively, 0.2 μL of 2 μM target genes forward and 0.2 μL of 2 μM reverse primers respectively, and 8.35 μL nuclease water to get a total volume of 20 μL in a PCR tube. The tubes with the samples were then put in the thermo-cycler (Primus 96 plus, MWG Biotech AG, Germany) with the thermal cycling profile as follows: denaturation of cDNA at 95$^{o}$C for 4 minutes followed by 30 cycles of denaturation at 95$^{o}$C for 1 minute, annealing at 60$^{o}$C for 1 minute and primer extension at 72$^{o}$C for 1 minute. Afterwards, the reaction followed a further extension step at 72$^{o}$C for 4 minutes. After completion, the cDNA samples were kept at -20$^{o}$C for further use. The specific primers for lumican, p-glycoprotein, β-actin were shown in Table 3.1. lumican and β-actin primers were ordered from Sino Biological (Beijing), while P-gp primers were ordered from Integrated DNA Technologies (USA).

**Table 3.1 Primer sequence of lumican, P-gp, β-actin in PCR reactions.**

| Gene | Primer | Sequence |
|---|---|---|
| **lumican** | Forward | 5′-CTTCAATCAGATAGCCAGACTGC-3′ |
| | Reverse | 5′-AGCCAGTTCGTTGTGAGATAAAC-3′ |
| **P-gp** | Forward | 5’-CCTTCACCCAGGCAATGATA-3’ |
| | Reverse | 5’-GCACCAAAGACAACAGCTGA-3’ |
| **β-actin** | Forward | 5'-GTGGGGCGCCCCAGGCACCA-3' |
| | Reverse | 5'-CTCCTTAATGTCACGCACGATTTC-3' |

## 3.15. Gel electrophoresis

1.5% agarose gel was prepared by dissolving 0.75 g agarose powder (Invitrogen, USA) in 50 mL 1 X TBE buffer, and heated by microwave for complete mixing. 0.01% (5 μL ） GelRed (Biotium, CA, USA) was then added for staining DNA. Gel electrophoresis was performed in 1X TBS buffer at 100 V for 1 hour (Bio-RAD, PowerPac BasicTM, USA). DNA samples were mixed with 6X loading dye (Promega, USA) and ran together was DNA marker. The DNA bands in the gel were then detected and analyzed by ChemiDoc XRS (Bio-Rad, USA), and DNA size was determined by comparing to GeneRuler 100 bp DNA ladder (Thermo scientific, USA).

## 3.16. Real-time quantitative PCR of cDNA

GoTaq qPCR system (Promega) was performed to analyze the relative mRNA expression of target genes by quantitively real-time PCR. Total RNA was extracted

from scratching the cells from the growth plate and reverse-transcribed into cDNA as mentioned in Section 3.11. Four μL of the synthesized cDNA was mixed with 10 μL of 2X qPCR Mastermix (Promega, USA), 2 μL of 2 μM forward and reverse primers of either target gene or reference gene (β-Actin was applied as reference gene), and 12 μL of RNase free water to get a total volume of 20 μL in a PCR tube. All 20 μL of sample mixtures were transferred into the wells of PikoReal 96-well strips (n=3). qPCR reactions were carried out by PikoReal Real-Time PCR System (Thermo Scientific, Erembodegem, Belgium). The thermocycling profile was progressed as follows: polymerase activation at 95°C for 2 minutes, then followed by 40 cycles of denaturation at 95°C for 15 seconds, annealing and primer extension at 60°C for 1 minute, then melt curve data was identified by gradually increasing temperature from 60 to 95°C until the fluorescent signal was dropped to zero. Cq (cycle of quantification) of each sample was determined and recorded by the program PikoReal Software 2.0 (Thermo Scientific, Erembodegem, Belgium).

For all the qPCR reactions, the relative expression of target genes in different samples were calculated and compared by using the $2^{-\Delta\Delta Ct}$ method. The expression level of target genes was normalized by the reference gene β-actin.

The calculation of $2^{-\Delta\Delta Ct}$ method was showed as follow[152]:

$$\Delta Cq \text{ of target gene} = Cq \text{ of target gene} - Cq \text{ of reference gene}$$

$$\Delta\Delta Cq \text{ of target gene} = \Delta Cq \text{ of the target gene in treated group} - \Delta Cq \text{ of the target gene in control group}$$

$$\text{Therefore, the fold change of gene expression level} = 2^{-(\Delta\Delta Cq \text{ of target gene})}$$

The expression level was regarded as overexpression if the fold change of gene expression level ratio ($\frac{\text{Target gene(tumor)/Reference gene(tumor)}}{\text{Target gene(non-tumor)/Reference gene(non-tumor)}}$) was larger than 1.2; a ratio between 0.8 and 1.2 was considered as no significant change, while a ratio smaller than 0.8 was considered as under expression of the target gene[153].

## 3.17. Cell cycle analysis

Approximately 8 $\times 10^5$ cells (KYSE450, A549 or LCC6 cells) were seeded into each well of a 6-well plate. After 24-hour incubation at 37°C with 5% $CO_2$, culture medium was replaced by fresh medium with compound 91b1 at a gradually increasing concentrations of 5, 10, 20, and 50 μg/mL, doxorubicin at 0.5 μg/mL as positive control, or 0.1% DMSO culture medium as vehicle control (n= 3). After 24-hour treatment at 37°C with 5% $CO_2$, cells were harvested by trypsinization as previously described in section 3.1 to get cell pellets, which were washed with cold PBS twice, and then resuspended in 300 μL PBS. The cells were fixed by injecting 300μl samples into 700 μL 100% ethanol drop by drop to get a final concentration of 70% ethanol with vortexing and were kept at 4°C overnight for fully fixing. On the next day, the cells were centrifuged at 500 rpm for 10 minutes to get the cell pellets and were washed with cold PBS twice, followed by resuspension with 0.5mL PI/RNase Staining Buffer (BD Biosciences, USA). After 15 minutes incubation at room temperature in darkness, the samples were analyzed by BD FACSCalibur Flow Cytometer (BD Biosciences, USA).

## 3.18. Trans-well matrigel invasion assay

Cancer cell invasion was evaluated by matrigel-coated membrane (8-μm pore size, BD Biocoat, Corning, USA) chambers in a 24-well plate. KYSE150 cells were investigated in this test. The lower chamber was filled with RPMI1640 medium containing 10% FBS with purified human recombinant lumican protein (reclumican, Beijing) at concentrations of 0 ng/mL, 50 ng/mL, 250 ng/mL and 500 ng/mL. Approximately 5,000 cancer cells were cultured in 200 μL serum free RPMI1640 culture medium in the upper chamber. At the same time, the same number of cells were cultured in uncoated membrane (8-μm pore size) chamber as a control. After 24-hour incubation at 37ºC with 5% $CO_2$, the uninvaded cells on the upper chamber were scraped off with a cotton swab, while the transmembrane cells which migrated to the opposite side of the membrane were fixed in 100% methanol for 10 min and then followed by staining with 0.5% crystal violet solution after washing twice with PBS. The transmembrane cells were counted under a microscope (Olympus CKX41, Japan) in 4 random fields at the magnification of 40 times. The invasion percent was calculated by $\text{invasion\%} = \frac{\text{number of cells invading through matrigel-coated membrane}}{\text{number of cells migrating through uncoated membrane}} \text{ X } 100$ to determine the cell invasion

## 3.19. *In vitro* wound healing assay

Wound healing assay was performed to evaluate cell migration and growth. Approximately 1 X $10^6$ cancer cells were cultured in a 6-well plate at 37ºC with 5% $CO_2$ overnight to let the cells adhered and grew to reach about 70~ 80% confluent

monolayers. On the second day, the monolayer was gently scratched with a new 1 ml pipette tip across the center of the well to generate a wound area without changing medium. After scratching, the well was gently washed twice with warm PBS buffer to remove detached cells and replenish the well with fresh medium or different concentrations of tested compound (compound 91b, or human recombinant lumican). The cells were incubated at 37ºC with 5% $CO_2$ again and observed by microscope (Olympus CKX41, Japan) at different time points (0, 6, 12, 24, or 48 hours after scratching depending on different cell types) for photography.

## 3.20. Multi-drug resistance assay

Multidrug Resistance Assay Kit (Cayman Chemical, USA) was used to analyze the modulation of cellular multidrug resistance machinery. Approximately 8 $\times 10^5$ cells were seeded into each well of a 6-well plate and allowed to grow for 24 hours at 37ºC with 5% $CO_2$ to let cells settle down. After 24-hour incubation, PBS buffer was used to rinse the cells once and1ml of the culture medium was then added with the gradually increasing concentration (2, 5 and 10 μg/mL) of compound 160a, verapamil (provided from kit, 1:1000 diluted in appropriate medium) as a positive control and 0.05% DMSO as a negative control (n=3). The treated cells were then incubated at 37ºC with 5% $CO_2$ for 30 minutes. Afterwards, 1ml of diluted calcein AM (2 μL in 10 ml medium) was added to the cells and the cells were incubated for another 25 minutes. After incubation, the cells were harvested by trypsin as previously described in Section 3.1 and put into a 1.5 mL Eppendorf tube. The tubes were then centrifuged at 8,000 rpm for 2 minutes to obtain the cell pellets, which were re-suspended by

appropriate medium and analyzed by the BD Accuri C6 flow cytometry (BD Biosciences, CA, USA).

## 3.21. Confocal microscopy

Approximately 8 $\times 10^5$ cells were seeded in glass bottom microwell dishes (MatTek, USA) and allowed to grow for 24 hours at 37°C with 5% $CO_2$. After 24-hour incubation, PBS was used to rinse the cells once and1ml of the culture medium was then added with the increasing concentration (2, 5 and 10 μg/mL) of 160a,

cyclosporin A (1:1000 diluted in appropriate medium; supplied with the Multi-drug resistance kit from Cayman Chemical, USA) as the positive control and 0.05% DMSO as the negative control. The cells were then incubated at 37°C with 5% $CO_2$ for 30 minutes. Afterwards, 1mL of diluted calcein AM (0.2 μL in 7 mL medium, offered from the Multi-drug resistance kit) was added and the cells were then incubated for another 25 minutes at 37°C with 5% $CO_2$. After incubation, the medium was replaced by PBS and the cells were then analyzed by Leica TCS SPE Confocal microscopy (Leica, USA)

## 3.22. cDNA microarray analysis

The cDNA microarray analysis and associated quality control were performed using Human Genome U133 Plus 2.0 arrays (Affymetrix, USA) according to Affymetrix's protocol at the Centre for Genomic Sciences of the University of Hong Kong.

Approximately 8 $\times 10^5$ KYSE150 cells were seeded in 75$cm^3$ flasks and were allowed to grow for 24 hours at 37°C with 5% $CO_2$ to settle down. After 24-hour incubation,

cells were treated with 9.5 μg/mL 91b1 or DMSO (0.05%, Sigma-Aldrich, USA) as blank control and then were incubated at 37°C with 5% $CO_2$ for 48 hours. Total RNA was extracted using RNeasy Mini Kit (Qiagen, Germany) as previously described in Section 3.11.

The RNA integrity was measured by the ratio of 28S/18S ribosomal RNA by Agilent 2100 Bioanalyzer (USA). cDNA was synthesized from 1μg of total RNA by reverse transcription kit (Invitrogen, USA) as previously described in Section 3.12. Biotin labelled-cRNA was produced by *in vitro* transcription kit (Invitrogen, USA) and was then purified by RNeasy mini columns (Qiagen, Germany). About 15 μg denatured cRNA was hybridized to each Human Genome U133 Plus 2.0 array (Affymetrix) and then was stained by a streptavidin phycoerythrin conjugate. The signals were detected by GeneArray scanner (Agilent, USA)and were analyzed by Agilent Genespring GX and Affymetrix GeneChip Operating Software. The signals of the differentially expressed genes of the treated samples were compared with the corresponding blank controls. The threshold levels of the corresponding up- or down-regulated genes with $\geq 2$ folds were included for further analyses[154].

## 3.23. BCA Assay

Pierce BCA Protein Assay Kit (Thermo Scientific, USA) was used to quantify the concentration of the whole cell protein lysates. The calibration curve was constructed by making the serial dilution of bovine serum albumin (BSA) standard from 0 μg/mL to 2000 μg/mL (0, 125, 250, 500, 750, 1000, 1500, 2000 μg/mL). BCA buffer A was

mixed with BCA buffer B at a ratio of 50:1 with the color of the mixture changed from blue to green after vortexing. The same volume of standard protein samples and protein lysate (25 μL) was respectively mixed with 200 μL BCA mixture (n=3) and then followed by incubation of each mixture at 37ºC for 30 minutes in water bath. After incubation, the absorbance of the serial dilutions of BCA standard and tested protein samples were measured by the microplate reader (Bio-RAD, Ultrmark, Microplate Imaging System, USA) at 562 nm. The standard curve of absorbance against protein concentrations was plotted to get a regression equation. Finally, the amount of protein in each sample can be obtained accordingly from the standard curve.

## 3.24. Analysis on signaling pathway

Bio-Plex Pro Cell Signaling Assay was performed to analysis involved signaling pathway. Based on magnetic bead immunoassays, intracellular phosphoproteins in cell lysates were detected with high sensitivity and specificity.

The assays were performed following the Bio-Plex Pro Cell Signaling Assays Instruction Manual. Approximately 8 $\times 10^5$ KYSE150 cells were seeded in 75$cm^3$ flasks and were allowed to grow for 24 hours at 37ºC with 5% $CO_2$. After 24-hour incubation, cells were treated with increasing concentrations of 91b1 (0, 5, 9.5, 20, and 50 μg/mL) or DMSO (0.05%, Sigma-Aldrich, USA) as blank control at 37ºC with 5% $CO_2$ for 48hours. Treatment reaction was stopped by aspirating culture medium and then adding ice-cold signaling cell wash buffer offered by the kit. Cells were

lysed by adding lysis buffer, scraping attached cells, and gently rocking or 20 mins at 4$^{o}$C to get the cell lysate. The cell lysate solution was then centrifuged at 14,000 rpm for 10 mins at 4 $^{o}$C to get the supernatant for measuring protein concentration by BCA test as previously described in Section 3.24. The protein concentration of cell lysates was diluted to 200 μg/mL for the next analysis or kept at -70 $^{o}$C until use. The coupled beads were diluted to 1X by washing buffer and 50 μL beads were added to each well of a 96-well flat bottom plate. The plate was washed two times with 200 μl wash buffer, and then 50 μl of each sample (KYSE150 cells treated with 0.05% DMSO; KYSE150 cells treated with 5, 9.5, 20, and 50 μg/mL 91b1; detection antibody diluent as blank control; phosphatase Hela lysate as negative control; UV-treated HEK293 lysate; EGF-treated SK-Br3 lysate; IFNa-treated Hela lysate and EGF-treated HEK293 lysate as positive control) was transferred to the appropriate wells of the plate, and followed by an incubation in dark at room temperature with shaking of 400 rpm for 18 hours. After incubation, the plate was washed three times with 200 μL wash buffer and 25 μL detection antibodies was transferred to each well of the assay plate. The plate was incubated in dark at room temperature with shaking of 400 rpm for 30 mins. The plate was washed three times with 200 μL wash buffer and 50 μL SA-PE was transferred to each well of the assay plate. The plate was incubated in dark at room temperature with shaking of 400 rpm for 10 mins. The plate was washed three times with 200 μL wash buffer, and then125 μL resuspension buffer was added to each well and the plate was shaked in dark at 1000 rpm for 30 seconds to resuspend the beads. Finally, the plate was placed in the reader of Bio-Rad

Bio-Plex 200 Suspension Array System to acquire the data.

## 3.25. Doxorubicin Accumulation

Because of the pumping-out effect for cytotoxic moieties by P-gp, the reversal effect of compound 160a or another P-gp inhibitor (verapamil) was studied by the corresponding increase in DOX (P-gp substrate) accumulation in cells. Doxorubicin accumulation test was performed as previously reported with minor modification. In brief, approximately 4 X $10^5$ cells of parental cell lines/ DOX-resistance cell lines (A549/DOX-resistance A549, KYSE150/ DOX-resistance KYSE150, LCC6/ LCC6MDR, and MCF-7/ MX-100 cell lines) were seeded in 6-well cell culture plate and were incubated with 20 μM DOX in the respective culture medium with different concentrations of compound 160a (10 μg/mL, 20 μg/mL, and 50μg/mL), 50 μg/mL verapamil (positive control), and 0.1 % DMSO (blank control). After 150-min incubation at 37$^o$C with 5% $CO_2$, cells were washed with cold PBS buffer and then lysed with lysis buffer (0.75 M HCl, 0.2% Triton-X100 in 2-propanol). The fluorescence level of DOX in the lysate was measured by CLARIOstar microplate reader (BMG LABTECH, Germany) using the excitation and emission wavelength pair of 460 and 587 nm respectively. A working solution of DOX (0, 0.05, 0.1, 0.2, 0.5, 1, 2, 5 μg/mL of DOX) was prepared, and a standard curve of DOX fluorescence signal against DOX concentration was plotted to calculate the intracellular concentration of DOX. Finally, a graph of intracellular DOX concentration against compound concentration was plotted to evaluate the reversal effect of compound 160a

comparing to verapamil.

## 3.26. Establishment of the analytical method for quantifying 91b1 and 160a

The primary standard stock solution of compound 91b1 or 160a was prepared by dissolving 1mg accurately weighed compound powder in 1.0 ml methanol to produce a concentration of 1.0 mg/mL, and stored at 4℃ for further use. Working solutions of compounds of 50 ng/mL, 100 ng/mL, 200 ng/mL, 500 ng/mL, 1 μg/mL, 2 μg/mL, 5 μg/mL, 10 μg/mL, 20 μg/mL, 50 μg/mL, 100 μg/mL, 200 μg/mL, and 500 μg/mL were prepared in methanol by appropriate serial dilution of the stock solution. Working solutions were freshly prepared every time together with samples analysis.

The quantitative test was performed using XEVO Triple Quadrupole MS (Waters Co. Milford, MA, USA) equipped with an ESI source which was set in positive ionization mode. Chromatographic separation was achieved using 2.1 X 50 mm column (part NO. 188002350, Serial NO. 024334240157 38at 25 ℃, Agilent, USA). Ioratadine (Sigma-Aladdin, USA) was used as internal standard (IS) to normalize compound response. Gradient elution was adopted to optimize well separation. The mobile phase consisted of methanol (A) and water (B). Gradient elution program: 0 min, A: B = 25: 75; 4 min, A: B = 60: 40; 6 min, A: B = 95: 5; 10 min, A: B = 95: 5, 11 min, A: B = 25: 75; 13 min, A: B = 25: 75. The ESI source was used at positive ion mode. The conditions of MS analysis were designed as follows: capillary voltage: 3.0 kV; source temperature: 150 ℃; desolvation temperature: 350 ℃; cone gas flow: 45L/H;

desolvation gas flow: 800L/H; the cone voltage (cv) and collision energy (CE) were set to match the MRM of each marker. The Masslynx V4.1 software (Waters) has been used for instrument control, data acquisition and handling.

The $[M+H]^+$ ions, and parents/daughter mass to charge ratio (m/z) were used for detection. The standard curve of ion abundance against compound concentrations was plotted to get a regression equation. Finally, the concentration of the tested compound in each sample was calculated using the standard curve accordingly.

## 3.27. Toxicity study of quinoline derivative 91b1

Ten SD rats were randomly divided into 2 groups (5 rats in each group) which separately received vehicle control or 800mg/kg of the quinoline compound 91b1 to evaluate acute toxicity.

Ten rats were randomly divided into 2 groups (5 rats in each group) which separately received the vehicle, and 500 mg/kg/day 91b1 for 7 days to evaluate chronic toxicity.

After treatment, 0.2 mL blood sample was collected into pre-heparinized tubes, centrifuged at 8000 rpm for 5 mins to get plasma samples, which were analyzed or stored at -20℃ for further use. The animals were sacrificed by $CO_2$ inhalation and the vital organs were collected including heart, liver, kidney, and lung. Dissected The organs were cut into two halves. One Half was preserved in 10% formalin for histopathological examination and the other half was kept in -80℃.Blood samples were collected and were allowed to stand for 30 mins to get the serum for biochemical parameter test by using automatic biochemical analyzer (Hitachi 7100 Japan) as

previously described in Section 3.22.

## 3.28. *In vivo* anti-cancer activity of quinoline compounds

*In vivo* nude-mice xenograft model was performed to evaluate the anti-cancer activity of the compounds in animals. For the preparation of cancer cell xenografts, approximately $1x10^6$ trypsinized cells suspended in HBSS (Life Technologies, USA) were implanted subcutaneously into the mid-doral region of each athymic nude mouse (BALB/c-*nu*/*nu*, female, 4-week old). Tumors were allowed to grow without treatment for 10 days. When the tumors became palpable (approximately 150 $mm^3$ in volume, calculated by formula as described [155]), each test agent (0.2 mL in volume) was injected into each mouse via the intraperitoneal (i.p.) route. 10 mg/kg/day and 50 mg/kg/day for the compound 91b1, 1 mg/kg/day for doxorubicin, or vehicle control. Compound 91b1 was dissolved into 6% PEG and then physiological saline to prepare the stock solution for testing its anti-cancer actions. Doxorubicin was dissolved in 6% PEG physiological saline as positive control. 6% PEG was dissolved in physiological saline as vehicle control. Each agent was given to each mouse from the tested groups as treatment. For each type of xenograft tumor, there were 5 mice in each treatment group for testing each test agent.

Tumor dimensions were assessed every other day with calipers, and tumor volumes were estimated using two-dimensional measurements of length and width and calculated with the formula [$l$ x $w^2$] x 0.52 (where $l$ is length and $w$ is width) as previously described[155]. Photos were taken every five days. After the 25-day

treatment, all animals were sacrificed by $CO_2$ inhalation and then dissected to collect the subcutaneous xenografts and vital organs (heart, liver, kidney, and lung). One half of each xenograft tumor or organs will be fixed in 10% formalin for histological and immunohistochemical assessment and the other half will be snap frozen in liquid nitrogen and stored at -85°C for further study. The whole blood of the animals was collected from eyeball and was allowed to stand for 30 mins to get the serum for biochemical parameter analysis by automatic biochemical analyzer (Hitachi 7100 Japan) as described in Section 3.29.

## 3.29. Serum biochemical parameter analysis

Blood samples were collected and allowed to stand for 30 mins, followed by 1500 rpm centrifugation to get 100 μL serum for analyzing the biochemical parameters by automatic biochemical analyzer (Hitachi 7100 Japan). Fully automatic test reagents were ordered from Kehua Bio-Engineering (Shanghai).

## 3.30. Statistical analysis

Two-tailed t-test was used to determine the statistical significance of the differences observed between groups. Statistical analyses were conducted by statistic program GraphPad Prism 5 or software Excel. A P-value of $< 0.05$ was considered statistically significant and marked with a * or ^, and a P-value of $< 0.01$ was considered remarkably statistically significant and marked with a ** or ^^.

Fluorescence intensity of photographs captured by confocal microscope were

measured by software Image J[156].Comparative ΔΔCt method was applied for relative quantification in qPCR analysis [152]. The analysis of the synergistic effects of the drug-drug combination was conducted by calculating combination index (CI value) through program CompuSyn[157].

# Chapter 4 Results

## 4.1. Study of the anti-cancer effect of compound 91b1

### 4.1.1. *In vitro* cytotoxicity test for compound 91b1

To evaluate the anti-cancer effect of compound 91b1 on cancer cell lines and non-tumor cell lines, MTS assay was performed. The percentage of MTS value was plotted against concentration of compound 91b1 (0, 1.562, 3.125, 6.250, 12.500, 25.000, and 50.000 μg/mL) and CDDP (0, 1.562, 3.125, 6.250, 12.500, 25.000, and 50.000 μg/ml). CDDP was applied as the positive control. Figure 4.1 shows the cytotoxic effect of 91b1 on 4 cancer cell lines (A549, AGS, KYSE150, and KYSE450) and one non-tumor cell (NE-3).

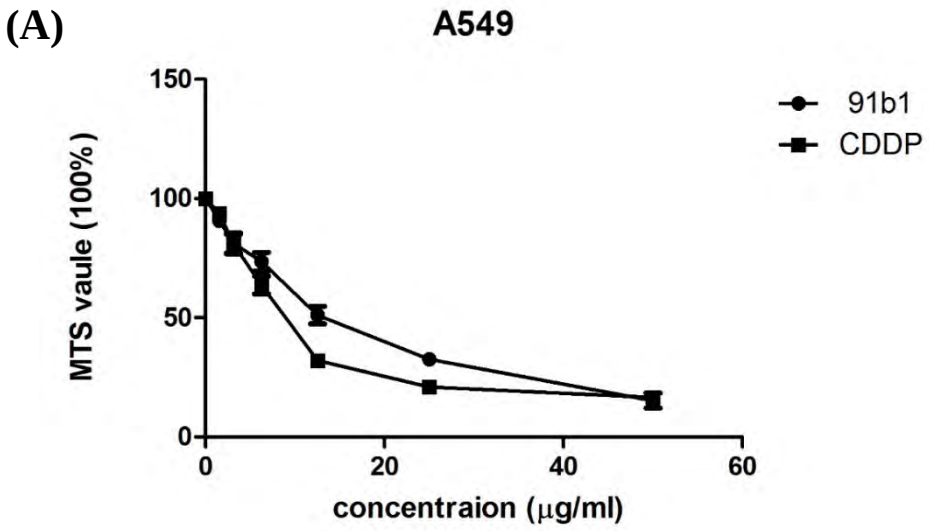

**(B)**

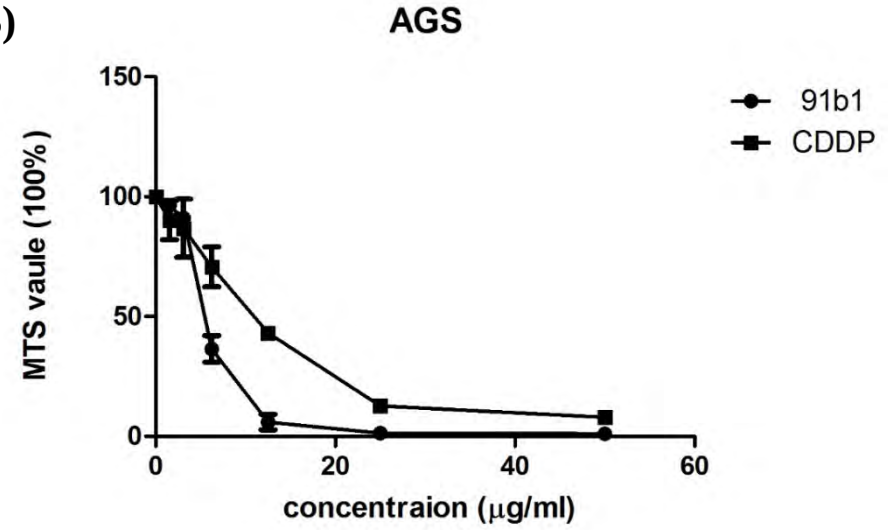
AGS
150
100
50
0
MTS vaule (100%)
0
20
40
60
concentraion (μg/ml)
91b1
CDDP

**(C)**

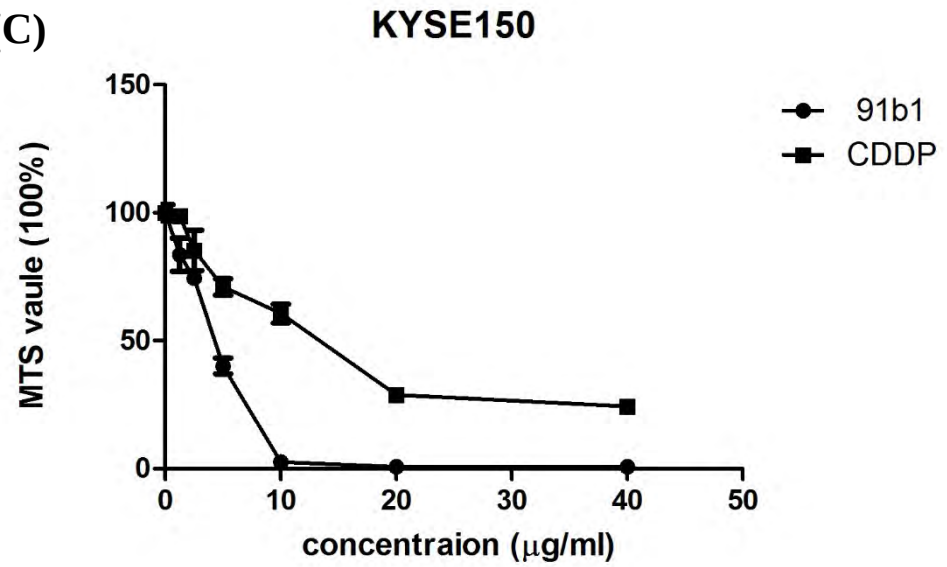
KYSE150
150
100
50
0
MTS vaule (100%)
0
10
20
30
40
50
concentraion (μg/ml)
91b1
CDDP

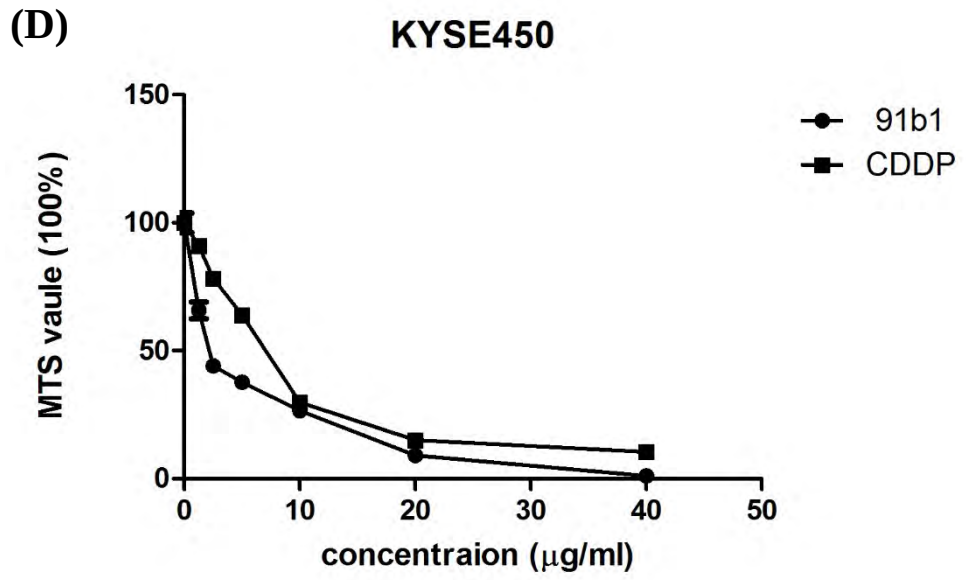


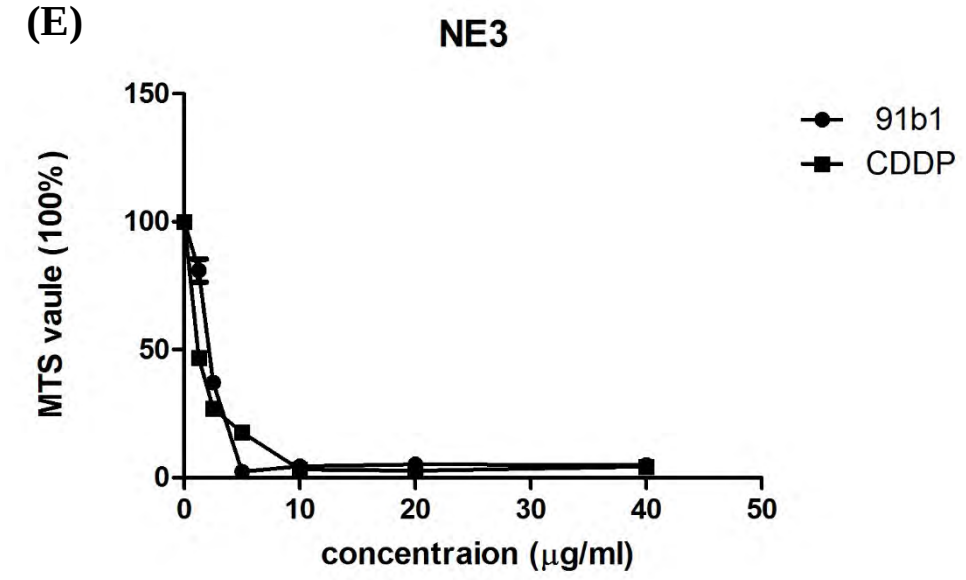


**Figure 4.1 Cytotoxic effect of compound 91b1 on tumor and non-tumor cell lines. CDDP was used as the positive control. Compound 91b1 and CDDP both showed dose-dependent manners for inducing cytotoxicity on the cell lines. (A): Cytotoxic effect of compound 91b1 on A549 cell lines; (B): Cytotoxic effect of compound 91b1 on AGS cell lines; (C): Cytotoxic effect of compound 91b1 on KYSE150 cell lines; (D): Cytotoxic effect of compound 91b1 on KYSE450 cell lines; (E): Cytotoxic effect of compound 91b1 on NE3 cell lines. CDDP: cisplatin. N=4. Vehicle control: 0.1% DMSO (dimethyl sulfoxide).**

The cytotoxic effect of compound 91b1 on tumor and non-tumor cell lines were compared with CDDP for the $MTS_{50}$ values which were determined as the concentration of tested compounds which showed 50% reduction of MTS signal comparing with vehicle control. Table 4.1 showed the inhibitory effects.

**Table 4.1 $MTS_{50}$ value(μg/mL) of compound 91b1 and CDDP on four cancer cell lines and one non-tumor cell line (NE3). Results were calculated by GraphPad Nonlinear regression analysis from four parallel experiments.**

| Cell Lines | $MTS_{50}$ value (μg/mL) | |
|---|---|---|
| | 91b1 | CDDP |
| **A549** | 15.38 | 6.23 |
| **AGS** | 4.28 | 13.00 |
| **KYSE150** | 4.17 | 13.2 |
| **KYSE450** | 1.83 | 6.83 |
| **NE3** | 2.17 | 1.17 |

CDDP: cisplatin. N=4. Vehicle control: 0.1% DMSO (dimethyl sulfoxide).

The $MTS_{50}$ values of compound 91b1 were 15.38 μg/mL, 4.28 μg/mL, 4.17 μg/mL, and 1.83 μg/mL for A549, AGS, KYSE150, and KYSE450 cell lines respectively. The $MTS_{50}$ values of CDDP were 6.23 μg/mL, 13.00 μg/mL, 13.2μg/mL, and 6.83 μg/mL for A549, AGS, KYSE150, and KYSE450 cell lines respectively. The $MTS_{50}$ values of compound 91b1 were lower than those of CDDP in AGS, KYSE150, and KYSE450 cell lines, implying that compound 91b1 showed stronger anti-cancer effect than CDDP in these three cancer cell lines. For the non-tumor cell line NE3, the $MTS_{50}$ values of compound 91b1 and CDDP were 2.17 μg/mL and 1.19 μg/mL respectively, indicating that compound 91b1 may be less toxic than CDDP to non-tumor cells.

### 4.1.2. Molecular Docking Analysis

To figure out the protein target for the compound 91b1, molecular docking analysis was performed by the SEA program(http://sea.bkslab.org)[151]. According to the instructions of the program, the binding probability of the compound to the protein target is significant if the expected value (P-Value) is lower than $1 \times 10^{-10}$, and the protein target with lower P-Value possess high infinity to the compound. The maximum target complementary value (MaxTC) indicates the level of the ligand-target complementarity, a higher MaxTC value suggested more suitable binding of the ligand to target. Table 4.2 shows the possible target for compound 91b1.

**Table 4.2 Predicted protein target of compound 91b1**

| Rank | Target Key | Target Name | Description | P-Value | MaxTC |
|---|---|---|---|---|---|
| 1 | ACEA-CANAX+5 | ICL1 | Isocitrate lyase | $2.865e^{-11}$ | 0.28 |

**MaxTC: maximum target complementary value.**

As shown in the Table 4.2, there is no human protein was the predicted target for the compound 91b1. The only significant binding protein in mouse was ICL1 from isocitrate lyase with the expected value of $2.865e^{-11}$ and maximum target complementary value of 0.28. Therefore, cDNA microarray analysis was performed to study the gene expression changes caused by compound 91b1 to figure out its anti-cancer mechanism.

### 4.1.3. cDNA microarray analysis

cDNA microarray analysis was performed to study the changes of gene expression level caused by compound 91b1 in cancer cells. The gene expression in compound 91b1 treated KYSE150 cells (treated with 9.5μg/mL (with reference to the $MTS_{50}$ value) compound 91b1 for 48 hours) was compared with control KYSE150 cells (parallel treatment was done with 0.1% vehicle DMSO for 48 hours). Gene expression changes was evaluated by signal-intensity fold change. The five most downregulated genes were CCL5, LUM, STON1, IGFBP5, and CP while the five most upregulated genes were C7orf57, ZBED2, CLGN, CSF2 and SLC16A6. Table 4.3 shows the five most downregulated genes and Table 4.4 shows the five most upregulated genes.

**Table 4.3 Five most down-regulated genes after treated with compound 91b1 (9.5 μg/ml) for 48 hours in KYSE150 cells.**

| Probe I.D. | Gene Title | Signal Intensity | | Intensity Fold Change (p9.5 / control) |
|---|---|---|---|---|
| | | 91b1 treated group | Control group | |
| 1405_i_at | CCL5 | 3.73491 | 7.911 | 47.21% |
| 201744_s_at | LUM | 3.71928 | 7.694374 | 48.34% |
| 213413_at | STON1 | 4.321197 | 7.786885 | 55.49% |
| 211959_at | IGFBP5 | 3.443796 | 6.158643 | 55.92% |
| 1558034_s_at | CP | 3.963314 | 7.085329 | 55.94% |

CCL5: chemokine (C-C motif) ligand 5; LUM: lumican; STON1: stonin 1; IGFBP5: insulin-like growth factor binding protein 5; CP: ceruloplasmin.

**Table 4.4 Five most up-regulated genes after treated with compound 91b1 (9.5 μg/ml) for 48 hours in KYSE150 cells.**

| Probe I.D. | Gene Title | Signal Intensity | | Intensity Fold Change (p9.5 / control) |
|---|---|---|---|---|
| | | 91b1 treated group | Control group | |
| 1557636_a_at | C7orf57 | 5.131972 | 2.715359 | 189.00% |
| 219836_at | ZBED2 | 10.007047 | 5.850765 | 171.04% |
| 205830_at | CLGN | 4.864191 | 2.923666 | 166.37% |
| 210229_s_at | CSF2 | 7.673194 | 4.657937 | 164.73% |
| 230748_at | SLC16A6 | 6.679981 | 4.237427 | 157.64% |

C7orf57: chromosome 7 open reading frame 57; ZBED2: zinc finger, BED-type containing 2; CLGN: calmegin; CSF2: colony stimulating factor 2; SLC16A6: solute carrier family 16, member 6 (monocarboxylic acid transporter 7)

The function of the top downregulated gene CCL5 was investigated by Dr Dessy Chan from our research group before. Thus, the function of the second top downregulated gene lumican (downregulated to 48.34% compared with the control group) was studied in this project.

### 4.1.4. Validation of cDNA microarray analysis by qPCR

To validate the downregulation of lumican after compound 91b1 treatment based on the cDNA microarray analysis, qPCR analysis was performed with primers specific for β-actin as the reference gene to detect the change in expression level of lumican in KYSE150 cells with the treatment of 91b1. The downregulation of relative expression level of lumican showed a dose-depend manner as the concentration of compound 91b1 was increased. The qPCR result was consistent with the cDNA microarray analysis result. Figure 4.2 shows the relative lumican expression level in KYSE150 cells after 48-hour treatment of different concentrations of compound 91b1 (5μg/mL, 9.5μg/mL, 20μg/mL, and 50μg/mL), and 0.1% DMSO was conducted in parallel as the vehicle control.

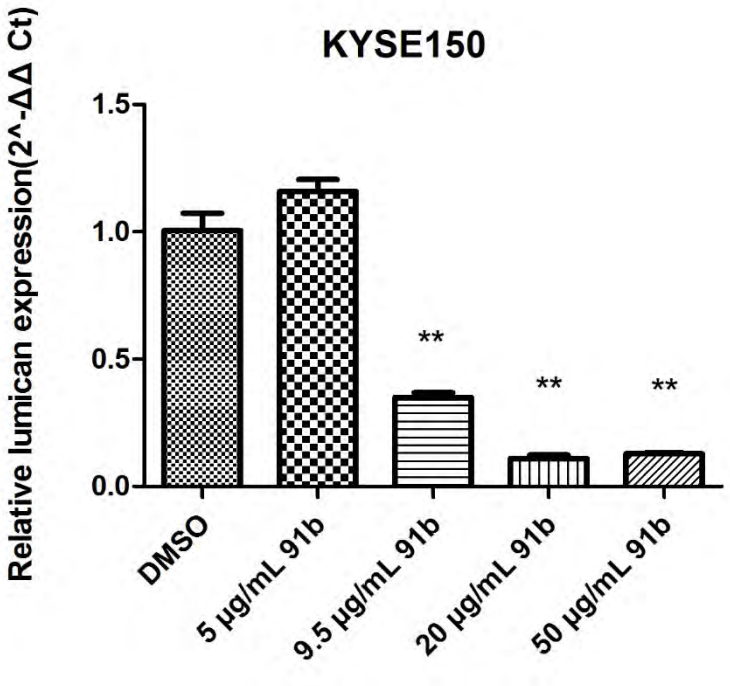

**Figure 4.2 Relative lumican expression level after 48-hour treatment with different concentrations of compound 91b1 (5μg/mL, 9.5μg/mL, 20μg/mL, and 50μg/mL) and vehicle (0.1% DMSO) in KYSE150. The relative lumican expression level was determined by comparing with cells treated with the vehicle after normalized with the expression of β-actin using qPCR. ** p<0.01.**

The lumican mRNA expression level of KYSE150 cells decreased after treatment with compound 91b1 and showed a dose-depend manner, suggesting that compound 91b1 may inhibit cancer growth by regulating the expression of lumican in cancer cells, which will be studied in the later sections.

### 4.1.5. Cell proliferation assay

To study the effect of compound 91b1 on cell proliferation, MTS cell proliferation assay was performed on A549, AGS, KYSE150, and KYSE450 cell lines. Results were shown in Figure 4.3.

**(A)**

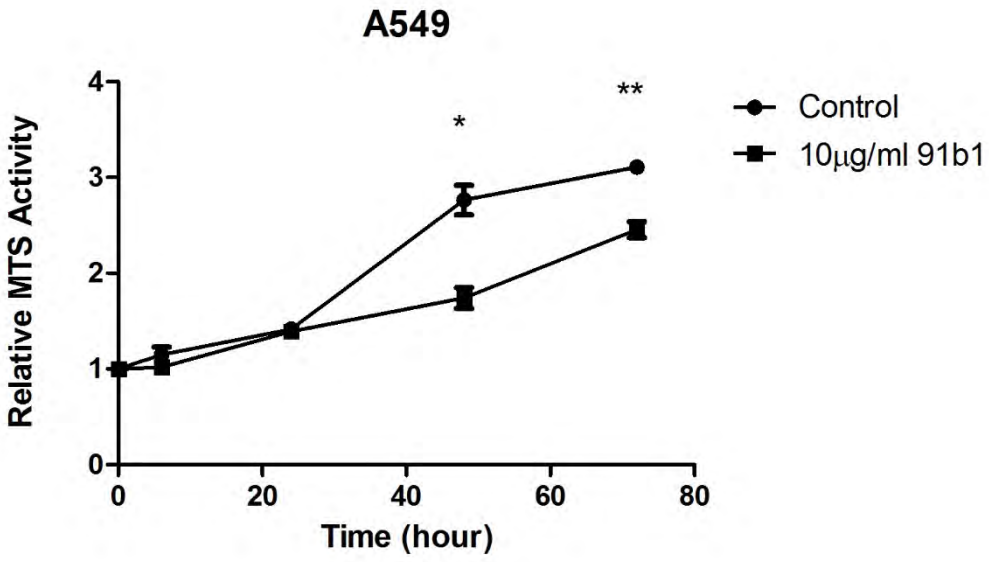

**(B)**

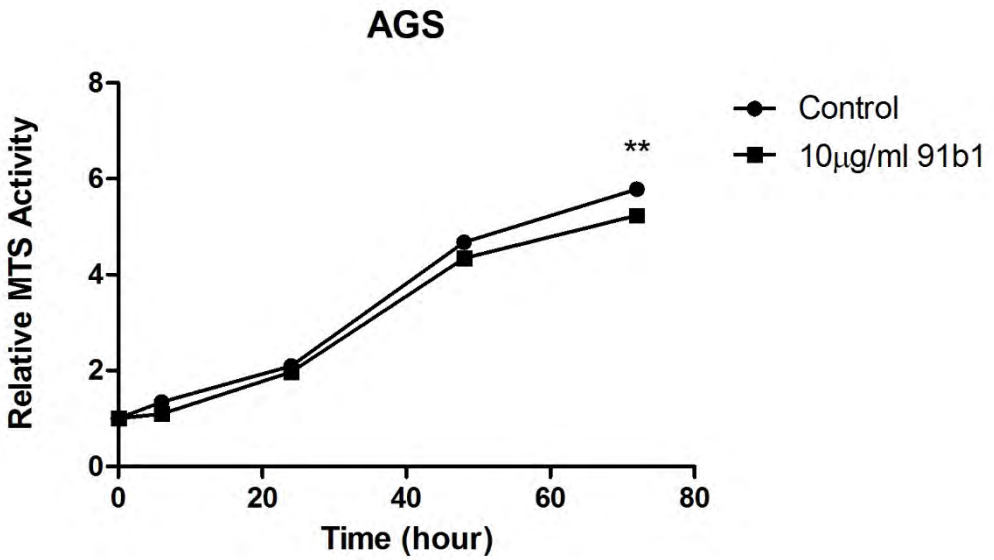
AGS
Relative MTS Activity
Time (hour)
Control
10μg/ml 91b1
**
0
2
4
6
8
0
20
40
60
80

**(C)**

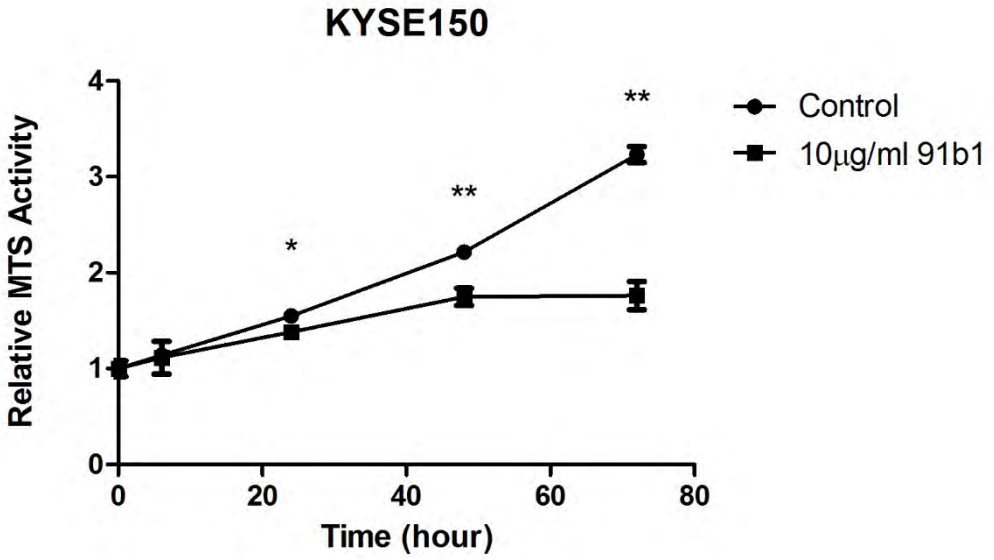
KYSE150
Relative MTS Activity
Time (hour)
Control
10μg/ml 91b1
*
**
**
0
1
2
3
4
0
20
40
60
80

**(D)**

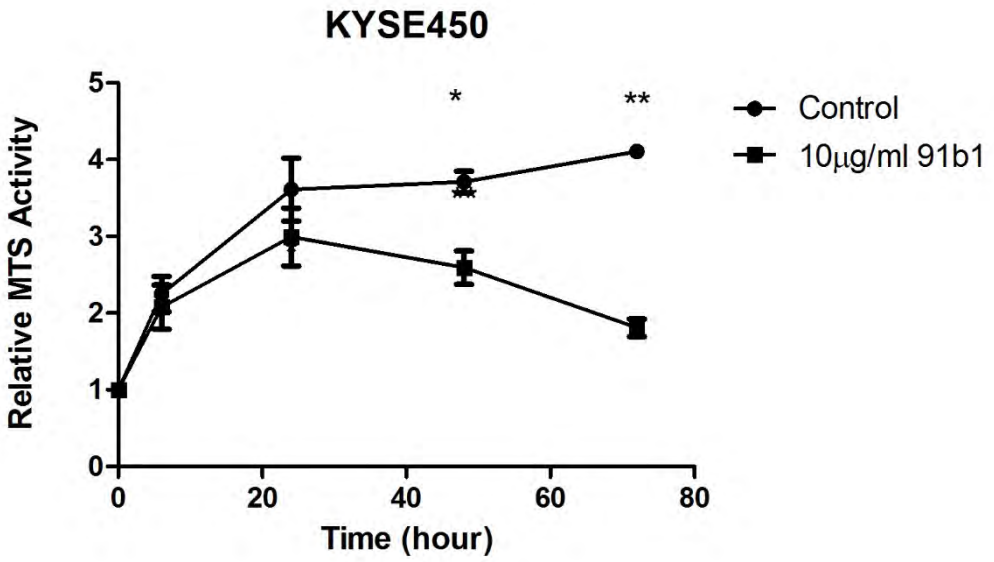


**Figure 4.3 Proliferation curves of cancer cells cultured in medium with or without 10 μg/mL compound 91b1. (A): Proliferation curves of A549 cells cultured with 10 μg/mL compound 91b1; (B): Proliferation curves of AGS cells cultured with 10 μg/mL compound 91b1; (C): Proliferation curves of KYSE150 cells cultured with 10 μg/mL compound 91b1; (D): Proliferation curves of KYSE450 cells cultured with 10 μg/mL compound 91b1. N=4. Vehicle control: 0.1% DMSO (dimethyl sulfoxide). * $p<0.05$; ** $p<0.01$.**

According to the results, the cell lines treated with compound 91b1 showed an obvious reduction in proliferation rate compared with vehicle control group on A549cells after 48-hours incubation, AGS cells after 72-hours incubation, KYSE150 cells after 24-hours incubation, and KYSE450 cells after 48-hours incubation respectively, indicating that compound 91b1 inhibited cancer cell growth usually when incubation time is 48 hours except AGS cells (cells were significantly inhibited after 72-hours), but stronger inhibited KYSE150 cell proliferation ( cells were

significantly inhibited after 24-hours incubation).

### 4.1.6. Cell cycle analysis

To further explain the effect of low proliferation rate in cancer cells after compound 91b1 treatment, cell cycle analysis was performed to reveal the cell cycle changes of A549 and KYSE450 with 91b1 treatment (Figure 4.3).

**(A)**

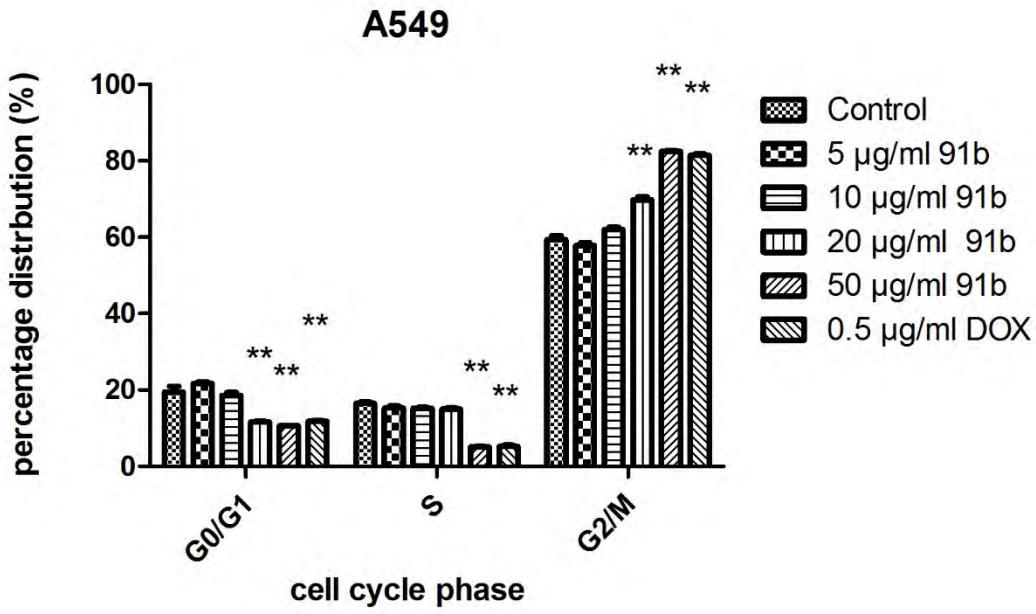

**(B)**

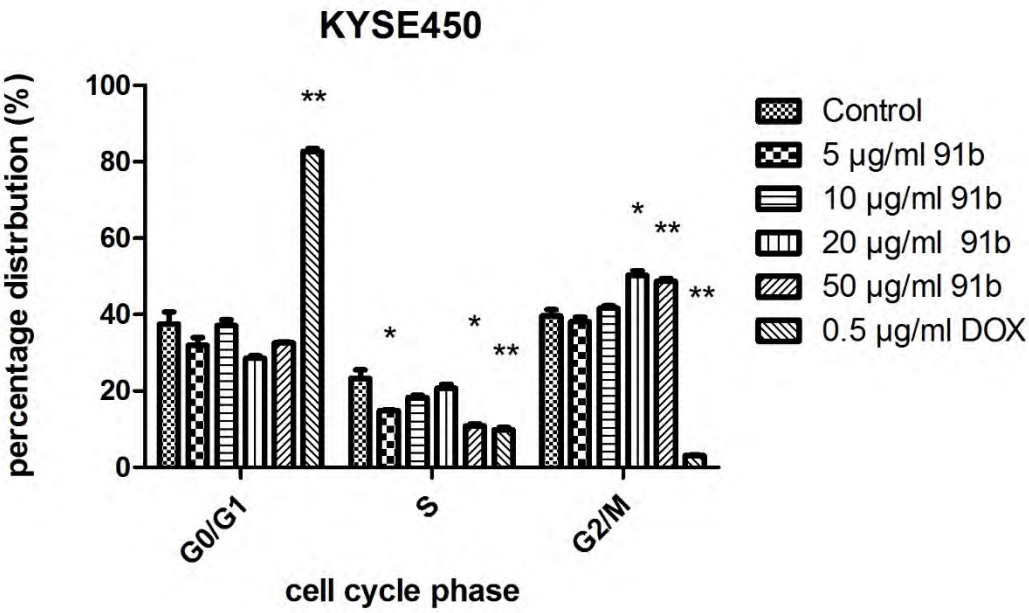


**Figure 4.4 Cell cycle analysis using flow cytometry on A549and KYSE450 cell lines. (A): cell cycle distribution of A549 cells after treatment of increasing concentrations of compound 91b1; (B): cell cycle distribution of KYSE450 cells after treatment of increasing concentrations of compound 91b1. 0.1% DMSO was applied as vehicle control. 0.5μg/ml doxorubicin was applied as the positive control. N=3. * p<0.05; ** p<0.01.**

The percentage of distribution of G0/G1 phase in A549 cells and KYSE450 cells were decreased dose dependently after the compound 91b1 treatment with the concentration from 5 μg/ml to 50 μg/ml and exhibited significance when compound 91b1 concentration reached 20 μg/ml. Although the percentage of distribution of G0/G1 phase in KYSE450 cells showed a decreasing trend after treated with compound 91b1, no significant difference was observed. For the G2/M phase of A549 cells and KYSE450 cells, the percentage of distribution was increased along with the concentrations of compound 91b1from 5 μg/ml to 50 μg/ml, exhibited significance

when compound 91b1 concentration reached 20 μg/ml. For the S phase of A549 cells, the percentage of distribution showed no significant difference after treated with low concentrations of compound 91b1 (5 μg/ml, 10 μg/ml, and 20 μg/ml), but decreased remarkably after treated with 50 μg/ml compound 91b1. The percentage of distribution of S phase in KYSE450 cells decreased significantly after treated with compound 91b1 at the concentration of 5 μg/ml and 50 μg/ml. It is suggested that compound 91b1 with the doses of 20 μg/ml may induce cancer cells to be arrested at the G2/M phase, interfere DNA synthesize at S phase, and finally resulted in the inhibition of cancer cell growth.

### 4.1.7. Wound healing Analysis

To evaluate the cell migration and growth properties affected by compound 91b1, wound healing analysis was performed on A549, KYSE150, AGS, KYSE70, and KYSE510 cell lines. A wound gap was created by scratching, and healing progress was captured at different time points. Cancer cells were treated with low (5 μg/mL) or high (10 μg/mL) dose of compound 91b1. Figure 4.4 shows the healing process of cancer cells after scratching under compound treatment culture.

**(A)**

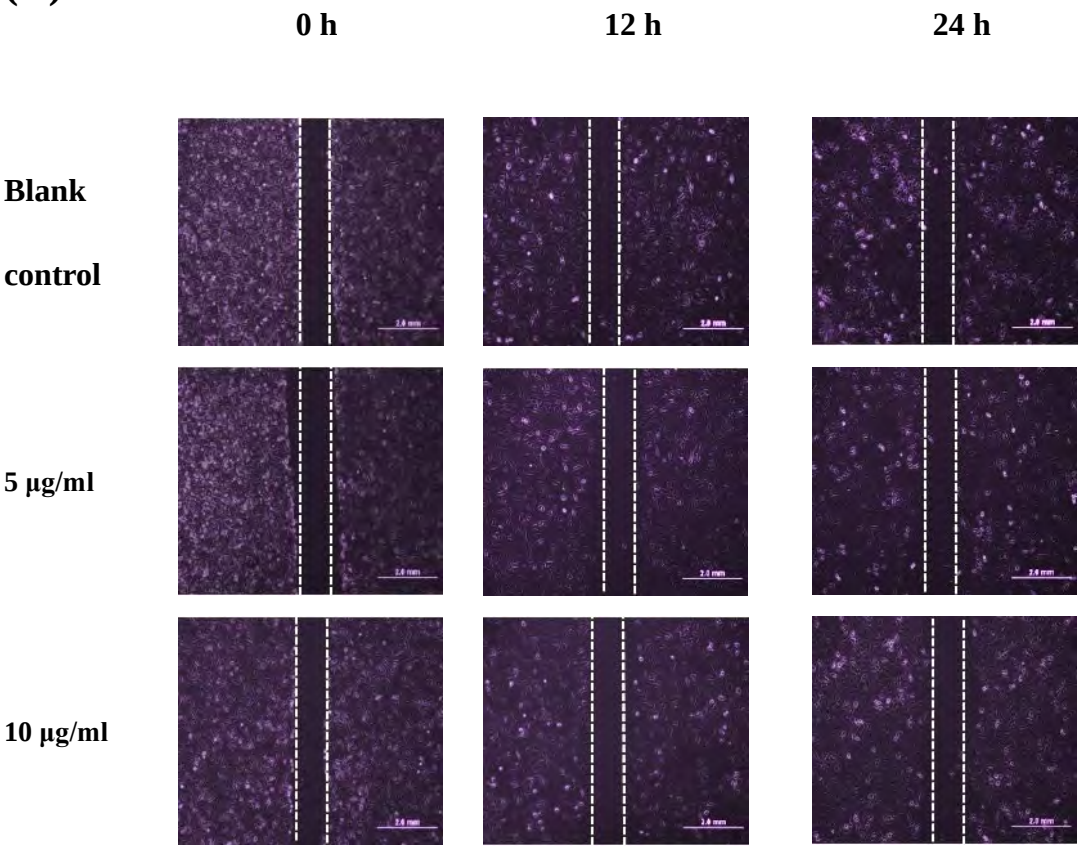


**Images of wound healing progress of A549 cells under 5μg/mL or 10μg/mL compound 91b1 at 0h, 12h, and 24h respectively**

**(B)**

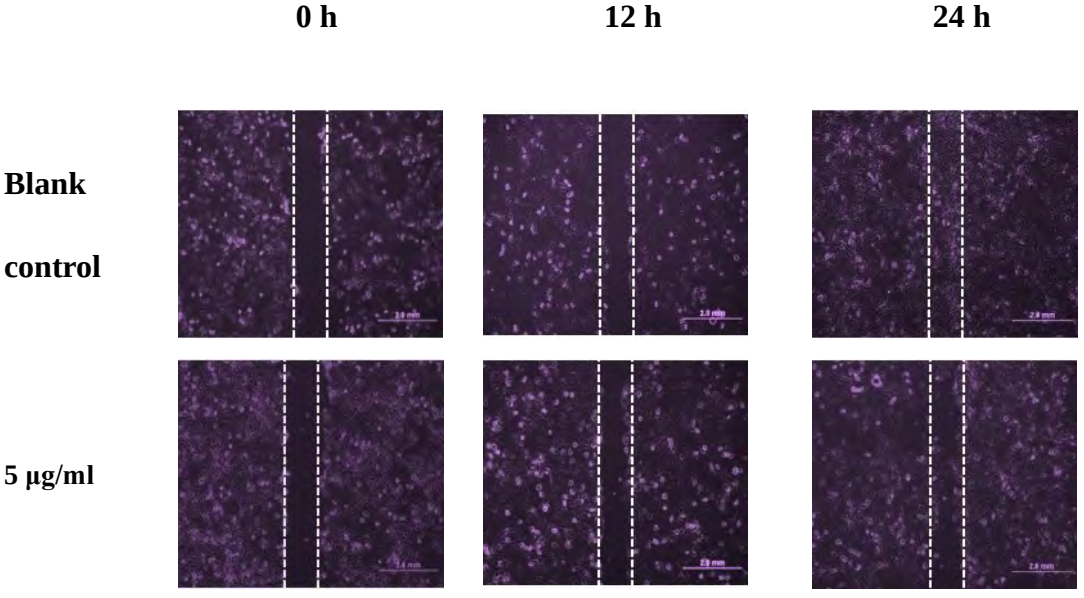

**10 μg/ml**

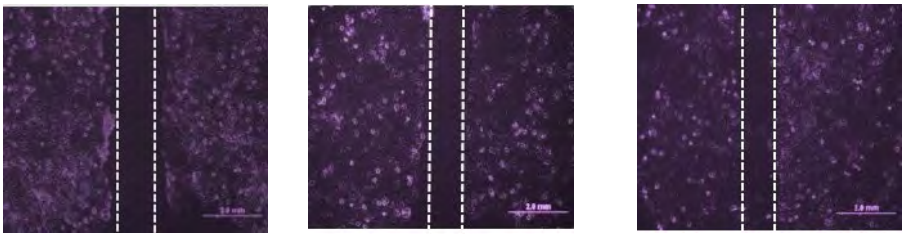

**Images of wound healing progress of KYSE150 cells under 5μg/mL or 10μg/mL compound 91b1 at 0h, 12h, and 24h respectively**

**(C)**

**0 h** **12 h** **24 h**

**Blank control**

**5 μg/mL**

**10 μg/mL**

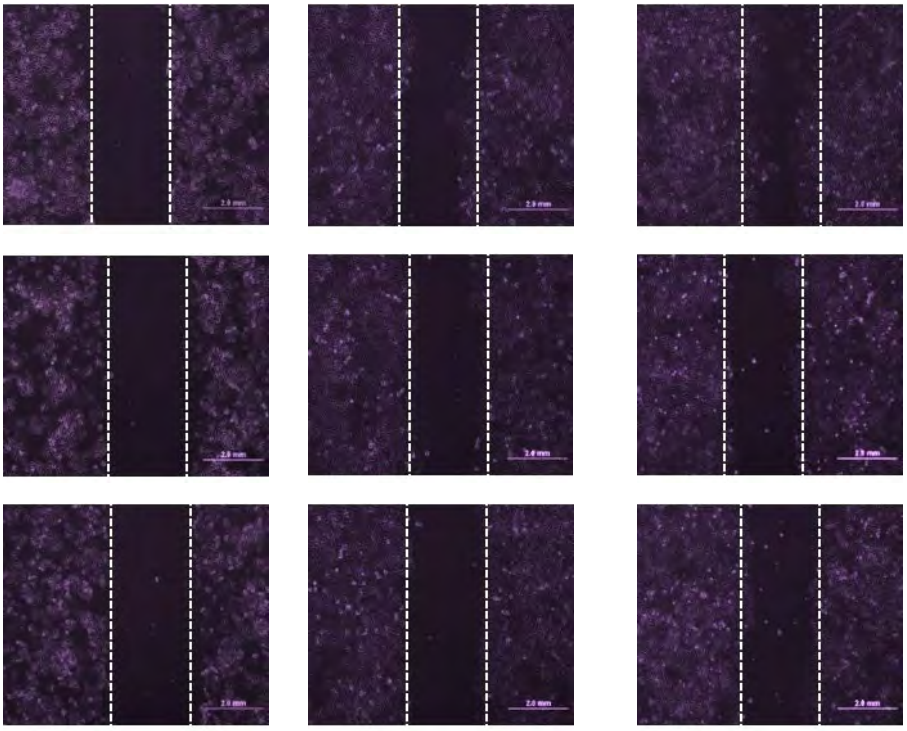

**Images of wound healing progress of AGS cells under 5μg/mL or 10μg/mL compound 91b1 at 0h, 12h, and 24h respectively**

**(D)**

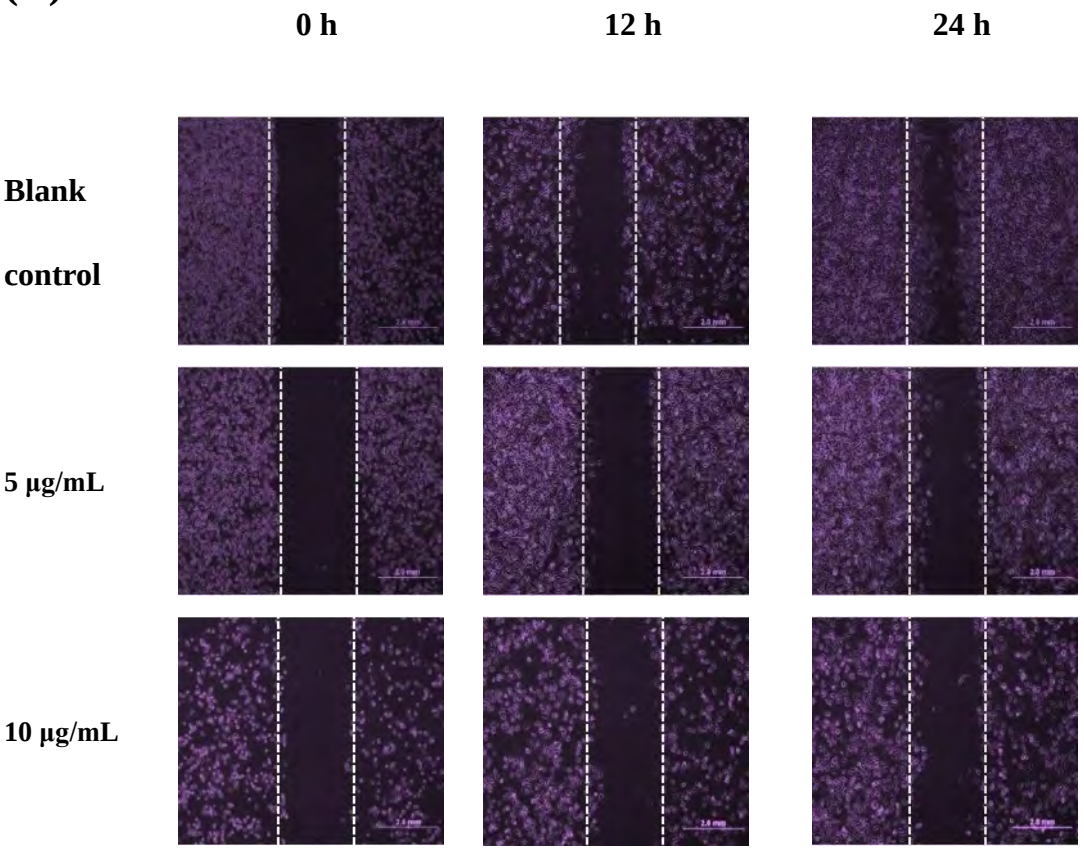


**Images of wound healing progress of KYSE70 cells under 5μg/mL or 10μg/mL compound 91b1 at 0h, 12h, and 24h respectively**

**(E)**

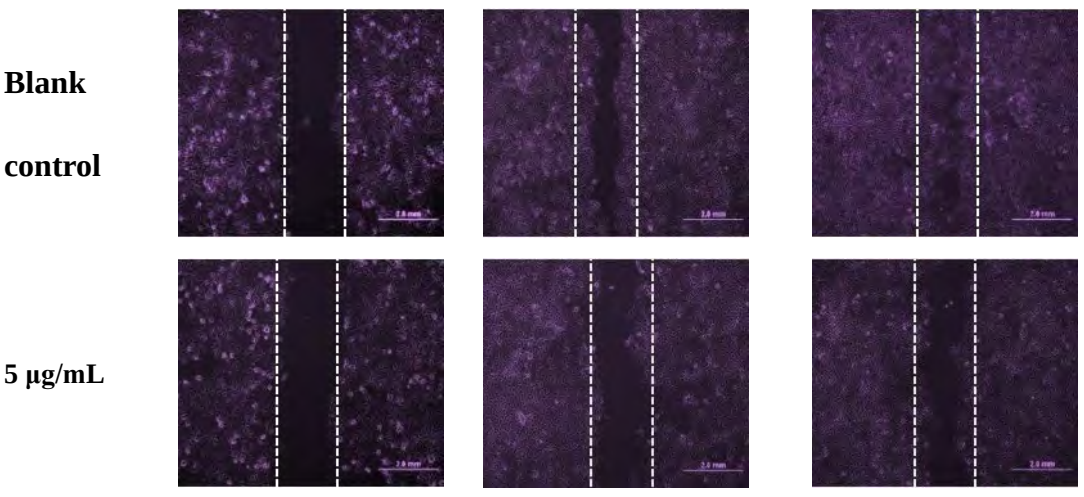

**10 µg/mL**

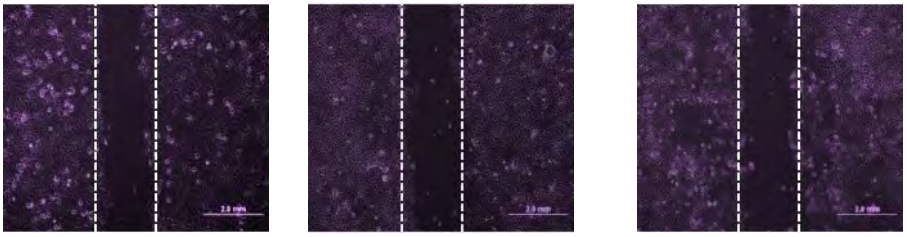

**Images of wound healing progress of KYSE510 cells under 5µg/mL or 10µg/mL compound 91b1 at 0h, 24h, and 48h respectively**

**Figure 4.5 Images of wound healing assay under compound 91b1 treatment on cancer cells. 0.1% DMSO was applied as the blank control. (A): Images of wound healing progress of A549 cells; (B): Images of wound healing progress of KYSE150 cells; (C): Images of wound healing progress of AGS cells; (D): Images of wound healing progress of KYSE70 cells; (E): Images of wound healing progress of KYSE510 cells. Fresh culture medium was applied as the blank control. Fresh culture medium was applied as the blank control Exposure time: 12.5 msec. Magnification: x 10. Scale: 2mm.**

According to the Figures 4.5 (A) to (E), after 12-hour (A549, KYSE150, AGS, and KYSE70 cell lines) or 24-hour (KYSE510 cell line) incubation, fewer cells of compound 91b1 treatment groups migrated into the scratched area than the control groups, indicating the reduction of cell migration of the cancer cells after 91b1 treatment.

## 4.1.8. Pathway Analysis

### 4.1.8.1. Bio-plex 200 system test

Bio-Plex Pro Cell Signaling Assay was performed to analyse the involved signaling pathways for the treatment with compound 91b1 on KYSE150 cells. Phosphorylated analytes (AKT($Ser^{473}$), ATF-2($Thr^{71}$), MEK1($Ser^{217}$/$Ser^{221}$), ErK1/2($Thr^{202}$/$Tyr^{204}$, $Thr^{185}$/$Tyr^{187}$), p38 MAPK($Thr^{180}$/$Tyr^{182}$), HSP27($Ser^{78}$), p53($Ser^{15}$),

JNK(Thr$^{183}$/Tyr$^{185}$), p90 RSK(Ser$^{380}$), Stat 3(Ser$^{727}$), and NF-κB p65(Ser$^{536}$)) from cell lysates treated with gradually increased concentrations of compound 91b1 (5, 9.5, and 20μg/mL) or vehicle control were detected by Bio-Rad Bio-Plex 200 Suspension Array System. Figure 4.6 shows the summary of phosphorylated analytes from compound 91b1 treated KYSE150 cells.

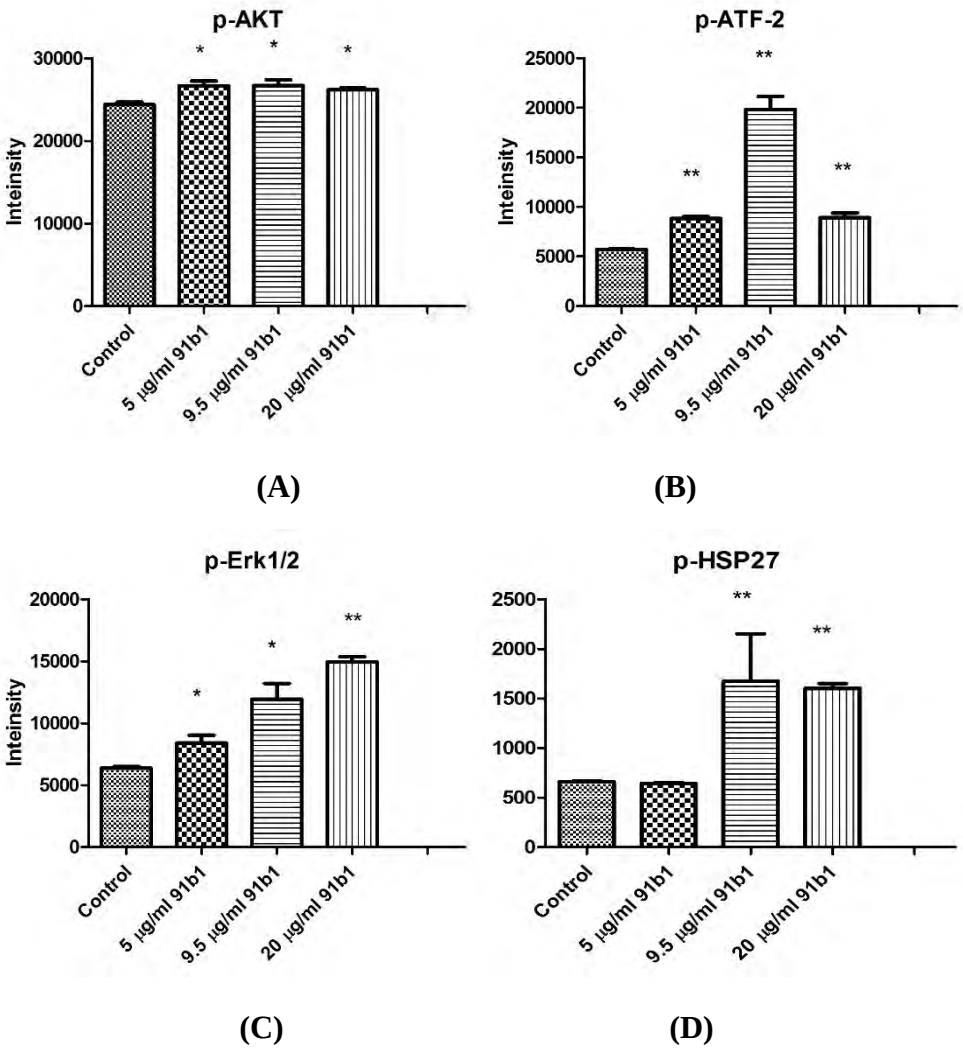

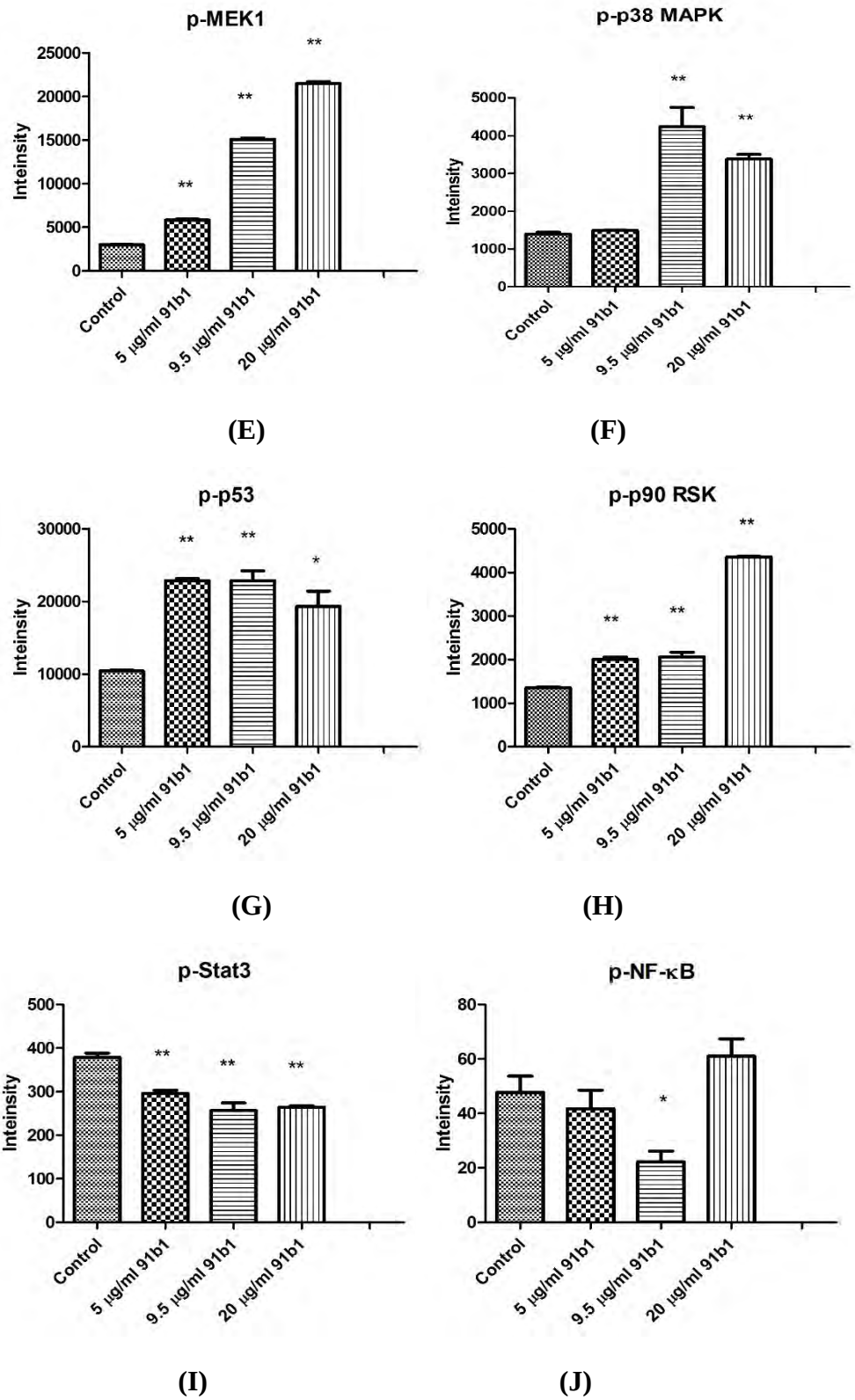


**Figure 4.6 Phosphorylated analytes from KYSE150 cells treated with different concentrations of compound 91b1 or vehicle control analyzed by Bio-plex 200. (A): Phosphorylated AKT(Ser$^{473}$); (B): Phosphorylated ATF-2 (Thr71); (C): Phosphorylated ErK1/2 (Thr202/Tyr204, Thr185/Tyr187); (D): Phosphorylated HSP27 (Ser78); (E): Phosphorylated MEK1 (Ser217/Ser221); (F):**

**Phosphorylated p38 MAPK (Thr180/Tyr182); (G): Phosphorylated p53 (Ser15); (H): Phosphorylated p90 RSK (Ser380) ; (I):Phosphorylated Stat 3 (Ser727); (J): Phosphorylated NF-κB p65(Ser$^{536}$). Compound 91b1 concentrations ranged from5, 9.5, and 20μg/mL. 0.1% DMSO was applied as the vehicle control. N=3.**

According to the results, the levels of phosphorylated AKT, ATF-2, ErK1/2, HSP27, MEK1, p38 MAPK, p53, and p90 RSK were increased significantly after treated with compound 91b1 and showed a dose-depend manner except for 20μg/mL in some groups (p-ATF-2, p-p38 MAPK, and p-p53 level after treated with 20μg/mL compound 91b1 were lower than those treated with 10μg/mL compound 91b1, but were still increased significantly than control). Phosphorylated Stat3 of cell lysates was decreased significantly as the concentrations of compound 91b1 were gradually increased.

### 4.1.8.2. IPA (Ingenuity Pathway Analysis)

To investigate the most associated pathways that the compound 91b1 involved, and together with its downstream effects on biological and disease processes, all the phosphorylated analytes were transformed to fold exchange format and analyzed by ingenuity pathway analysis software. Associated pathways were summarized in Figure 4.7.

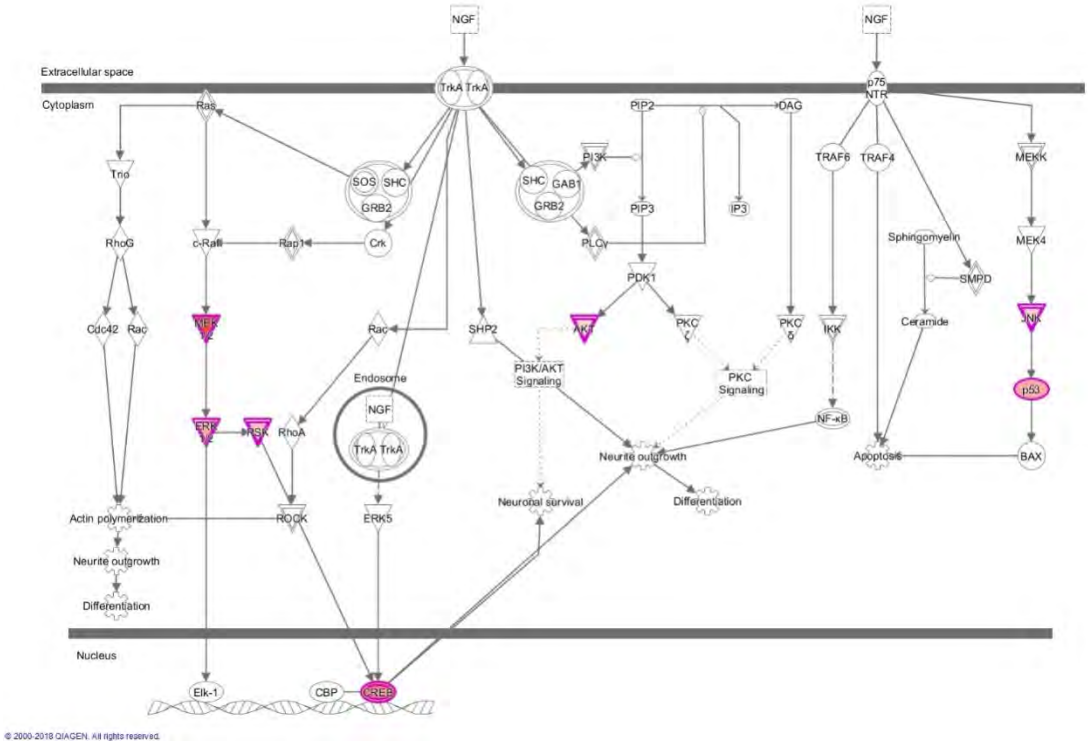


**Figure 4.7 Associated pathways and interactions analyzed by IPA software. Phosphorylated AKT, ATF-2, MEK1, ErK1/2, p38 MAPK, HSP27, p53, JNK, p90 RSK, and Stat 3 levels in the KYSE150 cell lysate after compound 91b1 treatment were detected by Bio-Plex 200 as described in the previous section. 0.1% DMSO was applied as vehicle control. N=3.**

According to the results of IPA software analysis, NGF (nerve growth factor) was screened out to be the most related pathway with all the pathways detected. The detailed analysis will be described in the discussion section.

### 4.1.9. Establishment of compound 91b1 analysis method by UPLC/MS

After analyzing the standard solution of compound 91b1 following the mentioned method in Section 3.26, the UPLC chromatogram and positive ion spectra of compound 91b1 and internal standard (IS) were obtained as shown in Figure 4.8.

Gradient elution program was summarized in Table 4.5. Mass spectrometry detection was performed by XEVO Triple Quadrupole MS equipped with an ESI source. The ESI source was set in positive ionization mode, the Capillary Voltage is 3.00kV, the Cone Voltage was 30V, the Source Temperature is 150 ℃, the Desolvation Temperature is 350 ℃, the Cone Gas Flow is 50 L/Hr, and the Desolvation Gas Flow is 800 L/Hr.

**Table 4.5 Gradient elution program of liquid chromatography method to analysis the compound 91b1.**

| Time (mins) | Flow Rate (ml/min) | A (%) 0.1% formic acid water | B (%) 0.1% formic acid acetonitrile |
|---|---|---|---|
| 0 | 0.35 | 90 | 10 |
| 2 | 0.35 | 90 | 10 |
| 6 | 0.35 | 10 | 90 |
| 7 | 0.35 | 10 | 90 |
| 9 | 0.35 | 90 | 10 |
| 11 | 0.35 | 90 | 10 |

**(A)**

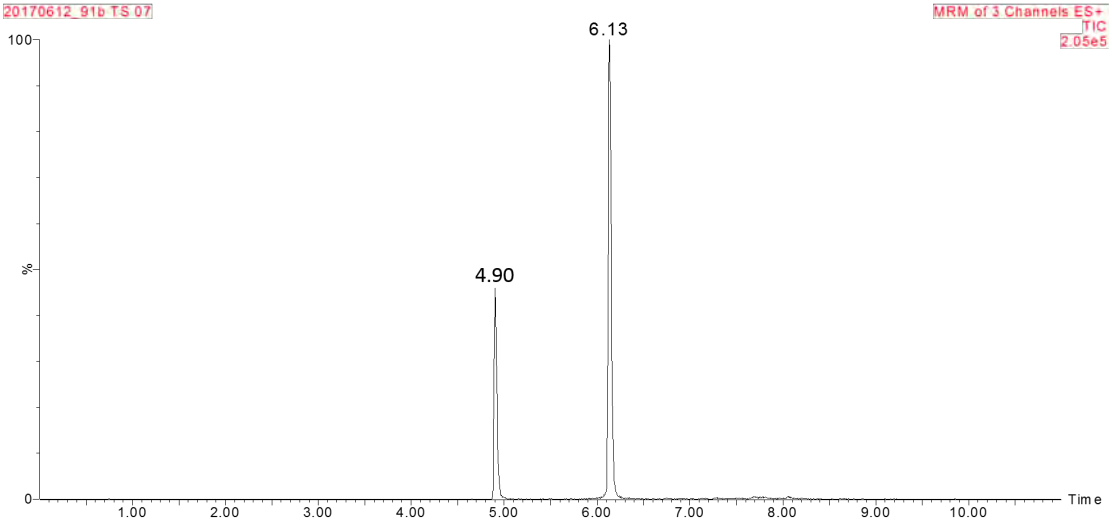
20170612_91b TS 07
MRM of 3 Channels ES+
TIC
2.05e5
100
%
0
6.13
4.90
1.00
2.00
3.00
4.00
5.00
6.00
7.00
8.00
9.00
10.00
Time

**(B)**

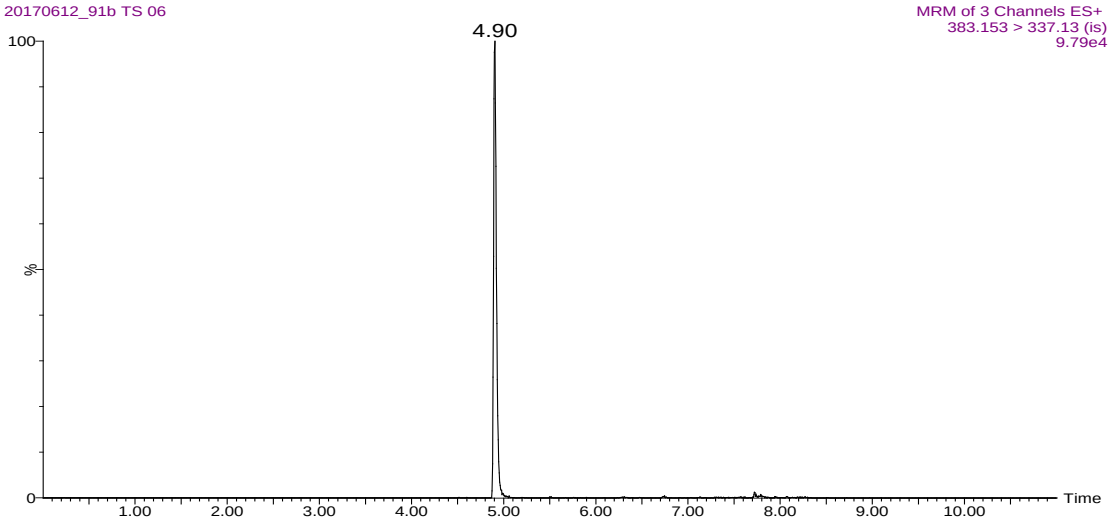
20170612_91b TS 06
MRM of 3 Channels ES+
383.153 > 337.13 (is)
9.79e4
100
%
0
4.90
1.00
2.00
3.00
4.00
5.00
6.00
7.00
8.00
9.00
10.00
Time

**(C)**

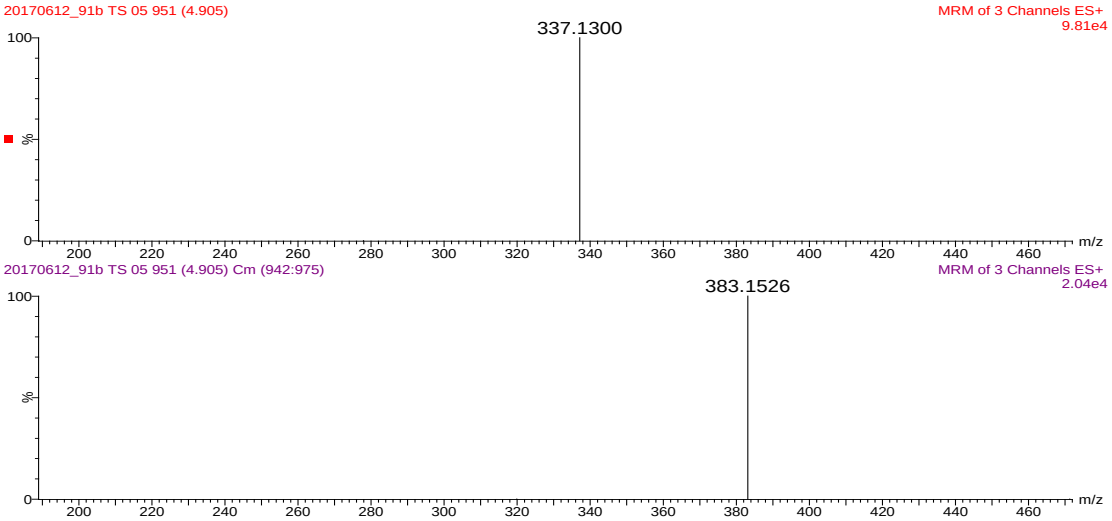
20170612_91b TS 05 951 (4.905)
MRM of 3 Channels ES+
9.81e4
337.1300
100
%
0
200 220 240 260 280 300 320 340 360 380 400 420 440 460
m/z
20170612_91b TS 05 951 (4.905) Cm (942:975)
MRM of 3 Channels ES+
2.04e4
383.1526
100
%
0
200 220 240 260 280 300 320 340 360 380 400 420 440 460
m/z

**(D)**

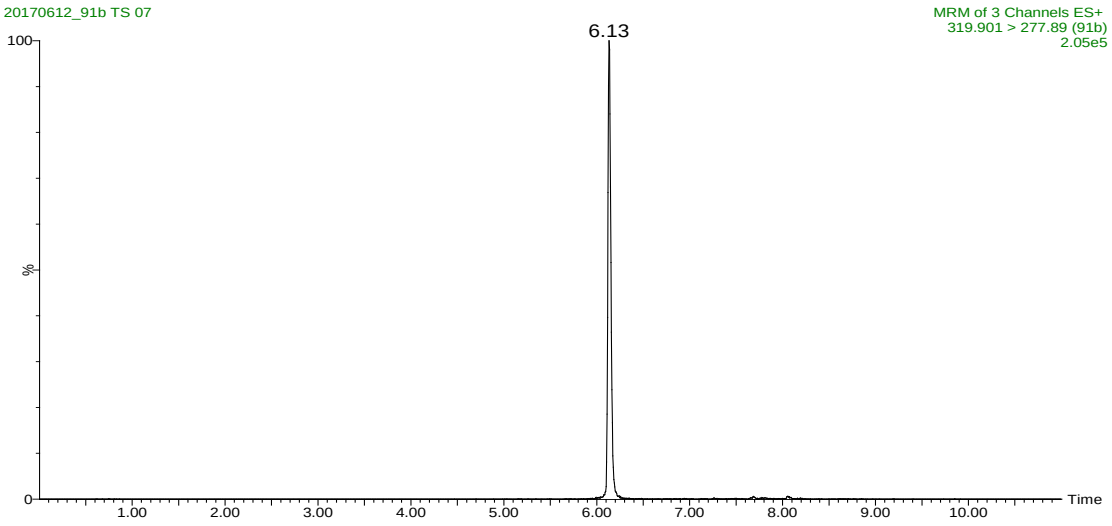
20170612_91b TS 07
MRM of 3 Channels ES+
319.901 > 277.89 (91b)
2.05e5
6.13
100
%
0
1.00 2.00 3.00 4.00 5.00 6.00 7.00 8.00 9.00 10.00
Time

**(E)**

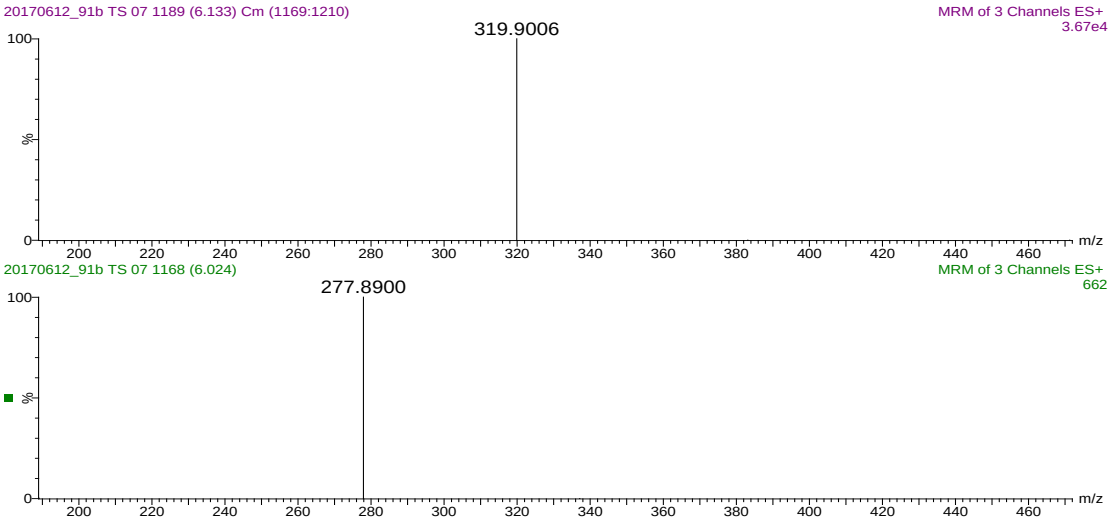


**Figure 4.8 Chromatograph of compound 91b1 analyzed by UPLC/MS. (A): Total ions chromatograph of compound 91b1 and IS (internal standard). The retention time of IS is 4.90 min, and the retention time of compound 91b1 is 6.13 min; (B): Ions chromatograph of IS; (C): Parents/daughter Mass to charge ratio (m/z) of IS is 383.153/337.13; (D): Ions chromatograph of compound 91b1; (E): Parents/daughter Mass to charge ratio (m/z) of compound 91b1 is 319.901/277.89. Compound 91b1 or internal standard was dissolved in methanol. Ioratadine was applied as internal standard.**

To establish a reliable quantitative analysis method, it is important to confirm the compounds studied in each test, as the compounds are probably degraded, or contaminated. The m/z showed by MS detection verified that the compound is the actual compound tested. Additionally, accurate concentrations of compound can be calculated by the area under the curve according to the standard curve to confirm the purity of the compound. Moreover, for the future research, pharmacokinetics behaviors will be studied *in vivo*. It is important to establish an analysis method to calculate the blood concentrations.

### 4.1.10. *In vivo* anti-cancer activity of compound 91b1

To study the *in vivo* anti-cancer activity of compound 91b1, tumor xenograft models induced by KYSE150 and KYSE450 cells were studied by monitoring the subcutaneous tumor sizes with the treatment of compound 91b1 compared to vehicle control group. Tumor size was calculated by the formula [$l$ x $w^2$] x 0.52 ( $l$ is length and $w$ is width)[158] and showed as relative volume ratio (relative tumor volume ratio on the measurement day = tumor volume on the measurement day/tumor volume of the first day). Table 4.6 and Table 4.7 summarized the relative tumor volume ratio data of KYSE450 xenograft compared with the vehicle control group, with the i.p. injection of 50 mg/kg/day for 25 days. Table 4.8 and Table 4.9 summarized the relative tumor volume ratio data of KYSE150 xenograft compared with the vehicle control group, with i.p, injection of 50 mg/kg/day for 25 days. Figure 4.8 shows the paired images of one animal from the vehicle control and the 91b1-treated group in KYSE450 on the first day and the 25$^{th}$ day. Figure 4.9 shows paired images of one animal from the vehicle control and the 91b1-treated group in KYSE150 on the first day and the 25$^{th}$ day. Figure 4.10 shows the changes of tumor size of the 91b1-treated group compared with the vehicle control group in KYSE450 xenograft by plotting the relative tumor volume ratio against the treatment time. Figure 4.11 shows tumor size changes of the 91b1-treated group compared with the vehicle control group in KYSE150 xenograft by plotting relative tumor volume ratio against the treatment time.

**Table 4.6 Relative tumor volume ratio derived from the vehicle control group in the KYSE450 tumor xenograft test for 25 days. 6% PEG saline was applied as vehicle control. N=5.**

| Ratio / Day | 1 | 2 | 3 | 4 | 5 | Mean | SD | RSD |
|---|---|---|---|---|---|---|---|---|
| 0 | 1.0 | 1.0 | 1.0 | 1.0 | 1.0 | 1.0 | 0.0 | 0.0 |
| 1 | 1.5 | 1.2 | 1.2 | 1.1 | 1.1 | 1.2 | 0.2 | 0.1 |
| 3 | 1.7 | 1.4 | 1.2 | 1.3 | 1.3 | 1.4 | 0.2 | 0.2 |
| 5 | 2.3 | 1.8 | 1.5 | 1.2 | 1.5 | 1.7 | 0.4 | 0.2 |
| 7 | 2.4 | 1.9 | 1.6 | 1.5 | 2.3 | 2.0 | 0.4 | 0.2 |
| 9 | 2.6 | 2.4 | 1.6 | 1.9 | 2.0 | 2.1 | 0.4 | 0.2 |
| 11 | 2.8 | 2.5 | 1.7 | 2.0 | 2.7 | 2.3 | 0.5 | 0.2 |
| 13 | 2.9 | 3.3 | 2.0 | 2.0 | 3.7 | 2.8 | 0.8 | 0.3 |
| 15 | 4.0 | 3.6 | 2.3 | 2.3 | 3.6 | 3.2 | 0.8 | 0.3 |
| 17 | 4.5 | 4.4 | 2.8 | 2.7 | 3.9 | 3.7 | 0.9 | 0.2 |
| 19 | 4.4 | 4.6 | 4.6 | 2.8 | 5.0 | 4.3 | 0.9 | 0.2 |
| 21 | 5.0 | 4.6 | 3.4 | 3.1 | 6.2 | 4.5 | 1.2 | 0.3 |
| 23 | 7.1 | 4.8 | 1.7 | 2.9 | 6.5 | 4.6 | 2.3 | 0.5 |
| 25 | 8.8 | 6.1 | 1.2 | 2.4 | 4.9 | 4.7 | 3.0 | 0.6 |

**Table 4.7 Relative tumor volume ratio derived from the compound 91b1 treated group (50mg/kg/day 91b1) in the KYSE450 tumor xenograft test for 25 days. N=5.**

| Ratio / Day | 1 | 2 | 3 | 4 | 5 | Mean | SD | RSD |
|---|---|---|---|---|---|---|---|---|
| 0 | 1.0 | 1.0 | 1.0 | 1.0 | 1.0 | 1.0 | 0.0 | 0.0 |
| 1 | 1.0 | 1.1 | 1.1 | 1.2 | 1.1 | 1.1 | 0.1 | 0.1 |
| 3 | 1.1 | 1.2 | 0.8 | 1.3 | 1.1 | 1.1 | 0.2 | 0.2 |
| 5 | 1.2 | 1.0 | 0.7 | 1.5 | 1.1 | 1.1 | 0.3 | 0.3 |
| 7 | 1.2 | 0.8 | 0.4 | 1.8 | 1.2 | 1.1 | 0.5 | 0.5 |
| 9 | 1.5 | 1.4 | 0.2 | 2.1 | 1.5 | 1.4 | 0.7 | 0.5 |
| 11 | 1.7 | 1.0 | 0.1 | 2.7 | 1.7 | 1.5 | 0.9 | 0.7 |
| 13 | 1.8 | 0.9 | 0.0 | 2.9 | 1.8 | 1.5 | 1.1 | 0.7 |
| 15 | 2.0 | 0.8 | 0.0 | 3.1 | 3.3 | 1.9 | 1.4 | 0.8 |
| 17 | 1.6 | 0.9 | 0.0 | 4.0 | 4.2 | 2.1 | 1.9 | 0.9 |
| 19 | 1.5 | 1.1 | 0.0 | 4.0 | 4.7 | 2.2 | 2.0 | 0.9 |
| 21 | 1.5 | 1.5 | 0.0 | 3.8 | 5.3 | 2.4 | 2.1 | 0.9 |
| 23 | 1.1 | 1.5 | 0.0 | 4.4 | 6.1 | 2.6 | 2.5 | 1.0 |
| 25 | 1.0 | 1.7 | 0.0 | 3.5 | 5.2 | 2.3 | 2.1 | 0.9 |

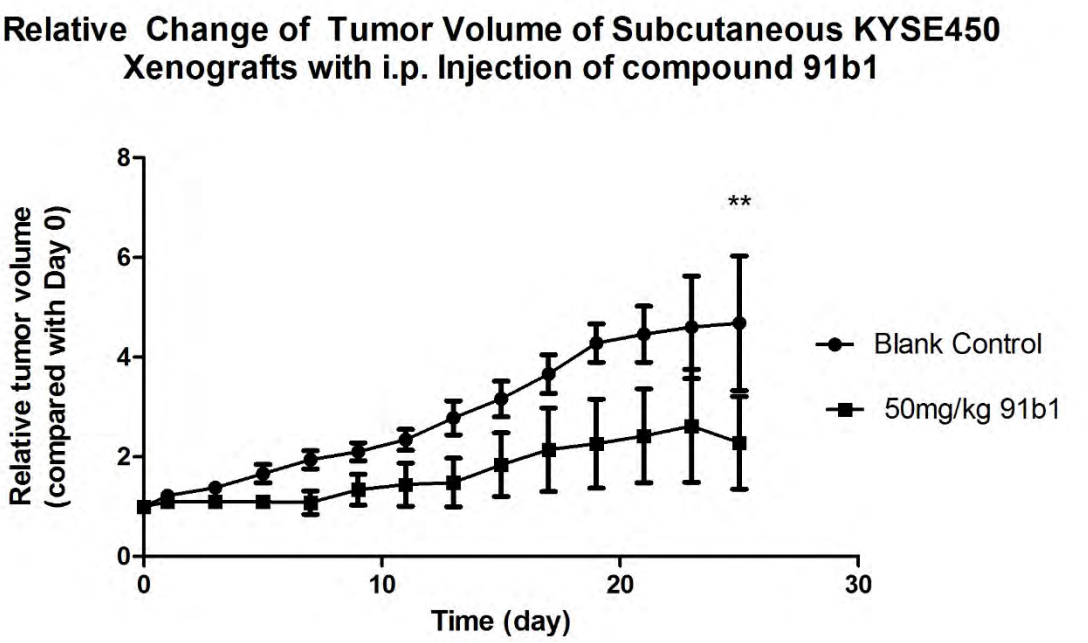


**Figure 4.9 Relative tumor volume changes of subcutaneous KYSE450 xenografts compared between the vehicle control group and compound 91b1 treated group (50mg/kg/day compound 91b1) after 25 days. 6% PEG saline was applied as vehicle control. N=5. ** P-value < 0.05.**

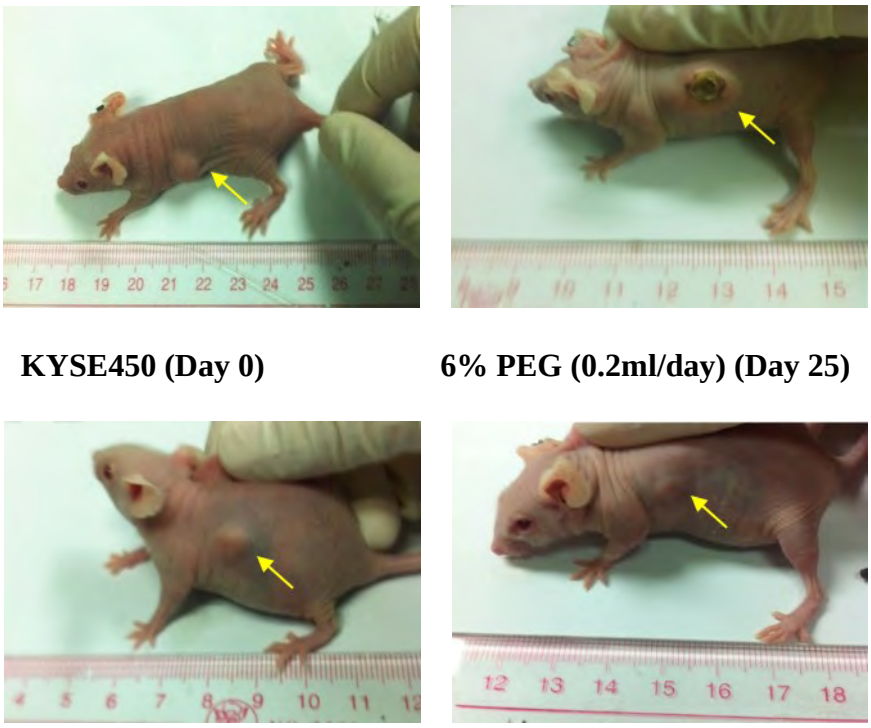

**KYSE450 (Day 0)** **6% PEG (0.2ml/day) (Day 25)**

**KYSE450 (Day 0)** **50mg/kg/day 91b1(0.2ml/day) (Day 25)**

**Figure 4.10 Images of one animal from the vehicle control group and compound 91b1 treated group in KYSE450 xenograft test at the first day and the 25th day.**

According to tables 4.6 and 4.7 and figures 4.9 and 4.10, in KYSE450 tumor xenograft test, the tumor volume of the nude mice in the vehicle control group increased gradually every day and reached about 5 times larger compared to the initial day. Whereas the average tumor volume of the nude mice with the administration of 50mg/kg/day compound 91b1 was controlled at 2 times volume comparing to the initial day, in which one of the tumor size was remained as the initial size, and the other tumor size was even totally invisible at 13$^{th}$ day without relapse. At the 25$^{th}$ day, the volume of the tumor in compound 91b1 treated group was significantly reduced ($p$=0.007) comparing to the vehicle control group. Therefore, compound 91b1 showed a significant *in vivo* anti-tumor effect on the KYSE450 tumor xenograft model.

**Table 4.8 Relative tumor volume ratio derived from the vehicle control group in the KYSE150 tumor xenograft test for 25 days. 6% PEG saline was applied as vehicle control. N=5.**

| Ratio / Day | 1 | 2 | 3 | 4 | 5 | Mean | SD | RSD |
|---|---|---|---|---|---|---|---|---|
| 0 | 1.0 | 1.0 | 1.0 | 1.0 | 1.0 | 1.0 | 0.0 | 0.0 |
| 1 | 1.3 | 1.2 | 1.1 | 1.0 | 1.3 | 1.2 | 0.1 | 0.0 |
| 3 | 2.3 | 1.9 | 1.6 | 1.6 | 1.5 | 1.8 | 0.3 | 0.1 |
| 5 | 3.6 | 2.4 | 1.8 | 1.8 | 3.0 | 2.5 | 0.8 | 0.2 |
| 7 | 2.9 | 2.8 | 2.1 | 2.1 | 5.2 | 3.0 | 1.3 | 0.2 |
| 9 | 3.5 | 3.0 | 2.1 | 2.9 | 5.2 | 3.3 | 1.2 | 0.2 |
| 11 | 3.5 | 3.2 | 2.8 | 3.2 | 6.8 | 3.9 | 1.6 | 0.2 |
| 13 | 4.6 | 3.6 | 3.6 | 3.6 | 7.9 | 4.7 | 1.9 | 0.2 |
| 15 | 4.9 | 3.2 | 4.7 | 4.9 | 10.7 | 5.7 | 2.9 | 0.3 |
| 17 | 4.8 | 3.6 | 5.5 | 7.0 | 10.9 | 6.4 | 2.8 | 0.2 |
| 19 | 6.4 | 4.5 | 5.4 | 9.3 | 13.3 | 7.8 | 3.6 | 0.2 |
| 21 | 5.7 | 3.3 | 5.9 | 9.6 | 13.6 | 7.6 | 4.0 | 0.3 |
| 23 | 5.7 | 5.3 | 5.2 | 12.1 | 14.1 | 8.5 | 4.3 | 0.3 |
| 25 | 6.9 | 4.7 | 7.8 | 12.6 | 16.0 | 9.6 | 4.6 | 0.2 |

**Table 4.9 Relative tumor volume ratio derived from the compound 91b1 treated group (50mg/kg/day 91b1) in the KYSE150 tumor xenograft test for 25 days. N=5.**

| Ratio / Day | 1 | 2 | 3 | 4 | 5 | Mean | SD | RSD |
|---|---|---|---|---|---|---|---|---|
| 0 | 1.0 | 1.0 | 1.0 | 1.0 | 1.0 | 1.0 | 0.0 | 0.0 |
| 1 | 1.3 | 1.1 | 1.2 | 1.2 | 1.1 | 1.2 | 0.1 | 0.0 |
| 3 | 1.4 | 1.8 | 1.5 | 1.4 | 1.3 | 1.5 | 0.2 | 0.1 |
| 5 | 1.5 | 2.4 | 1.7 | 1.5 | 1.4 | 1.7 | 0.4 | 0.1 |
| 7 | 1.7 | 2.7 | 2.5 | 2.1 | 1.8 | 2.2 | 0.4 | 0.1 |
| 9 | 1.9 | 3.7 | 2.7 | 2.9 | 2.0 | 2.6 | 0.7 | 0.1 |
| 11 | 3.1 | 4.2 | 3.2 | 3.9 | 1.3 | 3.1 | 1.1 | 0.2 |
| 13 | 3.6 | 5.2 | 3.4 | 4.5 | 2.2 | 3.8 | 1.1 | 0.2 |
| 15 | 5.3 | 6.2 | 4.1 | 5.7 | 2.0 | 4.7 | 1.7 | 0.2 |
| 17 | 5.6 | 8.4 | 5.2 | 6.9 | 3.1 | 5.9 | 1.9 | 0.2 |
| 19 | 7.4 | 9.0 | 5.4 | 8.2 | 4.3 | 6.9 | 1.9 | 0.1 |
| 21 | 9.7 | 10.4 | 7.2 | 9.9 | 4.7 | 8.4 | 2.4 | 0.1 |
| 23 | 9.9 | 12.9 | 7.2 | 12.1 | 6.4 | 9.7 | 2.9 | 0.1 |
| 25 | 11.0 | 13.8 | 9.7 | 13.3 | 7.3 | 11.0 | 2.7 | 0.1 |

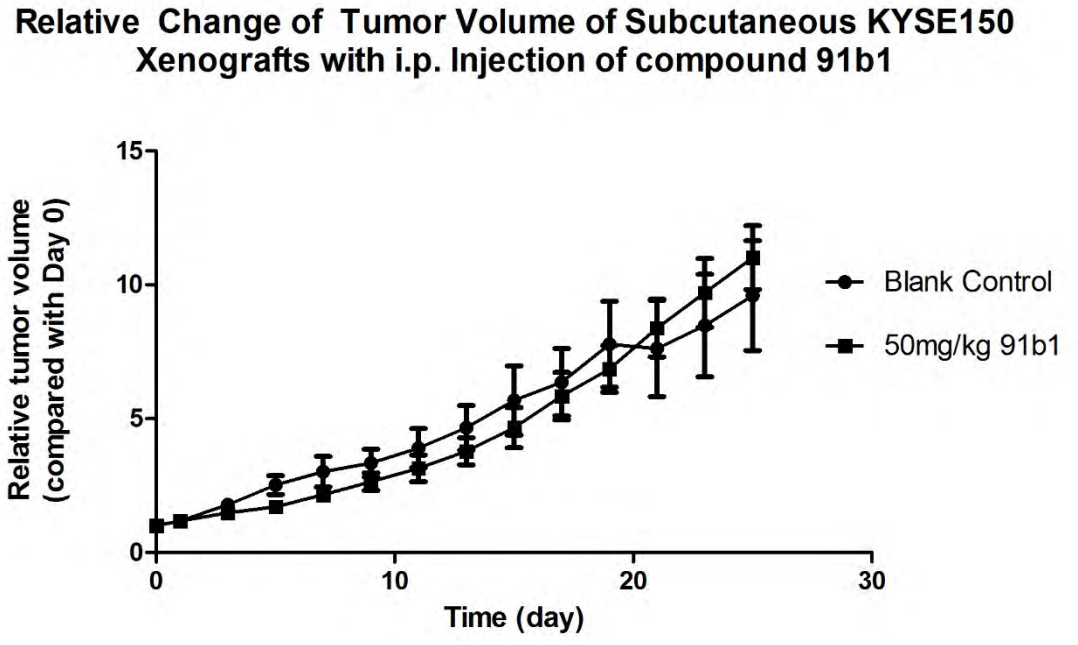


**Figure 4.11 Relative tumor volume changes of subcutaneous KYSE150 xenografts with vehicle control group and compound 91b1 treated group (50mg/kg/day compound 91b1). 6% PEG saline was applied as vehicle control. N=5. (p-value =0.007)**

**KYSE150 (Day 0)**

**6% PEG (0.2ml/day) (Day 25)**

**KYSE150 (Day 0)**

**50mg/kg/day 91b1(0.2ml/day) (Day 25)**

**Figure 4.12 Images of one animal from vehicle control group and compound 91b1 treated group in KYSE150 xenograft test on the first day and the 25$^{th}$ day.**

According to tables and figures, in KYSE150 tumor xenograft test, the tumor volume of the nude mice in vehicle control group was increased gradually every day and reached about 9.6 times larger comparing to the initial day, in which the tumor of one animal even grew to 16 times larger than the first day, suggesting that KYSE150 tumor developed quickly in nude mice. Whereas the average tumor volume of the nude mice with the administration of 50mg/kg/day compound 91b1 was increased to about 11 times larger than the initial day. The tumor volume of KYSE150 tumor xenografts for the compound 91b1 treated group showed no significant difference during the treatment period

### 4.1.11. Serum biomarker analysis

To analyze the possible changes in liver function after compound 91b1 treatment, some serum parameters including the level of albumin (ALB), alanine aminotransferase (ALT), aspartate aminotransferase (AST), urea and total bilirubin (TBil) were determined by Hitachi automatic biochemical analyzer. Table 4.10 summarizes the levels of serum biochemical parameters of the mice treated with 10mg/kg or 50mg/kg compound 91b1. Figure 4.12 shows that ALB and ALP level of compound-treated groups were significantly decreased compared to the blank control group (ALB from 27.6 to 26.6, and ALP from 92.00 to 56.40) in KYSE450 xenograft nude mice model. Table 4.11 summarizes the serum biochemical parameters in KYSE150 xenograft animals treated with either 10mg/kg or 50mg/kg compound 91b1 comparing with vehicle control.

**Table 4.10 Serum biochemical parameters in KYSE450 xenograft animals treated with either 10 mg/kg or 50 mg/kg compound 91b1 comparing with vehicle control.**

| | **Blank control** | | **91b1 10mg/kg** | | | **91b1 50mg/kg** | | |
|---|---|---|---|---|---|---|---|---|
| | Mean | RSD | Mean | RSD | P | Mean | RSD | p |
| **ALB** | 31.60 | 0.05 | 24.60 | 0.08 | 0.00 | 26.60 | 0.10 | 0.01 |
| **ALP** | 92.00 | 0.13 | 50.40 | 0.31 | 0.00 | 56.40 | 0.25 | 0.00 |
| **ALT** | 29.60 | 0.15 | 28.80 | 0.27 | 0.85 | 29.00 | 0.26 | 0.88 |
| **AST** | 195.00 | 0.06 | 170.20 | 0.13 | 0.05 | 162.40 | 0.37 | 0.27 |
| **TP** | 54.60 | 0.11 | 47.80 | 0.07 | 0.06 | 47.20 | 0.16 | 0.12 |

| | | | | | | | | |
|---|---|---|---|---|---|---|---|---|
| **TBil** | 0.54 | 0.43 | 0.82 | 0.43 | 0.18 | 0.34 | 0.61 | 0.19 |
| **Urea** | 17.00 | 0.52 | 8.60 | 0.44 | 0.09 | 21.60 | 0.39 | 0.42 |
| **AST/ALT** | 6.70 | 0.14 | 6.37 | 0.34 | 0.76 | 5.90 | 0.45 | 0.54 |

**ALB: albumin; ALP: alkaline phosphatase; ALT: alanine aminotransferase; AST: aspartate transaminase; TP: total protein; TBil: total bilirubin. P: p value calculated by t test. 6% PEG saline was applied as vehicle control. N=5.**

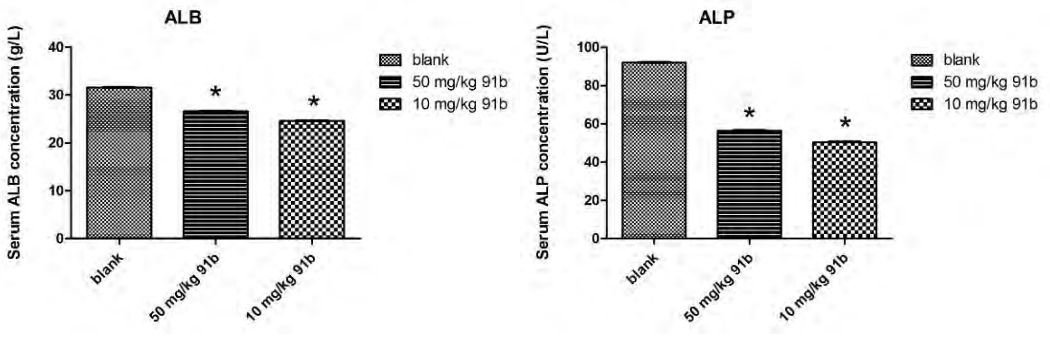


**(A)** **(B)**

**Figure 4.13 Assessment on liver function based on ALB and ALP changes inKYSE450 xenograft animals treated with either 10mg/kg or 50mg/kg compound 91b1 comparing with vehicle control. 6% PEG saline was applied as vehicle control. (A): Serum ALB changes of KYSE450 xenograft animals treated with compound 91b1 or vehicle control; (B): Serum ALP changes of KYSE450 xenograft animals treated with compound 91b1 or vehicle control. N=5. *: p<0.01.**

**Table 4.11 Serum biochemical parameters in KYSE150 xenograft animals treated with either 10 mg/kg or 50 mg/kg compound 91b1 comparing with vehicle control.**

| | **Blank control** | | **91b1 10mg/kg** | | | **91b1 50mg/kg** | | |
|---|---|---|---|---|---|---|---|---|
| | **Mean** | **RSD** | **Mean** | **RSD** | **p** | **Mean** | **RSD** | **p** |
| **ALB** | 21.80 | 0.23 | 24.60 | 0.09 | 0.30 | 22.80 | 0.12 | 0.71 |
| **ALP** | 32.60 | 0.34 | 44.00 | 0.24 | 0.13 | 41.40 | 0.27 | 0.25 |
| **ALT** | 26.60 | 0.33 | 55.40 | 1.40 | 0.43 | 21.60 | 0.33 | 0.35 |

| | | | | | | | | |
|---|---|---|---|---|---|---|---|---|
| **AST** | 163.00 | 0.39 | 156.20 | 0.29 | 0.85 | 119.20 | 0.25 | 0.20 |
| **TP** | 38.00 | 0.29 | 41.20 | 0.02 | 0.54 | 40.00 | 0.09 | 0.71 |
| **TBil** | 0.58 | 0.68 | 0.82 | 0.22 | 0.25 | 0.54 | 0.31 | 0.84 |
| **Urea** | 38.00 | 1.41 | 7.20 | 0.35 | 0.24 | 12.00 | 0.76 | 0.32 |
| **AST/ALT** | 6.19 | 0.33 | 6.10 | 0.66 | 0.97 | 5.77 | 0.23 | 0.71 |

**ALB: albumin; ALP: alkaline phosphatase; ALT: alanine aminotransferase; AST: aspartate transaminase; TP: total protein; TBil: total bilirubin. P: p value calculated by t test. 6% PEG saline was applied as vehicle control. N=5.**

## 4.1.12. *In vivo* toxicity test

### 4.1.12.1. Acute toxicity

To evaluate the acute toxicity of compound 91b1, either 800 mg/kg compound 91b1 or vehicle control was administrated orally to SD rats. The rates were observed at 5min, 30min, 1h, 4h, 8h, 12h, 24h, 48h after administration. All the animals in treated group and control group survived. There was no sign of deteriorated status of health in the animals that was observable. In general, there was no change of skin hair, movement activities, salivary secretion, eating, and drinking behaviors, and defecation activities compared with the vehicle control group. After 48-hour observation, the animals in each group were sacrificed and dissected. Animal livers were separated, and no visible pathological changes were observed. Figure 4.13 shows the images of liver from the vehicle control group and compound 91b1 treated group.

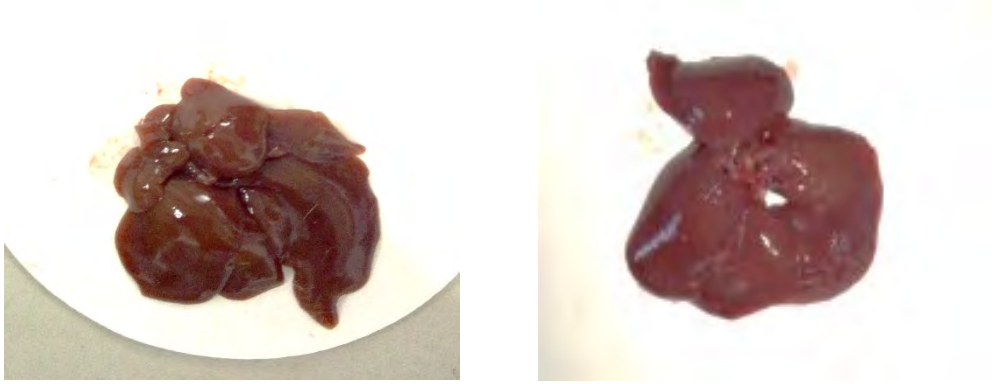

**(A)** **(B)**

**Figure 4.14 Images of liver condition from acute toxicity test. A: liver from vehicle control group; B: liver from compound 91b1 treated group in 800mg/kg.**

### 4.1.12.2. Chronic Toxicity

To evaluate the *in vivo* chronic toxicity of compound 91b1, 500 mg/kg/day compound 91b1 was administrated for 7 days, and 6% PEG saline was applied as the vehicle control. After 7-day administration and observation, the animals in the vehicle control group and compound treated group all survived. Then they were sacrificed and dissected to get the vital organs. There was no morphologically obvious injuries on heart, lung, and kidney. Figure 4.14 shows the images of liver from the vehicle control group and compound 91b1 treated group.

**(A)**

**(B)**

**(C)**

**(D)**

**Figure 4.15 Images of liver condition from chronic toxicity test. (A): Liver from vehicle control group; (B): liver from compound 91b1 treated group in 500mg/kg/day for 7 days; (C): liver andintestines observed from the vehicle control group; (D): liver and intestines observed from the compound 91b1 treated group. 6% PEG saline was applied as the vehicle control. N=5.**

Comparing the liver condition after dissection, the liver from compound 91b1 treated group was observed to be attached to intestines and revealed mild liver cirrhosis. Liver cirrhosis is defined as the histological development of regenerative nodules surrounded by fibrous band induced by chronic liver injury or liver disease[159]. It is reported that AST and ALT were often normal or moderately raised, ALP was increased by less than three-fold, and ALB was usually decreased in cirrhosis[160].

Additionally, data from serum biomarker tests showed consistent result. ALT and AST level of both KYSE450 and KYSE150 xenograft animals treated with compound 91b1 showed no significant difference. ALP level of KYSE 150 xenograft animals treated with compound 91b1 reveled increase trend. ALB level of KYSE450 xenograft animals treated with compound 91b1 exhibited decreased trend. However, the mentioned biomarkers changes were not significant according to statistic calculation, suggested that quinoline compound 91b1 showed no obvious toxicity to the rats at the maximum dose of 500 mg/kg in chronic treatment but induced a mild degree of liver damage.

## 4.2. Study of the functional roles of lumican in cancer cells

### 4.2.1. Induction of tumor formation in the lumican transfected non-tumor cells

To identify the function of lumican gene in tumorigenesis and development, NIH3T3 parental, NIH 3T3/Lum or NIH 3T3/Mock cells were subcutaneously injected into the franks of female Balb/c athymic nude mice. After a 14-day period, the possible formation of subcutaneous tumor was observed. Figure 4.16 shows images of each animal in NIH 3T3 parental group, NIH 3T3/Mock group, and NIH 3T3/Lum group on day 0, day 7 and day 14.

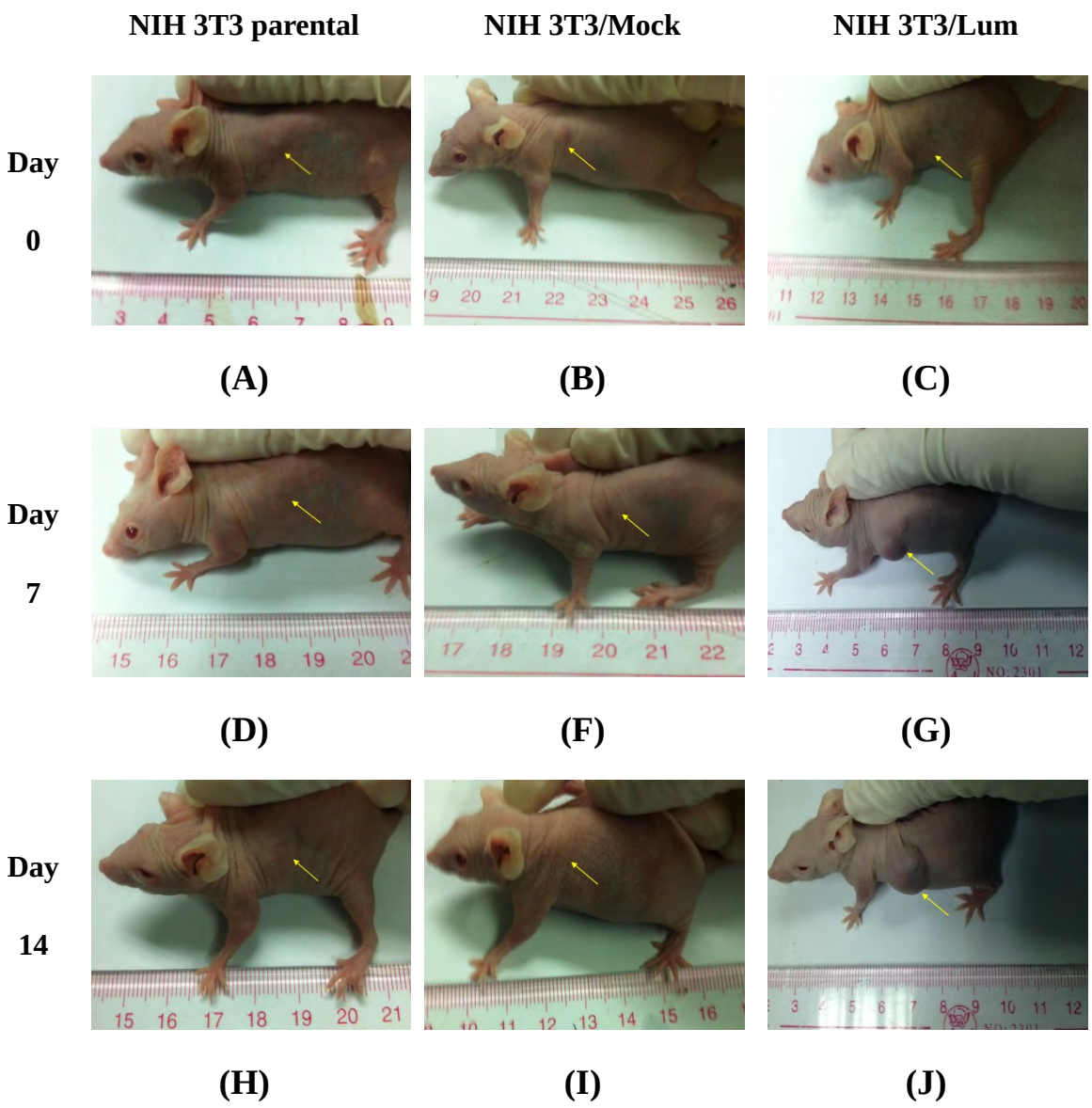


**Figure 4.16 Images of subcutaneous tumor formation in the nude mice with the injection of NIH 3T3 parental cells, Mock vector, or lumican Gene transfected NIH 3T3 cells on day 0, day 7, and day 14 respectively after injection. (A, D, and H): images of one animal from NIH 3T3 parental cells injected group on day 0, day 7, and day 14; (B, F, and I): images of one animal from Mock vector transfected NIH 3T3 cells injected group on day 0, day 7, and day 14; (C, G, and J): images of one animal from gene lumican transfected NIH 3T3 cells injected group on day 0, day 7, and day 14.**

According to the images, no visible subcutaneous mass was observed in the NIH 3T3 parental group and NIH 3T3/Mock group, whereas a gradually increased

subcutaneous tumor mass was observed in the animals injected with NIH 3T3/Lum group, suggesting that the gene lumican may play an important role in tumor tumorigenesis and development when it is overexpressed.

### 4.2.2. Lumican expression level in cancer cells and normal cells

Relative expression levels of lumican in seven cancer cell lines were compared with the non-tumor cell line (NE3) after normalized by the expression of β-actin and calculated by $2^{\wedge(-\Delta\Delta Ct)}$ method by qPCR.

**Table 4.12 Relative lumican expression level in seven cancer cell lines (KYSE30, KYSE70, KYSE150, KYSE450, KYSE510, HK3, and SLMT1) compared with the non-tumor cell line (NE-3).**

| Cell Lines | Cq | | ΔCq | ΔΔ Cq | 2^ (-ΔΔ Ct) | Lumican Expression Status |
|---|---|---|---|---|---|---|
| | Reference Gene | Lum | | | | |
| KYSE30 | 17.47 | 26.52 | 9.05 | -3.65 | 12.55 | overexpressed |
| KYSE70 | 15.38 | 26.68 | 11.3 | -1.40 | 2.64 | overexpressed |
| KYSE150 | 15.46 | 26.71 | 11.25 | -1.45 | 2.73 | overexpressed |
| KYSE450 | 14.61 | 27.22 | 12.61 | -0.09 | 1.06 | No significant difference |
| KYSE510 | 15.6 | 27.46 | 11.86 | -0.84 | 1.79 | overexpressed |
| HK3 | 13.43 | 26.74 | 13.31 | 0.61 | 0.66 | downregulated |
| SLMT1 | 14.29 | 25.57 | 11.28 | -1.42 | 2.681 | overexpressed |
| NE-3 | 14.55 | 27.25 | 12.7 | 0.00 | 1.00 | (Control) |

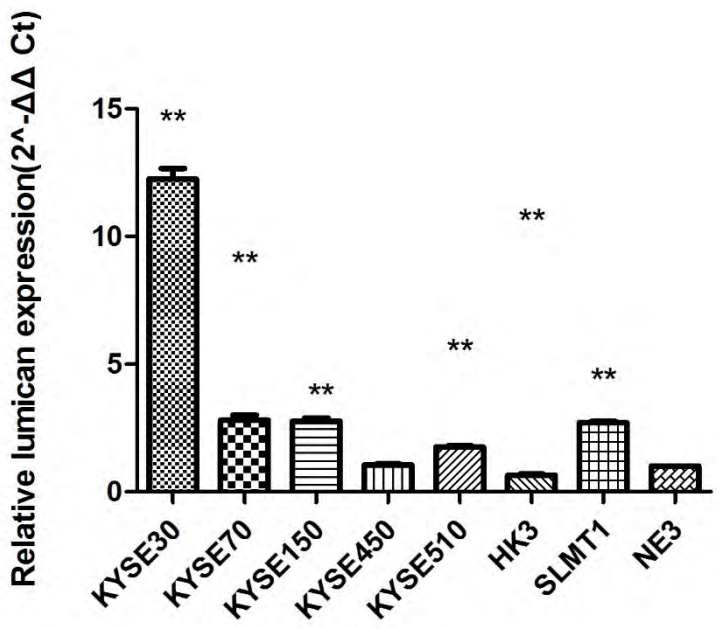


**Figure 4.17 Relative lumican expression levels in seven cancer cell lines and the non-tumor cell line (NE3). The relative lumican expression level was determined by comparing with NE-3, after being normalized with the expression of β-actin. ** p<0.01.**

Five out of seven (71.4%) cancer cell lines KYSE30, KYSE70, KYSE150, KYSE510, and SLMT1 showed higher relative expression level of lumican than NE-3, one cancer cell line HKESC3[161] showed lower relative expression level of lumican than NE-3, while one cancer cell line KYSE450 showed no significant difference of relative lumican expression comparing with NE-3.

### 4.2.3. Lumican expression level in ESCC patients' tumor specimen

Relative expression levels of lumican in tumor tissues were compared with the adjacent normal tissue after being normalized by the expression of β-actin and calculated by ΔCt (ΔCt = Cq of lumican – Cq of β-actin) by QRTPCR. The scatter plot was shown in Figure 4.18.

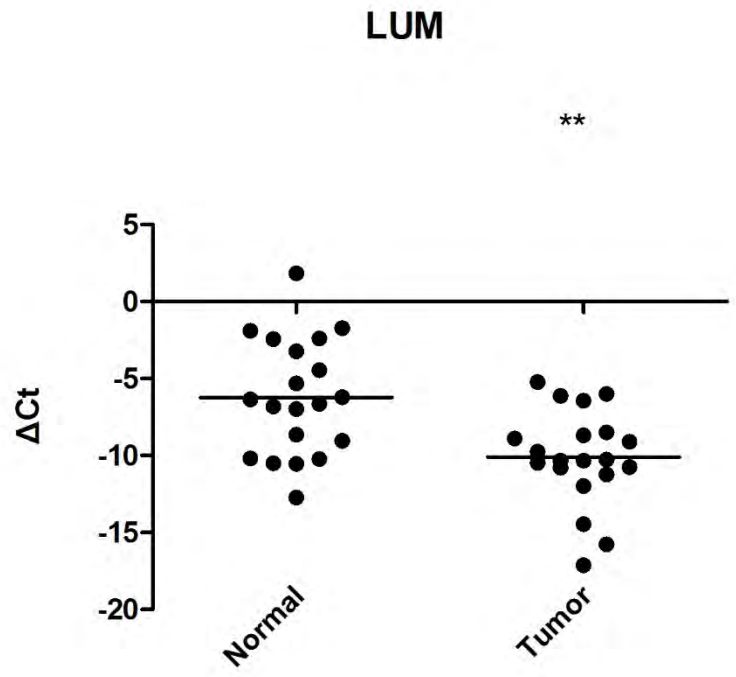


**Figure 4.18 Relative lumican expression level in tumor tissue and adjacent normal tissue isolated from cancer patients. β-actin was applied as the reference gene to normalize the lumican expression. N=20.** p<0.01.**

According to Figure 4.18, ΔCt of tumor sample group is lower than normal sample group, therefore, the Cq number of lumican of tumor sample group is less than normal sample group, indicating that the relative expression level of lumican if tumor sample group is in general higher than the non-tumor samples group. Therefore lumican is usually overexpressed in tumor patients.

### 4.2.4. Trans-well analysis

The change in cell invasion ability with or without the presence of lumican protein was tested by trans-well matrigel invasion assay. KYSE150 cells were seeded with increasing concentrations of purified human recombinant lumican (recLumican) for 24 hours. Transmembrane cells were stained with crystal violet and counted under the

microscope in a random 4 fields. Images of crystal violet stained cells were shown in Figure 4.19. The average invaded cell numbers among the groups were summarized in Figure 4.20.

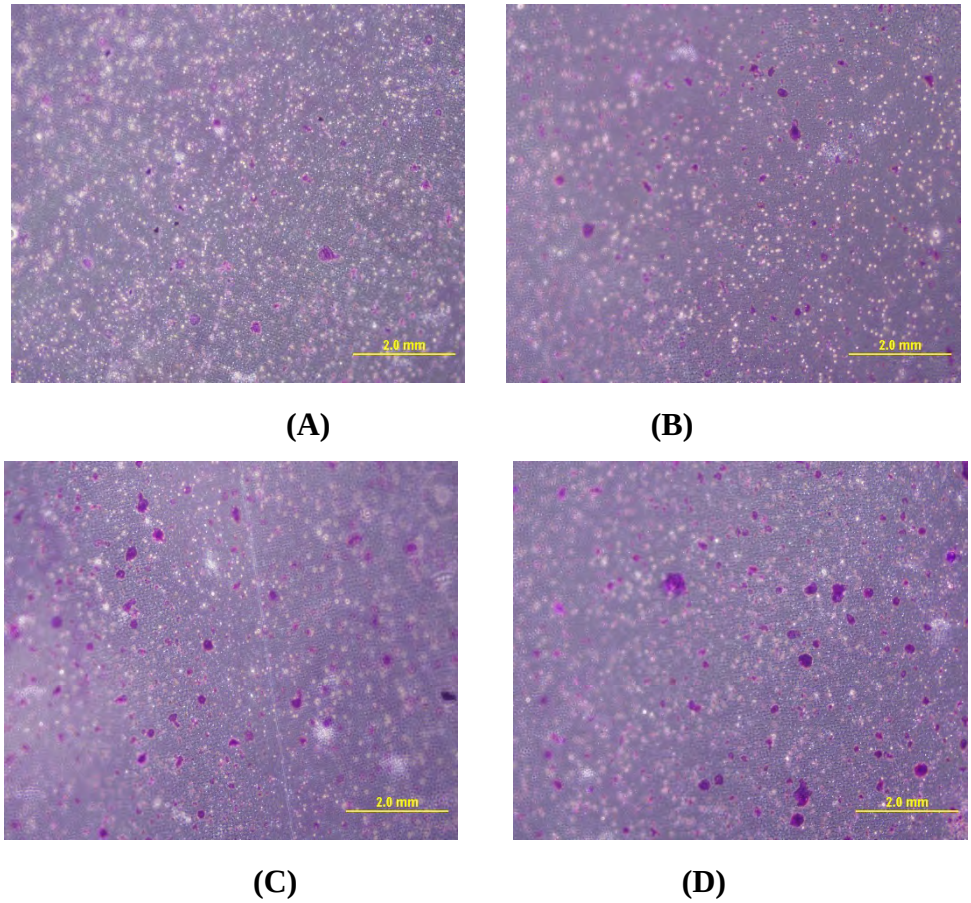


**Figure 4.19 Cell invasion assay with the use trans-well matrigel chamber and KYSE150 cells co-cultured with different concentrations of purified human recombinant lumican. (A): KYSE150 cells co-cultured with 0 ng/ml recLumican; (B): KYSE150 cells co-cultured with 50 ng/mL recLumican; (C): KYSE150 cells co-cultured with 250 ng/mL recLumican; (D): KYSE150 cells co-cultured with 500 ng/mL reclumican. Original magnification: x40.**

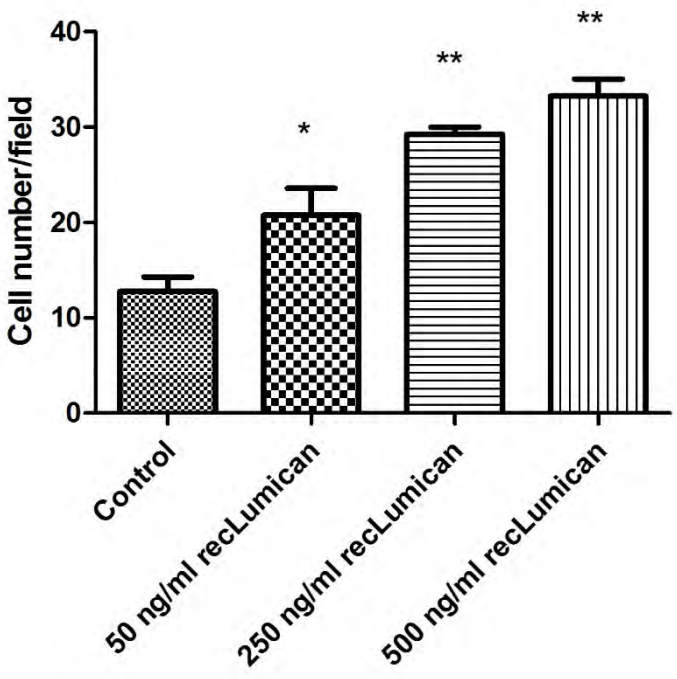


**Figure 4.20 Average invaded cell numbers of KYSE150 co-cultured with different concentrations of purified human recombinant lumican (0, 50, 250, 500 ng/mL recLumican). The invaded cells were counted under the microscope in 4 random fields at the original magnification of 40x. * $p < 0.05$; ** $p < 0.01$.**

The invaded cell number of KYSE150 co-cultured with recLumican was increased along with the increasing concentration of recLumican compared with the control group. The results suggested that protein lumincan enhances cancer-cell invasion.

### 4.2.5. Proliferation Assay

To further study the functional roles of lumican on cancer cell growth, cell proliferation assay was performed by MTS on A549, AGS, KYSE150, and KYSE450 cells co-cultured with or without recLumican at the concentration of 250 ng/mL (based on the results of cell invasion assay). The results are shown in Figure 4.21.

**(A)**

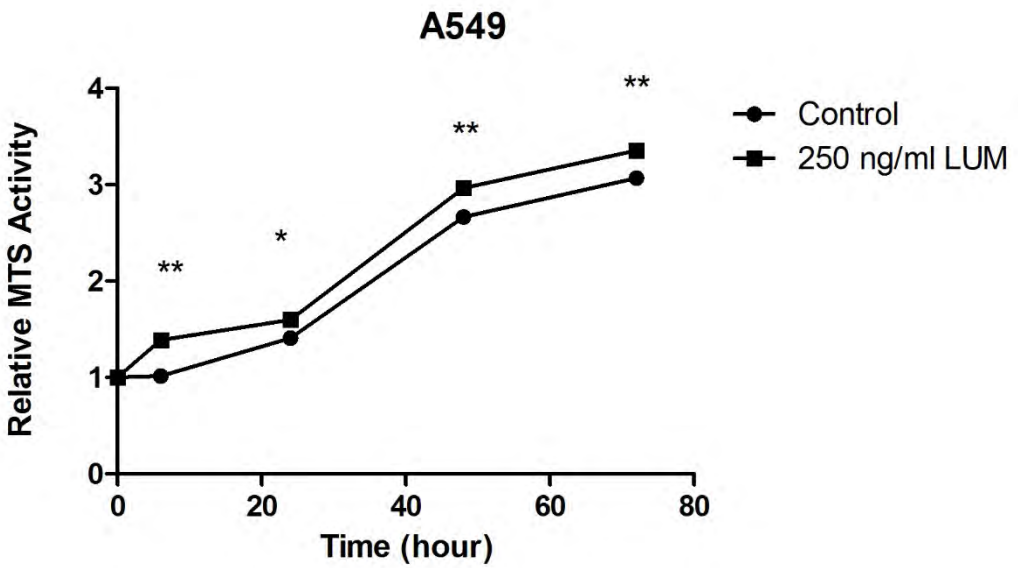
A549
Relative MTS Activity
Time (hour)
Control
250 ng/ml LUM
**
*
**
**
0
1
2
3
4
0
20
40
60
80

**(B)**

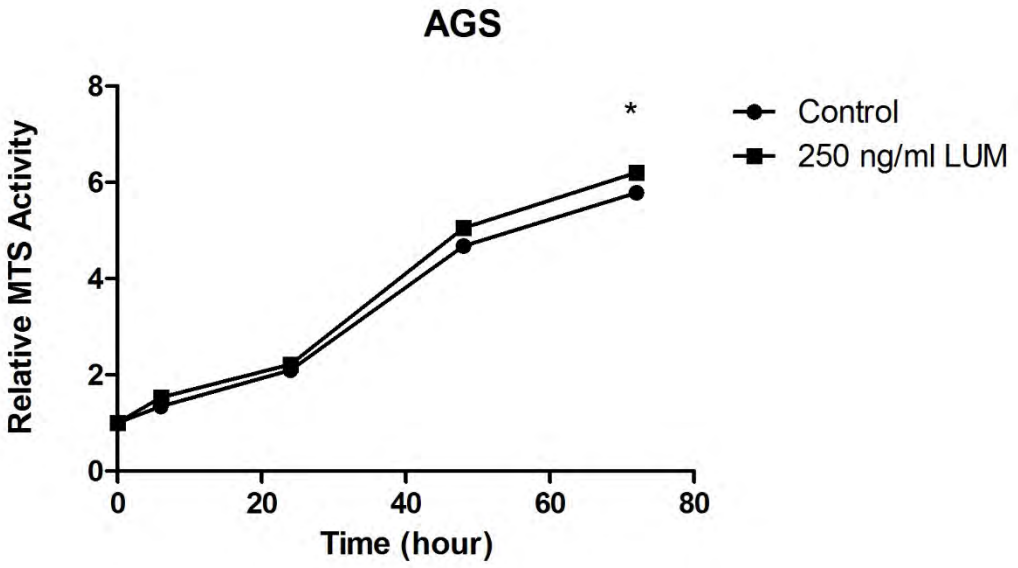
AGS
Relative MTS Activity
Time (hour)
Control
250 ng/ml LUM
*
0
2
4
6
8
0
20
40
60
80

**(C)**

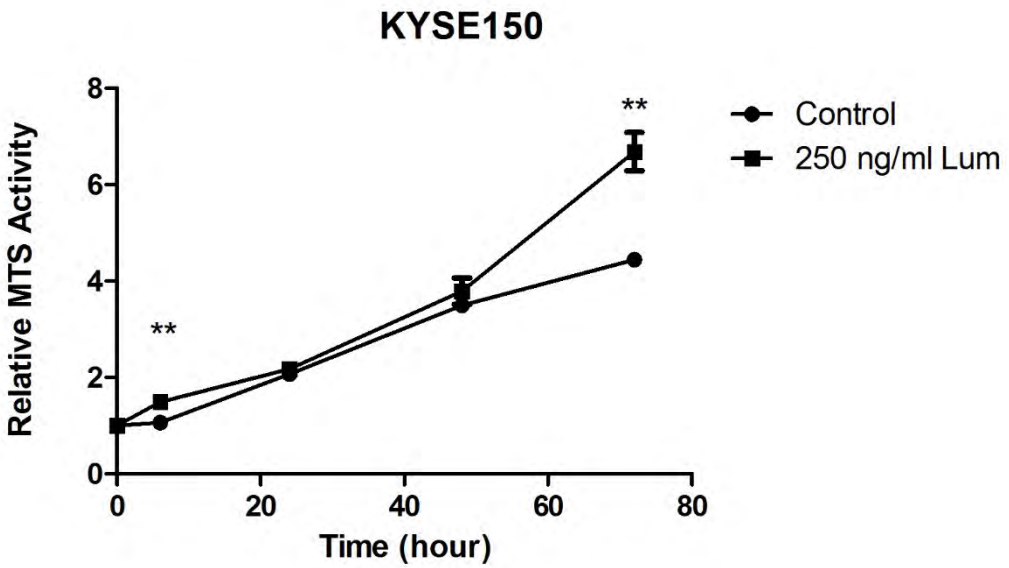


**(D)**

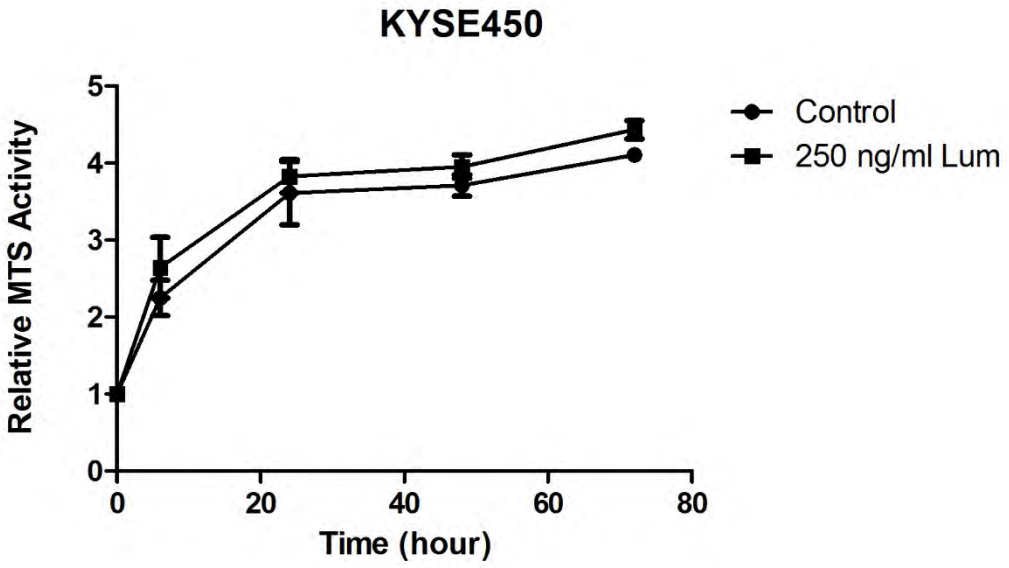


**Figure 4.21 Proliferation curves of cancer cells co-cultured with or without 250 ng/mL human recombinant lumican.(A): Proliferation curves of A549 cells; (B): Proliferation curves of AGS cells; (C): Proliferation curves of KYSE150 cells; (D): Proliferation curves of KYSE450 cells. N=3. Fresh culture medium was applied as the blank control. * $p<0.05$; ** $p<0.01$.**

According to the results, the cell lines co-cultured with 250ng/ml reclumican showed an increase in proliferation rate compared with the control group for A549, AGS, and KYSE150,indicating that lumican can promote the proliferation of cancer cells.

### 4.2.6. Wound healing analysis

To evaluate the effect of lumican on cancer cell migration and growth properties, wound healing analysis was performed on A549, AGS, and KYSE150 cancer cells. A wound gap was created by scratching, and healing progress was captured at different time points. Cancer cells were treated with low (50 ng/mL) or high (250 ng/mL) dose of purified human recombinant lumican (recLumican). Figure 4.22 shows the healing images of cancer cells co-cultured with recLumincan compared with the control after scratching.

**(A)**

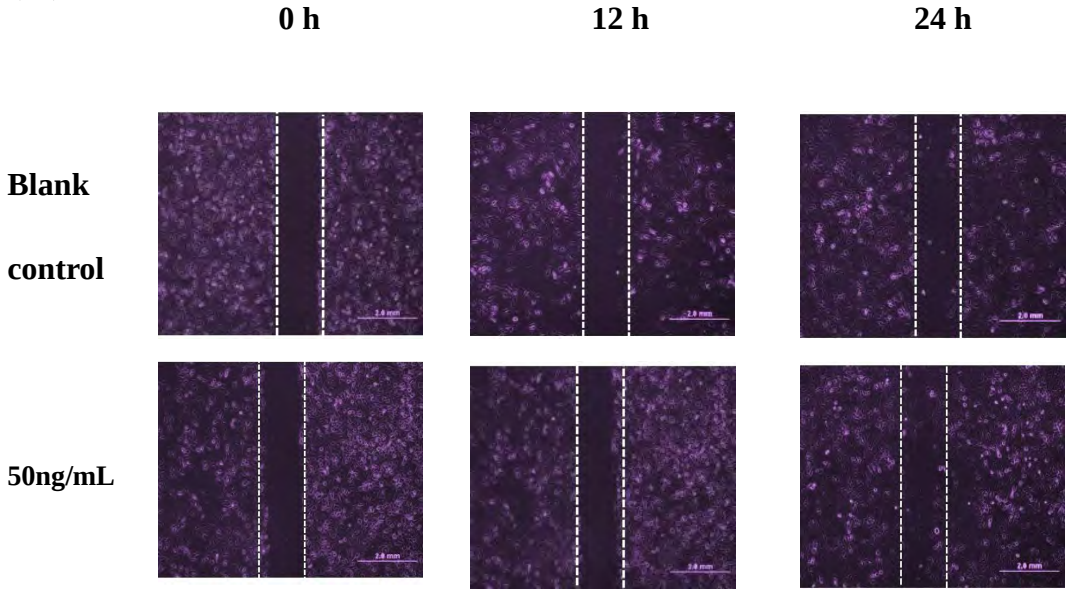

**250ng/mL**

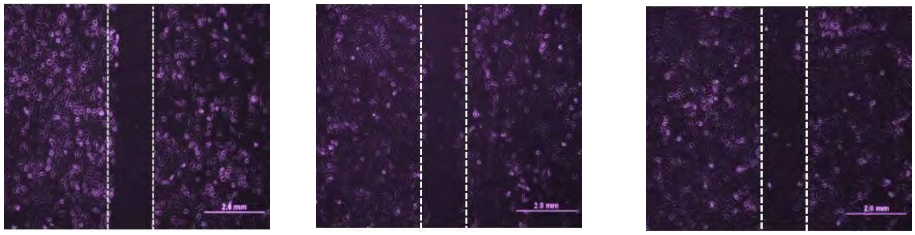

**Images of wound healing progress of A549 cells under 50ng/mL or 250μg/mL recombinant lumican protein at 0h, 12h, and 24h respectively**

**(B)**

**0 h** **24 h** **48 h**

**Blank control**

**50ng/mL**

**250ng/mL**

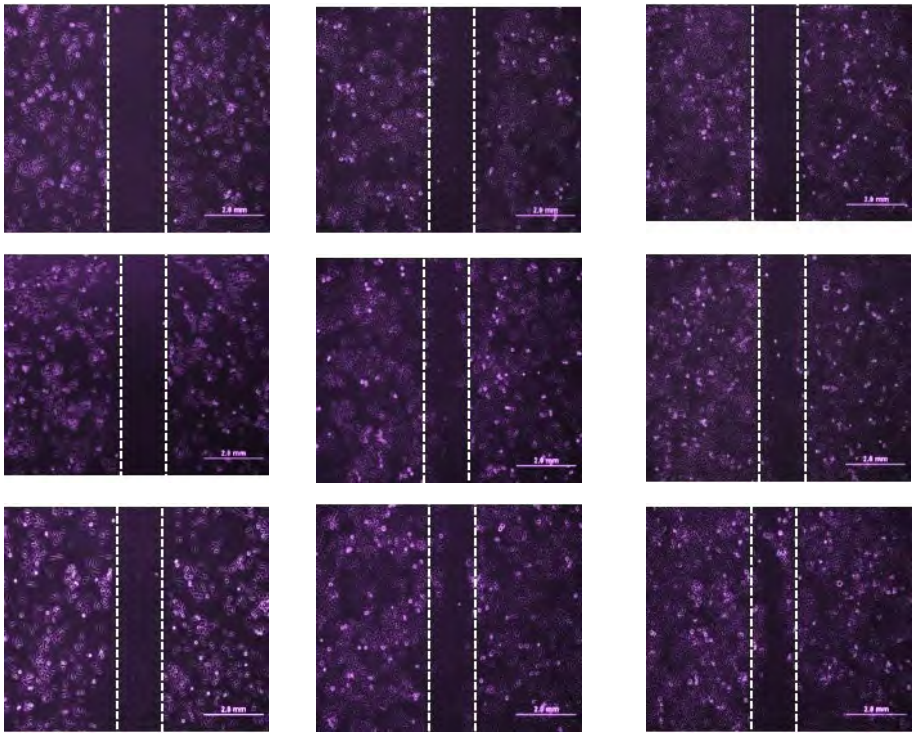

**Images of wound healing progress of AGS cells 50ng/mL or 250μg/mL recombinant lumican protein at 0h, 24h, and 48h respectively**

**(C)**

**0 h** **12 h** **24 h**

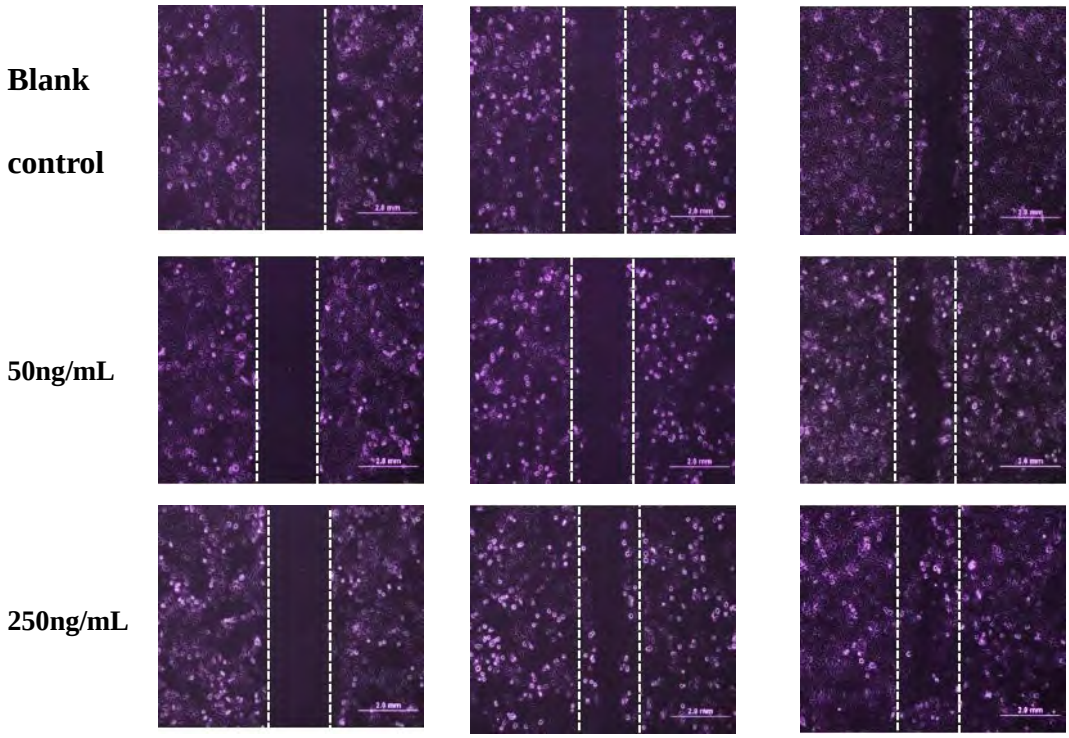


**Images of wound healing progress of KYSE150 cells 50ng/mL or 250μg/mL recombinant lumican protein at 0h, 12h, and 24h respectively**

**Figure 4.22 Images of wound healing assay with recombinant lumican protein treatment (50 ng/mL or 250ng/mL) on cancer cells at 0h, 12h, and 24h. (A): Images of wound healing progress of A549 cells; (B): Images of wound healing progress of AGS cells; (C): Images of wound healing progress of KYSE150 cells. Fresh culture medium was applied as the blank control. Exposure time: 12.5 msec. Original magnification: 10x. Scale: 2mm.**

According to the results, after 24-hour (A549 and KYSE150 cell lines) or 48-hour (AGS cell line) incubation, there were more cells from the reclumican treatment groups (both low dose and high dose groups) migrated into the scratched area than control groups, implying that the recombinant lumican protein increases the cell migration *in vitro*.

### 4.2.7. Pathway analysis by Bio-Plex 200 System

Bio-Plex Pro Cell Signaling Assay was performed to analyze the involved signaling pathways involving lumican in KYSE450 cells. Phosphorylated analytes (AKT($Ser^{473}$), ATF-2($Thr^{71}$), MEK1($Ser^{217}$/$Ser^{221}$), ErK1/2($Thr^{202}$/$Tyr^{204}$, $Thr^{185}$/$Tyr^{187}$), p38 MAPK($Thr^{180}$/$Tyr^{182}$), HSP27($Ser^{78}$), p53($Ser^{15}$), JNK($Thr^{183}$/$Tyr^{185}$), p90 RSK($Ser^{380}$), Stat 3($Ser^{727}$), NF-κB p65($Ser^{536}$)) from cell lysates treated with increasing concentrations of human recombinant lumican (50, 250, and 500 ng/mL) or control were detected by Bio-Rad Bio-Plex 200 Suspension Array System after 24-hour incubation. Figure 4.23 shows the summary of phosphorylated analytes from recLumican treated KYSE150 cells respectively.

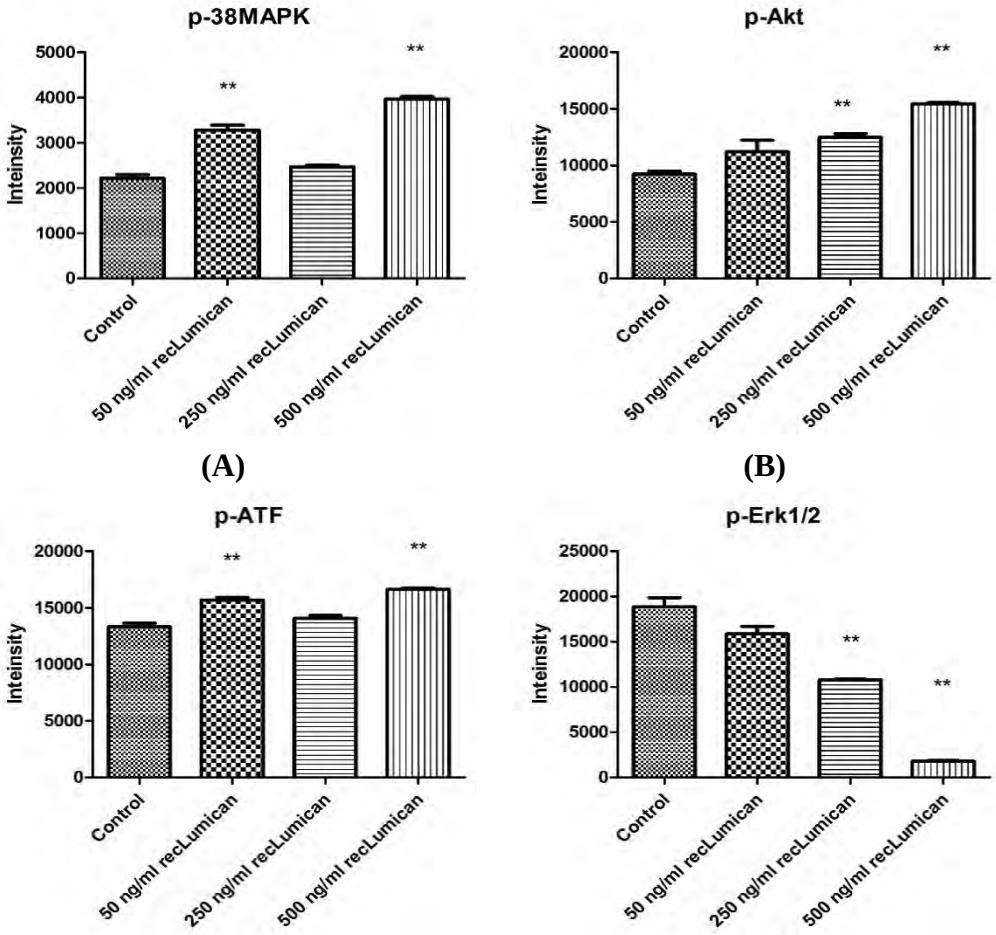

**(C)**

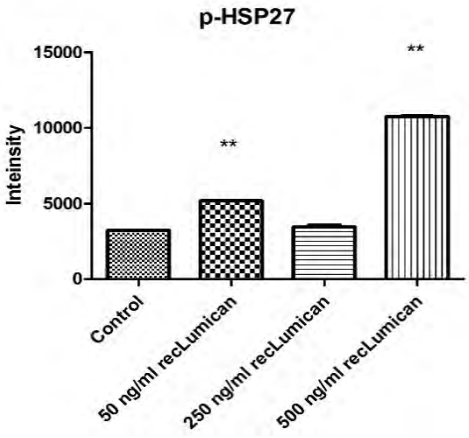
p-HSP27
Inteinsity
15000
10000
5000
0
**
**
Control
50 ng/ml recLumican
250 ng/ml recLumican
500 ng/ml recLumican

**(D)**

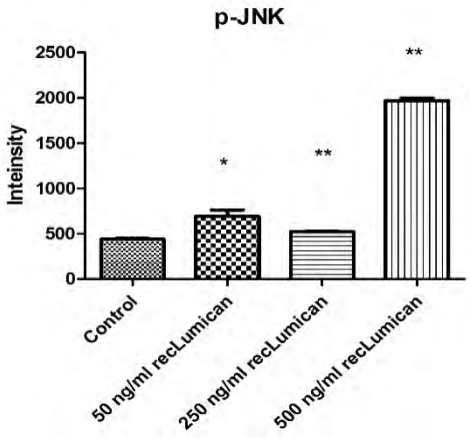
p-JNK
Inteinsity
2500
2000
1500
1000
500
0
*
**
**
Control
50 ng/ml recLumican
250 ng/ml recLumican
500 ng/ml recLumican

**(E)**

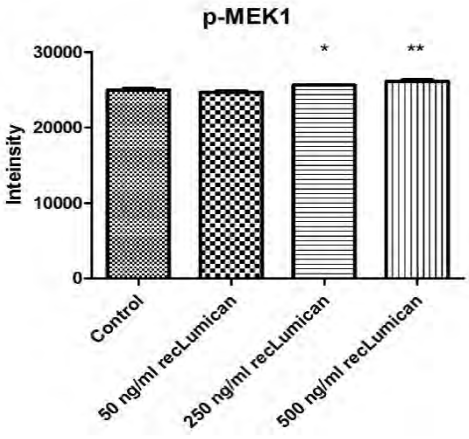
p-MEK1
Inteinsity
30000
20000
10000
0
*
**
Control
50 ng/ml recLumican
250 ng/ml recLumican
500 ng/ml recLumican

**(F)**

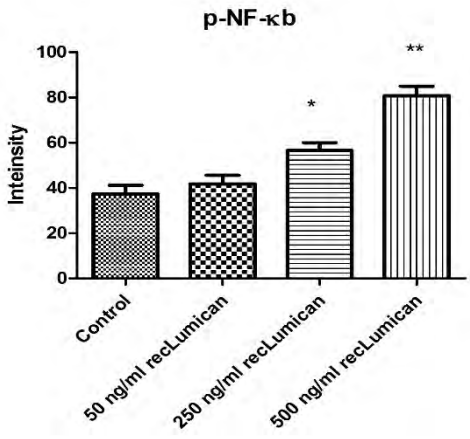
p-NF-κb
Inteinsity
100
80
60
40
20
0
*
**
Control
50 ng/ml recLumican
250 ng/ml recLumican
500 ng/ml recLumican

**(G)**

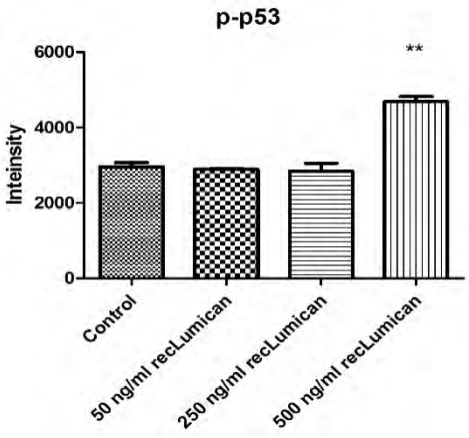
p-p53
Inteinsity
6000
4000
2000
0
**
Control
50 ng/ml recLumican
250 ng/ml recLumican
500 ng/ml recLumican

**(H)**

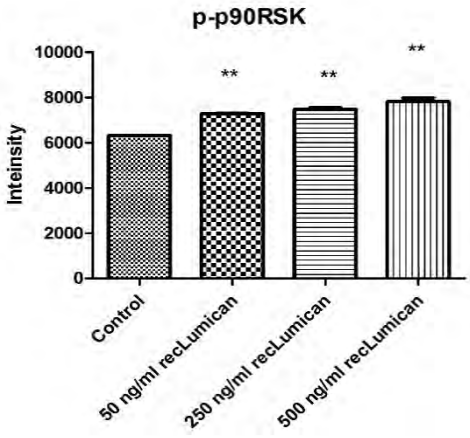
p-p90RSK
Inteinsity
10000
8000
6000
4000
2000
0
**
**
**
Control
50 ng/ml recLumican
250 ng/ml recLumican
500 ng/ml recLumican

**(I)**

**(J)**

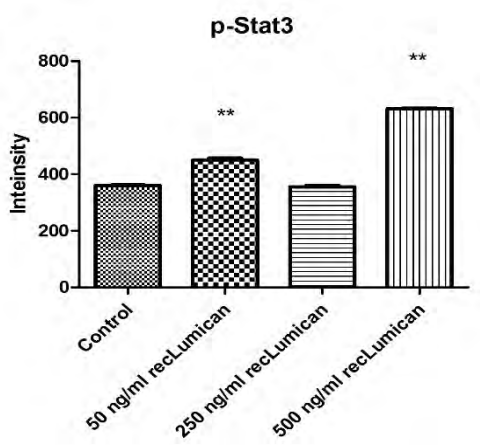


**(K)**

**Figure 4.23 Phosphorylated analytes from KYSE150 cells treated with different concentrations of recombinant lumican or vehicle control.(A); Phosphorylated p38 MAPK (Thr180/Tyr182) level;(B): Phosphorylated AKT(Ser$^{473}$)level; (C): Phosphorylated ATF-2 (Thr71) level;(D): Phosphorylated ErK1/2 (Thr202/Tyr204, Thr185/Tyr187) level; E: Phosphorylated HSP27 (Ser78) level; F: Phosphorylated JNK(Thr$^{183}$/Tyr$^{185}$) level; G: Phosphorylated MEK1 (Ser217/Ser221) level; H: Phosphorylated NF-κB p65(Ser$^{536}$) level; I: Phosphorylated p53 (Ser15) level; J: Phosphorylated p90 RSK (Ser380) level; K: Phosphorylated Stat 3 (Ser727) level. reclumican concentrations are50, 250, and 500 ng/mL. Fresh medium was applied as the control. N=3. * P < 0.05; ** p < 0.01.**

According to the results, phosphorylated AKT, ATF-2, MEK1, p38 MAPK, HSP27, p53, JNK, p90 RSK, Stat 3, and NF-κB p65 all increased significantly after the treatment with reclumincan in KYSE150 cells and to a certain extend showed the dose-depend manner. However, the phosphorylated Erk1/2 level of cell lysates decreased significantly as the concentration of reclumican was gradually increased.

## 4.3. Study of the reversal effect on the p-glycoprotein based multi-drug resistance using compound 160a

### 4.3.1. Molecular Docking Analysis

To figure out the possible molecular target for compound 160a, molecular docking analysis was first performed by the SEA program(http://sea.bkslab.org). According to the instructions of the program, the binding probability of the compound to the protein target is significant if the expected value (P-Value) is lower than $1 \times 10^{-10}$, the protein target with lower P-Value possesses high infinity to the test compound. The maximum target complementary value (MaxTC) indicates the level of the ligand-target complementarity, a higher MaxTC value suggests a more suitable binding to target ligand. Table 4.13 shows the possible targets for compound 160a.

**Table 4.13 The top three predicted human protein targets for compound 160a.**

| Rank | Target Key | Target Name | Description | P-Value | MaxTC |
|---|---|---|---|---|---|
| 1 | MTR1A_HUMAN+5 | MTNR1A | Melatonin receptor type 1A | $2.272e^{-19}$ | 0.40 |
| 2 | MDR1_HUMAN+5 | ABCB1 | Multidrug resistance protein 1 | $3.235e^{-18}$ | 0.46 |
| 3 | ROCK2_HUMAN+5 | ROCK2 | Rho-associated protein kinase 2 | $3.902e^{-18}$ | 0.32 |

**MaxTC: maximum target complementary value.**

As shown in the Table 4.13, the top three possible protein targets in human were summarized. The multi-drug resistance protein-1 (MDR-1, coded by ABCB1, also known as P-gp) possessed the second lowest expected value which is $3.24e^{-18}$and highest maximum target complementary value which is 0.46. Therefore, P-gp was predicted to be the most possible target for compound 160a and thus it was further investigated in this project.

### 4.3.2. Cytotoxic effect of doxorubicin combined with 160a

Doxorubicin (Dox) was one of the known substrates for p-glycoprotein. Dox-resistance cell lines were developed by the prolonged culturing the cells with doxorubicin (1.00 μg/mL doxorubicin in culture medium ). Cytotoxicity of doxorubicin was evaluated in parental and dox-resistance cell lines to check the development of Dox resistance (Figure 4.24 A and C). The Dox resistance effect of compound 160a was determined by co-culturing the dox-resistant cells with different concentrations of doxorubicin using MTS assay. The results were shown in Figure 4.24.

**(A)**

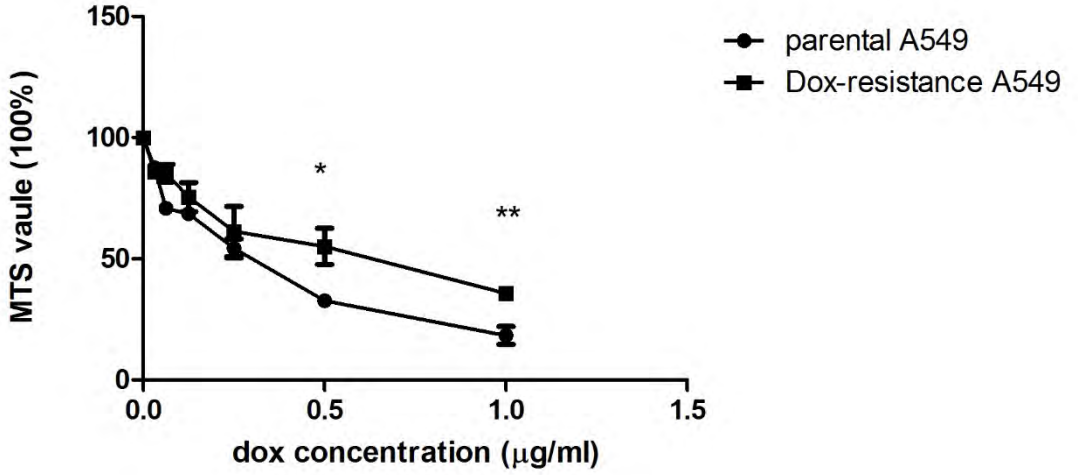
150
100
50
0
MTS vaule (100%)
0.0
0.5
1.0
1.5
dox concentration (μg/ml)
*
**
parental A549
Dox-resistance A549

**(B)**

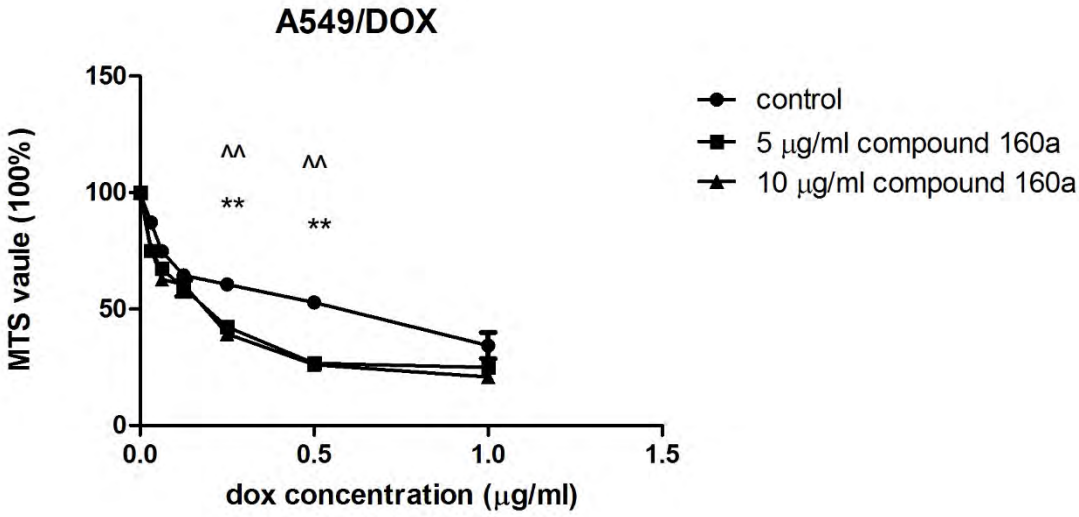
A549/DOX
150
100
50
0
MTS vaule (100%)
0.0
0.5
1.0
1.5
dox concentration (μg/ml)
^^
**
^^
**
control
5 μg/ml compound 160a
10 μg/ml compound 160a

**(C)**

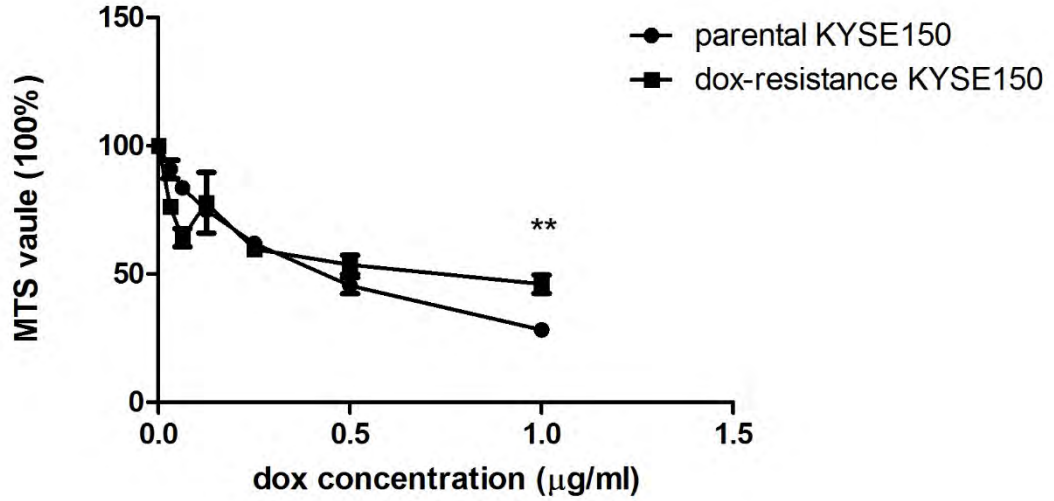


**(D)**

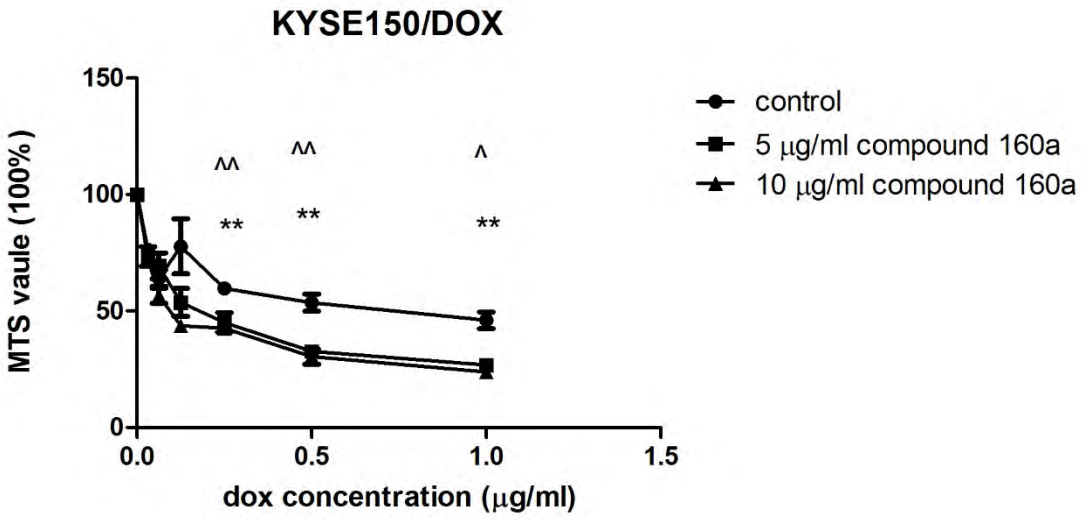


**Figure 4.24 Cytotoxic effect of different concentrations of doxorubicin on parental and doxorubicin resistance cancer cells co-cultured with compound 160a. (A): Relative MTS value of doxorubicin on parental and dox-resistance A549 cell lines; (B): Relative MTS value of doxorubicin combined with compound 160a (5 μg/mL, 10 μg/mL) in dox-resistance A549 cell lines; (C): Relative MTS value of doxorubicin on parental and dox-resistance KYSE150 cell lines; (D):Relative MTS value of doxorubicin combined with compound 160a (5 μg/ml, 10 μg/ml) in dox-resistance KYSE150 cells. 0.1% DMSO was applied as vehicle control. N=3. ^ $p < 0.05$, ^^ $p < 0.01$, comparing 5 μg/mL compound 160a group with control group; * $p < 0.05$, ** $p < 0.01$, comparing 10 μg/mL compound 160a group with control group.**

According to Figure 4.24 (A and C), A549/DOX cells and KYSE150/DOX cells revealed significant resistance effect comparing with parental A549 cells. Figure 4.24 (C and D) showed that compound 160a significantly reverse the cytotoxic effect of doxorubicin in both A549/DOX and KYSE/DOX cells.

### 4.3.3. Analysis of the synergistic effect of compound 160a

Although previous MTS assay data obtained in Section 4.3.2 showed that doxorubicin combined with compound 160a reveled high cytotoxic effect than doxorubicin alone, the synergistic effect of compound 160a on A549/DOX cells had to be evaluated by CI (combination index) value via Compusyn program. According to the concentration ratio of compound 160a verses doxorubicin, different CI values at different Fa were calculated and summarized in Table 3.14.

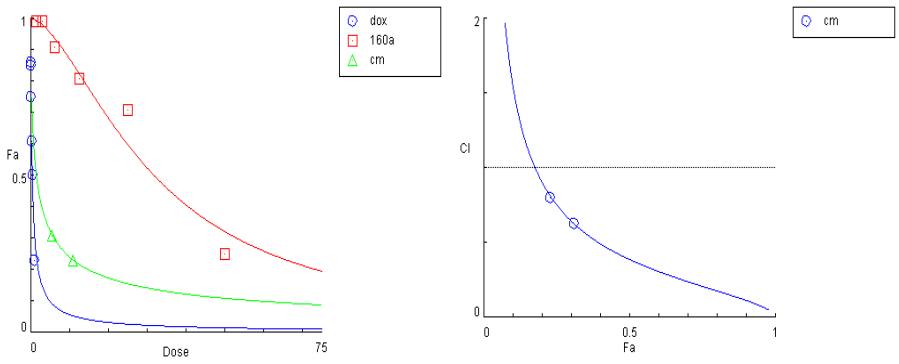


**(A)** **(B)**

**Figure 4.25 Analysis of the synergistic effect of compound 160a and doxorubicin on dox-resistance cancer cells A549/DOX using CompuSyn program. (A): Dose-effect curve of compound 160a, doxorubicin or compound 160a combined doxorubicin against relative MTS value; (B): Fa-CI plot (Chou-Talalay Plot). Fa: fraction of system affected. CI: combination index. CI = 1 indicates additive effect; CI <1 indicates synergism; CI > 1 indicates antagonism[162]. N=3. Cm:**

**combination; dox: doxorubicin.**

**Table 4.14 CI value calculated at different predicted Fa by Compusyn program.**

| Fa | 0.25 | 0.5 | 0.75 | 0.9 | 0.95 |
|---|---|---|---|---|---|
| **CI value** | 0.75051 | 0.38709 | 0.20716 | 0.11333 | 0.07577 |

From the results in Figure 4.25, the cytotoxic effect of doxorubicin combined with compound 160a group is higher than either doxorubicin alone or compound 160a alone group. The CI value was calculated by the cytotoxic effect of combinatory use of doxorubicin and compound 160a at the ration of 1:10 (doxorubicin dose: 1 μg/ml, compound 160a dose: 10 μg/ml, cell viability percentage: 0.23; doxorubicin dose: 0.5 μg/mL, compound 160a dose: 5 μg/mL, cell viability percentage: 0.31). Figure 4.25 (B) showed that the CI values of combination are all below 1, indicating that compound 160a plays a synergistic effect when combined with doxorubicin on A549/DOX cells. Additionally, from table 4.14, The CI values of doxorubicin combined with compound 160a are all below 1 when Fa range from 0.25 to 0.95, it further proved that compound 160a played a synergistic effect when combined with doxorubicin.

### 4.3.4. Effect of compound 160a on cancer cell proliferation

The effect of compound 160a on doxorubicin-resistance cancer cells' proliferation was assessed by MTS assay on A549/DOX, KYSE150/DOX, LCC6/MDR, and MX100 cells. Doxorubicin resistance cells were co-cultured with compound 160a,

doxorubicin, or compound 160a mixed with doxorubicin, and cell viability was determined by MTS at 0, 6, 24, 48, 72 hours. The results were shown in Figure 4.26.

**(A)**

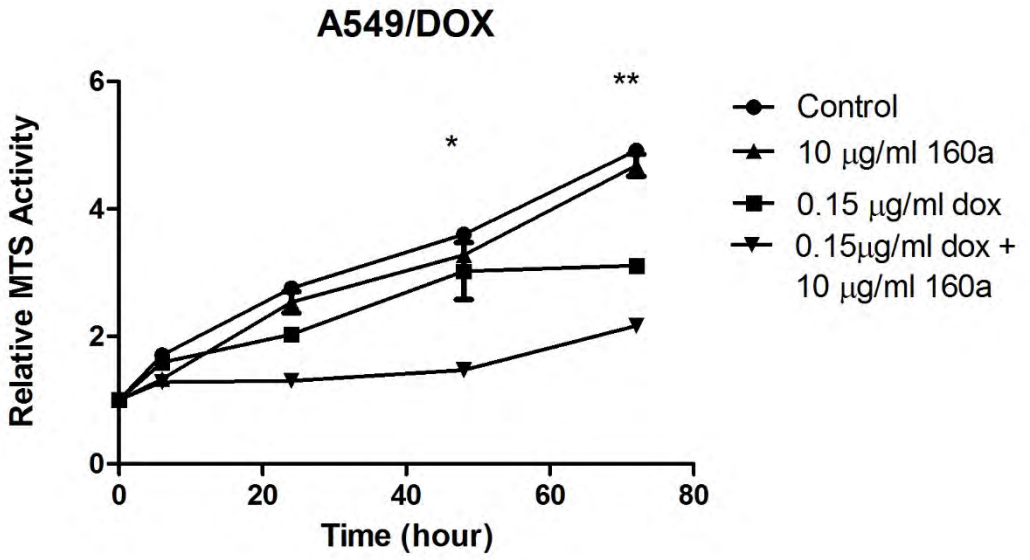


**(B)**

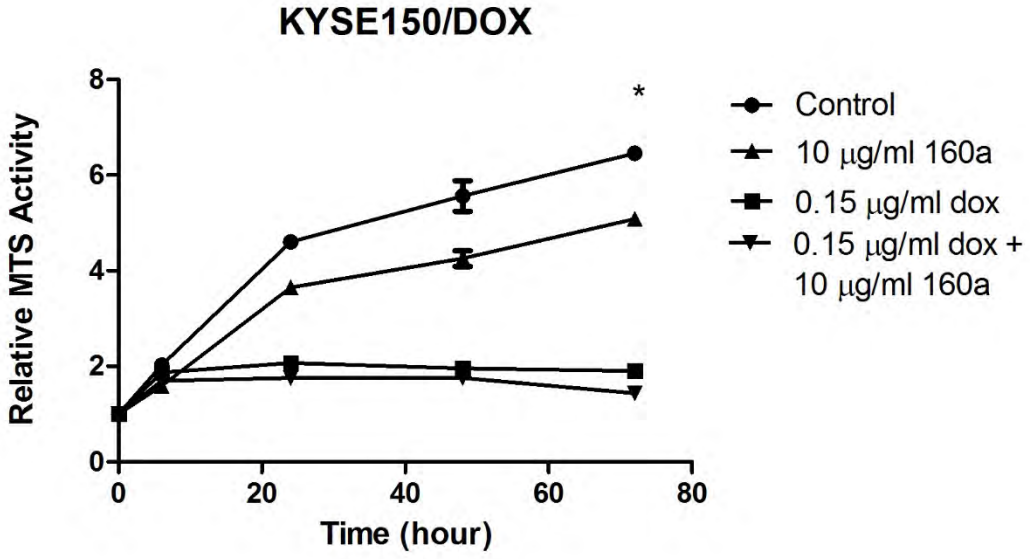

**(C)**

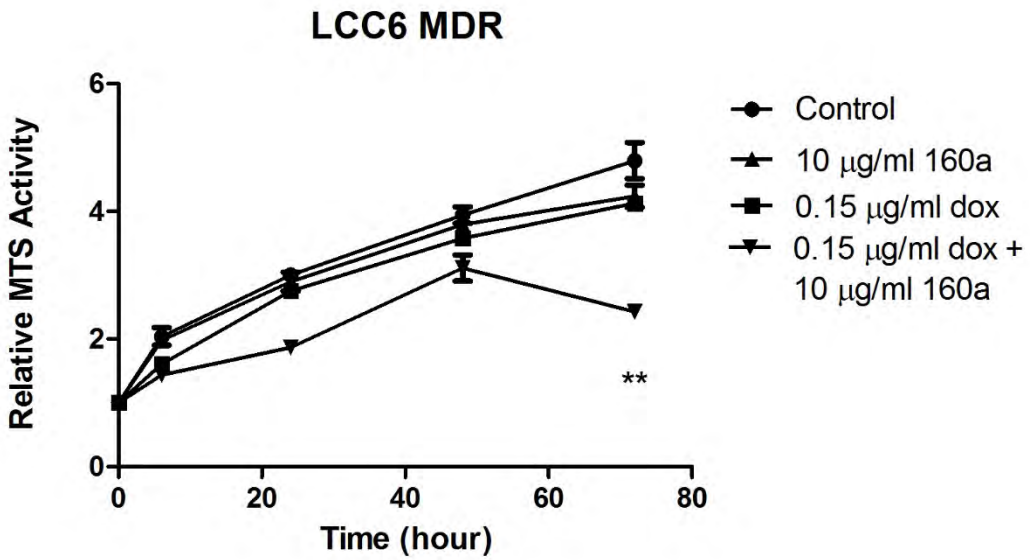


**(D)**

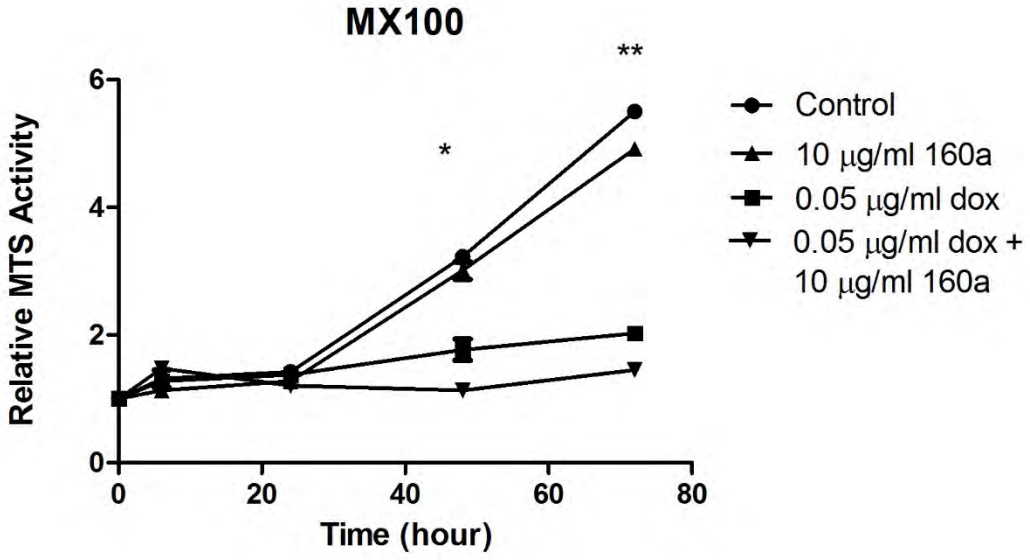


**Figure 4.26 Cell proliferation curves of doxorubicin resistance cells co-cultured with compound 160a, doxorubicin, and compound 160a combined with doxorubicin. (A): Cell proliferation curves of A549/DOX cells co-cultured with compound 160a, doxorubicin, and compound 160a combined with doxorubicin;**

**(B): Cell proliferation curves of KYSE150/DOX cells co-cultured with compound 160a, doxorubicin, and compound 160a combined with doxorubicin; (C): Cell proliferation curves of LCC6/MDR cells co-cultured with compound 160a, doxorubicin, and compound 160a combined with doxorubicin; (D): Cell proliferation curves of MX100 cells co-cultured with compound 160a, doxorubicin, and compound 160a combined with doxorubicin. 0.1% DMSO was applied as vehicle control. N=3. * p < 0.05; ** p <0.01, comparing the group of doxorubicin combined with compound 160a with the control group.**

Doxorubicin-resistance cancer cells in the control group grew faster compared with the treatment of either compound 160a, doxorubicin or combined groups. The growth of the cancer cells with the treatment of either doxorubicin or 160a was suppressed, whereas the treatment of doxorubicin combined with compound 160a showed stronger suppressive effects on cell growth. It was indicating that compound 160a enhanced the cytotoxic effects of doxorubicin on DOX-resistance cancer cells.

### 4.3.5. Multi-drug resistance analysis

To study the modulating effect of compound 160a on p-glycoprotein, multi-drug resistance kit (Cayman) was employed to determine the intracellular accumulation of calcein AM (a substrate for p-glycoprotein) using flow cytometry. Vehicle control, 2μg/mL, 10μg/mL, 20μg/mL compound 160a, and 50μg/mL verapamil (a positive control as the p-glycoprotein inhibitor) were tested to study their effect onthe intracellular accumulation of calcein AM, which could be evaluated by the intensity of green fluorescence. Figure 4.27 shows the percentage of calcein AM retention regulated by compound 160a on doxorubicin-resistance A549 cell lines.

**(A)**

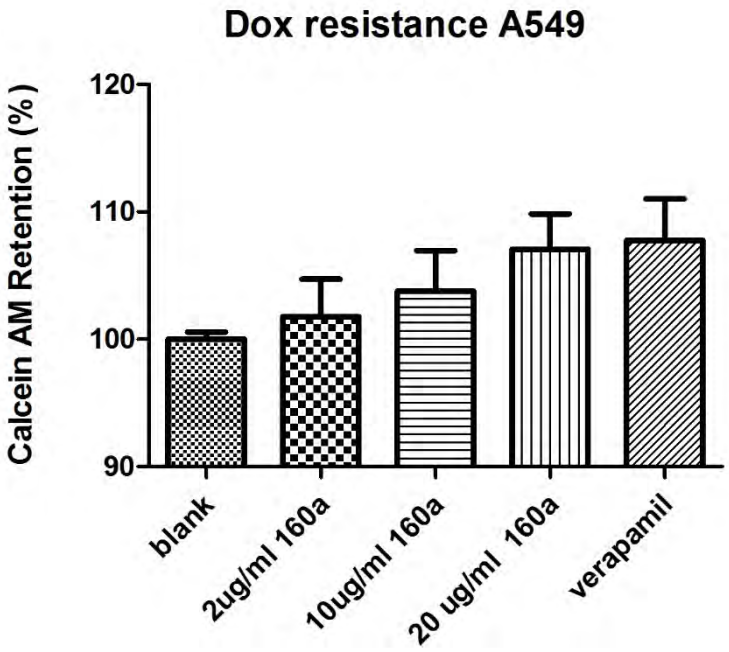
Dox resistance A549
Calcein AM Retention (%)
120
110
100
90
blank
2ug/ml 160a
10ug/ml 160a
20 ug/ml 160a
verapamil

**(B)**

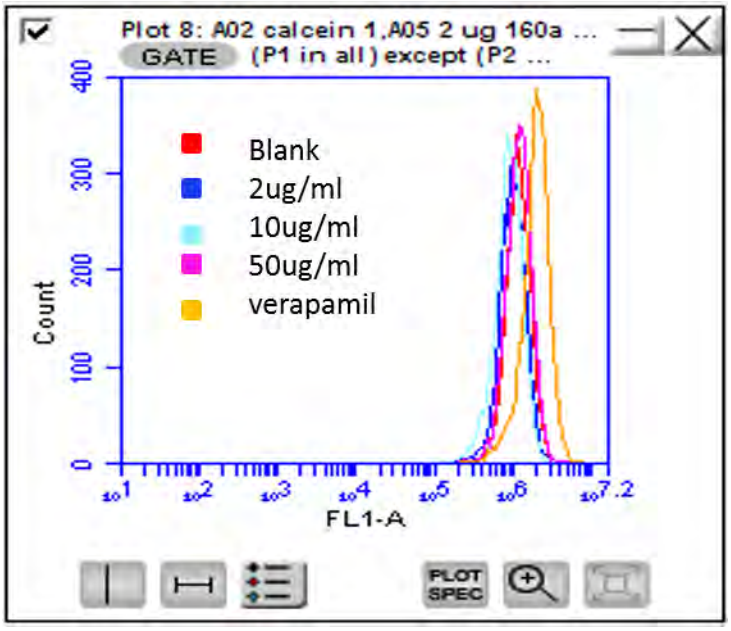
Plot 8: A02 calcein 1,A05 2 ug 160a ...
GATE (P1 in all) except (P2 ...
Blank
2ug/ml
10ug/ml
50ug/ml
verapamil
Count
400
300
200
100
0
FL1-A
PLOT SPEC

**Figure 4.27 Effects of reversing the MDR phenotype in doxorubicin resistance A549 cells line. (A): Calcein AM retention regulated by compound 160a on Doxorubicin A549 cell lines; (B): The intensity of green fluorescence from calcein AM counted by the filter channel (FL-1) using flow cytometric analysis of calcein AM with increasing concentrations compound 160a (2, 10 and 20 μg/mL). 0.1% DMSO was applied as vehicle control. 50 μg/ml verapamil was applied as the positive control. N=3**

According to the results, the retention of calcein AM showed an increasing trend after the treatment of either different concentrations of compound 160a or verapamil in doxorubicin resistance A549 cell line, indicating that compound 160a could increase the calcein AM (a p-glycoprotein substrate) accumulation into cells by inhibiting the pump out effect of p-glycoprotein.

### 4.3.6. Confocal Microscopy

To further study the p-glycoprotein inhibiting effect using compound 160a, SPE Confocal Microscope was used to observe the green fluorescence signal generated by calcein-AM on doxorubicin resistance A549 cell lines after being treated with different concentrations of compound 160a (5 μg/mL, 25 μg/mL, and 50 μg/mL) for 30 mins. Figure 4.28 shows the bright filed, overlayer, and calcein-AM signal images captured by the confocal microscope.

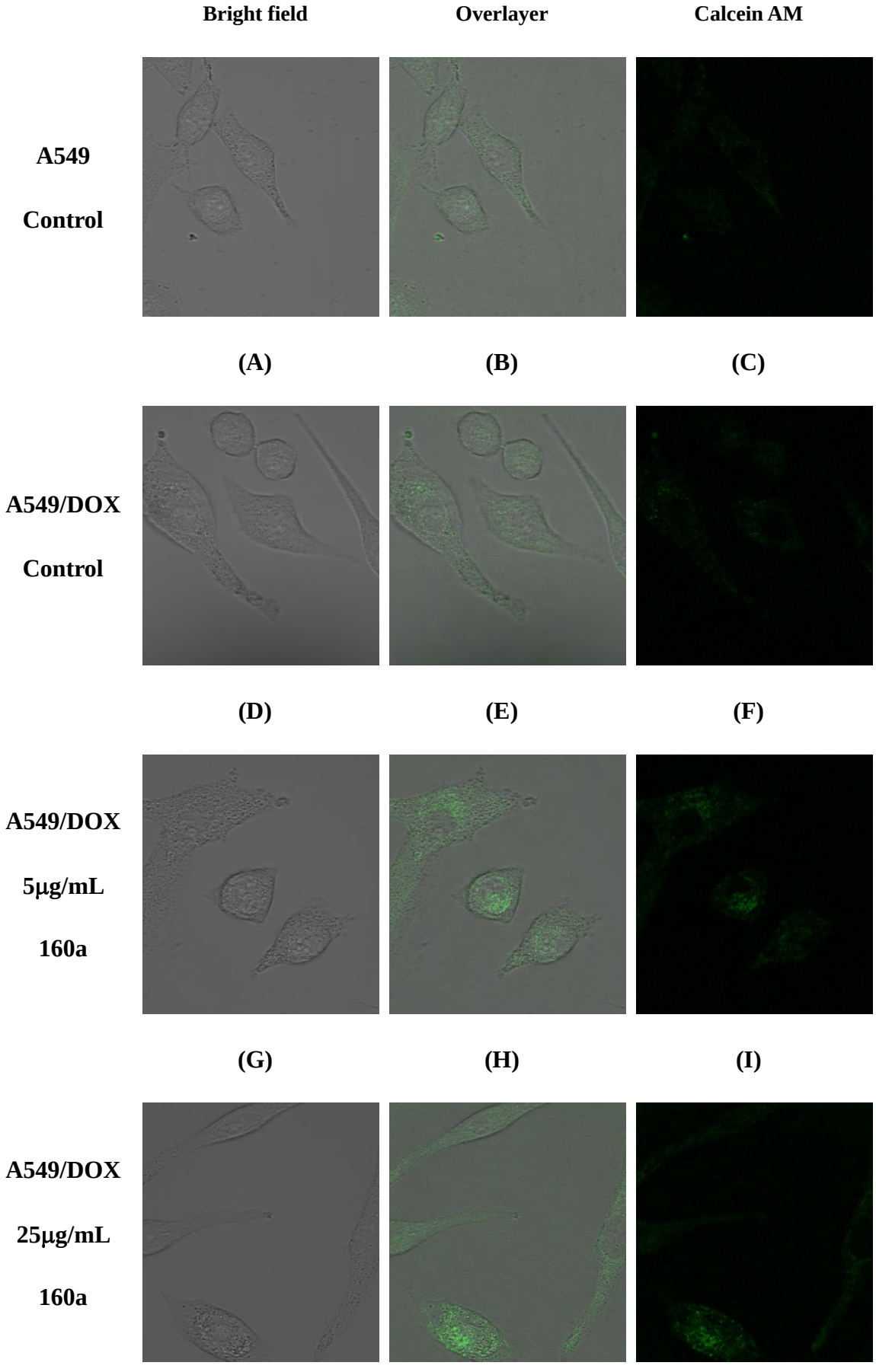
Bright field
Overlayer
Calcein AM
A549
Control
(A)
(B)
(C)
A549/DOX
Control
(D)
(E)
(F)
A549/DOX
5μg/mL
160a
(G)
(H)
(I)
A549/DOX
25μg/mL
160a

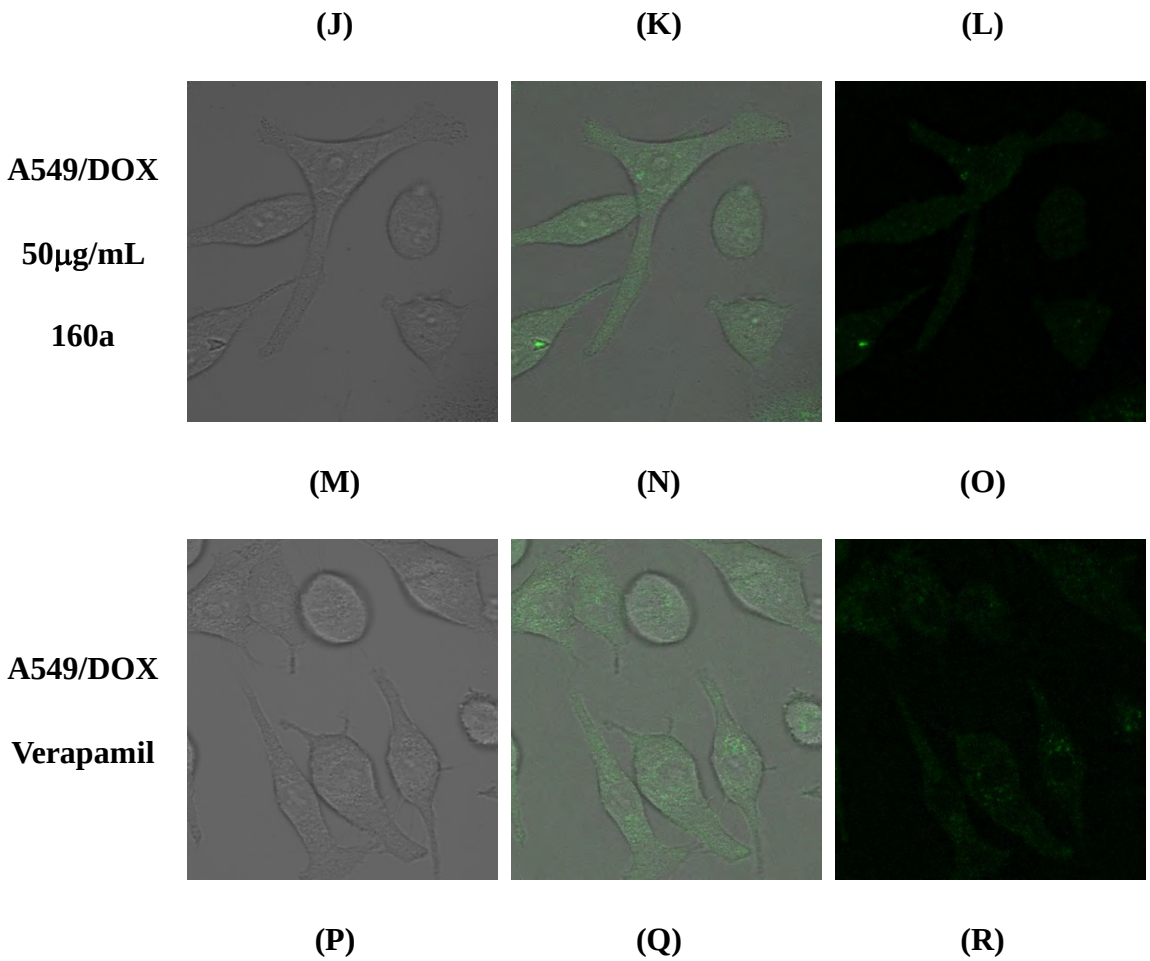


**Figure 4.28 Images of fluorescent signals of calcein AM accumulated in dox-resistance A549 cells after being treated with different concentration of compound 160a for30 mins. (A), (B) and (C): Calcein AM signal of A549 parental cells treated with DMSO; (D), (E) and (F): Calcein AM signal of dox-resistance A549 cells treated with DMSO; (G), (H) and (I): Calcein AM signal of dox-resistance A549 cells treated with 5 μg/ml compound 160a;(J), (K) and (L): Calcein AM signal of dox-resistance A549 cells treated with 25 μg/ml compound 160a; (M), (N) and (O): Calcein AM signal of dox-resistance A549 cells treated with 50 μg/ml compound 160a; (P), (Q) and (R): Calcein AM signal of dox-resistance A549 cells treated with verapamil. 0.1% DMSO was applied as vehicle control, 50 μg/ml verapamil was applied as the positive control.**

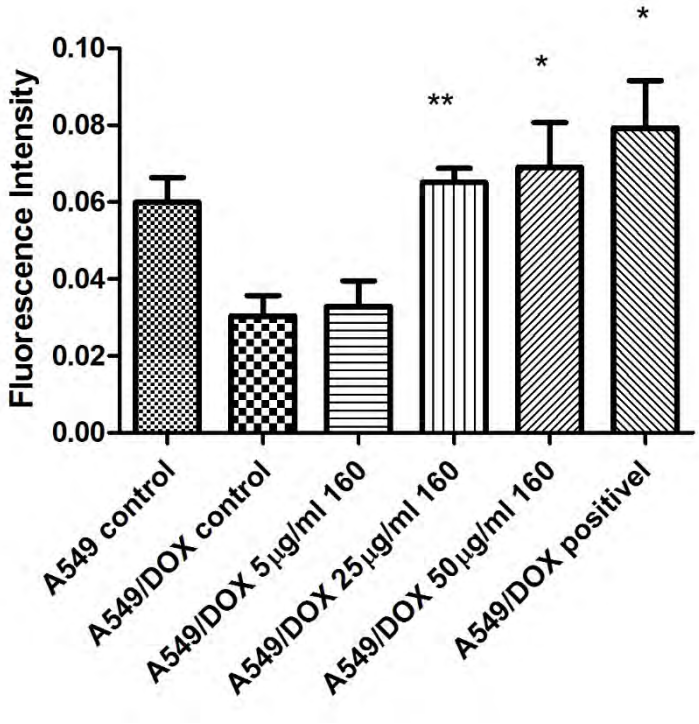


**Figure 4.29 Summary of fluorescence intensity of intracellular level of calcein AM in A549 andA549/DOX cell lines treated with compound 160a and observed by confocal microscope. 0.1% DMSO was applied as vehicle control, 50 μg/ml verapamil was applied as the positive control. Fluorescence intensity was measured by Image J.**

According to the confocal images, the fluorescence signal intensity generated by calcein-AM showed an increasing trend after the treatment of either increasing concentrations (5 μg/ml, 25 μg/ml, and 50 μg/ml)of compound 160a (calcein-AM fluorescence signal intensity showed a dose depend behavior) or verapamil in doxorubicin resistance A549 cell line, indicating that compound 160a could increase the calcein AM intracellular accumulation inside the cancer cells by inhibiting the pump out effect of p-glycoprotein.

### 4.3.7. Doxorubicin accumulation test

To provide the additional evidence for the compound 160a in reversing MDR effect,

doxorubicin accumulation test was performed on LCC6/LCC6 MDR cell lines, KYSE150/KYSE150-DOX cell lines, A549/A549-DOX cell lines, and MCF-7/MX-100 cell lines. The cells were cultured in 20μM doxorubicin and treated with different concentrations of compound 160a, and then were lysed for direct spectrophotometric detection. Figure 4.30 shows the effect of compound 160a on intracellular DOX accumulation in parental/DOX-resistance cells. Intracellular doxorubicin concentration was calculated by standard curve plotted by fluorescence intensity against concentration. Figure 4.31 shows the standard curve of intensity versus concentration.

**(A)**

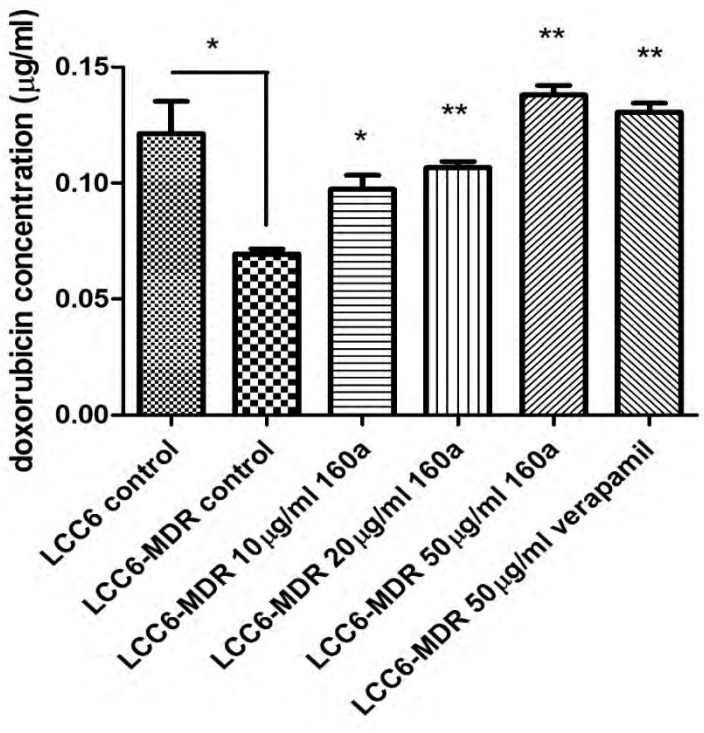

**(B)**

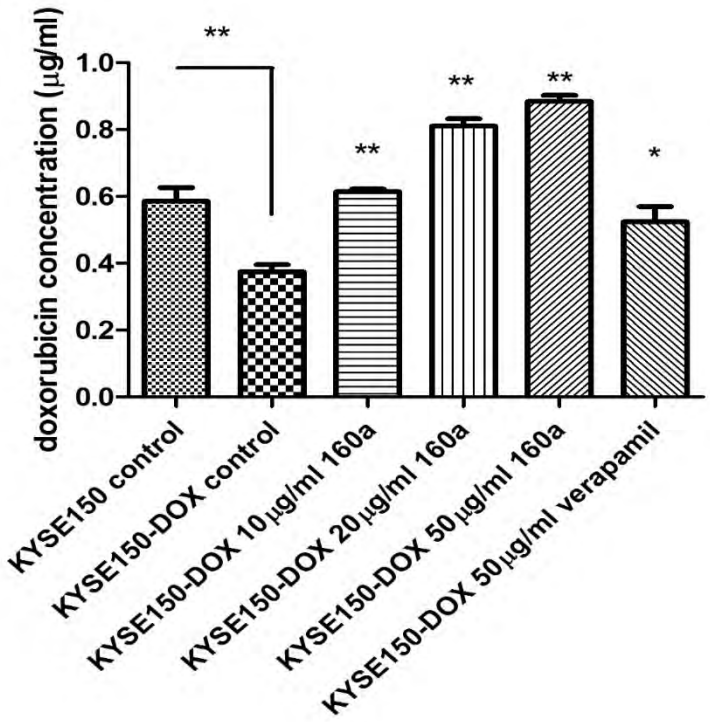
doxorubicin concentration (μg/ml)
1.0
0.8
0.6
0.4
0.2
0.0
**
**
**
**
*
KYSE150 control
KYSE150-DOX control
KYSE150-DOX 10μg/ml 160a
KYSE150-DOX 20μg/ml 160a
KYSE150-DOX 50μg/ml 160a
KYSE150-DOX 50μg/ml verapamil

**(C)**

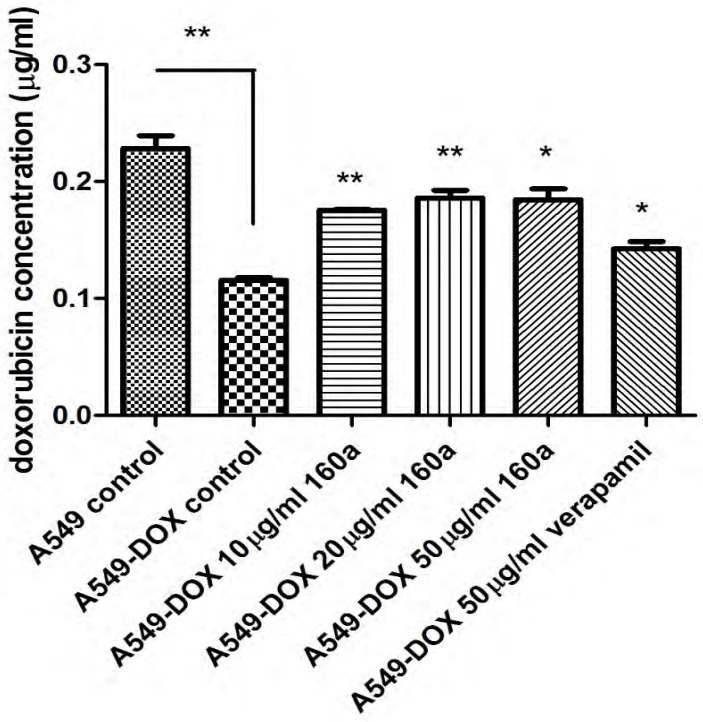
doxorubicin concentration (μg/ml)
0.3
0.2
0.1
0.0
**
**
**
*
*
A549 control
A549-DOX control
A549-DOX 10μg/ml 160a
A549-DOX 20μg/ml 160a
A549-DOX 50μg/ml 160a
A549-DOX 50μg/ml verapamil

**(D)**

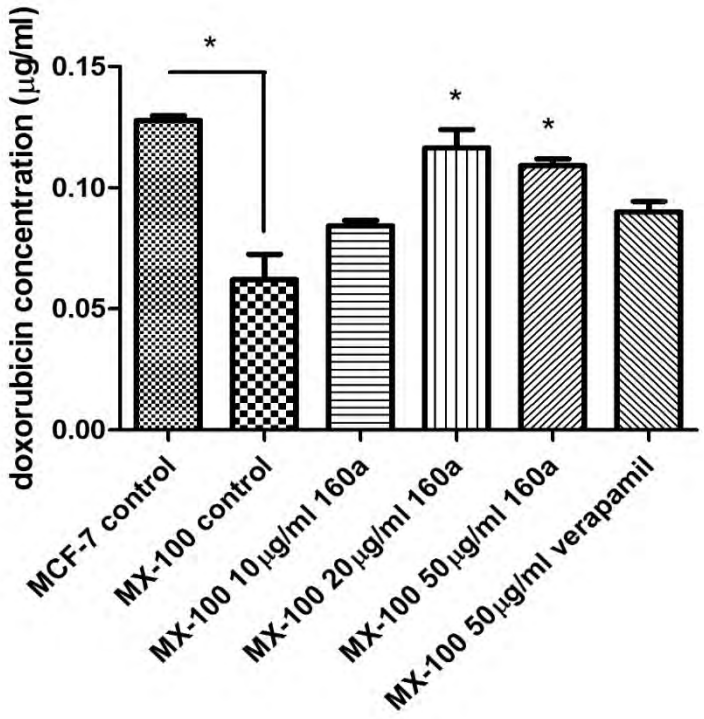


**Figure 4.30 Effect of compound 160a on intracellular DOX accumulation in parental/DOX-resistance cells. (A): Intracellular doxorubicin concentration of LCC6/LCC6 MDR cells treated with compound 160a; (B): Intracellular doxorubicin concentration of KYSE150/KYSE150-DOX cells treated with compound 160a; (C): Intracellular doxorubicin concentration of A549/A549-DOX cells treated with compound 160a; (D): Intracellular doxorubicin concentration of MCF-7/MX-100 cells treated with compound 160a. 0.1% DMSO was applied as the negative control. 50μg/ml verapamil was applied as the positive control. N=3. *<0.05, **<0.01.**

According to the results of the intracellular doxorubicin accumulation test, DOX concentrations in parental cells were all significantly higher than those in the corresponding DOX-resistance cells, indicating that DOX-resistance cell lines could pump out doxorubicin as the result of the p-glycoprotein function. Additionally, in

DOX-resistance cell lines, intracellular doxorubicin concentration increased in a dose-depend behavior with the increased concentration of compound 160a, suggesting that compound 160a may play a role in reversing the MDR effect by inhibiting p-glycoprotein function.

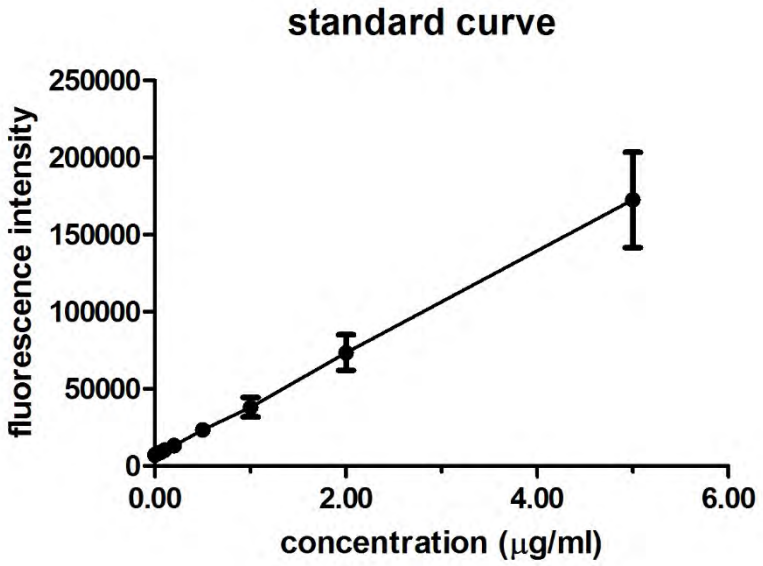


**Figure 4.31 A standard curve of fluorescence intensity against dox concentration (0.00, 0.05 μg/mL, 0.10 μg/mL, 0.20 μg/mL, 0.50 μg/mL, 1.00 μg/mL, 2.00 μg/mL, and 5.00 μg/mL doxorubicin). Doxorubicin was dissolved in cell lysis buffer. N=3. Regression equation: y = 43590x + 7471.3, $R^2$=0.9998.**

### 4.3.8. Potency of reversing the function of p-glycoprotein

From the above experiments results, it is concluded that compound 160a plays a synergistic effect when combined with p-glycoprotein substrate doxorubicin by reversing the effluxing effect of p-glycoprotein on its substrates. To evaluate the potency of the reversal effect of compound 160a, the dox-resistance cancer cell lines A549/DOX and MX100 cells were incubated with 10 μg/mL compound 160a overnight followed by the removal of compound 160a by washing and incubation

with fresh culture medium for different duration (0, 0.5, 1, and 2 hours) before doxorubicin treatment. Cell viability was determined by MTS assay, the relative MTS value at different time point was calculated by the ratio of MTS value at different time point (0.5, 1, or 2 hours) to the MTS value at time 0.and the results were shown in Figure 4.32.

**(A)**

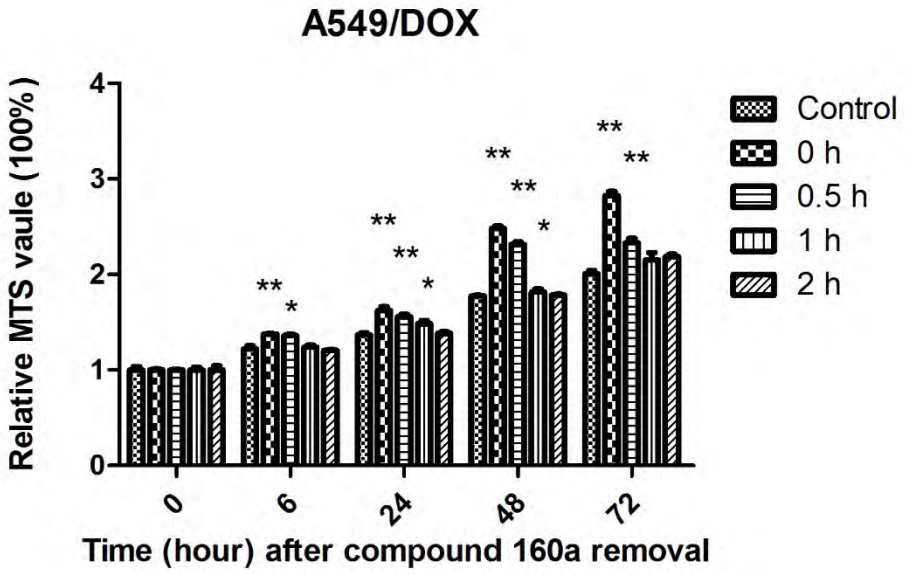


**(B)**

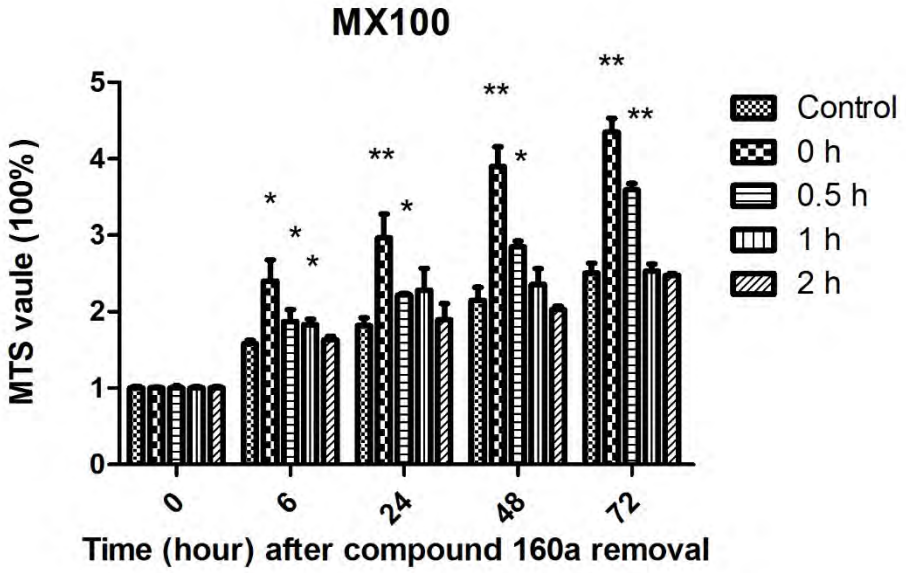


**Figure 4.32 Duration of the reversal effect of compound 160a on doxorubicin in DOX-resistance cancer cells. (A): Duration of the reversal effect of compound 160a on doxorubicin in A549/DOX cancer cells; B: Duration of the reversal effect of compound 160a on doxorubicin in MX100 cancer cells. 0.1% DMSO was applied as vehicle control. Cell viability was determined by MTS assay. N=3. * p < 0.05; ** p < 0.01.**

The potency for reversing the p-glycoprotein effect using compound 160a was still remarkable immediately after its removal and the reversal effect was still significant after 1 hour in A549/DOX cells and after 0.5 hours in MX100 cells. On the contrary, the p-glycoprotein reversal effect was not observed after 2 hours from the removal of compound 160a. These results demonstrated that the p-glycoprotein reversal effect of compound 160a could be persistent for at least 1 hour.

# Chapter 5 Discussion

## 5.1. Study of the anti-cancer effect of compound 91b1

In the first part of this study, both *in vitro* and *in vivo* anti-cancer effects of a novel quinoline compound 91b1 was characterized.

Compound 91b1 (R-5,7-dibromo-2-methyl-1,2,3,4-tetrahydroquinolin-8-ol) was prepared by Dr. Penny Chan Sau-hing from our research group in 2013. The structure of compound 91b1 was shown in Figure 2.3 and was confirmed by $^{1}$H-NMR (Figure 2.4). It was important to make sure the structure and purity is correct and consistent during the whole project to obtain reliable data.

The cytotoxic effect of compound 91b1 on cancer cells compared with non-cancer cells was evaluated by MTS cytotoxicity assay[163]. From Figure 4.1, compound 91b1 revealed cytotoxic effect by the $MTS_{50}$ value which is the concentration of 91b1to inhibit 50% of the cell viability. CDDP (cisplatin) is a well-known chemotherapeutic drug to treat various types of cancers, including carcinomas, germ cell tumors, lymphomas, and sarcomas[65], which was applied as the positive control to assess the anti-cancer potential of compound 91b1. The $MTS_{50}$ value was calculated by the software GraphPad Prism 5 and was summarized in Table 4.1. The $MTS_{50}$ values of compound 91b1 were lower than those of CDDP in AGS, KYSE150, and KYSE450 cell lines, implying that compound 91b1 showed stronger anti-cancer effect than CDDP in these three cancer cell lines. While in non-tumor cell line NE3, the $MTS_{50}$ values of compound 91b1 (2.17 μg/mL) was higher than it of

CDDP (1.19 μg/mL), indicating that compound 91b1 may be less toxic than CDDP to the non-tumor cells. Hence, compound 91b1 exhibited a good potential as an anti-cancer agent with higher anti-cancer activity and lower toxicity comparing with the first-line anti-cancer drug CDDP against cancers. Additionally, KYSE150 cells are more sensitive than other cancer cells to compound 91b1, therefore KYSE150 cells were selected for cDNA microarray analysis, Bio-plex pathway analysis, and qRT-PCR test to study the anti-cancer mechanisms in the later part of this project.

To predict the possible targets of compound 91b1 in human, molecular docking assay was performed using the SEA (Similarity ensemble approach) [151], which relates proteins based on the set-wise chemical similarity among their ligands. From Table 4.2, there was no human protein which was predicted to bind with compound 91b1. Therefore, KYSE150 cells treated with compound 91b1 were examined by cDNA microarray analysis to study the gene expression modulated by the compound 91b1.

The top 5 most downregulated and upregulated genes were identified and summarized in Table 4.3 and Table 4.4, which were considered as the most associated genes modulated by compound 91b1 against KYSE150 cells. The function of the top downregulated gene CCL5 (downregulated to 47.21% of control group) was investigated by Dr. Dessy Chan from our group previously. Thus, the function of the second top downregulated gene lumican (downregulated to 48.34% compared with the control group) was studied in this project. The 2-fold change was selected as threshold according to the instruction of Affymetrxi protocol. The same method has

been used and reported by our previous work[164]. The microarray test was performed by one of our group member Dr. Dessy Chan. She mainly studied the first top down-regulated gene CCL5 after compound 91b1 treatment. the second top down-regulated gene Lumican was studied in this project. According to the protocol of Affymetrix, 2-fold change was selected to determine the up- or down- regulation threshold. The purpose of cDNA microarray test is to identify the most associated genes. Therefore, the stringent approach can find the real down-regulated or up-regulated genes for further research. If we use the less stringent standard, there may be a lot of genes that could reach the requirements, but among these were not all have significance, and these are not the genes worthy for research.

cDNA microarray results were validated by qRT-PCR analysis. KYSE150 cells were treated with increasing concentrations (5 μg/mL, 9.5 μg/mL, 20 μg/mL, and 50 μg/mL) of compound 91b1 for 48 hours. The relative mRNA expression of lumican from treated KYSE150 cells were downregulated and showed a dose-dependent manner. It was suggested that quinoline compound 91b1 probably induced the anti-cancer effect by downregulating the expression of lumican, which modulated its upstream or downstream signaling pathway in cancer cells.

Lumican has been found accumulated frequently in cancer tissues[165]. It was reported that lumican is a key regulator of collagen fibrillogenesis, and participates in the maintenance of tissue homeostasis and modulates cellular functions including cell proliferation, migration, metastasis, and differentiation[77]. Hence, the effect of compound 91b1 on cancer cell proliferation, cell cycle, and invasion were

investigated in the next part of this project.

The proliferation rate of cancer cells with compound 91b1 was measured by MTS assay to evaluate the effect of compound 91b1 on cancer cell growth. The resulting change of MTS tetrazolium compound into colored formazan product, which is accomplished by NADPH or NADH produced via dehydrogenase enzymes in metabolically active cells indicates the cell viability[166]. According to Figure 4.3, for A549 and KYSE450 cells, cell proliferation was significantly inhibited after 48-hour incubation and co-cultured with compound 91b1. For AGS cells, the inhibition on cell growth rate exhibited the significant difference after 72-hour incubation and co-cultured with compound 91b1.For KYSE150 cells, the inhibitory effect of compound 91b1 was stronger than other three tested cell lines. Cell proliferation rate was significantly decreased after 24-hour incubation and co-cultured with compound 91b1. It was obvious that compound 91b1 suppressed cancer cell growth in varying degrees depending on cancer types. According to the results of cytotoxic assay and cell proliferation test, compound 91b1 showed remarkable anti-cancer effect on cancer in general.

Cell cycle is the series of events that lead to cell division with duplication of its DNA to produce two cells. A cell cycle consists of four distinct phases including G1/G0 phase, S phase, G2/M phase[167]. It was reported that there were many agents which exhibit anti-cancer activities by disturbing cell cycle processes[168]. According to Figure 4.4, the G0/G1 phase of A549 cells and KYSE450 cells were decreased, while the G2/M phase of A549 cells and KYSE450 cells was increased along with the

concentrations of compound 91b1. It is suggested that compound 91b1 may induce cancer cells accumulated at the G2/M phase and cannot complete the normal cell cycle as usual, and finally it results in the inhibition of cancer cell growth. Doxorubicin is a widely used chemotherapy medicine to treat many kinds of cancers, including breast cancer, bladder cancer, and lymphoma[69]. Doxorubicin was applied as the positive control in cell cycle assay, but according to Figure 4.4, doxorubicin revealed different behaviors compared with compound 91b1. It is reported that doxorubicin arrested G2/M phase of synchronized P388 cells[169].

Wound healing test was performed to evaluate the effect of compound 91b1 on cancer cell invasion. From Figure 4.5, after 12-hour (A549, KYSE150, AGS, and KYSE70 cell lines) or 24-hour (KYSE510 cell line) incubation and co-cultured with compound 91b1, less cells in the compound 91b1 treatment groups (both low dose groups and high dose groups) migrated into the scratched area than control groups. Additionally, the cells under the low dose(5μg/mL)treatment of compound 91b1 migrated with fewer amount of cells into the scratched area than the vehicle control group, but such the migration no. of cells was more than the group treated with compound 91b1 with high dose (10μg/mL), and the cells under the high dose (10 μg/mL)treatment of compound 91b1 migrated less amount of cells into the scratched area than both the vehicle control group and low dose compound 91b1 treated group, indicating that compound 91b1 arrested cancer cell migration dose dependently.

Furthermore, the *in vivo* anti-cancer activity and toxicity of compound 91b1 were assessed on animal models. The KYSE150 or KYSE450 induced tumor xenograft

model was applied on athymic nude mice by monitoring the tumor size with the treatment of compound 91b1 comparing to control group. The KYSE150 or KYSE450 tumor was allowed to grow to about 150 $mm^3$ large followed by i.p. administration of either 10mg/kg/day of compound 91b1, 50mg/kg/day of compound 91b, or vehicle control (6% PEG) to examine the effect of the compound on solid tumor development. From Figure 4.9, after 25-day treatment, KYSE450 tumor volume of the nude mice in the vehicle control group increased gradually every day and reached about 5 times larger compared to the initial day. Whereas the average tumor volume of the nude mice with the administration of 50 mg/kg/day compound 91b1 was controlled at 2 times volume comparing to the initial day, in which one of animal tumor size was controlled at the initial size, and one of the animals was even cured at $13^{th}$ day without relapse. Average tumor volume at 10 mg/kg/day compound 91b1 treated group showed a decreasing trend but no significant difference according to statistical analysis, so the volume against treatment time was not shown in Figure 4.9. At the $25^{th}$ day, the volume of the tumor in compound 91b1 treated group was significantly reduced ($p$=0.007) comparing to the vehicle control group. It was concluded that compound 91b1 showed a significant *in vivo* anti-tumor effect on the KYSE450 derived xenografts in nude mice. On the other side, according to Figure 4.11, in KYSE150 tumor xenograft test, the tumor volume of the nude mice in the vehicle control group increased gradually every day and reached about 9.6 times larger comparing to the initial day, in which the tumor of one animal even grew to 16 times larger than the first day, suggesting that KYSE150 tumor developed quickly in

nude mice and was difficult to control. As a result, the average tumor volume of the nude mice with the administration of 50 mg/kg/day compound 91b1 was increased to about 11 times larger than the initial day. Although the tumor volume of animals in compound 91b1 treated group showed no significant difference during the therapy period, tumors in compound 91b1 treated group was controlled at a relatively average level. On the contrary, tumors of Number 4 and Number 5 animals in vehicle group grew to 12.6 and 16.0 times larger. What's more, judging from the images of animals from vehicle control group and compound 91b1 group of KYSE450 tumor xenograft model, tumors in vehicle control group generated necrosis, inflammation and produced pus from inside, finally broke. But this phenomenon was not observed in compound 91b1 treated group. These results supported that compound 91b1 significantly suppress the development of tumor in animals.

Combining the results of cytotoxicity test and tumor xenograft test, it is interesting that both KYSE450 and KYSE150 cell lines were sensitive to 91b1 treatment in vitro but only KYSE450 was sensitive to 91b1 treatment in nude mice model. These results can be explained from two parts. Firstly, according to the cytotoxicity test, KYSE450 cells are more sensitive to compound 91b1 than KYSE150. Secondly, although both KYSE150 and KYSE450 were sensitive to compound 91b1, when the cancer cells were injected into animals, the microenvironment was different, KYSE150 cells maybe more adapted to the animal environment. But KYSE450 cells could not adapt to the animal's internal environment as KYSE150 did, due to the pressure from the animal's immune

system, for example, and at the same time, compound 91b1 were injected into animal body in attempt to suppress the growth of the cancer cells. As a result, the KYSE450 cells were hard to grow and develop inside the animals' bodies.

Besides high anti-cancer activity, low toxicity is also important to develop a new anti-cancer drug. Acute toxicity, chronic toxicity, and biochemical parameters analysis were performed to examine the toxicity of compound 91b1. Nude mice were special for tumor study as they don't have intact immune system, so they usually cannot reject the growth of the transplantated tumor. But when it comes to toxicity test, rats are commonly used animals to evaluated long-term toxicity test. Comparing with mice, rats are easier to survive for long-term administration of high dose compound. Additionally, SD rats grow fast, have strong resistance to respiratory diseases, and the genetic characteristics are consistent among different sources. Although low dose of compound 91b1 treated animals bearing tumors could not control their growth as significant as the high dose compound 91b1 treated groups, a series of serum biochemical parameters were tested to monitor the internal system changes. The level of ALB (albumin), ALP (alkaline phosphatase), ALT (alanine aminotransferase), AST (aspartate transaminase), urea and TBil (total bilirubin) in blood were measured to indicating the liver function conditions[170]. ALB is one of the main proteins generated by liver, which let it as a direct marker to reflect the functions of liver. The decrease of serum ALB usually implies to liver damage, or other factors which force liver focus on other functions such as detoxification of metabolites[171]. ALP is found across a multitude of organism, prokaryotes and eukaryotes alike, with the

function of dephosphorylating compounds. The elevation of ALP level suggested the probability of hepatitis, cirrhosis, liver cancer, or metastasis, while the reduced level of ALP suggested server chronic nephritis[172]. Table 4.10 summarizes the serum biochemical parameters of mice treated with 10 mg/kg or 50 mg/kg compound 91b1. The ALB and ALP level of compound-treated groups were significantly decreased compared to blank control group (ALB from 27.6 to 26.6, and ALP from 92.00 to 56.40) in KYSE450 xenograft nude mice model, while other biochemical parameters did not show significant changes after compound 91b1 treatment. It was indicated that the integrated systems are still fine after compound 91b1 treatment, with a certain kind of liver damage. Therefore, compound 91b1 is relatively safe for cancer therapy in animals at an effective dose.

There was no observable toxicity observed in the nude mice who bear the tumor xenografts after the treatment with compound 91b1. Acute and chronic toxicity test of compound 91b1 were conducted on SD rats. Judging from Figure 4.14, there were no visible pathological changes or signs of distress observed. Chronic toxicity tests were performed on SD rats at a dose of 500mg/kg/day compound 91b1 for 7 days. After 7-day administration and observation, all animals were survived, and then were sacrificed and dissected to get vital organs. There was no obvious injury on heart, lung, and kidney. Comparing the liver condition after anatomy, liver from compound 91b1 treated group was observed to be attached to intestines and revealed liver cirrhosis. Liver is the most important organ in drug metabolism processes, by which drugs are oxidized, reduced, or hydrolyzed by CYP450 enzymes in liver[173]. Many

kinds of anti-cancer drugs possess hepatotoxicity, such as methotrexate[174], nitidine chloride[175], and geldanamycin[176]. The therapeutic dose of compound 91b1 on tumor-bearing mice was 50 mg/kg/day, while the acute toxicity level for 91b1 was 800 mg/kg and its chronic toxicity level was 500 mg/kg/day for 7 days. The identified toxicity doses were much higher than therapeutic dose by at least 10 times. All the tested animals for therapeutic doses survived and there was only liver damage in chronic toxicity group. It is inferred that quinoline compound 91b1 displayed no obvious toxicity to the rats at the maximum dose of 500 mg/kg in chronic treatment and is safe to treat cancer in animals.

After both of the *in vitro* and *in vivo* cytotoxic assessment of compound 91b1 had been conducted, the mechanisms about how compound 91b1 suppresses tumor growth were then investigated. Bio-Plex Pro Cell Signaling Assay was performed to analysis involved signaling pathway of compound 91b1 on KYSE150 cell line. Phosphorylated analytes (AKT($Ser^{473}$), ATF-2($Thr^{71}$), MEK1($Ser^{217}$/$Ser^{221}$), ErK1/2($Thr^{202}$/$Tyr^{204}$, $Thr^{185}$/$Tyr^{187}$), p38 MAPK($Thr^{180}$/$Tyr^{182}$), HSP27($Ser^{78}$), p53($Ser^{15}$), JNK($Thr^{183}$/$Tyr^{185}$), p90 RSK($Ser^{380}$), Stat 3($Ser^{727}$)) from cell lysates treated with gradually increasing concentrations of compound 91b1 were detected by Bio-Rad Bio-Plex 200 Suspension Array System. From Figure 4.6, the phosphorylated AKT, ATF-2, Erk1/2, HSP27, MEK1, p38 MAPK, p53, and p90 RSK increased significantly, while the phosphorylated Stat3 of cell lysates decreased significantly after treated with compound 91b1. All phosphorylated analytes of mentioned pathways were analyzed by IPA (Ingenuity Pathway Analysis) system

software, and NGF (nerve growth factor) was screened out to be the most related pathway with all the pathways detected. NGF is important for the development and maintenance of the sympathetic and sensory nervous systems[177]. NGF is also associated with many kinds of diseases, including neuropathy[178], Alzheimer's disease[179], and Huntington's disease[180]. It is reported that NGF promoted cancer cell invasion[181], proliferation[182, 183], and involved in cancer cell apoptosis[183]. It is suggested that NGF pathway probably played an important role in the anti-tumor behaviors of compound 91b1. However, pathways associated with lumican which was selected by cDNA microarray assay were mainly studied in this project, while NGF pathway will be further investigated in the future work. From the results of Molecular Docking prediction, cDNA microarray assay, and qPTPCR test, the quinoline compound 91b1 probably induced the anti-cancer effect by downregulating the expression of lumican, which then modulates its upstream or downstream signaling pathway in cancer cells. The possibly associated pathways will be analyzed in the next sections.

## 5.2. Study of the function of lumican in progression of cancer cells

From the cDNA microarray results in Table 4.3, CCL5 is the most down-regulated gene of KYSE150 cells after treatment with compound 91b1, and lumican is the second most down-regulated gene, which were considered to be the associated genes regulated by compound 91b1. The function of gene CCL5 was investigated by Dr.

Dessy Chan from our group previously, so the function of lumican was investigated in this project. Additionally, Figure 4.2 showed that the lumican expression level of KYSE150 cells that was decreased after the treatment with compound 91b1 and showed a dose-dependent manner, suggesting that compound 91b1 may inhibit cancer progression by regulating the expression of lumican in cancer cells. To figure out how compound 91b1 induced the anti-cancer effect by downregulating the expression of lumican, the function of lumican in cancer cell progression was studied in this project. It was reported that lumicanis highly expressed in some types of cancers such as lung cancer[184], pancreatic cancer[81] and esophageal cancer[185] but downregulated in other types of cancers such as breast cancer[186]. Table 4.12 shows that lumican was overexpressed in KYSE30, KYSE70, KYSE150, KYSE510, and SLMT1 cancer cells comparing with non-tumor cells NE3. Patient specimens were tested by qRT-PCT to check the lumican expression. Twenty esophageal squamous cell carcinoma patients' tumor samples together with its adjacent non-tumor tissues were analyzed. Figure 4.18 showed that the relative expression level of lumican of tumor sample group is higher than the non-tumor sample group, which concluded that lumican is usually overexpressed in tumors of esophageal squamous cell carcinoma patients.

NIH 3T3 cells grow relatively fast, therefore there is a shortend time to get transfection results. Moreover, human gene expression is very stable when transfected into NIH 3T3 cells as previously reported[164].

To identify the role of lumican in tumorigenesis and development, either NIH 3T3 parental, NIH 3T3/Lum or NIH 3T3/Mock cells were subcutaneously injected into the

back of female Balb/c athymic nude mice via i.p. route. After 14-day formation of a subcutaneous tumor. No visible mass was observed in NIH 3T3 parental cells injected group and NIH 3T3/Mock cells injected group. Figure 4.16 shows the images of one animal in NIH 3T3/Lum group on day 0, day 7 and day 14. According to the images, a gradually increased tumor mass with time was observed in animals in NIH 3T3/Lum group, suggesting that lumican gene may play an important role in tumor development. Although there is no evidence that lumican is an oncogene to cause cancer, many researchers proved that lumican plays important roles in tumor pathogenesis and progression[88, 91]. The present study also offered some evidence to demonstrate the functional role of lumican in cancer formation.

The effect of lumican on cell invasion ability was tested by trans-well matrigel invasion assay in KYSE150 cells. Images of invaded cells which were stained by crystal violet were shown in Figure 4.19. The average invaded cell numbers were summarized in Figure 4.20. The invasion rate of KYSE150 cells co-cultured with purified human recombined lumican protein (recLumican) was increased along with the increasing concentration of reclumican comparing with the control group, suggesting that protein lumican enhances cancer cell invasion.

To further study the functional role of lumican on cancer cell growth, cell proliferation assay was performed by MTS on A549, AGS, KYSE150, and KYSE450 cells co-cultured with or without reclumican. Results in Figure 4.21 showed that the proliferation rate of cancer cells co-cultured with reclumican was increased remarkably, indicating that lumican promoted cancer cell growth.

To evaluate the effect of lumican on cancer cell migration and growth properties, wound healing analysis was performed on A549, AGS, and KYSE150 cancer cells. Figure 4.22 showed that there were more cells of reclumican treatment groups (both low dose groups and high dose groups) migrated into the scratched area than control groups in reclumican co-cultured groups, suggested that lumican enhances cancer cell migration. It is reported that lumican knock-out mice displayed delayed wound healing, and the over-expression of lumican in human corneal epithelial cells increased cell migration[79]. For gastric cancer, lumican was found to be highly expressed and promoted cancer cell proliferation, migration and invasion[90].In this project, lung cancer cell line A549, gastric cancer cell line AGS and esophageal cancer cell line KYSE150 were first applied to test the lumican function about migration and its promoting effect was proven.

It is concluded from the above results that lumican promotes tumor progression by enhancing cancer cell growth, invasion, and migration. Compound 91b1 displays its anti-cancer activity by downregulating the expression of lumican. But the specific mechanisms by which lumican affects cancer cell development have not yet fully understood. Bio-Plex Pro Cell Signaling Assay was performed to analyze the involved signaling pathways of lumican on KYSE150 cells. Phosphorylated analytes (AKT($Ser^{473}$), ATF-2($Thr^{71}$), MEK1($Ser^{217}$/$Ser^{221}$), Erk1/2($Thr^{202}$/$Tyr^{204}$, $Thr^{185}$/$Tyr^{187}$), p38 MAPK($Thr^{180}$/$Tyr^{182}$), HSP27($Ser^{78}$), p53($Ser^{15}$), JNK($Thr^{183}$/$Tyr^{185}$), p90 RSK($Ser^{380}$), Stat 3($Ser^{727}$), NF-κB p65($Ser^{536}$)) from cell lysates treated with gradually increased concentrations of human recombinant

lumican were detected by Bio-Rad Bio-Plex 200 Suspension Array System. Figure 4.23 shows the summary of phosphorylated analytes levels from the reclumican treated KYSE150 cells. According to the results, phosphorylated AKT, ATF-2, MEK1, p38 MAPK, HSP27, p53, JNK, p90 RSK, Stat 3, and NF-κB p65 were all increased significantly in levels after treatment with reclumincan and showed a certain kind of dose-dependent manner, while phosphorylated Erk1/2 of cell lysates was decreased significantly in level as the concentration of reclumicanwas gradually increased. Combining that pathway analysis results of compound 91b1 and reclumican (Figure 5.1), phosphorylated Erk1/2 and Stat3 levels after compound 91b1 treatment or reclumican co-cultured KYSE150 cells showed consistent results. Compound 91b1 downregulated the expression of lumican, followed by the decrease of lumican secreted outside cells, then the p-Erk1/2 level is increased, while p-Stat3 level is decreased. When KYSE150 cells co-cultured with purified recombined human lumican protein, the p-Erk1/2 level was decreased and p-Stat3 level was increased. These data suggested that compound 91b1 probably promotes p-Erk1/2 pathway and inhibits p-Stat3 pathway by downregulating the expression of lumican.

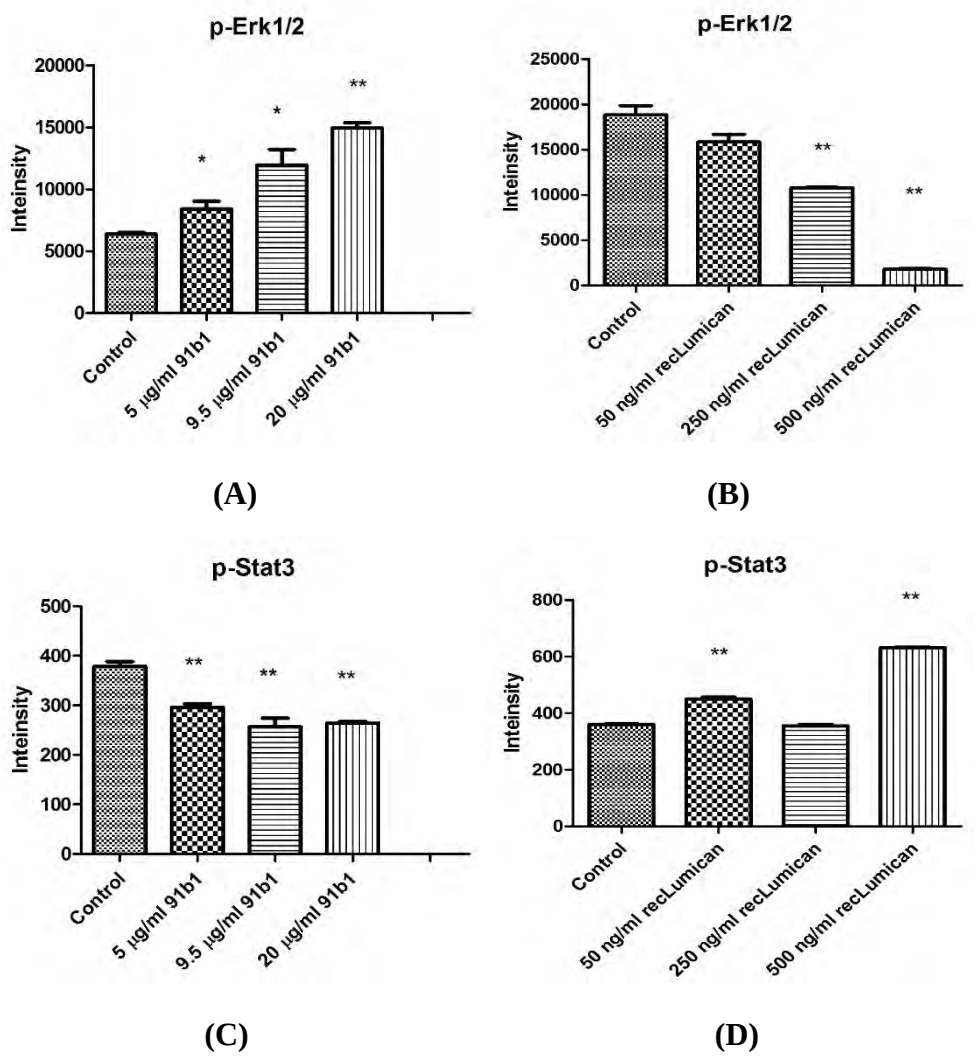


**Figure 5.1 Comparison of phosphorylated Erk1/2 and Stat3 levels of KYSE150 cells treated with compound 91b1 or recLumican with different doses. (A): Phosphorylated Erk1/2 (Thr202/Tyr204, Thr185/Tyr187) level from cell lysates of KYSE150treated with different concentrations of compound 91b1 or vehicle control; (B): Phosphorylated Erk1/2 (Thr202/Tyr204, Thr185/Tyr187) level from cell lysates of KYSE150 treated with different concentrations of reclumican or vehicle control; (C): Phosphorylated Stat 3 (Ser727) from cell lysates of KYSE150 treated with different concentrations of compound 91b1 or vehicle control; (D): Phosphorylated Stat 3 (Ser727) from cell lysates of KYSE150 treated with different concentrations of reclumican or vehicle control**

It has been reported that the mechanisms of lumican action in modulating cell functions were associated with integrin $\alpha_2\beta_1$ and $\beta_1$-FAK-Erk1/2 signaling pathways[92], TGFβ- TGFR- Smad-integrin signaling pathway[93], TLR4-MyD88-

NF-κB signaling pathway[94], and Fas−Fas ligand-immune response[95]. FAK signaling pathway has been reported to be closely related to tumor cell proliferation, motility, and survival[187]. From the present study, lumican expression in KYSE150 cells can be suppressed by compound 91b1, therefore the overall results suggested that compound 91b1 probably inhibits cancer cell growth through Erk1/2 signaling pathway to downregulate lumican expression.

Generally speaking, the activation of Ras/MEK/ERK signaling pathway promotes cell proliferation. Cells are a complicated organic whole, large amounts of signaling pathways, growths factors, hormones and extracellular microenvironment interact with each other and play varieties of functions. Hence at the same time compound 91b1 increased MER/ERK signaling pathway, the downstream effect which induce cancer cell death requires further study. Ganoderma lucidum polysaccharide (GLP) was found to show promising ant-cancer effect. In colorectal cancer HT-29 and HCT116 cells, GLP treatment induced autophagosome accumulation which caused cancer cell apoptosis. Additionally, the GLP induced autophagosome accumulation and apoptosis is mediated by MAPK/ERK activation[188]. Hepatocellular carcinoma is a common liver malignancy worldwide. It is reported that β-Thujaplicin inhibits the growth of HCC cells, but not normal liver cells. Furthermore, it is found that β-Thujaplicin induced cell apoptosis and the S-phase arrest mediated by activity of p38/ERK MAPK signaling pathway[189].

## 5.3. Study of the reversal effect on p-glycoprotein mediated multi-drug resistance function using compound 160a

The effect of reversing the p-glycoprotein based multi-drug resistance using quinoline compound 160a was investigated in this project. (8-(3-methoxybenzyloxy) quinoline-2-carbaldehyde (160a) was prepared previously by Dr. Penny Chan Sau-hing in 2012 from our research group. The structure of compound 160a was shown in Figure 2.5 and was confirmed by $^{1}$H-NMR (Figure 2.6).

As mentioned before, SEA program was first performed to predict the possible human targets for the compound 160a. Table 4.13 listed the top 3 predicted human protein targets for compound 160a. P-glycoprotein possessed the highest maximum target complementary value and the second lowest expected value ($3.235e^{-18}$). What's more, overexpression of p-glycoprotein is one of the major mechanisms of MDR in cancers[124]. On the other side, the predicted target with the lowest expected value ($2.272e^{-19}$) MTNR1A encodes one of the two high-affinity forms of a receptor for melatonin. Diseases related to MTNR1A include idiopathic scoliosis and scoliosis[190] which are not directly associated with this project, but deserve future efforts for further investigation. Hence, p-glycoprotein was selected as the target of compound 160a for further investigation in cancers.

Doxorubicin is extensively used to treat many types of cancers, including leukemias, bladder, breast and lung cancers[68], and is a well-known p-glycoprotein substrate which induces multi-dug resistance. Drug resistance is the main limitation in doxorubicin therapeutic progress[71]. Therefore, doxorubicin was chosen in this

project as an indicator to evaluate the possible anti-MDR effect of compound 160a.

Dox-resistance cell lines A549/DOX and KYSE150/DOX were cultured under doxorubicin with increasing concentration(from 0.1 μg/mL, 0.2 μg/mL, 0.5 μg/mL, 0.75 μg/mL to final 1.00 μg/mL) to maintained dox-resistance. Dox-resistance cell lines LCC6/MDR and MX100 were kindly provided by Professor Larry Chow in the Hong Kong Polytechnic University. According to Figure 4.24, in both A549/DOX and KYSE150/DOX cells, doxorubicin showed higher cytotoxicity when combined with compound 160a (no matter low or high dose). There are two inferred reasons to explain this phenomenon. One reason is that compound 160a also possesses cytotoxicity; another reason is that compound 160a produced synergistic effect when combined with doxorubicin by certain mechanisms. It was hypothesized that compound 160a probably reversed the drug-resistance effect induced by p-glycoprotein and enhanced the intercellular concentration of doxorubicin to obtain higher cytotoxicity. Therefore, the synergistic effect and its mechanisms were investigated in the next part of this project.

The synergistic effect of doxorubicin with the presence of compound 160a on A549/DOX cells was analyzed by Compusyn program. The percentage of cell viability which was determined by MTS value was applied as the effect to evaluate drug or drug-drug interaction related cytotoxicity. From Figure 4.25, the CI (combination index) values of compound 160a and doxorubicin combination were all below 1. It has been reported that after calculated by Chou-Talalay model [157], CI value < 1, =1 and > 1 indicates synergism, additive effect and antagonism respectively.

Therefore, it is concluded that compound 160a offered the synergistic effect when combined with doxorubicin on A549/DOX cells. Similar examples include the combination treatment with MEK and AKT inhibitors in human non-small cell lung cancer is more effective than each drug alone[191], the pre-use of propranolol before chemotherapy such as 5-fluorouracil or paclitaxel could increase the relapse-free and overall survival in breast cancer patients[192]. The synergistic effects were both evaluated by CI value according to Chou-Talalay model.

The proliferation rates of A549/DOX, KYSE150/DOX, LCC6/MDR, and MX100 cells treated with compound 160a, doxorubicin or compound 160a mixed with doxorubicin were further investigated. From the results in Figure 4.26, for all the four DOX-resistance cancer cell lines, the cells in the control group grew faster compared with the treatment of either compound 160a, doxorubicin or combined groups. The growth of cells with the treatment of either doxorubicin or 160a was suppressed, whereas the treatment of doxorubicin combined with compound 160a showed stronger suppressive effects on cell growth. This observation indicated that compound 160a enhanced the cytotoxic effects of doxorubicin on DOX-resistance cancer cells.

Afterward, the effect of compound 160a on reversing the p-glycoprotein based multi-drug resistance in DOX-resistance cell lines was determined by confocal microscopy and flow cytometry using the multi-drug resistance kit. Calcein AM was applied as the p-glycoprotein substrate instead of doxorubicin. Calcein AM is a cell-permeable non-fluorescent dye, and it exhibits strong green fluorescence once it been transported into viable cells because of the intracellular esterases-mediated

reaction[193]. Thus calcein A could be selected as a probe for identifying p-glycoprotein modulator effect.

According to Figure 4.27, the retention of calcein AM showed an increasing trend after the treatment of either different concentrations of compound 160a or verapamil (a well-known p-glycoprotein inhibitor; applied as a positive control[194])in doxorubicin-resistance A549 cell line. To further study the p-glycoprotein inhibiting effect using compound 160a, SPE Confocal Microscope was used to observe the green fluorescence signal generated by calcein-AM on doxorubicin-resistance A549 cell lines after being treated with compound 160a. Figure 4.28 showed that the fluorescence signal intensity generated by calcein-AM showed an increasing trend after the treatment of compound 160a in doxorubicin resistance A549 cell line. From the results of these two tests, it is suggested that compound 160a could increase the intracellular green fluorescence intensity produced by calcein AM in DOX-resistance cell lines, indicating the ability of compound 160a to reverse the multi-drug resistance conferred by p-glycoprotein by inhibiting the pumping-out effect of p-glycoprotein.

To provide more evidences about using compound 160a in reversing MDR effect, doxorubicin accumulation test was performed. Figure 4.30 shows the effect of compound 160a on intracellular DOX accumulation in parental/DOX-resistance cells. DOX accumulation was more intensive if the parental cells were remarkably showing higher DOX amount than the DOX-resistance cells. According to the results in Section 4.3.7, intracellular DOX concentration is 1.75 times higher in LCC6 than in LCC6/MDR cells; 1.56 times higher in KYSE150 than KYSE150/DOX cells; 1.97

times higher in A549 than in A549/DOX cells; and in MCF-7 it is 2.06 times higher in MX100 cells in the absence of compound 160a, which can be ascribed to p-glycoprotein mediated DOX efflux. Additionally, in DOX-resistance cell lines, intracellular doxorubicin concentration was increased in a dose-depend behavior with the increasing concentration of compound 160a, suggesting that compound 160a may play its MDR reversing effect by inhibiting p-glycoprotein function. Comparing with the effect of verapamil, both 20 μg/ml and 50 μg/ml compound 160a enhanced more intracellular DOX accumulation than 50 μg/ml verapamil. On LCC6/MDR, KYSE150/DOX, and A549/DOX cells, even 10 μg/ml of compound 160a revealed a stronger enhancing effect than verapamil in DOX accumulation. These data suggested that compound 160a exhibited stronger effect in increasing DOX accumulation into DOX-resistance cancer cells than verapamil with the use of lesser dose. The hypothesis mechanisms of compound 160a reverse MDR effect by inhibiting P-gp based drug efflux function was summarized in Figure 5.2

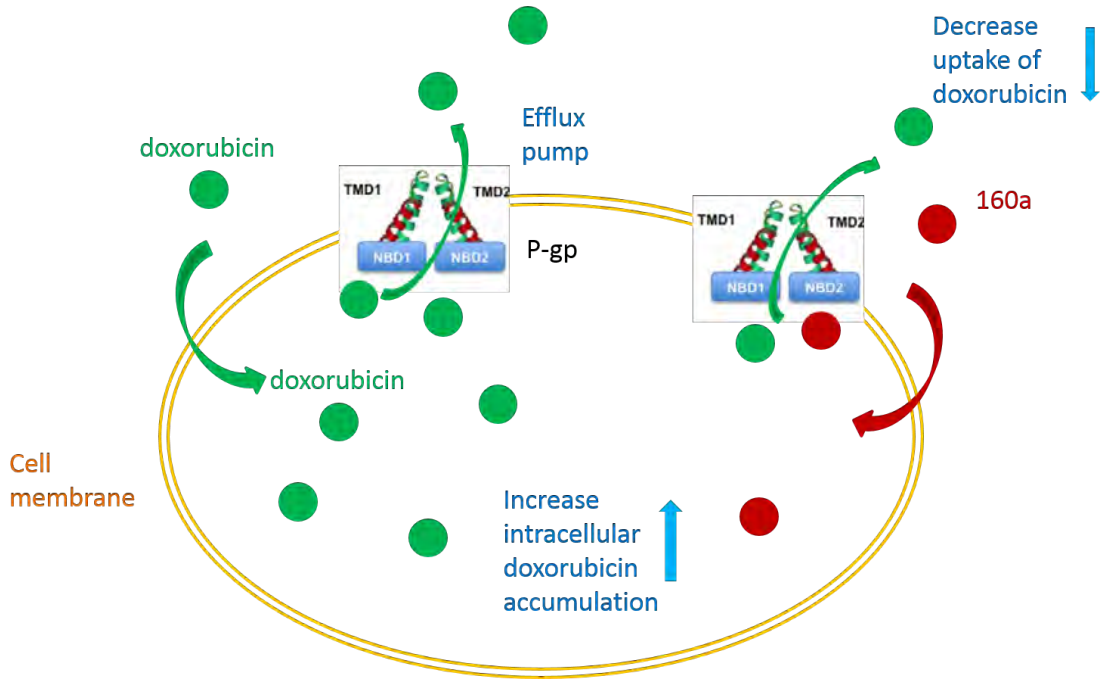


**Figure 5.2 Hypothesized mechanisms of compound 160a reverse MDR effect by inhibiting p-gp based drug efflux function.**

It was reported previously that a serios of novel quinoline compounds 6,7-dimethoxy-2-(2-(4-(1H-1, 2, 3- triaxol-1-yl) phenyl) ethyl)-1, 2, 3, 4-tetrahydroisoquinolines possess MDR-reverse potency which could enhance the effect of other MDR-related cytotoxic agents and increase the accumulation of DOX in K562/A02 MDR cells using the similar experiment[195].

From the above experimental results, it is concluded that compound 160a plays a synergistic effect when it is present with p-glycoprotein substrate doxorubicin by reversing the efflux action of p-glycoprotein. To evaluate the duration of the reversal effect of compound 160a, the DOX-resistance cancer cells were incubated with compound 160a overnight followed by removal of compound 160a with washing and then incubated with fresh culture medium for various times before doxorubicin treatment. Cell viability was determined by MTS assay, and the results were shown in

Figure 4.32. The potency for p-glycoprotein mediated MDR-reversal effect of compound 160a was existed after its removal and was still significant after 1 hour in A549/DOX cells and 0.5 hours in MX100 cells. On the contrary the p-glycoprotein reversal effect was not observed in 2 hours after the removal of compound 160a. These results demonstrated that the MDR reversal effect on p-glycoprotein induced by compound 160a could persist at least for 1 hour. Similar results were reported previously with the use of verapamil whose MDR-reversing potency was decreased immediately after removal[196], and the use of cyclosporin A which lost the MDR-reversing activity within 60 mins after removal[138].

The development of drug resistance during chemotherapy is one of the major obstacles in cancer therapy, hence anti-cancer drugs combined with anti-MDR agents is a desirable strategy [7]. Most drugs are metabolized by liver CYP450 enzymes, whose activities are usually inhibited or induced by many kinds of drugs, resulting in drug-drug interactions when two or more drugs are combined and administrated at the same time to cause serious adverse reactions or even toxicity. Therefore, anti-MDR drugs whose reversal effect is decreased quickly after administration or only lasts for a very short time are less desirable, as at the same time it may be required to administer the patients with more drugs (anti-MDR drugs and anti-cancer drugs)and this probably induces unnecessary drug-drug interactions[197]. From the doxorubicin duration assay, the MDR-reversing potency of compound 160a persisted for about 0.5 to 1 hour and this observation may provide a more reasonable administration scheme to give anti-MDR drugs first, and then followed by other anti-cancer drugs after a

period of time, in order to minimize the drug-drug interaction and reversing the multi-drug resistance at the same time.

# Chapter 6 Conclusions

## 6.1. Study of the anti-cancer effect of compound 91b1

The novel quinoline compound 91b1 demonstrated strong anti-cancer effect both *in vitro* and *in vivo* with relatively low toxicity. Compound 91b1 suppressed cell proliferation, migration, invasion, and modulated cell cycle of cancer cells. Compound 91b1 down regulated lumican mRNA expression.

The above results suggest the great potential of quinoline compound 91b1 to be developed as a novel anti-cancer drug. Apart from the high activity and low toxicity of compound 91b1 both *in vitro* and *in vivo*, the pharmacokinetic behavior is also very important, and the study is required in the future work.

## 6.2. Study of the functional role of lumican in cancer progression

Lumican was found frequently upregulated in cancer cells and tumor tissues from ESCC patient samples. This project provided the evidence that lumican protein enhanced cancer cell proliferation, migration, and invasion in ESCC KYSE150, lung cancer cell line A549, and gastric cancer cell line AGS. It is hypothesized that compound 91b1 inhibits cancer cell progression by down regulating lumican expression through modulating Erk1/2 signaling pathway. The upstream signaling pathway such as FAK signaling pathway, and other associated proteins such as

integrins will be the next focus in future work. The overall results offer a new perspective that lumican could be developed as a new therapeutic target in cancer treatment.

## 6.3. Study of the reversal effect on p-glycoprotein based multi-drug resistance using compound 160a

The quinoline-based compound 160a possesses synergistic effect when combined with doxorubicin against DOX-resistance cancer cells. The compound 160a probably reverses the multi-drug resistance by modulating the p-glycoprotein based drug-efflux effect. The strong and persisted MDR reversal effect suggested the potential of compound 160a as anti-MDR drug to combine with anti-cancer drugs for higher therapeutic effect and lower toxicity.

# APPENDICES

## Appendix A - Information of *lumican*

### I General Information for lumican

| | |
|---|---|
| **Gene ID** | 4060 |
| **Gene Symbol** | LUM |
| **Source** | Homo sapiens (human) |
| **Gene type** | Protein coding |
| **Location** | Chromosome 12q21.33 |
| **Exon count** | 3 |
| **Predicted protein** | lumican |
| **Protein size** | 338 amino acids |
| **Protein molecular mass** | 38429 Da |

### II Homo sapiens lumican (LUM), mRNA

```
   1 ACAGTGAGCT TCCTTATTTG AAGCAGGACT CAATTCTTGG TTAAAAGCTA TGGTATTTGA
  61 GCTAGTTAAA CACATATCTC TCTCCCATTC CATAGGGAAT GAGCTGGGCT GTCCTTTCTC
 121 CCCACGTTCA CCTGCACTTC GTTAGAGAGC AGTGTTCACA TGCCACACCA CAAGATCCCC
 181 ACAATGACAT AACTCCATTC AGAGACTGGC GTGACTGGGC TGGGTCTCCC CACCCCCCTT
 241 CAGCTCTTGT ATCACTCAGA ATCTGGCAGC CAGTTCCGTC CTGACAGAGT TCACAGCATA
 301 TATTGGTGGA TTCTTGTCCA TAGTGCATCT GCTTTAAGAA TTAACGAAAG CAGTGTCAAG
 361 ACAGTAAGGA TTCAAACCAT TTGCCAAAAA TGAGTCTAAG TGCATTTACT CTCTTCCTGG
 421 CATTGATTGG TGGTACCAGT GGCCAGTACT ATGATTATGA TTTTCCCCTA TCAATTTATG
 481 GGCAATCATC ACCAAACTGT GCACCAGAAT GTAACTGCCC TGAAAGCTAC CCAAGTGCCA
 541 TGTACTGTGA TGAGCTGAAA TTGAAAAGTG TACCAATGGT GCCTCCTGGA ATCAAGTATC
 601 TTTACCTTAG GAATAACCAG ATTGACCATA TTGATGAAAA GGCCTTTGAG AATGTAACTG
 661 ATCTGCAGTG GCTCATTCTA GATCACAACC TTCTAGAAAA CTCCAAGATA AAAGGGAGAG
 721 TTTTCTCTAA ATTGAAACAA CTGAAGAAGC TGCATATAAA CCACAACAAC CTGACAGAGT
 781 CTGTGGGCCC ACTTCCCAAA TCTCTGGAGG ATCTGCAGCT TACTCATAAC AAGATCACAA
 841 AGCTGGGCTC TTTTGAAGGA TTGGTAAACC TGACCTTCAT CCATCTCCAG CACAATCGGC
 901 TGAAAGAGGA TGCTGTTTCA GCTGCTTTTA AAGGTCTTAA ATCACTCGAA TACCTTGACT
```

```
 961 TGAGCTTCAA TCAGATAGCC AGACTGCCTT CTGGTCTCCC TGTCTCTCTT CTAACTCTCT
1021 ACTTAGACAA CAATAAGATC AGCAACATCC CTGATGAGTA TTTCAAGCGT TTTAATGCAT
1081 TGCAGTATCT GCGTTTATCT CACAACGAAC TGGCTGATAG TGGAATACCT GGAAATTCTT
1141 TCAATGTGTC ATCCCTGGTT GAGCTGGATC TGTCCTATAA CAAGCTTAAA AACATACCAA
1201 CTGTCAATGA AAACCTTGAA AACTATTACC TGGAGGTCAA TCAACTTGAG AAGTTTGACA
1261 TAAAGAGCTT CTGCAAGATC CTGGGGCCAT TATCCTACTC CAAGATCAAG CATTTGCGTT
1321 TGGATGGCAA TCGCATCTCA GAAACCAGTC TTCCACCGGA TATGTATGAA TGTCTACGTG
1381 TTGCTAACGA AGTCACTCTT AATTAATATC TGTATCCTGG AACAATATTT TATGGTTATG
1441 TTTTTCTGTG TGTCAGTTTT CATAGTATCC ATATTTTATT ACTGTTTATT ACTTCCATGA
1501 ATTTTAAAAT CTGAGGGAAA TGTTTTGTAA ACATTTATTT TTTTTAAAGA AAAGATGAAA
1561 GGCAGGCCTA TTTCATCACA AGAACACACA CATATACACG AATAGACATC AAACTCAATG
1621 CTTTATTTGT AAATTTAGTG TTTTTTTATT TCTACTGTCA AATGATGTGC AAAACCTTTT
1681 ACTGGTTGCA TGGAAATCAG CCAAGTTTTA TAATCCTTAA ATCTTAATGT TCCTCAAAGC
1741 TTGGATTAAA TACATATGGA TGTTACTCTC TTGCACCAAA TTATCTTGAT ACATTCAAAT
1801 TTGTCTGGTT AAAAAATAGG TGGTAGATAT TGAGGCCAAG AATATTGCAA AATACATGAA
1861 GCTTCATGCA CTTAAAGAAG TATTTTTAGA ATAAGAATTT GCATACTTAC CTAGTGAAAC
1921 TTTTCTAGAA TTATTTTTCA CTCTAAGTCA TGTATGTTTC TCTTTGATTA TTTGCATGTT
1981 ATGTTTAATA AGCTACTAGC AAAATAAAAC ATAGCAAATG GCATCACTGT GTTTGACTTC
2041 TTGTGAAATT TCTGTACTTT GTATATAAAA TACATAAAAC AATAGATTAG AAATCAAAAG
2101 ATATCTCTGG CCTGCA
```

## III Protein sequence

```
1 mtlnslpifl llisgifcqy dygpaddygy dpfgpssavc apecncplsy ptamycdnlk
  61 lktipivpsg ikylylrnnm iegieentfd nvtdlqwlil dhnhlenski kgrvfsklkh
 121 lkklhinynn lteavgplpk tlddlqlshn kitkvnpgal eglvnltvih lqnnqlkads
 181 isgafkglns llyldlsfnr ltklptglph sllmlyfdnn qisnvpdeyf qgfkalqylr
 241 lshnkltdsg ipgnvfnits lveldlsfnq lksiptvsen lenfylqvnk inkfplssfc
 301 kvvgpmtysk ithlrldgnn ltradlpqem ynclrvaaei sleqtmtlkv ytsllllflv
 361 navwtrtvrq vydeldpdhw shytfecpqe cfcppsfpna lycdnkglke ipaipariwy
 421 lylqnnliet isekpfvnat hlrwinlnkn kitnsgigsg vlsklkrlly lflednelee
 481 vpaplpvgle qlrlarnkis ripegvfsnl enltmldlhq nslldsalqs dtfqglnnlm
 541 qlniaknslk kmplsipant lqlfldnnsi evipenyfsa ipkvtflrln ynklsddgip
 601 pngfnvssil dlqlshnqlt kippinahle hlhldhnrik svngtqicpv sisvaedhgf
 661 ygniprlryl rldgneiqpp ipldimicfr llqavii
```

# Appendix B - Information of P-gp

## I General Information for P-gp

| | |
|---|---|
| **Gene ID** | 5243 |
| **Gene Symbol** | P-gp/ABCB1 |
| **Official Full Name** | ATP binding cassette subfamily B member 1 |
| **Gene type** | Protein coding |
| **Source** | Homo sapiens (human) |
| **Location** | Chromosome 7p21.12 |
| **Exon count** | 32 |
| **Predicted protein** | Multidrug resistance protein 1 |
| **Protein size** | 1280 amino acids |
| **Protein molecular mass** | 141470 Da |

## II Coding sequence of P-gp

```
  1 GATATCAGCT CGATGAGTTT ACTGATTACG GCCTTGGTAC CGTAAGAGGA CGCCATTGGA
 61 AAACATTCCA CCCATTTACT ATAAGCGTCG ACAACAATAA AAAACATTTG ATTATTCAAC
121 GGCCCCAAAA AGTCAACGTG AATACGATAG AATGCATGTG GTGGTAGCGG CCATGGCGAG
181 AGTGGTGCGC GCGGGGGAGC GGGACGAAGC GCAGCGCATA TAGCACATTC GACTGCGAGC
241 CGTTCTAGCT GCTCGTCGAC GCCTGGGAAC CAAAACCGTT TTCGCGCCTC CGCTTTCATC
301 TTCACTATGC CGAAATGTGA GCTATGCAAT TCATTACATA CTATATTTCG GAGTGAAGTC
361 GGCAGTATGA CCTTGTGACC TCGCATGAGA CATCCGTTTT CATACGATAT TTGCATACGA
421 CAGTTATGAT AAGGTTTCAG AGCTGAATCG ATTATCTTTC TCGGCCAACC GTTTAACACG
481 TAATCCTTTA CTTTGCCTAG GGTGACATCT TTGTTAGTTT CTACCTGAAC TCGTTGTAAC
541 GTTACGGGCA TATCTCCCTG CATTACGAAA TTAACGTATG TAGCACGGTC TATGACATCA
601 CAGCACTCCT CCGACGTTTG TGCCGGCAAC GGAACTCGCG AAAAGTAATC CGCGCTATTA
661 TCACTACTTC TAACGTATTC AATAGTATAG TTGTAAGCGG TCAAAAATAT CGCGTAACGT
721 TGCAGTCGGT TCGCCGAGAT CTCATCGTCA TCATCAACAG ACTCTTCAAT GGTCTATCAA
781 TGGGATTACT TTACTTCTGC ATCTTCTGTT CTTACGCTGT TTCCTTTTGG TTTGGGTACA
```

841 AATTGATGAT TGACGAACCG GAAAATTACG ATGTCAATAC CATGATTGCT GTGTTTTTTG
901 GTATCATGAC GGGATCACAA AACTTTGGTA TCTCATCGAC TATTATGGAA GTGTTCGGAG
961 TAGCGCAAGG CGCTGGTGCA CAAATATTCC ATTTGATAGA CAACGTACCG ACAATAAACC
1021 CTTTGCGAAA CGAGGGTGAT GTACCTAAGT TGATAAACGG TAATATTGAA TTGAAGAATG
1081 TCGTATTCCA CTATCCGTCA CGACCCGATG TACCGGTACT AAAAGGTGTC AACCTCACAA
1141 TAAAACACGG ACAATCCGTT GCCTTAGTTG GACATTCCGG ATGCGGCAAG TCTACTATCA
1201 TACAACTGCT ATCCAGGTAC TACGATGTCA TCGATGGAAG CGTGATATTA GATGGTAAAG
1261 ATATACGCAA ATTGTCAGTT CGTTGGTTAC GAGCACAAAT CGGTCTGGTA GGCCAGGAGC
1321 CAGCACTATT TAACACCACA GTAAGAGAGA ACATCCGTTA CGGCCGCAAA GATGCTTCCG
1381 ATGCAGATAT AGAAGCAAGT TCCAAACAAG CTAACGCTCA CCACTTCATA ATGAAATTAC
1441 CAAAGGGTTA TGATACGCAA GTTGGCGAAC ATGGAGCTTC ACTTTCAGGC GGACAGAAGC
1501 AAAGGATCGC TATAGCTCGT GCTCTCGTTC GAAATCCGAA ACTCCTCTTA CTCGATGAAG
1561 CGACCAGTGC TTTGGACACC TCCTCAGAAG CTAAAGTTCA AAAAGCTTTG GACAAGGCTC
1621 AAGAAGGTCG AACGACAGTG GTAGTGGCTC ACAGATTATC GACAATAAGA CACGTGGATA
1681 TAATTTACGT TTTCAAAAGT GGAGAAATCA TAGAAAGCGG CAATCACGAA GACTTGATGA
1741 AGAAGAAGGG TCATTATTAC GATATGGTTA TGGTCCAAGC GGCACCAGAG GCGGAAGAGA
1801 AAAAAGATAA TGAAATCCTT AATCGTCAAA TGTCACTCAT CAGCGAAGAA GATGAAGACG
1861 AAGTGATAGA AATAAAACAG AAAGAAGTAG ATGAAAAGGA AGTTAAAGAA CCGGAAGTGT
1921 CTTTTTGGAA AGTACTGCAT TTGAATGCAC CGGAATGGAA ATCTGTAGGG ACGGCTAGCC
981 TGTCTTCACT AATTAGCGGG TTCGCTATGC CCGTATTTGC TATTATCCTT GGAGATTTTA
2041 TCGGTGTATT GTCAGATCCA AATCAAGATG AAGTTATGAG ACAGATCATC AAATACGCGT
2101 TGATATTTTT AGGGGTAGGC ATTTATTCTG GCGTCTCCAA CTTCATCGTG GTATACTTTT
2161 ACGCTATTGG TGGAGAATAT TTGACAGAAC GACTGAGATT TTTAATCTTC GAACATTTAC
2221 TCCAACAAGA TATGGGGTTT TACGATGACA AAATGAACTC TACAGGTGCT CTGTGCGCAA
2281 GGTTGTCAGG TGAAAGTGCA AAAGTACAAG GAGCAACAGG TCAACGAATC GGTACAGTAG
2341 TGCAAGCTAT CGGAACGTTT TCCTTAGCAT TAGTACTTTC TTTGTATTAC GAATGGAGAG
2401 TGGGACTTGT GGCACTTACA TTTGTGCCAC TGATGGTTGC CCTTTTATAC AAAGAAGCCA
2461 GAATGGCGAA TGCTGAGTCA TTCGGTACAG CCAAAACAAT GGAAGAAAGC TCAAAGATTG
2521 CTGTAGAAGC AGTAGCTAAC ATTCGCACGG TAGCGTCATT GGGACGTGAA GAGACTTTTC
2581 TAGAAGAATA TTCAGCGAAA CTGTTACCAG GATTAGTTCT CGCGAAACGC AGTGCTCACT
2641 GGCGAGGCTT GGTATTCGGC ATGTCTCGAG GTTTATTCAG CTTTGTATAC GGCGTTTCTT
2701 TGTATTACGG AGGAACCTTA ATAGTATATC ACAACGTTCC CTATGCTGTA ATTTTAAAGT
2761 CGTCAGAGGC ACTTCTTATG GGGGCGATGA CCGCCGCGGA AGCCTTTGCG TTCGCTCCGA
2821 ATTTCCAAAA AGGTATTAAA GCAGCCGGAC GTATCCTTAT AATGCTAAAA GGAAAATCAA
2881 AAATAGTTGA TCCAGATAAA CCGGTTCTCG ATTTCAAAGG AACTGGTAAA GCCAATTTAC
2941 AGAATGTAAC ATTTAAATAC CCGACCAGAC CATCAATAAA AGTACTGAAG AGTATAAACC
3001 TAGATATTGA AAAAGGTAAA ACGATAGCTC TGGTTGGCGC CAGCGGATGT GGTAAGAGTA
3061 CGGTCATACA ACTACTGGAG AGATATTACG ACCCCGATGA AGGAATAGTG TCTCAAGATA
3121 ACGTACCGCT ACAAAAGTTG CGATTATCTG ACGCAAGACA ACCGATAGGA TTTGTACAAC
3181 AAGAGCCGAT ATTATTCGAC CGGACGATCG GTGAAAATAT CGCATATGGA GACAACTCTC
3241 GGACTGCAAA TATGGACGAC ATCATTGCGG TCGCCAAGGA AGCGAACATA CATACGTTTA
3301 TATCATCATT ACCACTAGGT TACGATACAA ATATCGGCTC AAAGGGAACA CAACTTTCCG
3361 GTGGTCAAAA GCAAAGAATA GCGATAGCCA GAGCATTGTT ACGACGACCC AAGATGCTGC
3421 TGCTTGATGA AGCGACCAGC GCTCTCGACA CAGAGAGTGA AAAGGTTGTA CAAGAAGCGT

```
3481 TGGACGCCGC CAAAGCGGGC CGCACGTGCG TCATGATCGC GCACAGACTG AGCACAGTCC
3541 GCGACGCTGA CGTCATCTGT GTGCTCAGCG ACGGCCGCGT CGCGGAAGCG GGCACACACT
3601 CGCAACTCAT GGATCTCAAG GGACTATACT ATAAACTAAA CTCTCAAGGC TATGCTTAAC
3661 GTTACATTTT ACTCTTCAAG GATAGATTAT AATGACTATT TATATTGTTT AGAATTAGAA
3721 ACAATTTTCT ACCAAATGTT CAAGTTTACG ATGATATTTA TTGTAGGCCA ATAATTGTAT
3781 ATAGTACATA CATTACCATA TAGGGGTACT TAATATTATA TAATAAACGA CATGAATTAA
3841 GAAAA
```

## III Protein sequence afterP-gptranslation

```
   1 mdlegdrngg akkknffkln nksekdkkek kptvsvfsmf rysnwldkly mvvgtlaaii
  61 hgaglplmml vfgemtdifa nagnledlms nitnrsdind tgffmnleed mtryayyysg
 121 igagvlvaay iqvsfwclaa grqihkirkq ffhaimrqei gwfdvhdvge lntrltddvs
 181 kinegigdki gmffqsmatf ftgfivgftr gwkltlvila ispvlglsaa vwakilssft
 241 dkellayaka gavaeevlaa irtviafggq kkelerynkn leeakrigik kaitanisig
 301 aaflliyasy alafwygttl vlsgeysigq vltvffsvli gafsvgqasp sieafanarg
 361 aayeifkiid nkpsidsysk sghkpdnikg nlefrnvhfs ypsrkevkil kglnlkvqsg
 421 qtvalvgnsg cgksttvqlm qrlydptegm vsvdgqdirt invrflreii gvvsqepvlf
 481 attiaeniry grenvtmdei ekavkeanay dfimklphkf dtlvgergaq lsggqkqria
 541 iaralvrnpk illldeatsa ldteseavvq valdkarkgr ttiviahrls tvrnadviag
 601 fddgvivekg nhdelmkekg iyfklvtmqt agnevelena adeskseida lemssndsrs
 661 slirkrstrr svrgsqaqdr klstkealde sippvsfwri mklnltewpy fvvgvfcaii
 721 ngglqpafai ifskiigvft riddpetkrq nsnlfslllfl algiisfitf flqgftfgka
 781 geiltkrlry mvfrsmlrqd vswfddpknt tgalttrlan daaqvkgaig srlavitqni
 841 anlgtgiiis fiygwqltll llaivpiiai agvvemkmls gqalkdkkel egsgkiatea
 901 ienfrtvvsl tqeqkfehmy aqslqvpyrn slrkahifgi tfsftqammy fsyagcfrfg
 961 aylvahklms fedvllvfsa vvfgamavgq vssfapdyak akisaahiim iiektplids
1021 ysteglmpnt legnvtfgev vfnyptrpdi pvlqglslev kkgqtlalvg ssgcgkstvv
1081 qllerfydpl agkvlldgke ikrlnvqwlr ahlgivsqep ilfdcsiaen iaygdnsrvv
1141 sqeeivraak eanihafies lpnkystkvg dkgtqlsggq kqriaiaral vrqphillld
1201 eatsaldtes ekvvqealdk aregrtcivi ahrlstiqna dlivvfqngr vkehgthqql
1261 laqkgiyfsm vsvqagtkrq
```

# Appendix C- Information of Human LUM ORF mammalian expression plasmid

## Ⅰ Information of Human LUM ORF mammalian expression plasmid

| | |
|---|---|
| **Vector Name** | pCMV3-C-Myc |
| **Vector Size** | 6164 bp |
| **Vector Type** | Mammalian Expression Vector |
| **cDNA Size** | 1017 bp |
| **Expression Method** | Constitutive, Stable / Transient |
| **Promoter** | CMV |
| **Antibiotic Resistance** | Kanamycin |
| **Selection in Mammalian Cells** | Hygromycin |
| **Protein Tag** | GAGCAGAAACTCATCTCAGAAGAGGATCTG |
| **Sequencing Primer** | Forward T7: 5’ TAATACGACTCACTATAGGG 3’<br>ReverseBGH: 5’TAGAAGGCACAGTCGAGG 3’ |

## Ⅱ Sequences of Human LUM ORF mammalian expression plasmid

ATGAGTCTAAGTGCATTTACTCTCTTCCTGGCATTGATTGGTGGTACCAGTGGCCAGTACTATGA
TTATGATTTTCCCCTATCAATTTATGGGCAATCATCACCAAACTGTGCACCAGAATGTAACTGCC
CTGAAAGCTACCCAAGTGCCATGTACTGTGATGAGCTGAAATTGAAAAGTGTACCAATGGTGCC
TCCTGGAATCAAGTATCTTTACCTTAGGAATAACCAGATTGACCATATTGATGAAAAGGCCTTTG
AGAATGTAACTGATCTGCAGTGGCTCATTCTAGATCACAACCTTCTAGAAAACTCCAAGATAAA
AGGGAGAGTTTTCTCTAAATTGAAACAACTGAAGAAGCTGCATATAAACCACAACAACCTGACA

GAGTCTGTGGGCCCACTTCCCAAATCTCTGGAGGATCTGCAGCTTACTCATAACAAGATCACAA
AGCTGGGCTCTTTTGAAGGATTGGTAAACCTGACCTTCATCCATCTCCAGCACAATCGGCTGAA
AGAGGATGCTGTTTCAGCTGCTTTTAAAGGTCTTAAATCACTCGAATACCTTGACTTGAGCTTCA
ATCAGATAGCCAGACTGCCTTCTGGTCTCCCTGTCTCTCTTCTAACTCTCTACTTAGACAACAATA
AGATCAGCAACATCCCTGATGAGTATTTCAAGCGTTTTAATGCATTGCAGTATCTGCGTTTATCTC
ACAACGAACTGGCTGATAGTGGAATACCTGGAAATTCTTTCAATGTGTCATCCCTGGTTGAGCTG
GATCTGTCCTATAACAAGCTTAAAAACATACCAACTGTCAATGAAAACCTTGAAAACTATTACCT
GGAGGTCAATCAACTTGAGAAGTTTGACATAAAGAGCTTCTGCAAGATCCTGGGGCCATTATCC
TACTCCAAGATCAAGCATTTGCGTTTGGATGGCAATCGCATCTCAGAAACCAGTCTTCCACCGG
ATATGTATGAATGTCTACGTGTTGCTAACGAAGTCACTCTTAATGGGGGTGGAGGCTCTGAGCA
GAAACTCATCTCAGAAGAGGATCTGTAA

MSLSAFTLFLALIGGTSGQYYDYDFPLSIYGQSSPNCAPECNCPESYPSAMYCDELKLKSVPMVPPGIK
YLYLRNNQIDHIDEKAFENVTDLQWLILDHNLLENSKIKGRVFSKLKQLKKLHINHNNLTESVGPLPKSL
EDLQLTHNKITKLGSFEGLVNLTFIHLQHNRLKEDAVSAAFKGLKSLEYLDLSFNQIARLPSGLPVSLLTL
YLDNNKISNIPDEYFKRFNALQYLRLSHNELADSGIPGNSFNVSSLVELDLSYNKLKNIPTVNENLENYY
LEVNQLEKFDIKSFCKILGPLSYSKIKHLRLDGNRISETSLPPDMYECLRVANEVTLNGGGGSEQKLISEE
DL-

# Appendix D - Information of pcMv/hygro-negative control vector

## I Information of pcMv/hygro-negative control vector

| | |
|---|---|
| Vector Name | pCMV/hygro-Myc |
| Vector Size | 5558bp |
| Vector Type | Mammalian Expression Vector |
| Expression Method | Constitutive, Stable / Transient |
| Promoter | CMV |
| Antibiotic Resistance | Ampicillin |
| Selection in Mammalian Cells | Hygromycin |
| Protein Tag | GAGCAGAAACTCATCTCAGAAGAGGATCTG |
| Sequencing Primer | ForwardT7:5’ TAATACGACTCACTATAGGG 3’<br>ReverseBGH: 5’ TAGAAGGCACAGTCGAGG 3’ |

## II Sequences of pcMv/hygro-negative control vector

```
1       GACGGATCGG GAGATCTCCC GATCCCCTAT GGTGCACTCT CAGTACAATC TGCTCTGATG
61      CCGCATAGTT AAGCCAGTAT CTGCTCCCTG CTTGTGTGTT GGAGGTCGCT GAGTAGTGCG
121     CGAGCAAAAT TTAAGCTACA ACAAGGCAAG GCTTGACCGA CAATTGCATG AAGAATCTGC
181     TTAGGGTTAG GCGTTTTGCG CTGCTTCGCG ATGTACGGGC CAGATATACG CGTTGACATT
241     GATTATTGAC TAGTTATTAA TAGTAATCAA TTACGGGGTC ATTAGTTCAT AGCCCATATA
301     TGGAGTTCCG CGTTACATAA CTTACGGTAA ATGGCCCGCC TGGCTGACCG CCCAACGACC
361     CCCGCCCATT GACGTCAATA ATGACGTATG TTCCCATAGT AACGCCAATA GGGACTTTCC
421     ATTGACGTCA ATGGGTGGAG TATTTACGGT AAACTGCCCA CTTGGCAGTA CATCAAGTGT
481     ATCATATGCC AAGTACGCCC CCTATTGACG TCAATGACGG TAAATGGCCC GCCTGGCATT
541     ATGCCCAGTA CATGACCTTA TGGGACTTTC CTACTTGGCA GTACATCTAC GTATTAGTCA
601     TCGCTATTAC CATGGTGATG CGGTTTTGGC AGTACATCAA TGGGCGTGGA TAGCGGTTTG
661     ACTCACGGGG ATTTCCAAGT CTCCACCCCA TTGACGTCAA TGGGAGTTTG TTTTGGCACC
721     AAAATCAACG GGACTTTCCA AAATGTCGTA ACAACTCCGC CCCATTGACG CAAATGGGCG
781     GTAGGCGTGT ACGGTGGGAG GTCTATATAA GCAGAGCTCT CTGGCTAACT AGAGAACCCA
841     CTGCTTACTG GCTTATCGAA ATTAATACGA CTCACTATAG GGAGACCCAA GCTGGCTAGG
901     CCGCCACCAA GCTTGGTACC GCTGAGCAGA AACTCATCTC AGAAGAGGAT CTGTAAAGGG
961     CCCGTTTAAA CCCGCTGATC AGCCTCGACT GTGCCTTCTA GTTGCCAGCC ATCTGTTGTT
1021    TGCCCCTCCC CCGTGCCTTC CTTGACCCTG GAAGGTGCCA CTCCCACTGT CCTTTCCTAA
1081    TAAAATGAGG AAATTGCATC GCATTGTCTG AGTAGGTGTC ATTCTATTCT GGGGGGTGGG
1141    GTGGGGCAGG ACAGCAAGGG GGAGGATTGG GAAGACAATA GCAGGCATGC TGGGGATGCG
1201    GTGGGCTCTA TGGCTTCTGA GGCGGAAAGA ACCAGCTGGG GCTCTAGGGG GTATCCCCAC
1261    GCGCCCTGTA GCGGCGCATT AAGCGCGGCG GGTGTGGTGG TTACGCGCAG CGTGACCGCT
```

1321 ACACTTGCCA GCGCCCTAGC GCCCGCTCCT TTCGCTTTCT TCCCTTCCTT TCTCGCCACG
1381 TTCGCCGGCT TTCCCCGTCA AGCTCTAAAT CGGGGGCTCC CTTTAGGGTT CCGATTTAGT
1441 GCTTTACGGC ACCTCGACCC CAAAAAACTT GATTAGGGTG ATGGTTCACG TAGTGGGCCA
1501 TCGCCCTGAT AGACGGTTTT TCGCCCTTTG ACGTTGGAGT CCACGTTCTT TAATAGTGGA
1561 CTCTTGTTCC AAACTGGAAC AACACTCAAC CCTATCTCGG TCTATTCTTT TGATTTATAA
1621 GGGATTTTGC CGATTTCGGC CTATTGGTTA AAAAATGAGC TGATTTAACA AAAATTTAAC
1681 GCGAATTAAT TCTGTGGAAT GTGTGTCAGT TAGGGTGTGG AAAGTCCCCA GGCTCCCCAG
1741 CAGGCAGAAG TATGCAAAGC ATGCATCTCA ATTAGTCAGC AACCAGGTGT GGAAAGTCCC
1801 CAGGCTCCCC AGCAGGCAGA AGTATGCAAA GCATGCATCT CAATTAGTCA GCAACCATAG
1861 TCCCGCCCCT AACTCCGCCC ATCCCGCCCC TAACTCCGCC CAGTTCCGCC CATTCTCCGC
1921 CCCATGGCTG ACTAATTTTT TTTATTTATG CAGAGGCCGA GGCCGCCTCT GCCTCTGAGC
1981 TATTCCAGAA GTAGTGAGGA GGCTTTTTTG GAGGCCTAGG CTTTTGCAAA AAGCTCCCGG
2041 GAGCTTGTAT ATCCATTTTC GGATCTGATC AGCACGTGAT GAAAAAGCCT GAACTCACCG
2101 CGACGTCTGT CGAGAAGTTT CTGATCGAAA AGTTCGACAG CGTCTCCGAC CTGATGCAGC
2161 TCTCGGAGGG CGAAGAATCT CGTGCTTTCA GCTTCGATGT AGGAGGGCGT GGATATGTCC
2221 TGCGGGTAAA TAGCTGCGCC GATGGTTTCT ACAAAGATCG TTATGTTTAT CGGCACTTTG
2281 CATCGGCCGC GCTCCCGATT CCGGAAGTGC TTGACATTGG GGAATTCAGC GAGAGCCTGA
2341 CCTATTGCAT CTCCCGCCGT GCACAGGGTG TCACGTTGCA AGACCTGCCT GAAACCGAAC
2401 TGCCCGCTGT TCTGCAGCCG GTCGCGGAGG CCATGGATGC GATCGCTGCG GCCGATCTTA
2461 GCCAGACGAG CGGGTTCGGC CCATTCGGAC CGCAAGGAAT CGGTCAATAC ACTACATGGC
2521 GTGATTTCAT ATGCGCGATT GCTGATCCCC ATGTGTATCA CTGGCAAACT GTGATGGACG
2581 ACACCGTCAG TGCGTCCGTC GCGCAGGCTC TCGATGAGCT GATGCTTTGG GCCGAGGACT
2641 GCCCCGAAGT CCGGCACCTC GTGCACGCGG ATTTCGGCTC CAACAATGTC CTGACGGACA
2701 ATGGCCGCAT AACAGCGGTC ATTGACTGGA GCGAGGCGAT GTTCGGGGAT TCCCAATACG
2761 AGGTCGCCAA CATCTTCTTC TGGAGGCCGT GGTTGGCTTG TATGGAGCAG CAGACGCGCT
2821 ACTTCGAGCG GAGGCATCCG GAGCTTGCAG GATCGCCGCG GCTCCGGGCG TATATGCTCC
2881 GCATTGGTCT TGACCAACTC TATCAGAGCT TGGTTGACGG CAATTTCGAT GATGCAGCTT
2941 GGGCGCAGGG TCGATGCGAC GCAATCGTCC GATCCGGAGC CGGGACTGTC GGGCGTACAC
3001 AAATCGCCCG CAGAAGCGCG GCCGTCTGGA CCGATGGCTG TGTAGAAGTA CTCGCCGATA
3061 GTGGAAACCG ACGCCCCAGC ACTCGTCCGA GGGCAAAGGA ATAGCACGTG CTACGAGATT
3121 TCGATTCCAC CGCCGCCTTC TATGAAAGGT TGGGCTTCGG AATCGTTTTC CGGGACGCCG
3181 GCTGGATGAT CCTCCAGCGC GGGGATCTCA TGCTGGAGTT CTTCGCCCAC CCCAACTTGT
3241 TTATTGCAGC TTATAATGGT TACAAATAAA GCAATAGCAT CACAAATTTC ACAAATAAAG
3301 CATTTTTTTC ACTGCATTCT AGTTGTGGTT TGTCCAAACT CATCAATGTA TCTTATCATG
3361 TCTGTATACC GTCGACCTCT AGCTAGAGCT TGGCGTAATC ATGGTCATAG CTGTTTCCTG
3421 TGTGAAATTG TTATCCGCTC ACAATTCCAC ACAACATACG AGCCGGAAGC ATAAAGTGTA
3481 AAGCCTGGGG TGCCTAATGA GTGAGCTAAC TCACATTAAT TGCGTTGCGC TCACTGCCCG
3541 CTTTCCAGTC GGGAAACCTG TCGTGCCAGC TGCATTAATG AATCGGCCAA CGCGCGGGGA
3601 GAGGCGGTTT GCGTATTGGG CGCTCTTCCG CTTCCTCGCT CACTGACTCG CTGCGCTCGG
3661 TCGTTCGGCT GCGGCGAGCG GTATCAGCTC ACTCAAAGGC GGTAATACGG TTATCCACAG
3721 AATCAGGGGA TAACGCAGGA AAGAACATGT GAGCAAAAGG CCAGCAAAAG GCCAGGAACC
3781 GTAAAAAGGC CGCGTTGCTG GCGTTTTTCC ATAGGCTCCG CCCCCCTGAC GAGCATCACA
3841 AAAATCGACG CTCAAGTCAG AGGTGGCGAA ACCCGACAGG ACTATAAAGA TACCAGGCGT
3901 TTCCCCCTGG AAGCTCCCTC GTGCGCTCTC CTGTTCCGAC CCTGCCGCTT ACCGGATACC

3961 TGTCCGCCTT TCTCCCTTCG GGAAGCGTGG CGCTTTCTCA TAGCTCACGC TGTAGGTATC
4021 TCAGTTCGGT GTAGGTCGTT CGCTCCAAGC TGGGCTGTGT GCACGAACCC CCCGTTCAGC
4081 CCGACCGCTG CGCCTTATCC GGTAACTATC GTCTTGAGTC CAACCCGGTA AGACACGACT
4141 TATCGCCACT GGCAGCAGCC ACTGGTAACA GGATTAGCAG AGCGAGGTAT GTAGGCGGTG
4201 CTACAGAGTT CTTGAAGTGG TGGCCTAACT ACGGCTACAC TAGAAGAACA GTATTTGGTA
4261 TCTGCGCTCT GCTGAAGCCA GTTACCTTCG GAAAAAGAGT TGGTAGCTCT TGATCCGGCA
4321 AACAAACCAC CGCTGGTAGC GGTTTTTTTG TTTGCAAGCA GCAGATTACG CGCAGAAAAA
4381 AAGGATCTCA AGAAGATCCT TTGATCTTTT CTACGGGGTC TGACGCTCAG TGGAACGAAA
4441 ACTCACGTTA AGGGATTTTG GTCATGAGAT TATCAAAAAG GATCTTCACC TAGATCCTTT
4501 TAAATTAAAA ATGAAGTTTT AAATCAATCT AAAGTATATA TGAGTAAACT TGGTCTGACA
4561 GTTACCAATG CTTAATCAGT GAGGCACCTA TCTCAGCGAT CTGTCTATTT CGTTCATCCA
4621 TAGTTGCCTG ACTCCCCGTC GTGTAGATAA CTACGATACG GGAGGGCTTA CCATCTGGCC
4681 CCAGTGCTGC AATGATACCG CGAGACCCAC GCTCACCGGC TCCAGATTTA TCAGCAATAA
4741 ACCAGCCAGC CGGAAGGGCC GAGCGCAGAA GTGGTCCTGC AACTTTATCC GCCTCCATCC
4801 AGTCTATTAA TTGTTGCCGG GAAGCTAGAG TAAGTAGTTC GCCAGTTAAT AGTTTGCGCA
4861 ACGTTGTTGC CATTGCTACA GGCATCGTGG TGTCACGCTC GTCGTTTGGT ATGGCTTCAT
4921 TCAGCTCCGG TTCCCAACGA TCAAGGCGAG TTACATGATC CCCCATGTTG TGCAAAAAAG
4981 CGGTTAGCTC CTTCGGTCCT CCGATCGTTG TCAGAAGTAA GTTGGCCGCA GTGTTATCAC
5041 TCATGGTTAT GGCAGCACTG CATAATTCTC TTACTGTCAT GCCATCCGTA AGATGCTTTT
5101 CTGTGACTGG TGAGTACTCA ACCAAGTCAT TCTGAGAATA GTGTATGCGG CGACCGAGTT
5161 GCTCTTGCCC GGCGTCAATA CGGGATAATA CCGCGCCACA TAGCAGAACT TTAAAAGTGC
5221 TCATCATTGG AAAACGTTCT TCGGGGCGAA AACTCTCAAG GATCTTACCG CTGTTGAGAT
5281 CCAGTTCGAT GTAACCCACT CGTGCACCCA ACTGATCTTC AGCATCTTTT ACTTTCACCA
5341 GCGTTTCTGG GTGAGCAAAA ACAGGAAGGC AAAATGCCGC AAAAAAGGGA ATAAGGGCGA
5401 CACGGAAATG TTGAATACTC ATACTCTTCC TTTTTCAATA TTATTGAAGC ATTTATCAGG
5461 GTTATTGTCT CATGAGCGGA TACATATTTG AATGTATTTA GAAAAATAAA CAAATAGGGG
5521 TTCCGCGCAC ATTTCCCCGA AAAGTGCCAC CTGACGTC

# Appendix E - Reagents and solutions

## Ⅰ Preparation of stock solution of quinoline compounds

Accurately weight 10 mg of quinoline compounds (compound 91b1 or compound 160a) was added to 200 μL DMSO to get a final concentration of 50 mg/mL. The stock solution was kept at 4 ℃in darkness.

## Ⅱ Preparation of saline

About 9 g sodium chloride (NaCl, Sigma,USA) were added with 1 L ofdouble-distilled water to get a final concentration of 0.9 % saline.

## Ⅲ Preparation of 6% PEG saline vehicle

6% PEG saline was applied as vehicle control in animal test. About 0.6 g PEG was added to 10 mL 0.9 % saline to get a final concentration of 6% PEG saline. The vehicle solution was kept at 4 ℃, and warmed up to 37 ℃ in water bath before administrated to animals.

## Ⅳ Preparation of CDDP

Accurately weight 10 mg of CDDP was added to 200 μL Milli-Q water to get a final concentration of 50 mg/mL. The stock solution was kept at 4 ℃ in darkness.

## Ⅴ Preparation of doxorubicin

Accurately weight 10 mg of doxorubicin was added to 1 mL Milli-Q water to get a final concentration of 10 mg/mL. The stock solution was kept at 4 ℃ in darkness.

## Ⅵ Preparation of verapamil

Accurately weight 10 mg of verapamil was added to 1 mL Milli-Q water to get a final concentration of 10 mg/mL. The stock solution was kept at 4 ℃ in darkness.

## Ⅶ Preparation of LB broth

About 2 g of LB powder (Sigma,USA) was added to 100 mL of double-distilled water and autoclaved for about 20 mins(Gibco,USA)

## Ⅷ Preparation of phosphate buffered saline (PBS) buffer

About 8 g of sodium chloride (NaCl, Sigma,USA), 0.2 g of potassium chloride (KCl,Sigma), 1.44 g of disodium hydrogen phosophate ($Na_2HPO_4$, Sigm, USA) and 0.24 gof potassium dihydrogen phosphate ($KH_2PO_4$, Sigma, USA) were added with 1 L ofdouble-distilled water to give 1x of PBS buffer with pH ranged from 7.2 to 7.4.The PBS buffer was autoclaved for about 20 mins before use.

## Ⅸ Preparation of antibiotics

About 5 g of antibiotics (ampicillin or kanamycin) was dissolved in 100 mL ofdistilled water to give a final working concentration of 50 mg/mL.

## X Preparation of 10x *tris*-borate-EDTA (TBE) buffer

TBE buffer was used for the agarose gel electrophoresis of nucleic acids as it hada high buffer capacity. About 108 g of *tris*-(hydroxymethyl)-aminomethane,*tris*-base ($C_4H_{11}NO_3$, Sigma-Aldrich), 55 g of boric acid ($H_3BO_3$, Sigma-Aldrich) and 9.3 g ofethylenediaminetetraacetate, EDTA ($C_{10}H_{16}N_2O_8$, Sigma-Aldrich) were added with 1 L ofdouble-distilled water to give rise to 10x of TBE buffer. The pH is 8.3 andrequired no adjustment. The working buffer of agarose gel electrophoresis fornucleic acid was 1x TBE.

## XI Preparation of crystal violet staining solution

50mg of crystal violet (Sigma-Aldrich, USA) was added to 25mL of methanol and 75 mLdouble-distilled water to give 0.05% w/v crystal violet staining solution. The staining solution was stored in dark and room temperature.

# Reference


1. Jemal, A., et al., *Cancer statistics, 2008.* CA Cancer J Clin, 2008. **58**(2): p. 71-96.
2. Siegel, R.L., K.D. Miller, and A. Jemal, *Cancer Statistics, 2018.* Ca-a Cancer Journal for Clinicians, 2018. **68**(1): p. 7-30.
3. Bray, F., et al., *Global estimates of cancer prevalence for 27 sites in the adult population in 2008.* International Journal Of Cancer, 2013. **132**(5): p. 1133-1145.
4. Ferlay, J., et al., *Cancer incidence and mortality worldwide: Sources, methods and major patterns in GLOBOCAN 2012.* International Journal Of Cancer, 2015. **136**(5): p. E359-E386.
5. Anand, P., et al., *Cancer is a Preventable Disease that Requires Major Lifestyle Changes.* Pharmaceutical Research, 2008. **25**(9): p. 2097-2116.
6. Hanahan, D. and R.A. Weinberg, *Hallmarks of Cancer: The Next Generation.* Cell, 2011. **144**(5): p. 646-674.
7. Seebacher, N.A., D.R. Richardson, and P.J. Jansson, *A mechanism for overcoming P-glycoprotein-mediated drug resistance: novel combination therapy that releases stored doxorubicin from lysosomes via lysosomal permeabilization using Dp44mT or DpC.* Cell Death & Disease, 2016. **7**: p. 13.
8. Konopka, J.B., et al., *Cell lines and clinical isolates derived from Ph1-positive chronic myelogenous leukemia patients express c-abl proteins with a common structural alteration.* Proceedings of the National Academy of Sciences, 1985. **82**(6): p. 1810-1814.
9. Croce, C.M., *ROLE OF CHROMOSOME TRANSLOCATIONS IN HUMAN NEOPLASIA.* Cell, 1987. **49**(2): p. 155-156.
10. Heldin, C.H. and B. Westermark, *Mechanism of action and in vivo role of platelet-derived growth factor.* Physiological Reviews, 1999. **79**(4): p. 1283-1316.
11. Arteaga, C.L., *Epidermal growth factor receptor dependence in human tumors: More than just expression?* Oncologist, 2002. **7**: p. 31-39.
12. Peterson, C.L. and J.L. Workman, *Promoter targeting and chromatin remodeling by the SWI/SNF complex.* Current Opinion In Genetics & Development, 2000. **10**(2): p. 187-192.
13. Pawson, T. and N. Warner, *Oncogenic re-wiring of cellular signaling pathways.* Oncogene, 2007. **26**(9): p. 1268-1275.
14. Adams, J.M. and S. Cory, *The Bcl-2 apoptotic switch in cancer development and therapy.* Oncogene, 2007. **26**(9): p. 1324-1337.
15. Goldman, J.M. and J.V. Melo, *Targeting the BCR-ABL tyrosine kinase in chronic myeloid leukemia.* New England Journal Of Medicine, 2001. **344**(14): p. 1084-1086.
16. Collins, M.K. and A. Lopez Rivas, *The control of apoptosis in mammalian cells.* Trends Biochem Sci, 1993. **18**(8): p. 307-9.
17. Wyllie, A.H., *Apoptosis and the regulation of cell numbers in normal and neoplastic tissues: an overview.* Cancer Metastasis Rev, 1992. **11**(2): p. 95-103.
18. Elmore, S., *Apoptosis: A review of programmed cell death.* Toxicologic Pathology, 2007. **35**(4): p. 495-516.
19. Robertson, J.D. and S. Orrenius, *Molecular mechanisms of apoptosis induced by cytotoxic chemicals.* Crit Rev Toxicol, 2000. **30**(5): p. 609-27.

20. Gamet-Payrastre, L., et al., *Sulforaphane, a naturally occurring isothiocyanate, induces cell cycle arrest and apoptosis in HT29 human colon cancer cells.* Cancer Res, 2000. **60**(5): p. 1426-33.
21. O'Connor, P.M., et al., *G2 delay induced by nitrogen mustard in human cells affects cyclin A/cdk2 and cyclin B1/cdc2-kinase complexes differently.* J Biol Chem, 1993. **268**(11): p. 8298-308.
22. Khan, S.N., et al., *Effect of mitoxantrone on proliferation dynamics and cell-cycle progression.* Biosci Rep, 2010. **30**(6): p. 375-81.
23. Kuo, P.L., et al., *The mechanism of ellipticine-induced apoptosis and cell cycle arrest in human breast MCF-7 cancer cells.* Cancer Lett, 2005. **223**(2): p. 293-301.
24. Fidler, I.J., *Timeline - The pathogenesis of cancer metastasis: the 'seed and soil' hypothesis revisited.* Nature Reviews Cancer, 2003. **3**(6): p. 453-458.
25. Chaffer, C.L. and R.A. Weinberg, *A Perspective on Cancer Cell Metastasis.* Science, 2011. **331**(6024): p. 1559-1564.
26. Gupta, G.P., et al., *Mediators of vascular remodelling co-opted for sequential steps in lung metastasis.* Nature, 2007. **446**(7137): p. 765-U2.
27. Pennathur, A., et al., *Oesophageal carcinoma.* Lancet, 2013. **381**(9864): p. 400-412.
28. Umar, S.B. and D.E. Fleischer, *Esophageal cancer: epidemiology, pathogenesis and prevention.* Nature Clinical Practice Gastroenterology & Hepatology, 2008. **5**(9): p. 517-526.
29. Zhang, Y.W., *Epidemiology of esophageal cancer.* World Journal Of Gastroenterology, 2013. **19**(34): p. 5598-5606.
30. Levine, M.S., et al., *Carcinoma of the esophagus and esophagogastric junction: Sensitivity of radiographic diagnosis.* American Journal Of Roentgenology, 1997. **168**(6): p. 1423-1426.
31. Jeon, J.H., C.H. Lee, and H.S. Lee, *Antimicrobial activities of 2-methyl-8-hydroxyquinoline and its derivatives against human intestinal bacteria.* Journal of the Korean Society for Applied Biological Chemistry, 2009. **52**(2): p. 202-205.
32. Nieman, D.R. and J.H. Peters, *Treatment Strategies for Esophageal Cancer.* Gastroenterology Clinics Of North America, 2013. **42**(1): p. 187-+.
33. Torre, L.A., et al., *Global cancer statistics, 2012.* CA Cancer J Clin, 2015. **65**(2): p. 87-108.
34. Sohlberg, T., *Tobacco: science, policy and public health, 2nd edition.* Nordic Studies on Alcohol And Drugs, 2011. **28**(4): p. 397-400.
35. Samet, J.M., et al., *LUNG-CANCER MORTALITY AND EXPOSURE TO RADON PROGENY IN A COHORT OF NEW-MEXICO UNDERGROUND URANIUM MINERS.* Health Physics, 1991. **61**(6): p. 745-752.
36. Alberg, A.J., et al., *Epidemiology of Lung Cancer Diagnosis and Management of Lung Cancer, 3rd ed: American College of Chest Physicians Evidence-Based Clinical Practice Guidelines.* Chest, 2013. **143**(5): p. E1-E29.
37. Valk, P.E., et al., *Staging non-small cell lung cancer by whole-body positron emission tomographic imaging.* Annals Of Thoracic Surgery, 1995. **60**(6): p. 1573-1581.
38. Molina, J.R., et al., *Non-small cell lung cancer: Epidemiology, risk factors, treatment, and survivorship.* Mayo Clinic Proceedings, 2008. **83**(5): p. 584-594.
39. Jemal, A., et al., *Global Cancer Statistics.* Ca-a Cancer Journal for Clinicians, 2011. **61**(2): p.

69-90.
40. McPherson, K., C.M. Steel, and J.M. Dixon, *ABC of breast disease: Breast cancer-epidemiology, risk factors, and genetics.* British Medical Journal, 2000. **321**(7261): p. 624-628.
41. Fisher, B., et al., *Twenty-year follow-up of a randomized trial comparing total mastectomy, lumpectomy, and lumpectomy plus irradiation for the treatment of invasive breast cancer.* New England Journal Of Medicine, 2002. **347**(16): p. 1233-1241.
42. Huang, E.H., et al., *Postmastectomy radiation improves local-regional control and survival for selected patients with locally advanced breast cancer treated with neoadjuvant chemotherapy and mastectomy.* Journal Of Clinical Oncology, 2004. **22**(23): p. 4691-4699.
43. Bonadonna, G., et al., *30 years' follow up of randomised studies of adjuvant CMF in operable breast cancer: cohort study.* British Medical Journal, 2005. **330**(7485): p. 217-220.
44. Bange, J., E. Zwick, and A. Ullrich, *Molecular targets for breast cancer therapy and prevention.* Nature Medicine, 2001. **7**(5): p. 548-552.
45. Danaei, G., et al., *Causes of cancer in the world: comparative risk assessment of nine behavioural and environmental risk factors*. Lancet, 2005. **366**(9499): p. 1784-1793.
46. Goldie, S.J., et al., *Projected clinical benefits and cost-effectiveness of a human papillomavirus 16/18 vaccine.* Journal Of the National Cancer Institute, 2004. **96**(8): p. 604-615.
47. Mitra, A.P., et al., *Biomarker profiling for cancer diagnosis, prognosis and therapeutic management.* National Medical Journal Of India, 2005. **18**(6): p. 304-312.
48. Reubi, J.C., *Peptide receptors as molecular targets for cancer diagnosis and therapy.* Endocrine Reviews, 2003. **24**(4): p. 389-427.
49. Kosaka, N., H. Iguchi, and T. Ochiya, *Circulating microRNA in body fluid: a new potential biomarker for cancer diagnosis and prognosis.* Cancer Science, 2010. **101**(10): p. 2087-2092.
50. Vogelstein, B. and K.W. Kinzler, *Cancer genes and the pathways they control.* Nature Medicine, 2004. **10**(8): p. 789-799.
51. Wan, P.T.C., et al., *Mechanism of activation of the RAF-ERK signaling pathway by oncogenic mutations of B-RAF.* Cell, 2004. **116**(6): p. 855-867.
52. Downward, J., *Targeting ras signalling pathways in cancer therapy.* Nature Reviews Cancer, 2003. **3**(1): p. 11-22.
53. Hennessy, B.T., et al., *Exploiting the PI3K/AKT pathway for cancer drug discovery.* Nature Reviews Drug Discovery, 2005. **4**(12): p. 988-1004.
54. Bjornsti, M.A. and P.J. Houghton, *The TOR pathway: A target for cancer therapy.* Nature Reviews Cancer, 2004. **4**(5): p. 335-348.
55. Hupp, T.R., D.P. Lane, and K.L. Ball, *Strategies for manipulating the p53 pathway in the treatment of human cancer.* Biochemical Journal, 2000. **352**: p. 1-17.
56. Siegel, R., et al., *Cancer treatment and survivorship statistics, 2012.* Ca-a Cancer Journal for Clinicians, 2012. **62**(4): p. 220-241.
57. Kufe DW, P.R., Weichselbaum RR, et al., , *Holland-Frei Cancer Medicine. .* 6th edition ed. 2003., Hamilton (ON):: BC Decker; .

58. Hill, R., et al., *Advances in kilovoltage x-ray beam dosimetry.* Physics In Medicine And Biology, 2014. **59**(6): p. R183-R231.
59. Lind, M.J., *Principles of cytotoxic chemotherapy.* Medicine, 2008. **36**(1): p. 19-23.
60. Lind, M.J. and C. Ardiet, *PHARMACOKINETICS OF ALKYLATING-AGENTS.* Cancer Surveys, 1993. **17**: p. 157-188.
61. Belani, C.P., *Recent updates in the clinical use of platinum compounds for the treatment of lung, breast, and genitourinary tumors and myeloma.* Seminars In Oncology, 2004. **31**(6): p. 25-33.
62. Dumontet, C. and M.A. Jordan, *Microtubule-binding agents: a dynamic field of cancer therapeutics.* Nat Rev Drug Discov, 2010. **9**(10): p. 790-803.
63. Pommier, Y., *Topoisomerase I inhibitors: camptothecins and beyond.* Nature Reviews Cancer, 2006. **6**(10): p. 789-802.
64. Hamid, O., *Emerging Treatments in Oncology: Focus on Tyrosine Kinase (erbB) Receptor Inhibitors.* Journal of the American Pharmacists Association, 2004. **44**(1): p. 52-58.
65. Dasari, S. and P.B. Tchounwou, *Cisplatin in cancer therapy: Molecular mechanisms of action.* European Journal Of Pharmacology, 2014. **740**: p. 364-378.
66. Florea, A.-M. and D. Büsselberg, *Cisplatin as an anti-tumor drug: cellular mechanisms of activity, drug resistance and induced side effects.* Cancers, 2011. **3**(1): p. 1351-1371.
67. Galluzzi, L., et al., *Molecular mechanisms of cisplatin resistance.* Oncogene, 2012. **31**(15): p. 1869-1883.
68. Honda, M., et al., *Doxorubicin, cisplatin, and fluorouracil combination therapy for metastatic esophageal squamous cell carcinoma.* Dis Esophagus, 2010. **23**(8): p. 641-5.
69. Tacar, O., P. Sriamornsak, and C.R. Dass, *Doxorubicin: an update on anticancer molecular action, toxicity and novel drug delivery systems.* Journal Of Pharmacy And Pharmacology, 2013. **65**(2): p. 157-170.
70. Mimeault, M., R. Hauke, and S.K. Batra, *Recent advances on the molecular mechanisms involved in the drug resistance of cancer cells and novel targeting therapies.* Clinical Pharmacology & Therapeutics, 2008. **83**(5): p. 673-691.
71. Yu, L., et al., *Enhancement of doxorubicin cytotoxicity on human esophageal squamous cell carcinoma cells by indomethacin and 4-[5-(4-chlorophenyl)-3-(trifluoromethyl)-1H-pyrazol-1-yl]benzenesulfonamide (SC236) via inhibiting P-glycoprotein activity.* Mol Pharmacol, 2009. **75**(6): p. 1364-73.
72. Blochberger, T.C., P.K. Cornuet, and J.R. Hassell, *ISOLATION AND PARTIAL CHARACTERIZATION OF LUMICAN AND DECORIN FROM ADULT CHICKEN CORNEAS - A KERATAN SULFATE-CONTAINING ISOFORM OF DECORIN IS DEVELOPMENTALLY REGULATED.* Journal Of Biological Chemistry, 1992. **267**(29): p. 20613-20619.
73. Nikitovic, D., et al., *Lumican, a Small Leucine-rich Proteoglycan.* Iubmb Life, 2008. **60**(12): p. 818-823.
74. Kobe, B. and A.V. Kajava, *The leucine-rich repeat as a protein recognition motif.* Current Opinion In Structural Biology, 2001. **11**(6): p. 725-732.
75. Chakravarti, S., et al., *PRIMARY STRUCTURE OF HUMAN LUMICAN (KERATAN SULFATE PROTEOGLYCAN) AND LOCALIZATION OF THE GENE (LUM) TO CHROMOSOME 12Q21.3-Q22.* Genomics, 1995. **27**(3): p. 481-488.
76. Cornuet, P.K., T.C. Blochberger, and J.R. Hassell, *Molecular polymorphism of lumican*

*during corneal development.* Invest Ophthalmol Vis Sci, 1994. **35**(3): p. 870-7.
77. Ishiwata, T., et al., *Role of lumican in cancer cells and adjacent stromal tissues in human pancreatic cancer.* Oncology Reports, 2007. **18**(3): p. 537-543.
78. Yeh, L.K., et al., *Soluble lumican glycoprotein purified from human amniotic membrane promotes corneal epithelial wound healing.* Investigative Ophthalmology & Visual Science, 2005. **46**(2): p. 479-486.
79. Seomun, Y. and C.K. Joo, *Lumican induces human corneal epithelial cell migration and integrin expression via ERK 1/2 signaling.* Biochemical And Biophysical Research Communications, 2008. **372**(1): p. 221-225.
80. Chakravarti, S., et al., *Lumican regulates collagen fibril assembly: Skin fragility and corneal opacity in the absence of lumican.* Journal Of Cell Biology, 1998. **141**(5): p. 1277-1286.
81. Lu, Y.P., T. Ishiwata, and G. Asano, *Lumican expression in alpha cells of islets in pancreas and pancreatic cancer cells.* Journal Of Pathology, 2002. **196**(3): p. 324-330.
82. Lu, Y.P., et al., *Expression of lumican in human colorectal cancer cells.* Pathology International, 2002. **52**(8): p. 519-526.
83. Nikitovic, D., et al., *Lumican expression is positively correlated with the differentiation and negatively with the growth of human osteosarcoma cells.* FEBS J, 2008. **275**(2): p. 350-61.
84. Brezillon, S., et al., *Expression of lumican, a small leucine-rich proteoglycan with antitumour activity, in human malignant melanoma.* Clinical And Experimental Dermatology, 2007. **32**(4): p. 405-416.
85. Coulson-Thomas, V.J., et al., *Lumican expression, localization and antitumor activity in prostate cancer.* Experimental Cell Research, 2013. **319**(7): p. 967-981.
86. Troup, S., et al., *Reduced expression of the small leucine-rich proteoglycans, lumican, and decorin is associated with poor outcome in node-negative invasive breast cancer.* Clinical Cancer Research, 2003. **9**(1): p. 207-214.
87. Matsuda, Y., et al., *Expression and roles of lumican in lung adenocarcinoma and squamous cell carcinoma.* International Journal Of Oncology, 2008. **33**(6): p. 1177-1185.
88. Nikitovic, D., et al., *Lumican affects tumor cell functions, tumor-ECM interactions, angiogenesis and inflammatory response.* Matrix Biology, 2014. **35**: p. 206-214.
89. Nikitovic, D., et al., *Lumican affects tumor cell functions, tumor-ECM interactions, angiogenesis and inflammatory response.* Matrix Biol, 2014. **35**: p. 206-14.
90. Wang, X.F., et al., *Cancer-associated fibroblast-derived Lumican promotes gastric cancer progression via the integrin beta 1-FAK signaling pathway.* International Journal Of Cancer, 2017. **141**(5): p. 998-1010.
91. Brezillon, S., et al., *Lumican effects in the control of tumour progression and their links with metalloproteinases and integrins.* Febs Journal, 2013. **280**(10): p. 2369-2381.
92. Zhao, Y., et al., *Lumican alleviates hypertrophic scarring by suppressing integrin-FAK signaling.* Biochemical and Biophysical Research Communications, 2016. **480**(2): p. 153-159.
93. Nikitovic, D., et al., *Lumican expression is positively correlated with the differentiation and negatively with the growth of human osteosarcoma cells.* Febs Journal, 2008. **275**(2): p. 350-361.
94. Chakravarti, S., F. Wu, and L. Roberts, *Extracellular matrix proteoglycan lumican regulates innate immune response via the CD14-TLR4 pathway.* Gastroenterology, 2007. **132**(4): p.

A78-A79.

95. Vij, N., et al., *Lumican suppresses cell proliferation and aids Fas-Fas ligand mediated apoptosis: implications in the cornea*. Experimental Eye Research, 2004. **78**(5): p. 957-971.
96. Russo, C.M., et al., *Synthesis and initial evaluation of quinoline-based inhibitors of the SH2-containing inositol 5'-phosphatase (SHIP).* Bioorg Med Chem Lett, 2015.
97. Kumar, S., S. Bawa, and H. Gupta, *Biological activities of quinoline derivatives.* Mini Rev Med Chem, 2009. **9**(14): p. 1648-54.
98. Ekengard, E., et al., *Antimalarial activity of ruthenium(ii) and osmium(ii) arene complexes with mono- and bidentate chloroquine analogue ligands.* Dalton Trans, 2015.
99. Chan, S.H., et al., *Synthesis of 8-hydroxyquinoline derivatives as novel antitumor agents.* ACS medicinal chemistry letters, 2013. **4**(2): p. 170-174.
100. Michael, J.P., *Quinoline, quinazoline and acridone alkaloids.* Natural product reports, 1998. **16**(6): p. 697-709.
101. Kumar, S., S. Bawa, and H. Gupta, *Biological activities of quinoline derivatives.* Mini reviews in medicinal chemistry, 2009. **9**(14): p. 1648-1654.
102. Madapa, S., et al., *Search for new pharmacophores for antimalarial activity. Part I: synthesis and antimalarial activity of new 2-methyl-6-ureido-4-quinolinamides.* Bioorg Med Chem, 2009. **17**(1): p. 203-21.
103. Eswaran, S., et al., *New quinoline derivatives: synthesis and investigation of antibacterial and antituberculosis properties.* Eur J Med Chem, 2010. **45**(8): p. 3374-83.
104. Savarino, A., et al., *The anti-HIV-1 activity of chloroquine.* J Clin Virol, 2001. **20**(3): p. 131-5.
105. Chojnacka-Wójcik, E. and A. Naparzewska, *Pharmacological properties of new 11H-indeno[1,2-b]-quinolin-11-one derivatives.* Pol J Pharmacol Pharm, 1982. **34**(5-6): p. 357-63.
106. Chan, B., T.M. Khadem, and J. Brown, *A review of tuberculosis: Focus on bedaquiline.* Am J Health Syst Pharm, 2013. **70**(22): p. 1984-94.
107. Kakadiya, R., et al., *Potent DNA-directed alkylating agents: Synthesis and biological activity of phenyl N-mustard-quinoline conjugates having a urea or hydrazinecarboxamide linker.* Bioorg Med Chem, 2010. **18**(6): p. 2285-99.
108. Wang, Y., et al., *Expeditious one-pot synthesis of C3-piperazinyl-substituted quinolines: key precursors to potent c-Met inhibitors.* Org Biomol Chem, 2011. **9**(17): p. 5930-3.
109. Li, S., et al., *Synthesis and biological evaluation of quinazoline and quinoline bearing 2,2,6,6-tetramethylpiperidine-N-oxyl as potential epidermal growth factor receptor(EGFR) tyrosine kinase inhibitors and EPR bio-probe agents*. Eur J Med Chem, 2012. **49**: p. 271-8.
110. Yang, Y., et al., *Design, synthesis and biological evaluation of quinoline amide derivatives as novel VEGFR-2 inhibitors*. Bioorg Med Chem Lett, 2010. **20**(22): p. 6653-6.
111. Lee, H.Y., et al., *5-Amino-2-aroylquinolines as highly potent tubulin polymerization inhibitors. Part 2. The impact of bridging groups at position C-2.* J Med Chem, 2011. **54**(24): p. 8517-25.
112. Jones, P., et al., *A novel series of potent and selective ketone histone deacetylase inhibitors with antitumor activity in vivo.* J Med Chem, 2008. **51**(8): p. 2350-3.

113. Mistry, P., et al., *In vitro and in vivo reversal of P-glycoprotein-mediated multidrug resistance by a novel potent modulator, XR9576.* Cancer Res, 2001. **61**(2): p. 749-58.
114. Atalay, C., *Multi-drug resistance and cancer.* Expert Opinion on Therapeutic Patents, 2007. **17**(5): p. 511-520.
115. Ojima, I., P.Y. Bounaud, and C.F. Oderda, *Recent strategies for the treatment of multi-drug resistance in cancer cells.* Expert Opinion on Therapeutic Patents, 1998. **8**(12): p. 1587-1598.
116. Kapse-Mistry, S., et al., *Nanodrug delivery in reversing multidrug resistance in cancer cells.* Frontiers in Pharmacology, 2014. **5**.
117. Wu, Q., et al., *Multi-drug resistance in cancer chemotherapeutics: Mechanisms and lab approaches.* Cancer Letters, 2014. **347**(2): p. 159-166.
118. Sharom, F.J., *ABC multidrug transporters: structure, function and role in chemoresistance.* Pharmacogenomics, 2008. **9**(1): p. 105-27.
119. Vinod, B.S., T.T. Maliekal, and R.J. Anto, *Phytochemicals As Chemosensitizers: From Molecular Mechanism to Clinical Significance.* Antioxidants & Redox Signaling, 2013. **18**(11): p. 1307-1348.
120. Casorelli, I., C. Bossa, and M. Bignami, *DNA Damage and Repair in Human Cancer: Molecular Mechanisms and Contribution to Therapy-Related Leukemias.* International Journal Of Environmental Research And Public Health, 2012. **9**(8): p. 2636-2657.
121. Ivanova, T., et al., *Integrated epigenomics identifies BMP4 as a modulator of cisplatin sensitivity in gastric cancer.* Gut, 2013. **62**(1): p. 22-33.
122. Stewart, A., et al., *Phase I trial of XR9576 in healthy volunteers demonstrates modulation of P-glycoprotein in CD56(+) lymphocytes after oral and intravenous administration.* Clinical Cancer Research, 2000. **6**(11): p. 4186-4191.
123. Patil, Y.B., et al., *The use of nanoparticle-mediated targeted gene silencing and drug delivery to overcome tumor drug resistance.* Biomaterials, 2010. **31**(2): p. 358-365.
124. Fardel, O., V. Lecureur, and A. Guillouzo, *The P-glycoprotein multidrug transporter.* General Pharmacology, 1996. **27**(8): p. 1283-1291.
125. Liang, Y., et al., *In vitro to in vivo evidence of the inhibitor characteristics of Schisandra lignans toward P-glycoprotein.* Phytomedicine, 2013. **20**(11): p. 1030-1038.
126. Borst, P., et al., *A family of drug transporters: the multidrug resistance-associated proteins.* J Natl Cancer Inst, 2000. **92**(16): p. 1295-302.
127. Aller, S.G., et al., *Structure of P-Glycoprotein Reveals a Molecular Basis for Poly-Specific Drug Binding.* Science, 2009. **323**(5922): p. 1718-1722.
128. Zinzi, L., et al., *Small and innovative molecules as new strategy to revert MDR.* Frontiers in Oncology, 2014. **4**.
129. Ling, V., *Multidrug resistance: Molecular mechanisms and clinical relevance.* Cancer Chemotherapy And Pharmacology, 1997. **40**: p. S3-S8.
130. Ambudkar, S.V., et al., *Biochemical, cellular, and pharmacological aspects of the multidrug transporter.* Annual Review Of Pharmacology And Toxicology, 1999. **39**: p. 361-398.
131. Aller, S.G., *Structure of P-Glycoprotein Reveals a Molecular Basis for Poly-Specific Drug Binding.* Biophysical Journal, 2010. **98**(3): p. 755A-755A.
132. Zhou, S.F., *Structure, function and regulation of P-glycoprotein and its clinical relevance*

*in drug disposition.* Xenobiotica, 2008. **38**(7-8): p. 802-32.

133. Dantzig, A.H., D.P. de Alwis, and M. Burgess, *Considerations in the design and development of transport inhibitors as adjuncts to drug therapy.* Advanced Drug Delivery Reviews, 2003. **55**(1): p. 133-150.
134. Thomas, H. and H.M. Coley, *Overcoming Multidrug Resistance in Cancer: An Update on the Clinical Strategy of Inhibiting P-Glycoprotein.* Cancer Control, 2003. **10**(2): p. 159-165.
135. Ozben, T., *Mechanisms and strategies to overcome multiple drug resistance in cancer.* Febs Letters, 2006. **580**(12): p. 2903-2909.
136. Foote, S.J., et al., *SEVERAL ALLELES OF THE MULTIDRUG-RESISTANCE GENE ARE CLOSELY LINKED TO CHLOROQUINE RESISTANCE IN PLASMODIUM-FALCIPARUM.* Nature, 1990. **345**(6272): p. 255-258.
137. Qi, J., et al., *Pyronaridine, a novel modulator of P-glycoprotein-mediated multidrug resistance in tumor cells in vitro and in vivo.* Biochemical And Biophysical Research Communications, 2004. **319**(4): p. 1124-1131.
138. Mistry, P., et al., *In vitro and in vivo reversal of P-glycoprotein-mediated multidrug resistance by a novel potent modulator, XR9576.* Cancer Research, 2001. **61**(2): p. 749-758.
139. Tang, J.C.O., et al., *Establishment and characterization of a new xenograft-derived human esophageal squamous cell carcinoma cell line SLMT-1 of Chinese origin.* Cancer genetics and cytogenetics, 2001. **124**(1): p. 36-41.
140. Zhang, H., et al., *Cytogenetic aberrations in immortalization of esophageal epithelial cells.* Cancer Genetics and Cytogenetics, 2006. **165**(1): p. 25-35.
141. Leonessa, F., et al., *MDA435/LCC6 and MDA435/LCC6(MDR1): Ascites models of human breast cancer.* British Journal of Cancer, 1996. **73**(2): p. 154-161.
142. Tharayil, N., et al., *Dual purpose secondary compounds: phytotoxin of Centaurea diffusa also facilitates nutrient uptake.* New Phytologist, 2009. **181**(2): p. 424-434.
143. Lam, K.H., et al., *Anti-tumour and pharmacokinetics study of 2-Formyl-8-hydroxy-quinolinium chloride as Galipea longiflora alkaloid analogue.* Phytomedicine, 2014. **21**(6): p. 877-882.
144. Lam, K.H., et al., *Preparation of 8-hydroxyquinoline derivatives as potential antibiotics against Staphylococcus aureus.* Bioorganic & medicinal chemistry letters, 2014. **24**(1): p. 367-370.
145. Chan, A.S.C., et al., *Method of making and administering quinoline derivatives as anti-cancer agents*. 2009, Google Patents.
146. Lam, K.H., et al., *Preparation of Galipea officinalis Hancock type tetrahydroquinoline alkaloid analogues as anti-tumour agents.* Phytomedicine, 2013. **20**(2): p. 166-171.
147. Lam, K.H., et al., *Highly enantioselective iridium-catalyzed hydrogenation of quinoline derivatives using chiral phosphinite H8-BINAPO.* Advanced Synthesis & Catalysis, 2005. **347**(14): p. 1755-1758.
148. Wen, D.S., et al., *A rapid and sensitive UHPLC-MS/MS method for quantification of 83b1 in plasma and its application to bioavailability study in rats.* Journal Of Pharmaceutical And Biomedical Analysis, 2017. **134**: p. 71-76.
149. Pun, I.H.Y., et al., *Anti-cancer Effects of a Novel Quinoline Derivative 83b1 on Human*

*Esophageal Squamous Cell Carcinoma through Down-Regulation of COX-2 mRNA and PGE(2).* Cancer Research And Treatment, 2017. **49**(1): p. 219-229.
150. Qiu, Q.Q., et al., *XR9576.* Journal Of Medicinal Chemistry, 2017. **60**(8): p. 3289-3302.
151. Keiser, M.J., et al., *Relating protein pharmacology by ligand chemistry.* Nature Biotechnology, 2007. **25**(2): p. 197-206.
152. Schmittgen, T.D. and K.J. Livak, *Analyzing real-time PCR data by the comparative CT method.* Nature protocols, 2008. **3**(6): p. 1101-1108.
153. Zhou, C., et al., *Overexpression of human pituitary tumor transforming gene (hPTTG), is regulated by beta-catenin /TCF pathway in human esophageal squamous cell carcinoma.* Int J Cancer, 2005. **113**(6): p. 891-8.
154. Mariani, T.J., et al., *A variable fold-change threshold determines significance for expression microarrays.* Faseb Journal, 2002. **16**(14): p. 321-+.
155. Guba, M., et al., *Rapamycin inhibits primary and metastatic tumor growth by antiangiogenesis: involvement of vascular endothelial growth factor.* Nat Med, 2002. **8**(2): p. 128-35.
156. Schneider, C.A., W.S. Rasband, and K.W. Eliceiri, *NIH Image to ImageJ: 25 years of image analysis.* Nature Methods, 2012. **9**: p. 671.
157. Zhang, N., J.N. Fu, and T.C. Chou, *Synergistic combination of microtubule targeting anticancer fludelone with cytoprotective panaxytriol derived from panax ginseng against MX-1 cells in vitro: experimental design and data analysis using the combination index method.* American Journal Of Cancer Research, 2016. **6**(1): p. 97-104.
158. Guba, M., et al., *Rapamycin inhibits primary and metastatic tumor growth by antiangiogenesis: involvement of vascular endothelial growth factor.* Nature Medicine, 2002. **8**(2): p. 128-135.
159. Schuppan, D. and N.H. Afdhal, *Liver cirrhosis.* Lancet, 2008. **371**(9615): p. 838-851.
160. Pratt, D.S. and M.M. Kaplan, *Evaluation of the liver.* 1999. **1**: p. 205-244.
161. Hu, Y.C., et al., *Establishment, characterization, karyotyping, and comparative genomic hybridization analysis of HKESC-2 and HKESC-3: two newly established human esophageal squamous cell carcinoma cell lines.* Cancer Genetics and Cytogenetics, 2002. **135**(2): p. 120-127.
162. Chou, T.C., *Theoretical basis, experimental design, and computerized simulation of synergism and antagonism in drug combination studies.* Pharmacological Reviews, 2006. **58**(3): p. 621-681.
163. Barltrop, J.A., et al., *5-(3-CARBOXYMETHOXYPHENYL)-2-(4,5-DIMETHYLTHIAZOLYL)-3-(4-SULFOPHENYL) TE TRAZOLIUM, INNER SALT (MTS) AND RELATED ANALOGS OF 3-(4,5-DIMETHYLTHIAZOLYL)-2,5-DIPHENYLTETRAZOLIUM BROMIDE (MTT) REDUCING TO PURPLE WATER-SOLUBLE FORMAZANS AS CELL-VIABILITY INDICATORS.* Bioorganic & Medicinal Chemistry Letters, 1991. **1**(11): p. 611-&.
164. Chan, D., et al., *Expression of Insulin-Like Growth Factor Binding Protein-5 (IGFBP5) Reverses Cisplatin-Resistance in Esophageal Carcinoma.* Cells, 2018. **7**(10): p. 15.
165. Kelemen, L.E., et al., *Genetic variation in stromal proteins decorin and lumican with breast cancer: investigations in two case-control studies.* Breast Cancer Res, 2008. **10**(6): p. R98.
166. Berridge, M.V. and A.S. Tan, *Characterization of the Cellular Reduction of*

*3-(4,5-dimethylthiazol-2-yl)-2,5-diphenyltetrazolium bromide (MTT): Subcellular Localization, Substrate Dependence, and Involvement of Mitochondrial Electron Transport in MTT Reduction.* Archives of Biochemistry and Biophysics, 1993. **303**(2): p. 474-482.

167. Wang, J.D. and P.A. Levin, *Metabolism, cell growth and the bacterial cell cycle.* Nature Reviews Microbiology, 2009. **7**: p. 822.
168. Wang, J.N., et al., *Rabdocoestin B exhibits antitumor activity by inducing G2/M phase arrest and apoptosis in esophageal squamous cell carcinoma.* Cancer Chemotherapy And Pharmacology, 2018. **81**(3): p. 469-481.
169. Ling, Y.H., et al., *Cell cycle-dependent cytotoxicity, G2/M phase arrest, and disruption of p34(cdc2)/cyclin B-1 activity induced by doxorubicin in synchronized P388 cells.* Molecular Pharmacology, 1996. **49**(5): p. 832-841.
170. Sallie, R., J.M. Tredger, and R. Williams, *DRUGS AND THE LIVER .1. TESTING LIVER-FUNCTION.* Biopharmaceutics & Drug Disposition, 1991. **12**(4): p. 251-259.
171. Hutchinson, D.R., et al., *SERUM PRE-ALBUMIN AS AN INDEX OF LIVER-FUNCTION IN HUMAN HEPATOBILIARY DISEASE.* Clinica Chimica Acta, 1981. **114**(1): p. 69-74.
172. Alvaro, D., et al., *The function of alkaline phosphatase in the liver: Regulation of intrahepatic biliary epithelium secretory activities in the rat.* Hepatology, 2000. **32**(2): p. 174-184.
173. Guengerich, F.P., *Common and Uncommon Cytochrome P450 Reactions Related to Metabolism and Chemical Toxicity.* Chemical Research in Toxicology, 2001. **14**(6): p. 611-650.
174. Famurewa, A.C., et al., *Virgin coconut oil supplementation attenuates acute chemotherapy hepatotoxicity induced by anticancer drug methotrexate via inhibition of oxidative stress in rats.* Biomedicine & Pharmacotherapy, 2017. **87**: p. 437-442.
175. Li, W.Y., et al., *Supramolecular formulation of nitidine chloride can alleviate its hepatotoxicity and improve its anticancer activity.* Food And Chemical Toxicology, 2017. **109**: p. 923-929.
176. Samuni, Y., et al., *Superoxide-dependent hepatotoxicity of the Hsp90 inhibiting anticancer drugs geldanamycin and its two derivatives.* Cancer Research, 2009. **69**: p. 1.
177. Eibl, J.K., B.C. Strasser, and G.M. Ross, *Structural, biological, and pharmacological strategies for the inhibition of nerve growth factor.* Neurochemistry International, 2012. **61**(8): p. 1266-1275.
178. Carvalho, O.P., et al., *A novel NGF mutation clarifies the molecular mechanism and extends the phenotypic spectrum of the HSAN5 neuropathy.* Journal of Medical Genetics, 2011. **48**(2): p. 131-135.
179. Olson, L., *NGF AND THE TREATMENT OF ALZHEIMERS-DISEASE.* Experimental Neurology, 1993. **124**(1): p. 5-15.
180. Galpern, W.R., et al., *NGF attenuates 3-nitrotyrosine formation in a 3-NP model of Huntington's disease.* Neuroreport, 1996. **7**(15-17): p. 2639-2642.
181. Festuccia, C., et al., *Tyrosine kinase inhibitor CEP-701 blocks the NTRK1/NGF receptor and limits the invasive capability of prostate cancer cells in vitro.* International Journal of Oncology, 2007. **30**(1): p. 193-200.
182. Darnell, R.B. and J.B. Posner, *Paraneoplastic syndromes affecting the nervous system.*

Seminars in Oncology, 2006. **33**(3): p. 270-298.
183. Anagnostopoulou, V., et al., *Differential Effects of Dehydroepiandrosterone and Testosterone in Prostate and Colon Cancer Cell Apoptosis: The Role of Nerve Growth Factor (NGF) Receptors.* Endocrinology, 2013. **154**(7): p. 2446-2456.
184. Okano, T., et al., *Plasma proteomics of lung cancer by a linkage of multi-dimensional liquid chromatography and two-dimensional difference gel electrophoresis.* Proteomics, 2006. **6**(13): p. 3938-48.
185. Kashyap, M.K., et al., *Overexpression of periostin and lumican in esophageal squamous cell carcinoma.* Cancers (Basel), 2010. **2**(1): p. 133-42.
186. Eshchenko, T.Y., et al., *Expression of different proteoglycans in human breast tumors.* Biochemistry (Mosc), 2007. **72**(9): p. 1016-20.
187. Zhao, J. and J.L. Guan, *Signal transduction by focal adhesion kinase in cancer.* Cancer Metastasis Rev, 2009. **28**(1-2): p. 35-49.
188. Pan, H.T., et al., *Autophagic flux disruption contributes to Ganoderma lucidum polysaccharide-induced apoptosis in human colorectal cancer cells via MAPK/ERK activation.* Cell Death & Disease, 2019. **10**.
189. Zhang, G.Y., et al., *beta-Thujaplicin induces autophagic cell death, apoptosis, and cell cycle arrest through ROS-mediated Akt and p38/ERK MAPK signaling in human hepatocellular carcinoma.* Cell Death & Disease, 2019. **10**.
190. Qiu, X.S., et al., *Lack of association between the promoter polymorphism of the MTNR1A gene and adolescent idiopathic scoliosis.* Spine, 2008. **33**(20): p. 2204-2207.
191. Meng, J.R., et al., *Combination Treatment with MEK and AKT Inhibitors Is More Effective than Each Drug Alone in Human Non-Small Cell Lung Cancer In Vitro and In Vivo.* Plos One, 2010. **5**(11).
192. Pasquier, E., et al., *Propranolol potentiates the anti-angiogenic effects and antitumor efficacy of chemotherapy agents: implication in breast cancer treatment.* Oncotarget, 2011. **2**(10): p. 797-809.
193. Tiberghien, F. and F. Loor, *Ranking of P-glycoprotein substrates and inhibitors by a calcein-AM fluorometry screening assay.* Anti-Cancer Drugs, 1996. **7**(5): p. 568-578.
194. Aszalos, A., et al., *Combinations of P-glycoprotein blockers, verapamil, PSC833, and cremophor act differently on the multidrug resistance associated protein (MRP) and on P-glycoprotein (Pgp).* Anticancer Research, 1999. **19**(2A): p. 1053-1064.
195. Liu, B.M., et al., *6,7-Dimethoxy-2-{2- 4-(1H-1,2,3-triazol-1-yl)phenyl ethyl}-1,2,3,4-tetra hydroisoquinolines as Superior Reversal Agents for P-Glycoprotein-Mediated Multidrug Resistance.* Chemmedchem, 2015. **10**(2): p. 336-344.
196. Qiu, Q., et al., *Design, Synthesis, and Pharmacological Characterization of N-(4-(2 (6,7-Dimethoxy-3,4-dihydroisoquinolin-2(1H)yl)ethyl)phenyl)quinazolin-4-amine Derivatives: Novel Inhibitors Reversing P-Glycoprotein-Mediated Multidrug Resistance.* Journal of Medicinal Chemistry, 2017. **60**(8): p. 3289-3302.
197. Thummel, K.E. and G.R. Wilkinson, *In vitro and in vivo drug interactions involving human CYP3A.* Annual Review Of Pharmacology And Toxicology, 1998. **38**: p. 389-430.